AD-A048 165 DEFENSE NUCLEAR AGENCY WASHINGTON D C F/G 18/3
HUSSAR SWORD SERIES. MIGHTY EPIC EVENT, CONSOLIDATED MIGHTY EPI--ETC(U)
APR 77 H L PIPER

UNCLASSIFIED DNA-POR-6962 ERDA-WT-6962 NL

1 OF 3
ADA
048165

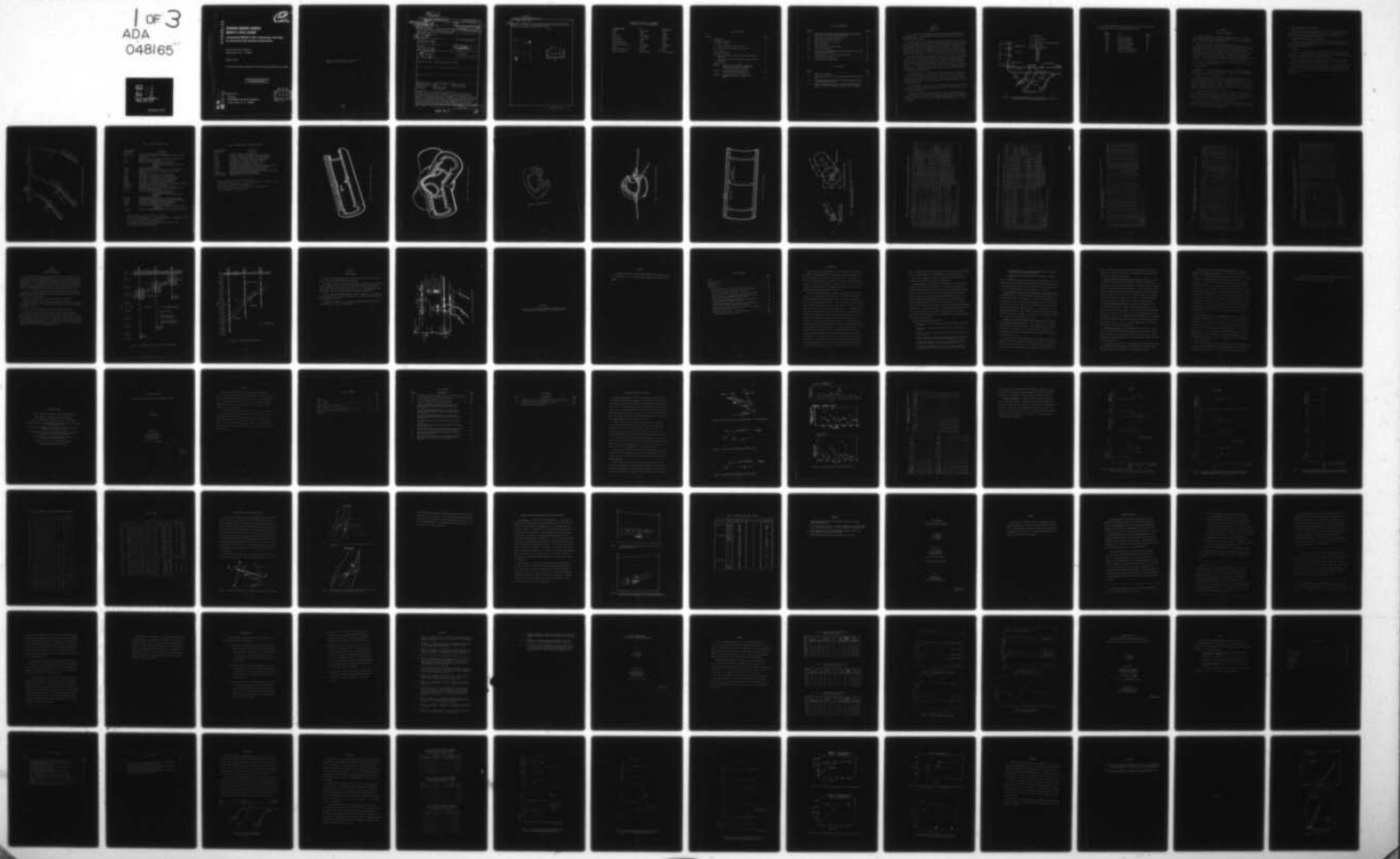

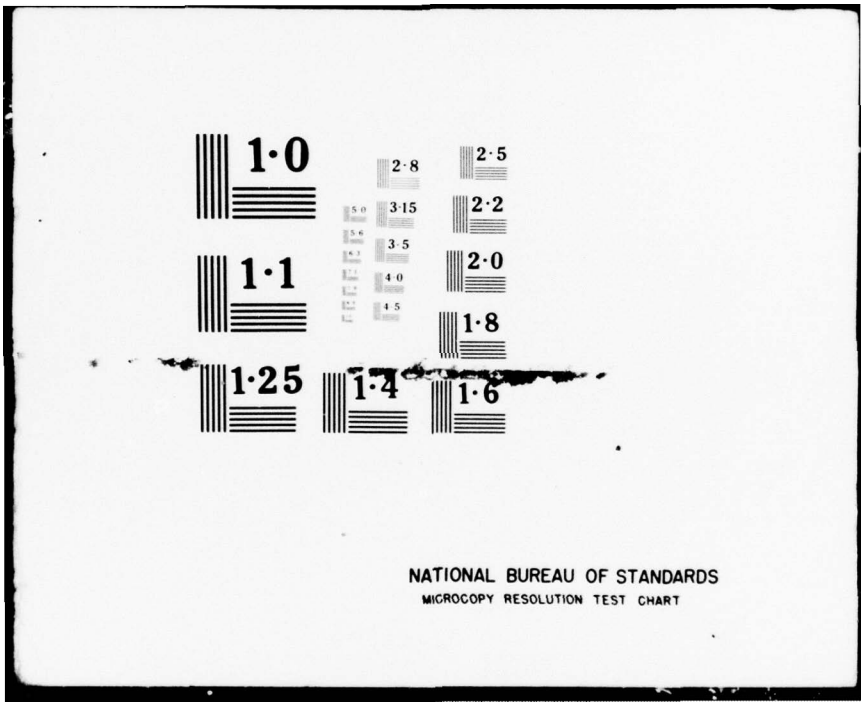
1·0
1·1
1·25
1·4
1·6
1·8
2·0
2·2
2·5
2·8
3·15
3·5
4·0
4·5
5·0
5·6
NATIONAL BUREAU OF STANDARDS
MICROCOPY RESOLUTION TEST CHART

HUSSAR SWORD SERIES
MIGHTY EPIC EVENT

Consolidated MIGHTY EPIC Compression Test Data for Structures and Interface Experiments

Defense Nuclear Agency
Washington, D.C. 20305

26 April 1977

Final Project Officers Report for Period October 1975—June 1976

Prepared for
Director
DEFENSE NUCLEAR AGENCY
Washington, D. C. 20305

Destroy this report when it is no longer needed. Do not return to sender.

(18) ERDA

UNCLASSIFIED

SECURITY CLASSIFICATION OF THIS PAGE *(When Data Entered)*

(19) **REPORT DOCUMENTATION PAGE**

READ INSTRUCTIONS BEFORE COMPLETING FORM

(14) REPORT NUMBER: DNA-POR-6962 WT-6962	2. GOVT ACCESSION NO.
	3. RECIPIENT'S CATALOG NUMBER (9)
(6) TITLE *(and Subtitle)*: HUSSAR SWORD SERIES, MIGHTY EPIC EVENT, Consolidated MIGHTY EPIC Compression Test Data for Structures and Interface Experiments.	5. TYPE OF REPORT & PERIOD COVERED: Final Project Officers Report for Period Oct 75—Jun 76,
	6. PERFORMING ORG. REPORT NUMBER
7. AUTHOR(s): (10) H. L. Piper, LCDR, USN	8. CONTRACT OR GRANT NUMBER(s)
9. PERFORMING ORGANIZATION NAME AND ADDRESS: Defense Nuclear Agency, Washington, D.C. 20305	10. PROGRAM ELEMENT, PROJECT, TASK AREA & WORK UNIT NUMBERS
11. CONTROLLING OFFICE NAME AND ADDRESS: Director, Defense Nuclear Agency, Washington, D.C. 20305	(11) 12. REPORT DATE: 26 Apr 1977
	13. NUMBER OF PAGES: 270
14. MONITORING AGENCY NAME & ADDRESS *(if different from Controlling Office)*: (12) 266p.	15. SECURITY CLASS *(of this report)*: UNCLASSIFIED
	15a. DECLASSIFICATION/DOWNGRADING SCHEDULE

16. DISTRIBUTION STATEMENT *(of this Report)*

Approved for public release; distribution unlimited.

17. DISTRIBUTION STATEMENT *(of the abstract entered in Block 20, if different from Report)*

18. SUPPLEMENTARY NOTES

19. KEY WORDS *(Continue on reverse side if necessary and identify by block number)*

MIGHTY EPIC Event	Compression Strength	Concrete Test Data
HUSSAR SWORD Series	Loads	Material Properties
Grout Data	Physical Properties	
Core Samples	Interface Holes	

20. ABSTRACT *(Continue on reverse side if necessary and identify by block number)*

This report consolidates the compression test data and the physical properties data for the various structures, grouts and cores used in the MIGHTY EPIC underground nuclear test. The purpose of this report is to provide data for use in interpreting damage to the MIGHTY EPIC test structures before and after the reloading of the structures in the DIABLO HAWK nuclear event. This report contains the results obtained ~~by~~ Terra Tek, Inc., U.S. Army Engineer Waterways Experiment Station (WES), Flood Testing Laboratories, Holmes and Narver, Concrete Technology and Fenix and Scisson, Inc. for total load and → next page

DD FORM 1 JAN 73 1473 EDITION OF 1 NOV 65 IS OBSOLETE

UNCLASSIFIED

SECURITY CLASSIFICATION OF THIS PAGE *(When Data Entered)*

406 762

JB

20. ABSTRACT (Continued)

cont. compressive strength tests on the various structures and surrounding grout mixtures. In addition, it contains descriptions of the material properties of the N Tunnel complex at the Nevada Test Site.

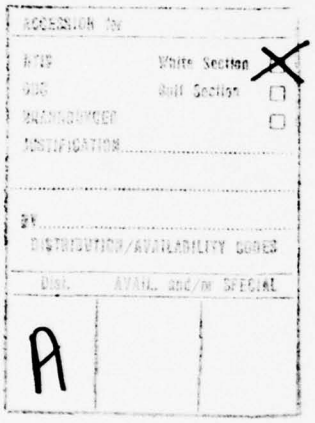

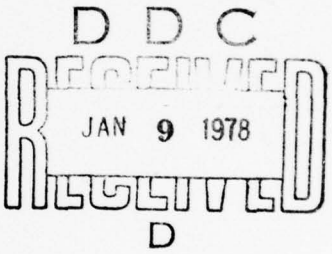

CONVERSION FACTORS FOR U.S. CUSTOMARY
TO METRIC (SI) UNITS OF MEASUREMENTS

TO CONVERT FROM	TO	MULTIPLY BY
Inches	Centimeters	2.54
Feet	Meters	0.3048
Square Feet	Square Meters	0.0929
Cubic Yards	Cubic Meters	0.764555
Gallons (U.S.)	Liters	3.785
Gallons (Imperial)	Liters	4.542
Gallons (U.S. Liquid)	Cubic Meters	0.003785412
Pounds	Kilograms	0.454
Pounds Per Square Inch	Pascals	6,894.757
Degrees Fahrenheit	Degrees Kelvin	$t_K = (t_F^\circ + 459.67)/1.8$

TABLE OF CONTENTS

LIST OF ILLUSTRATIONS

LIST OF TABLES

SECTION 1

INTRODUCTION

MIGHTY EPIC was a nuclear weapons effects test sponsored by the Defense Nuclear Agency (DNA). It was executed 12 May 1976 in the U12n.10 tunnel drift at the Nevada Test Site (NTS).

The event was primarily a radiation effects test; however, two sets of experiments to investigate critical aspects of shock hardened and deep basing technology were included. The first set consisted of structural models to investigate the response of new concepts of structural designs to withstand high intensity shock loading and the second set investigated the underground nuclear explosion induced shock and ground motions across a geological media interface of tuff and quartzite.

These two experiments were located near the device working point of the MIGHTY EPIC test bed. This test bed offered the unique opportunity to shock load test structures twice since the DIABLO HAWK Event is planned for the same tunnel complex. The structures models were located in three separate drifts as shown in Figure 1.1. The geological interface was located in a plane underlaying the MIGHTY EPIC test bed. The experiment measurements were made in drill holes that penetrated down through the interface.

This Project Officers Report (POR) consolidates the MIGHTY EPIC compression test data and the physical properties data for the various structures, grouts, and cores that were tested by Terra Tek, Inc., the U.S. Army Engineers Waterways Experiment Station (WES), Flood Testing Laboratories, Holmes and Narver, and Concrete Technology Corp.

Data extracted from the Terra Tek, Inc. report are contained in the tables in Section 2. The Terra Tek complete report and the reports from Fenix and Scisson are included as appendices.

The data from the Flood Testing Laboratories, Holmes and Narver Materials Testing Laboratory, and the Concrete Technology Corporation have been included in total in the table in Section 2 and the laboratory data sheets are not included in the POR.

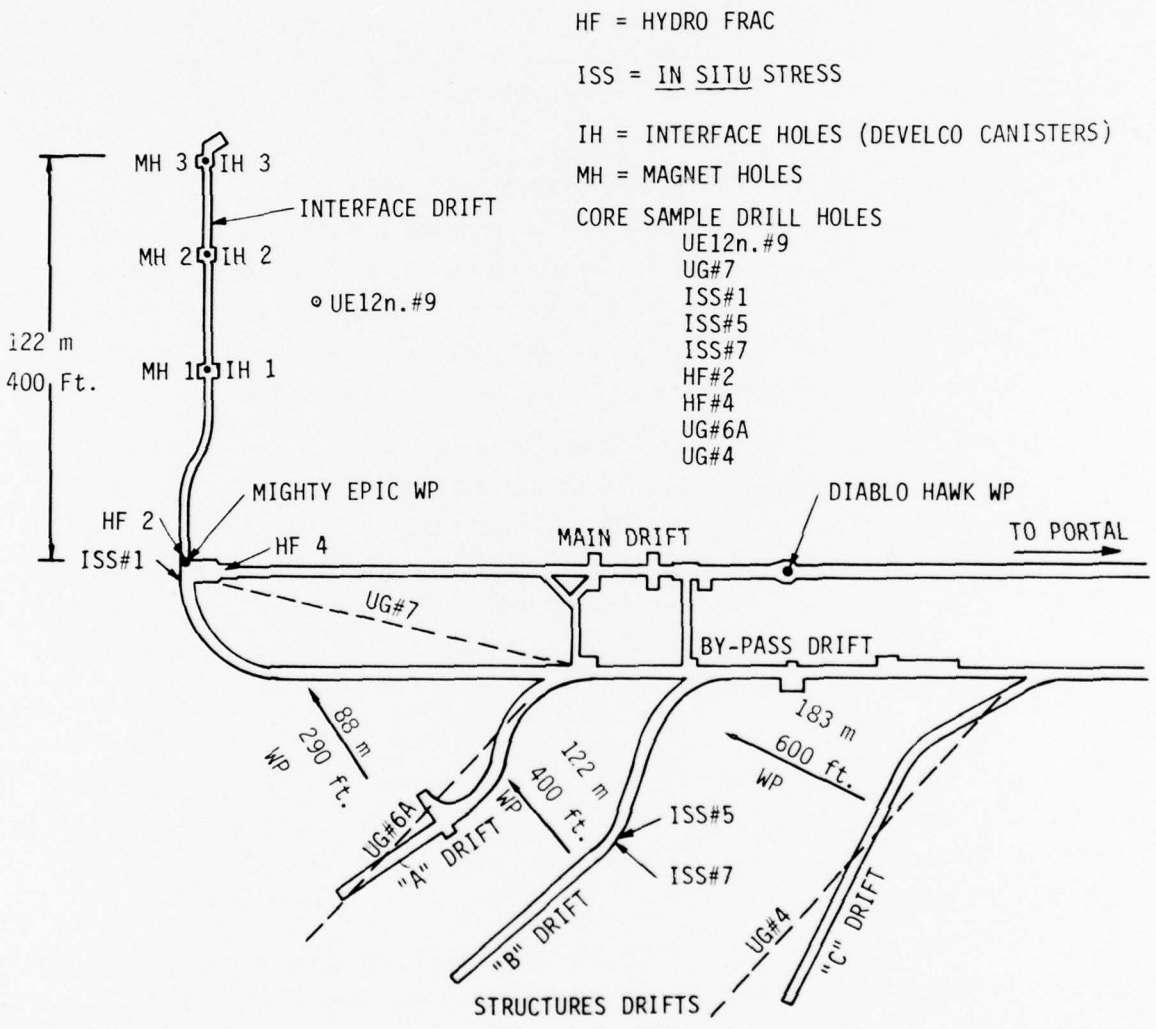

Figure 1.1 Plan view of the MIGHTY EPIC area showing the structures and interface drifts and the related drill holes.

This report contains data on the grout and cores in the vicinity of the experiments described in the following MIGHTY EPIC PORs.

POR NUMBER	TITLE	AGENCY
6949	Structures Response	CASE
6950	Structures Response	SRI
6951	Spherical Structures	AA
6952	Interface Experiments	WES
6953	Interface Magnetic	S^3
6954	Structures Instrumentation	PI
6963	Interface Calculations	S^3

SECTION 2

STRUCTURES EXPERIMENTS

Structural models used were designed by MERRITT-CASES, Inc., formerly J. L. Merritt Consulting and Special Engineering Services (CASES); Stanford Research Institute (SRI); and Agbabian Associates (AA).

Most of the structures were designed to withstand shock pressures in the MPa (tenths of kbar) range. However, models were placed in the drifts at three anticipated peak stress levels as shown in the Preliminary Results Report (POR 6940-2). This was done to hedge against high or low device yields, uncertainties associated with structural material properties and site geological properties. The test structures consisted of two types of composite steel-concrete cylindrical shells and a steel-fiber-reinforced concrete spherical shell.

Figure 2.1 shows the details of the structures experimental layout. Table 2.1 gives a description of each structure.

2.1 CASES STRUCTURES

Figures 2.2, 2.3, and 2.4 show the various kinds of structures designed by MERRITT-CASES, Inc. The compression tests were performed on the CASES MIGHTY EPIC structures by the following organizations:

Holmes and Narver, Inc., Materials Testing Laboratory, Nevada Test Site, P.O. Box 1, Mercury, Nevada 89023, tested cores of the grout in the vicinity of 13 of the 15 CASES composite integral structures. They did not test near C-X-9 and C-Z-1. They tested adjacent to one of the CASES "X" intersections, C-Y-13, and one of CASES "T" intersection structures and in the vicinity of all nine of the CASES dome closures. Their data are included in Table 2.2.

Flood Testing Laboratories, Inc., 1945 East 87th Street, Chicago, Illinois 60617, tested 14 of the 15 CASES composite integral structures. They did not test C-Z-3. They tested both of the CASES "X" intersections and the one CASES "T" intersection structures. Their data are included in Table 2.3.

Concrete Technology Corp., 1123 Port of Tacoma Road, Tacoma, Washington 98421, tested all nine of the CASES dome closures, and two of the CASES slabs, C-X-6/S and C-Y-13/S. The results are included in Table 2.2.

2.2 AGBABIAN ASSOCIATES (AA) STRUCTURES

Figure 2.5 shows pictorially the type of spherical concrete structures that AA fielded in the nine locations shown in Figure 2.1. Concrete Technology Corp. tested the Agbabian structures and the results are given in Table 2.2.

2.3 STANFORD RESEARCH INSTITUTE (SRI) STRUCTURES

Figures 2.6 and 2.7 show sketches of the SRI built-up structures and the models fielded in the MIGHTY EPIC Event. Table 2.4 contains the Terra Tek, Inc., test data for the SRI structures.

2.4 TEST DATA

Table 2.2 is a consolidation of all the MIGHTY EPIC structures compression test data. It summarizes the data from Terra Tek, Inc., WES, Flood Testing Laboratories, Holmes and Narver, and Concrete Technology Corp.

Table 2.3 shows the physical properties and the results of the Flood Test Laboratories compression tests on the CASES structures in A, B, and C drifts.

Table 2.4 shows the types of compression and strain tests performed by Terra Tek, Inc., on various structures and on cores taken in the vicinity of the structures drifts. This table also summarizes the physical properties for the structures and cores.

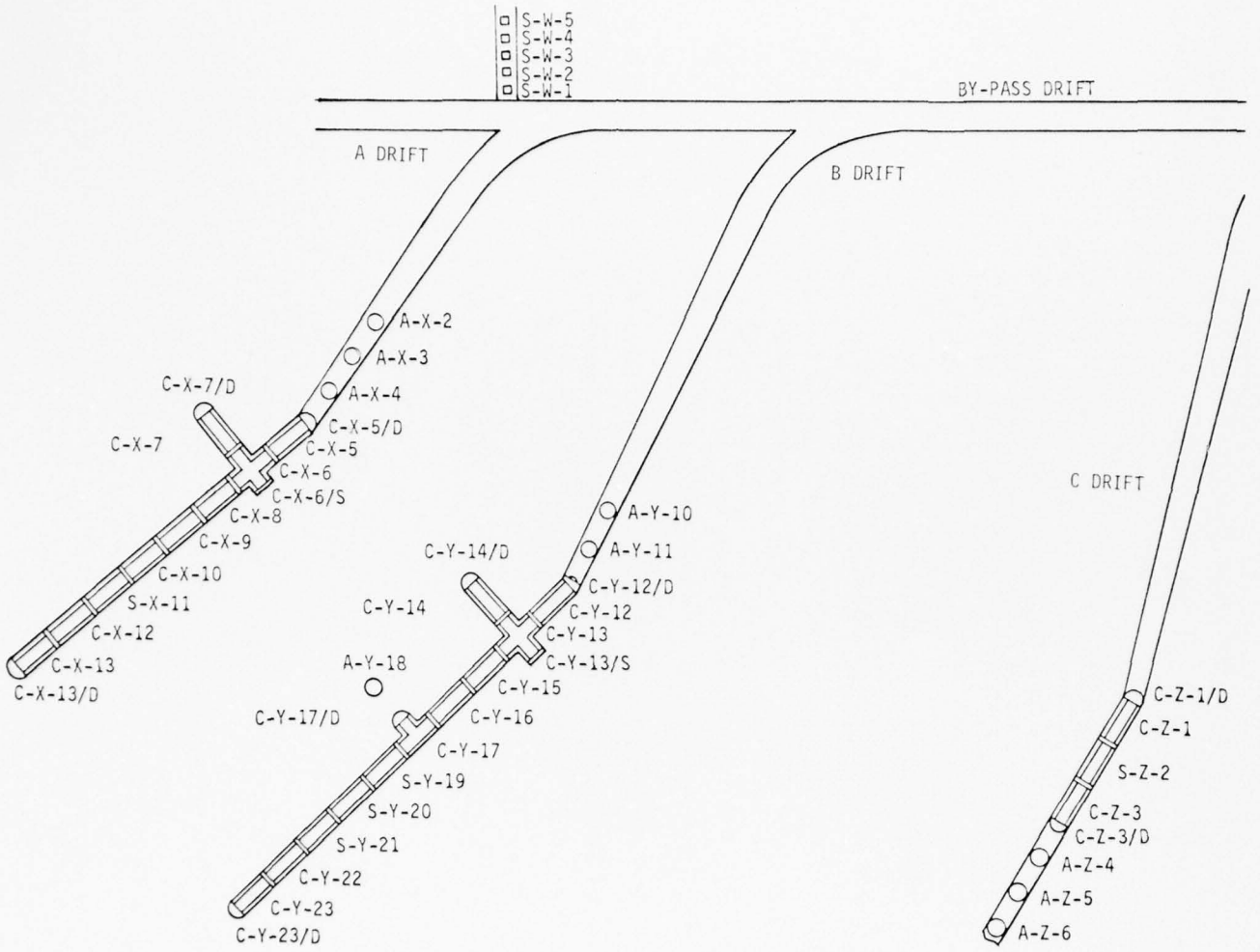

Figure 2.1 MIGHTY EPIC structures experiment layout

Table 2.1 MIGHTY EPIC structures

LAYOUT DRAWING* DESIGNATION	DESCRIPTION
A-X-1 thru 4	Concrete Spheres; 6'-0" OD; 12,000 lb.
C-X-5	3/4" Steel, 15" Concrete, 12" Cellular Concrete; 8'-7½" OD; 80,000 lb.
C-X-5/D	Dome End Closure with Cable Penetration and Manhole, 3/4" Steel, 15" Concrete; 7,500 lb.
C-X-6	X-Intersection - Forward End-On Stub; 19,000 lb. - Aft End-On Stub; 19,000 lb. - Side-On Unit (Two stubs and center unit); 66,000 lb.
C-X-6/S	Slab End Closure; 3,300 lb.
C-X-7	End-On; 3/4" Steel, 11" Concrete; 5'-11½" OD; 41,000 lb.
C-X-7/D	Dome End Closure-No Cable Penetration and no Manhole; 3,000 lb.
C-X-8	1½" Steel, 18" Concrete; 7'-3" OD; 78,000 lb.
C-X-9	3/4" Steel, 15" Concrete; 6'-7½" OD; 57,000 lb.
C-X-10	3/4" Steel, 11" Concrete; 5'-11½" OD; 41,000 lb.
S-X-11	2" Steel, 8" Cellular Concrete; 5'-8" OD; 27,000 lb.
C-X-12	3/4" Steel, 7" Concrete; 5'-3½" OD; 27,000 lb.
C-X-13	3/4" Steel, 5" Concrete; 4'-11½" OD; 21,000 lb.
C-X-13/D	Dome End Closure-No Cable Penetration and no Manhole; 3,000 lb.
A-Y-10 and 11	Concrete Spheres; 6'-0" OD: 12,000 lb.
C-Y-12	3/4" Steel, 15" Concrete; 6'-7½" OD; 57,000 lb.
C-Y-12/D	Dome End Closure with Cable Penetration and Manhole, 3/4" Steel, 15" Concrete; 7,500 lb.
C-Y-13	X-Intersection - Forward End-On Stub; 19,000 lb. - Aft End-On Stub; 19,000 lb. - Side-On Unit (Two stubs & center unit); 66,000 lb.
C-Y-13/S	Slab End Closure; 3,300 lb.
C-Y-14	End-On, 3/4" Steel, 5" Concrete; 4'-11½" OD; 21,000 lb.
C-Y-14/D	Dome End Closure-No Cable penetration and Manhole; 3,000 lb.
C-Y-15	3/4" Steel, 7" Concrete; 5'-3½" OD; 27,000 lb.
C-Y-16	3/4" Steel, 5" Concrete; 4'-11½" OD, 21,000 lb.
C-Y-17	Tee Intersection - End-On Stub; 19,000 lb. - Side-On Unit (Two stubs and center unit); 66,000 lb.
C-Y-17/D	Dome End Closure with Cable Penetration and Manhole; 7,500 lb.

*Identification of structure is derived as follows:

First Letter Designates Agency: A = Agbabian Associates; C = CASES and S = SRI.

Second Letter Designates Anticipated Shock Level

Third Position Designates Structures Number in Each Particular Drift

/D Designates Domes; /S Designates Slabs

Table 2.1 MIGHTY EPIC structures (Continued)

LAYOUT DRAWING* DESIGNATION	DESCRIPTION
A-Y-18	Concrete Sphere; 6'-0" OD; 12,000 lb.
S-Y-19	2" Steel, 8" Cellular Concrete; 5'-8" OD; 27,000 lb.
S-Y-20	1½" Steel, 6" Cellular Concrete; 5'-3" OD; 21,000 lb.
S-Y-21	1" Steel, 4" Cellular Concrete; 4'-10" OD; 14,000 lb.
C-Y-22	3/4" Steel, 3½" Concrete; 4'-8½" OD; 16,000 lb.
C-Y-23	3/4" Steel, 2½" Concrete; 4'-6½" OD; 13,000 lb.
C-Y-23/D	Dome End Closure - No Manhole; 3,000 lb.
C-Z-1	3/4" Steel, 5" Concrete; 4'-11½" OD; 21,000 lb.
C-Z-1/D	Dome End Closure with Cable Penetration and Manhole; 3,000 lb.
S-Z-2	1" Steel, 4" Cellular Concrete; 4'-10" OD; 14,000 lb.
C-Z-3	3/4" Steel, 2½" Concrete; 4'-6½" OD; 13,000 lb.
C-Z-3/D	Dome End Closure with Cable Penetration and Manhole; 3,000 lb.
A-Z-4 through 6	Concrete Spheres; 6'-0" OD; 12,000 lb.
S-W-1 through 5	SRI Models; 3' long; 2'-6" OD; 3,200 lb.

*Identification of structure is derived as follows:

First Letter Designates Agency: A = Agbabian Associates; C = CASES and S = SRI.

Second Letter Designates Anticipated Shock Level

Third Position Designates Structures Number in Each Particular Drift

/D Designates Domes; /S Designates Slabs

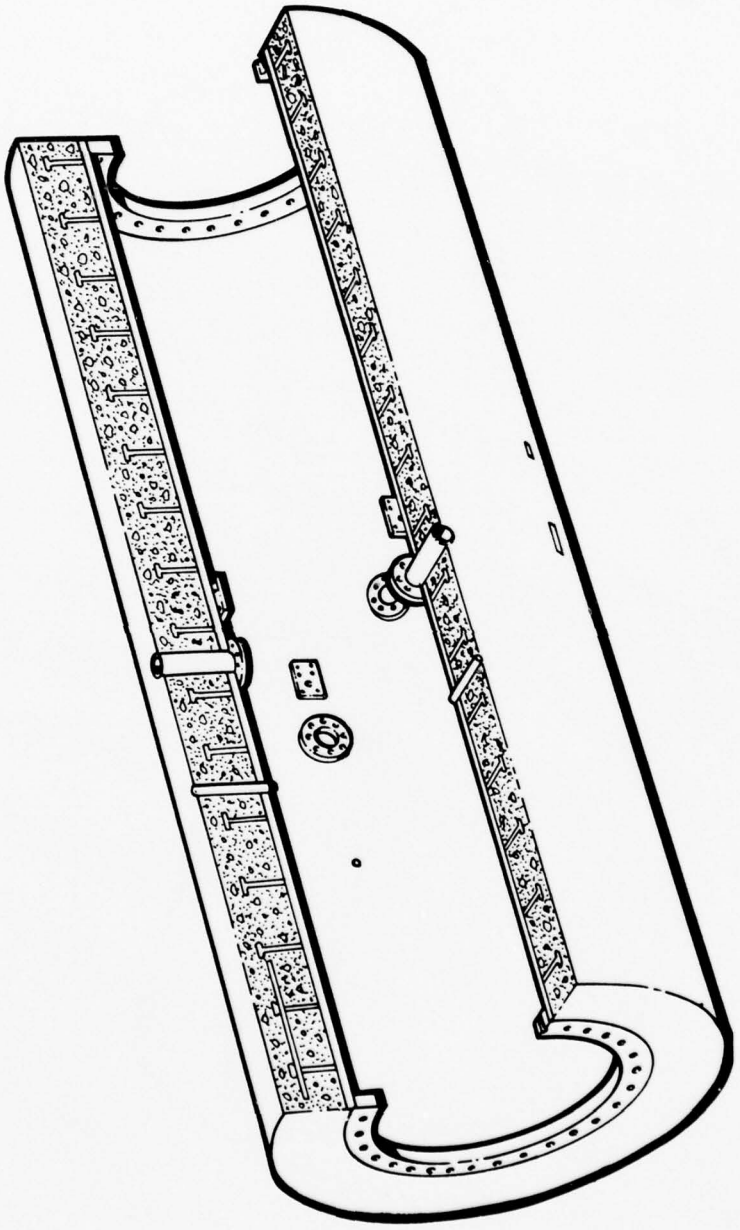

Figure 2.2 CASES composite integral structure

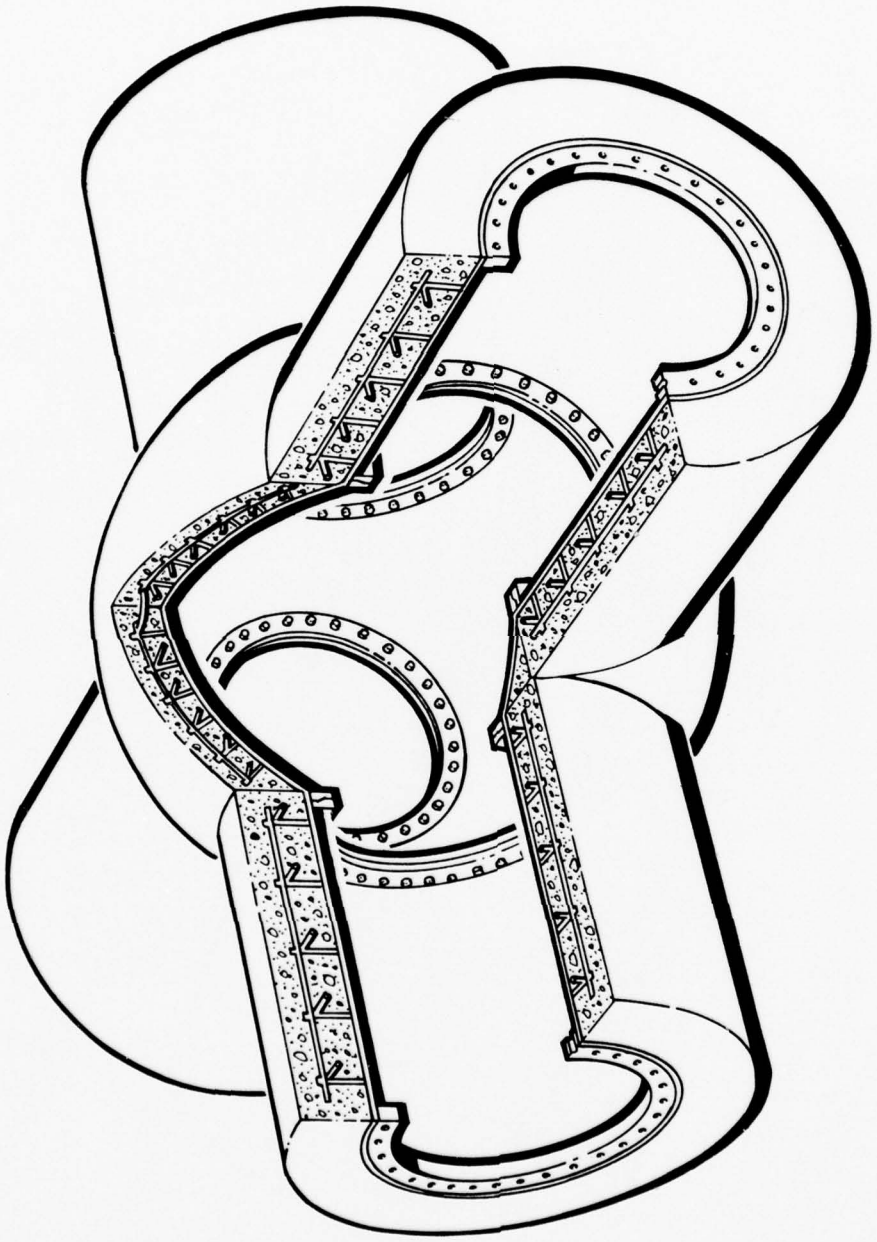

Figure 2.3 CASES intersection (X) structure

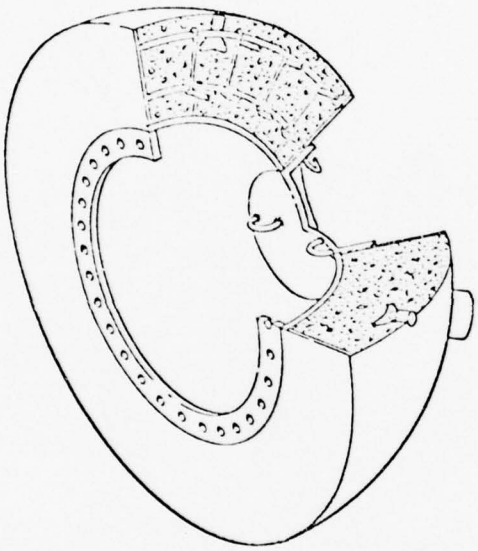

Figure 2.4 CASES dome closure

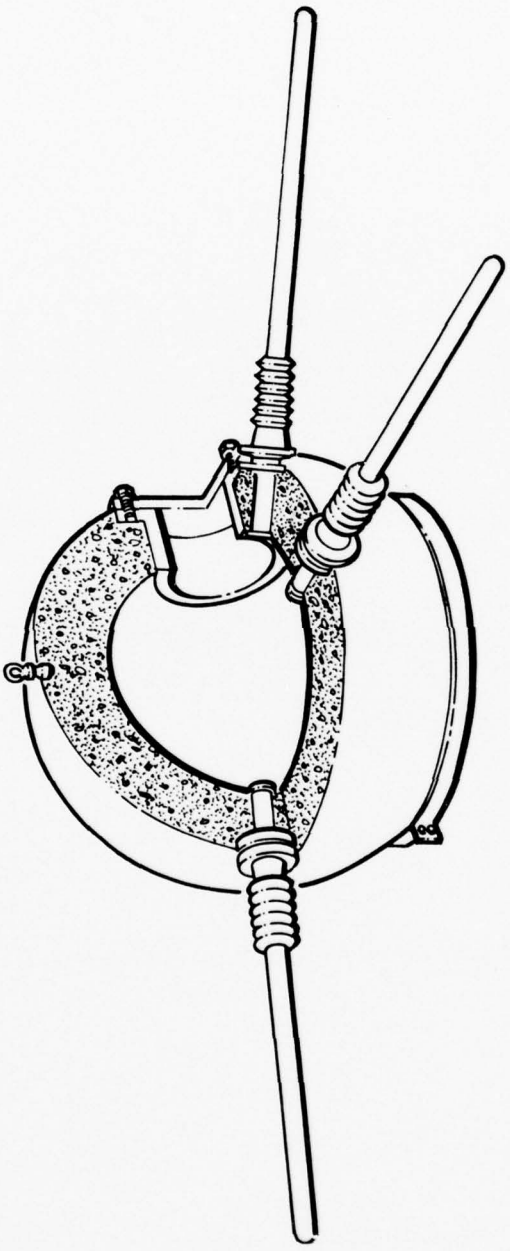

Figure 2.5 Agbabian Associates concrete sphere

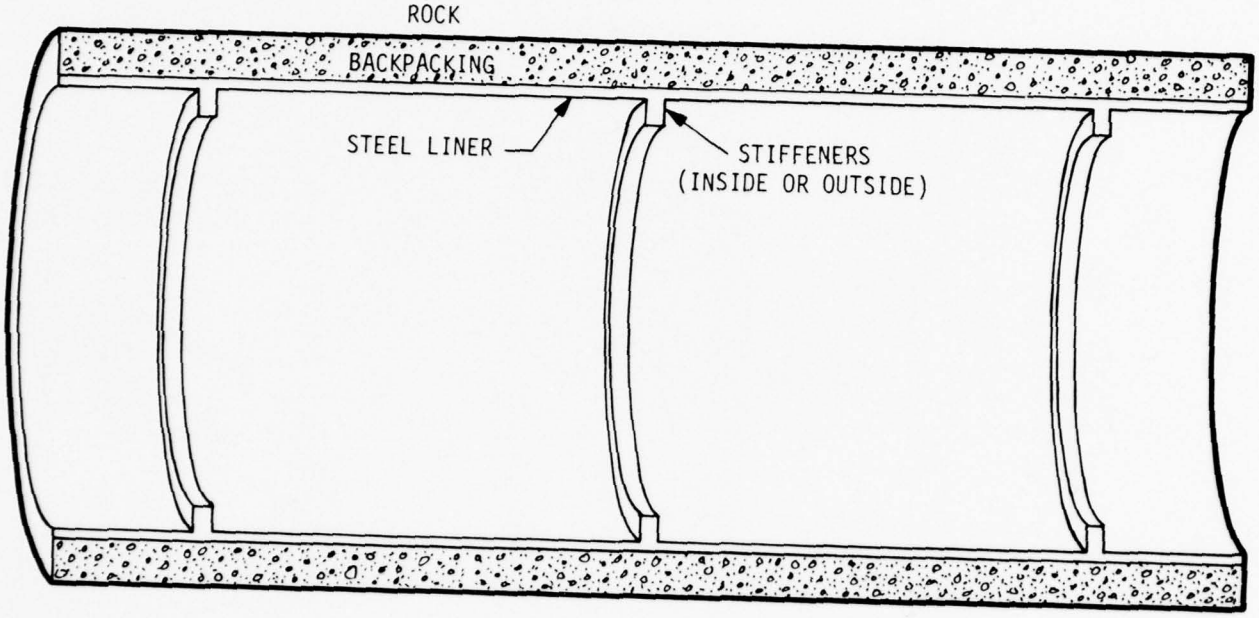

Figure 2.6 SRI built-up structure

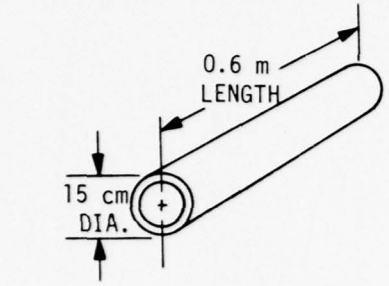

(a) MODELS DIRECTLY IN TUFF
(BOTH END-ON AND SIDE-ON)

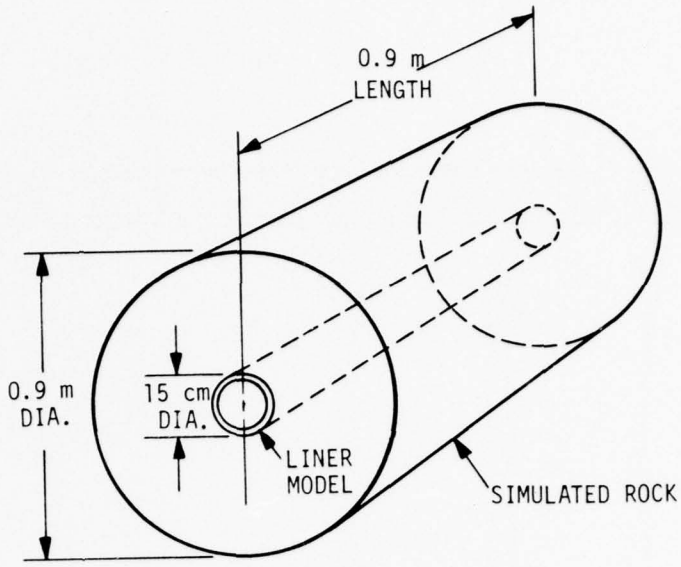

(b) MODELS IN SIMULATED INTACT ROCK

Figure 2.7 Sketches of 15-cm-diameter SRI models fielded directly in tuff and in simulated intact rock.

Table 2.2. Consolidated MIGHTY EPIC structures unconfined compression test data

STRUCTUR	TOTAL LOAD								COMPRESSIVE STRENGTH									Physical Properties Data Available
	7 day			28 day					7 day			28 day					Grout Test	
	lbs	lbs	Average lbs	lbs	lbs	lbs	lbs	Average lbs	PSI	PSI	Avg PSI	PSI	PSI	PSI	PSI	Avg PSI	PSI	
A-X-2									7960[3]	8880[3]	8450	10010[3]	10010[3]	10540[3]	10500[3]	10260	1120[5]	
A-X-3									8560[3]	8735[3]	8675	10565[3]	10210[3]	10495[3]	10070[3]	10340	1120[5]	
A-X-4									7780[3]	8770[3]	8420	10045[3]	10150[3]	10225[3]	10635[3]	10260	1120[5]	
C-X-5	173,000	170,000	171,500	239,500	233,000	172,000[2]	167,000[2]	202,900	6120	6010	6065	8470	8240	6080[2]	5910[2]	7180	1590[5]	
C-X-5/D									7074[3]	6968[3]	7021	9055[3]	9019[3]	8810[4]	8120[4]	8750		
C-X-6	175,500	171,500	173,500	211,000	205,500			208,300	6210	6070	6140	7460	7270			7370	1590[5]	
C-X-6/S	163,000	158,000	160,500	208,000	203,500			205,800	5770	5590	3080	7360	7200			7280		
C-X-6/S									7498[3]	7463[3]	7480	9055[3]	8878[3]			8970		
C-X-7	166,500	162,500	164,500	196,000	199,500	172,000[2]	142,000[2]	177,400	5890	5750	5820	6930	7060	6080[2]	5020[2]	6270	1590[5]	
C-X-7/D									7605[3]	7675[3]	7640	9090[3]	9055[3]	7890[4]	7850[4]	8470		
C-X-8	158,000	161,500	160,000	183,000	199,000			191,000	5590	5710	5650	6470	7040	8630[4]		7380	1485[5]	
C-X-8	131,000	132,000	131,500	186,500	204,500	138,000[2]	145,500[2]	168,600	4630	4670	4650	6600	7230	4880[2]	5160[2]	5970		Appendix A
C-X-9	157,000	154,000	155,500	188,000	183,000			193,500	5550	5450	5500	6650	6470			6560	1520[5]	Appendix A
C-X-10	173,500	176,000	174,800	221,000	216,000	176,500[2]	172,000[2]	196,400	6140	6230	6185	7820	7640	6240[2]	6080[2]	8500	1765[5]	Appendix A
C-X-11																	1290[5]	Appendix A
C-X-12	162,000	160,500	161,300	209,000	207,500	173,500[2]	185,500[2]	193,900	5730	5680	5705	7390	7160	6140[2]	6540[2]	6810	985[5]	
C-X-13	156,500		156,500	178,000		153,000[2]	170,000[2]	167,000	5540	6300	5920	5411[2]	6013[2]	8070[4]	8720[4]	7050	1510[5]	
C-X-13/D									8170[3]	8277[3]	8224	8843[3]	8913[3]	6600[4]	5040[4]	7350		
A-Y-10									8135[3]	8630[3]	8375	10530[3]	10151[3]	9833[3]	9550[3]	10020	1210[5]	
A-Y-11									7445[3]	8135[3]	7880	9338[3]	9550[3]	9585[3]	10080[3]	9640	1210[5]	
C-Y-12	156,500	151,000	153,800	204,500	207,500	173,500[2]	187,000[2]	193,100	5540	5340	5440	7230	7340	6140[2]	6610[2]	6830	1960[5]	
C-Y-12/D									7109[3]	7074[3]	7092	8666[3]	8701[3]	8260[4]	7820[4]	8360		
C-Y-13	129,000	127,000	128,000	166,000	170,500			168,300	4560	4490	4525	5870	6030	9530[4]	10170[4]	7900	1960[5]	

Data without a superscript is from Flood Testing Laboratories, Inc.

1. Terra Tek Report TR 76-21, April 1976 - Appendix A
2. Holmes & Narver data
3. Concrete Technology Corp data
4. WES data on ME8-11 (R) grout and structures tested for 56 days or more
5. WES data on ME8-11 (R) grout tested at 28 days, except C-X-10 which was tested at 56 days

A-X-2, A-X-3, A-X-4, A-Y-10, A-Y-11: Concrete Technology Corp data. High and Low data only. The average includes 4 data points.

Table 2.2. Consolidated MIGHTY EPIC structures unconfined compression test data (Continued)

STRUCTURE	TOTAL LOAD								COMPRESSIVE STRENGTH								Grout Test PSI	Physical Properties Data Available
	7 day			28 day					7 day			28 day						
	lbs	lbs	Average lbs	lbs	lbs	lbs	lbs	Average lbs	PSI	PSI	Avg. PSI	PSI	PSI	PSI	PSI	Avg. PSI		
C-Y-13/S	156,000	153,000	154,500	207,500	215,000	185,500[2]	197,000[2]	201,400	5520	5410	5465	7340	7610	6560[2]	6970[2]	7145		
C-Y-13	184,500	179,000	181,800	235,000	230,500			232,800	6530	6330	6430	8310	8150			8230		
C-Y-14	151,000	156,000	153,500	200,500	202,000	162,000[2]	170,500[2]	183,800	5340	5520	5430	7090	7150	5730[2]	6030[2]	6500	1960[5]	
C-Y-14 D									7675[3]	7711[3]	7693	9232[3]	9479[3]	8670[4]	8370[4]	8940		
C-Y-15	141,500	143,500	142,500	181,500	186,000	150,000[2]	155,500[2]	168,300	4990	5080	5035	6420	6580	5310[2]	5500[2]	5955	2050[5]	Appendix A
C-Y-16	164,000	168,500	166,300	215,000	220,500	179,000[2]	167,000[2]	195,400	5800	5960	5880	7610	7800	6360[3]	5910[3]	6920	1630[5]	Appendix A
C-Y-17	197,000	200,000	198,500	250,000	242,000	209,000[2]	213,500[2]	228,700	6970	7080	7025	8840	8560	7390[3]	7530[3]	8080	1445[5]	
C-Y-17/D									7923[3]	7392[3]	7658	9125[3]	9161[3]	9550[4]	9370[4]	9300		
A-Y-18									6970[3]	7685[3]	7330	9125[3]	8745[3]	9630[3]	9365[3]	9215	1445[5]	Appendix A
S-Y-19																	1655[5]	Appendix A
S-Y-20																	1410[5]	Appendix A
S-Y-21																	1370[5]	
C-Y-22	148,000		148,000	208,000		120,000[2]	122,000[2]	150,000	5240		5240	7360		4240[2]	4240[2]	5280	1695[5]	Appendix A
C-Y-23	140,000	142,000	141,000	169,500[2]	176,500[2]	186,500	182,000	178,600	4950	5020	4985	6600	6440	6000[2]	6240[2]	6320	1505[5]	
C-Y-23/D									7438[3]	7463[3]	7480	9055[3]	8878[3]	10630[4]	10810[4]	9845		
C-Z-1	203,000	199,000	201,000	236,000	231,500			233,800	7180	7040	7110	8350	8190	8250[4]	9445[4]	8560	1790[5]	
C-Z-1/D									7781[5]	7428[3]	7605	9904[3]	9939[3]			9920		
S-Z-2																		
C-Z-3				202,500[2]	194,500[2]			198,500	5910	6510	6210	7570	7680	7162[2]	6879[2]	7320		
C-Z-3 D									6685[3]	6791[3]	6740	9373[3]	9196[3]	7300[4]	8955[4]	8700		
A-Z-4									7640[3]	8956[3]	8300	8950[3]	9265[3]	10955[3]	10850[3]	10005	1705[5]	
A-Z-5									8215[3]	8660[3]	8440	10495[3]	10850[3]	10080[3]	10705[3]	10530	1705[5]	
A-Z-6									8700[3]	9170[3]	8935	10390[3]	10245[3]	10390[3]	10285[3]	10325	1705[5]	

Data without a superscript is from Flood Testing Laboratories, Inc.

1. Terra Tek Report TR 76-21, April 1976 - Appendix A
2. Holmes & Narver data
3. Concrete Technology Corp data
4. WES data on ME8-11 (R) grout and structures tested for 56 days or more
5. WES data on ME8-11 (R) grout tested at 28 days, except C-Y-22 which was tested at 56 days.

A-Y-18, A-Z-4, A-Z-5, A-Z-6: Concrete Technology Corp Data. High and low data only. The average includes 4 data points.

Table 2.3. Flood Testing Laboratory report of unconfined compression test of CASES concrete cylinders

Structure	ID No[1]	Date of Report	Age at Breaking (days)	Wt/yd³ #	Cement Wt/yd³	Fine Aggregate	Fly Ash #	Pozzolith 122-N fl.oz.	Darex AEA fl.oz.	Slump inches	Air Content Net %	Temperatures Concrete (degrees F)	Temperatures Air (degrees F)	Weather	TEST DATA[2] Lab #	TEST DATA[2] Compressive Strength # Actual	TEST DATA[2] Compressive Strength psi	TEST DATA[2] Lab #	TEST DATA[2] Compressive Strength # Actual	TEST DATA[2] Compressive Strength psi
C-X-5	27	12/16/75	7	611	1175	1800[3]	75	18.3	6.0	3 1/2	5.3	65	38	Cloudy	7523384	173,000	6120	385	170,000	6010
C-X-5	35	1/6/76	28	611	1175	1800[3]	75	18.3	6.0	3 1/2	5.3	65	38	Cloudy	7523386	239,500	8470	387	233,000	8240
C-X-6	21	12/[illegible]/75	7	611	1175	1800[3]	75	18.3	6.0	3 3/4	5.0	64	34	Snow	7522939	175,500	6210	940	171,500	6070
C-X-6	30	12/22/75	7	705	1180	1600*	75	21.2	5.0*	4	6.1	73	34	Cloudy	7523653	163,000	5770	654	158,000	5590
C-X-6	32	12/29/75	28	611	1175	1800[3]	75	18.3	6.0	3 3/4	5.0	64	34	Snow	7522941	211,000	7460	942	205,500	7270
C-X-6	37	1/12/76	28	705	1180	1600*	75	21.2	5.0*	4	6.1	73	34	Cloudy	7523655	208,000	7360	656	203,500	7200
C-X-7	9	11/12/75	7	564	1225	1790[3]	75	16.9	5.0	4	5.0	66	69	Cloudy	7521493	166,500	5890	494	162,500	5750
C-X-7	20	12/3/75	28	564	1225	1790[3]	75	16.9	5.0	4	5.0	66	69	Cloudy	7521495	196,000	6930	496	199,500	7060
C-X-8	10	9/13/75	28	705	1180	1600*	75	21.2	5.0*	3 1/2	3.5	70	64	Sunny	7519858	214,000	7570	857	210,000	7430
C-X-8	10	9/13/75	28	705	1180	1600*	75	21.2	5.0*	3 1/2	3.5	70	64	Sunny	7519855	217,000	7680	856	215,000	7610
C-X-8	19	12/1/75	7	611	1175	1800[3]	75	18.3	6.0	3 3/4	5.0	65	58	Cldy&Rain	7522645	131,000	4630	646	132,000	4670
C-X-8	19	12/1/75	7	611	1175	1800[3]	75	18.3	6.0	3 3/4	5.1	67	60	Cldy&Rain	7522649	158,000	5590	650	161,500	5710
C-X-8	29	12/19/75	28	611	1175	1800[3]	75	18.3	6.0	3 3/4	5.0	65	58	Cldy&Rain	7522647	183,000	6470	648	199,000	7040
C-X-8	29	12/19/75	28	611	1175	1800[3]	75	18.3	6.0	3 3/4	5.1	67	60	Clyd&Rain	7522651	186,500	6600	652	204,500	7230
C-X-9	12	11/14/75	7	564	1225	1790[3]	75	16.9	5.0	3 1/2	5.0	66	69	Ptly Cldy	7521675	157,000	5550	676	154,000	5450
C-X-9	23	12/5/75	28	564	1225	1790[3]	75	16.9	5.0	3 1/2	5.0	66	69	Ptly Cldy	7521677	188,000	6650	678	183,000	6470
C-X-10	6	11/6/75	7	611	1175	1800[3]	75	18.3	6.0	3	4.5	65	54	Ptly Cldy	7521014	173,500	6140	015	176,000	6230
C-X-10	17	11/28/75	28	611	1175	1800[3]	75	18.3	6.0	3	4.9	65	54	Ptly Cldy	7521016	221,000	7820	017	216,000	7640
C-X-12	3	10/24/75	7	705	1180	1600*	75	21.2	5.0*	3 1/2	4.0	68	60's	Sunny	7520001	162,000	5730	003	160,500	5680
C-X-12	11	11/14/75	28	705	1180	1600*	75	21.2	5.0*	3 1/2	4.0	68	60's	Sunny	7520002	209,000	7390	004	202,500	7160
C-X-13	4	10/29/75	7							4 1/2			65	Fair	7520614	156,500	5540			
C-X-13	14	11/19/75	28							4 1/2			65	Fair	7520615	178,000	6300			

*Daravair not Darex.
[1]Flood Testing Laboratories, Inc., ID#.
[2]All samples were 6" dia x 12" height with 28.27 in² in compression area and all fractures were conical with specifications of 5500 lbs./sq inch in 28 days.
[3]No. 57 Crushed Stone.
[4]No. 8, Gravel, 31.0 gal water.

Table 2.3. Flood Testing Laboratory report of unconfined compression test of CASES concrete cylinders (Continued)

Structure	ID No[1]	Data of Report	Age at Breaking (days)	Wt/yd³ #	Cement Wt/yd³	Fine Aggregate	Fly Ash #	Pozzolith 122-N fl. oz.	Darex AEA fl. oz.	Slump inches	Air Content Net %	Temperatures Concrete (degrees F)	Temperatures Air (degrees F)	Weather	TEST DATA[2] Lab #	TEST DATA[2] Compressive # Actual	TEST DATA[2] Strength psi	TEST DATA[2] Lab #	TEST DATA[2] Compressive # Actual	TEST DATA[2] Strength psi
C-Y-12	7	11/7/75	7	(5)						3 1/2	6.7	64	52	Ptly Cldy	7521228	164,000	5800	229	168,500	5960
C-Y-12	27	12/16/75	7	611	1175	1800[3]	75	18.3	6.0	4	5.5	67	38	Cloudy	7523385	156,500	5540	389	151,000	5340
C-Y-12	35	1/6/75	28	611	1175	1800[3]	75	18.3	6.0	4	5.5	67	38	Cloudy	7523390	204,500	7230	391	207,500	7340
C-Y-13	1	10/22/75	7	611	1175	1800[3]	75	18.3	6.0						7519744	129,000	4560	745	127,000	4490
C-Y-13	8	11/11/75	28	611	1175	1800[3]	75	18.3	6.0						7519746	166,000	5870	747	170,500	6030
C-Y-15	31	12/24/75	7	705	1180	1600[4]	75	21.2	5.0*	4	5.5	74	28	Cloudy	7523810	156,000	5520	811	153,000	5410
C-Y-15	38	1/14/76	28	705	1180	1600[4]	75	21.2	5.0*	4	5.5	74	28	Cloudy	7523812	207,500	7340	813	215,000	7610
C-Y-13	25	12/1/75	7	611	1175	1800[3]	75	18.3	6.0	3 1/2	5.1	65	34	Cloudy	7523187	184,500	6530	188	179,000	6330
C-Y-13	34	1/5/76	28	611	1175	1800[3]	75	18.3	6.0	3 1/2	5.1	65	34	Cloudy	7523189	235,000	8310	190	230,500	8150
C-Y-14	16	11/24/75	7	611	1175	1800[3]	75	18.3	6.0	4	5.5	64	34	Sunny	7522306	151,000	5340	307	156,000	5520
C-Y-14	26	12/15/75	28	611	1175	1800[3]	75	18.3	6.0	4	5.5	64	34	Sunny	7522308	200,500	7090	309	202,000	7150
C-Y-15	13	11/18/75	7	611	1175	1800[3]	75	18.3	6.0	3 1/2	5.0	66	55	Ptly Cldy	7521899	141,500	4990	900	143,500	5080
C-Y-15	24	12/9/75	28	611	1175	1800[3]	75	18.3	6.0	3 1/2	5.0	66	55	Ptly Cldy	7521901	181,500	6420	902	186,000	6580
C-Y-16	7	11/7/75	7	(5)						3 1/2	6.7	64	52	Ptly Cldy	7521228	164,000	5800	229	168,500	5960
C-Y-16	18	11/28/75	27	705	1180	1600[4]	75	21.2	5.0*	3 1/2	6.7	64	52	Ptly Cldy	7521230	215,000	7610	231	220,500	7800
C-Y-17	22	12/4/75	7	705	1180	1600[4]	75	21.2	5.0*	3 1/2	6.7	65	31	Snow	7522943	197,000	6970	444	200,000	7080
C-Y-17	33	12/29/75	28	705	1180	1600[4]	75	21.2	5.0*	3 1/2	6.7	65	31	Snow	7522946	250,000	8840	946	242,000	8560
C-Y-22	2	10/24/75	7	705	1180	1600[4]	75	21.2	5.0*	2 1/2	4.0				7519854	148,000	5240			
C-Y-22	10	11/13/75								2 1/2	4.0				7519859	208,000	7360			
C-Y-23	5	11/3/75	7	(5)						3	6.5	67	75	Cloudy	7520634	140,000	4950	635	142,000	5020
C-Y-23	15	11/24/75	28	705	1180	1600[4]	75	21.2	5.0*	3	6.5	67	75	Cloudy	7520636	186,500	6600	637	182,000	6440
												Drift								
C-Z-1	28	12/18/75	7	705	1180	1600[4]	75	21.2	5.0*	4	6.3	65	35	Ptly Cldy	7523501	203,000	7180	502	199,000	7040
C-Z-1	36	1/8/76	28	705	1180	1600[4]	75	21.2	5.0*	4	6.3	65	35	Ptly Cldy	7523503	236,000	8350	504	231,500	8190
C-Z-3	2	10/24/75	7	705	1180	1600[4]	75	21.2	5.0*	3 1/2	3.5	70	64	Sunny	7519852	184,000	6510	853	167,000	5910

*Daravair not Darex.
[1]Flood Testing Laboratories, Inc., ID#.
[2]All samples were 6" dia x 12" height with 28.27 in² in compression area and all fractures were conical with specifications of 5500 lbs./sq inch in 28 days.
[3]No. 57 Crushed Stone.
[4]No. 8 Gravel, 31.0 gal water.
[5]) 7.5 Sack.

Table 2.4. Terra Tek compression and strain references and physical properties for specified structures, grout and cores for MIGHTY EPIC.

Structure or Grout or Core	TRIAXIAL COMPRESSION (Stress Difference Vs % Strain-Axial and Transverse)	UNCONFINED COMPRESSION (Stress Difference Vs % Strain-axial and Transverse)	UNIAXIAL STRAIN (Axial Stress Vs Volume Change %)	UNIAXIAL STRAIN (Mean Stress Vs % Vol Change)	UNIAXIAL STRAIN (Stress Diff Vs Confining Pressure)	UNIAXIAL STRAIN (Axial Stress Vs Axial Strain)	PHYSICAL PROPERTIES										
							Age Days or Feet	DENSITY(gm/cc) As-Rec	Dry	Grain	Water by Wet Weight %	Porosity %	Saturation %	Calc Air Voids %	Meas Perm Comp %	Ultrasonic Vel(ft/sec) Long	Shear
C-X-9					16b	16a	150	2.19	1.83	3.07	16.5	40	90	4.2		9,570	5179
C-X-10				2/5/76	14b	14a	56	2.12	1.75	3.03	17.5	42	87	5.4	5.4	10,500	5540
S-X-11				2/5/76	14b	14a	58	2.09	1.73	2.94	17.5	41	88	5.1	4.7	11,260	5600
C-X-12				2/5/76	14b, 16b	14a, 16a	64	2.14	1.77	3.05	17.6	42	90	4.3	4.9	10,490	5300
C-Y-16					16b	16a	120	2.12	1.75	3.03	17.3	42	87	5.6		10,287	5520
C-Y-17				2/5/76	14b	14a	22	2.11	1.73	2.96	17.8	42	90	4.1	3.9	9,700	4970
A-Y-18				2/5/76	14b	14a	22	2.11	1.73	2.96	17.8	42	90	4.1	3.9	9,700	4970
S-Y-19				2/5/76	14b	14a	49	2.12	1.73	3.00	18.1	42	91	3.9	4.0	11,150	5360
S-Y-20					16b	16a	156	2.17	1.79	3.03	17.5	41	93	2.9		10,564	5721
S-Y-21					16b	16a	164	2.09	1.73	3.00	17.5	43	86	6.0		10,614	5425
C-Y-22				2/5/76	14b	14a	71	2.12	1.75	3.01	17.7	42	90	4.3	4.0	10,240	5300
A Drift			A13a		A13b		31'	1.92	1.61	2.39	16.2	33	94	1.9	0.9	11,206	6162
UG6A	A6	A5	12a	A1	2,3,4A,12,A-15		216'	2.03	1.82	2.34	10.2	22	95	1.1	0.6	12,342	7306
B Drift			A13a		A13b		25'	1.91	1.50	2.45	18.5	36	97	0.9	0.8	9,567	4512
ISS5	A7,A8,A9			A2	3,4,A16		9'	1.91	1.55	2.48	18.5	37	94	2.1		8,960	4070
ISS7	A10			A3	3,4,A17												
C Drift			A13a		A13b		30'	1.84	1.44	2.46	22.0	41	98	0.9	0.6	10,801	5382
UG4		A4	A11a		2,3,4,A11b, A14		282'	1.96	1.64	2.45	16.3	33	97	0.9	1.3	9,370	4104
ME8-11			B15a		12,15b,B14, 15a, B15b												

Cols. Compressions and Strains refer to Figures (i.e. A6) in Terra Tek TR 76-21, April 1976, subject "Characterization of Tuff and Development of Grouts for MIGHTY EPIC Structures Program," (Appendix A) Except 2/5/76 refers to an enclosure to a letter (February 5, 1976) from Scott W. Butters of Terra Tek, Inc. to Mr. J.W. LaComb, DNA, Mercury, NV

Physical properties are from Terra Tek TR 76-21, April 1976 (Appendix A)

SECTION 3

INTERFACE EXPERIMENTS

Geological media interface experiments were conducted to evaluate uncertainties in protecting deep underground facilities against nuclear weapon produced ground shock. The major uncertainty is the extent of relative motion between the two media layers. To better define this uncertainty, both active and passive experiments were emplaced across the interface to measure ground motions and stress levels. These measurements were made at three ranges from the working point.

Figure 3.1 shows the details of the active interface holes which were used in determining the relative displacement and stress wave modifications across the tuff/quartzite interface region.

3.1 WATERWAYS EXPERIMENT STATION (WES) ACTIVE INTERFACE EXPERIMENTS

Active measurements of the relative displacements between the tuff and quartzite media were made by WES at five points in each of three vertical drill holes as illustrated in Figure 3.1.

3.2 SYSTEMS, SCIENCE AND SOFTWARE (SSS) PASSIVE INTERFACE EXPERIMENTS

SSS fielded a passive measurement scheme in which magnetic sources were placed in three vertical drill holes at differing ranges along a radial from the working point as shown in Figure 3.2. The magnets were placed at intervals in each hole, both above and below the interface. Preshot, each drill hole was accurately surveyed. Residual displacements will be determined postshot by drilling adjacent parallel holes and conducting a magnetometer survey.

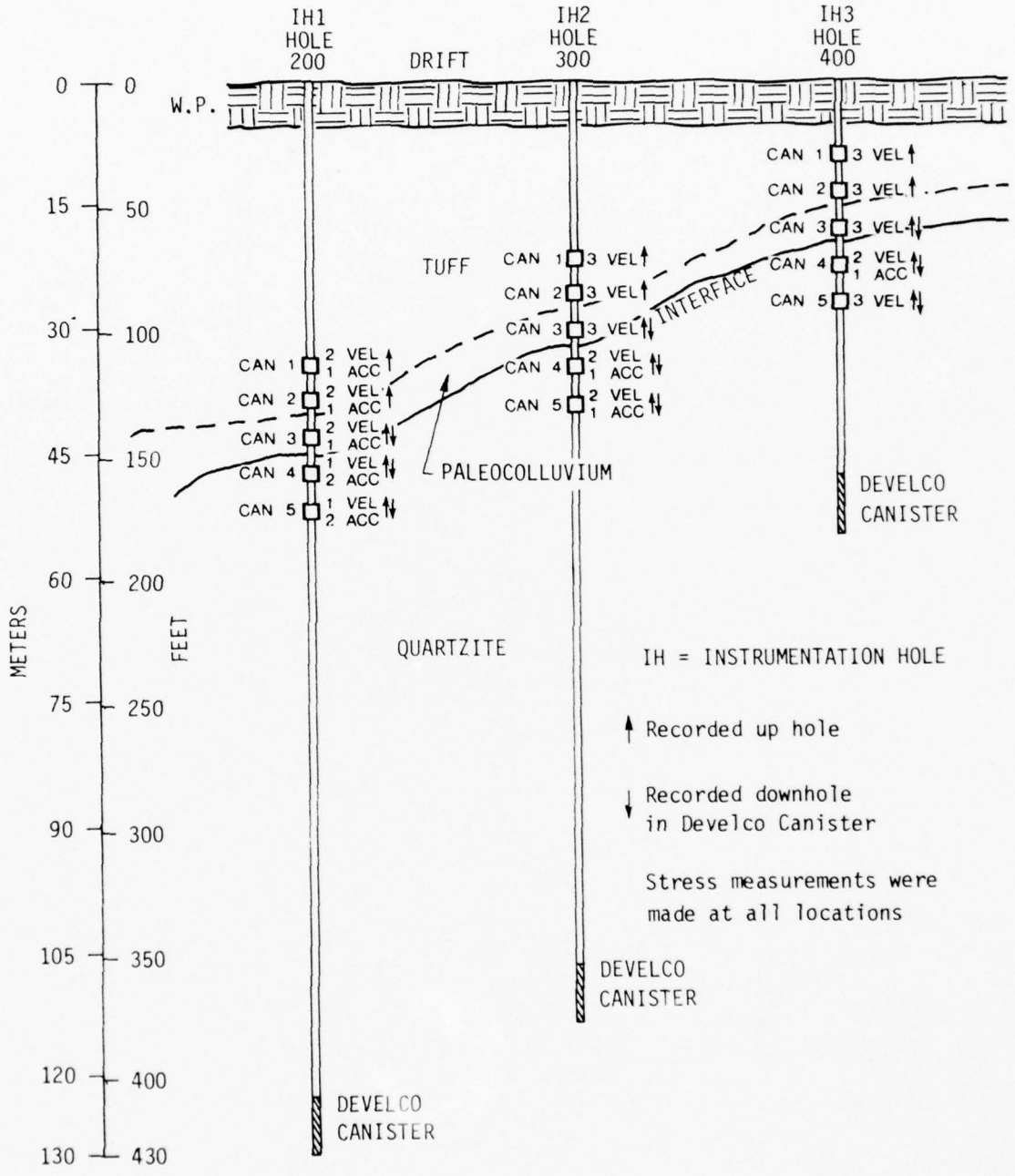

Figure 3.1 Instrumentation for active interface experiment

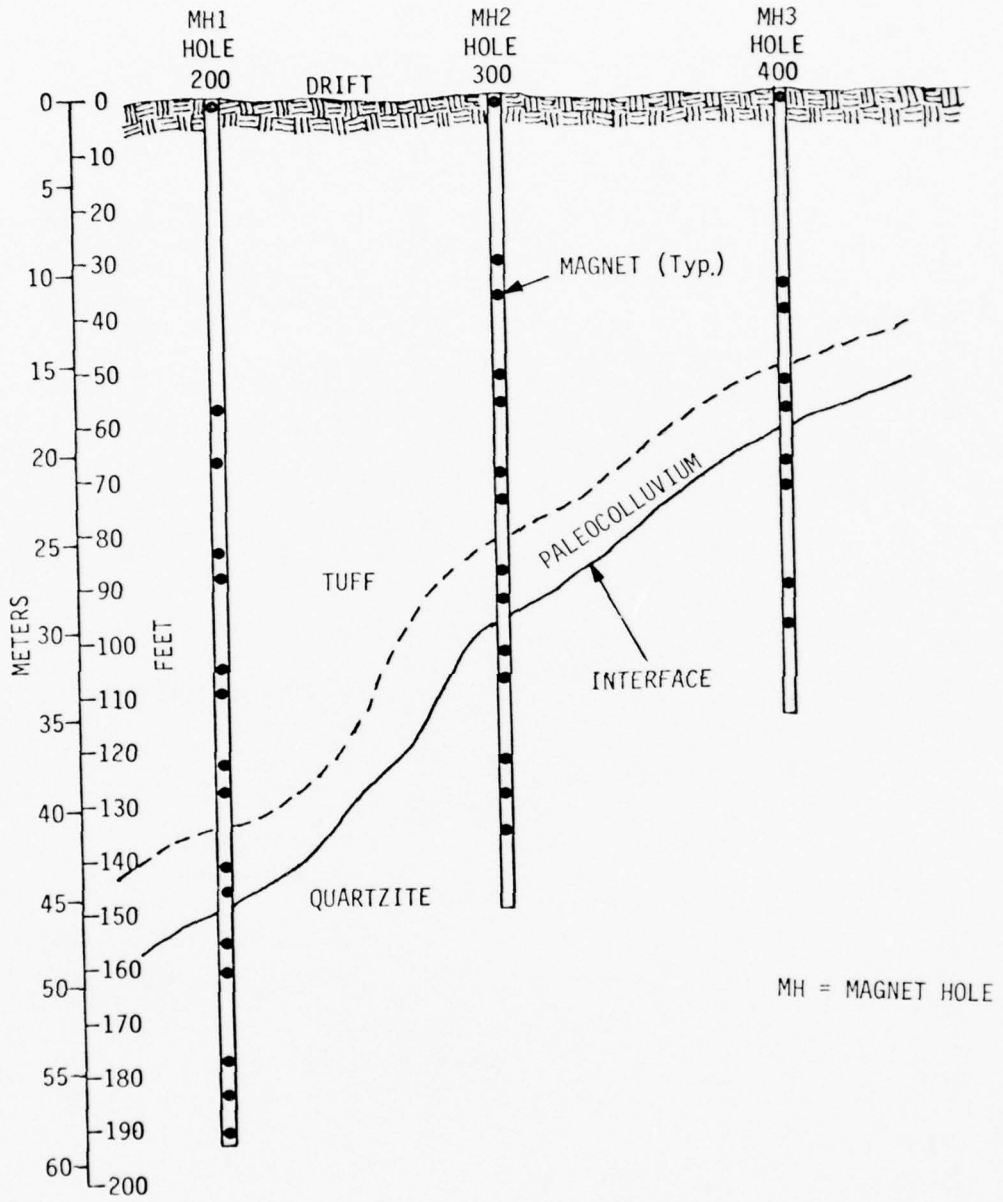

Figure 3.2 Passive interface experiment

SECTION 4

CORES AND GROUT

Figure 1.1 shows the location of the drill holes from which the cores were taken. Figure 4.1 shows the MIGHTY EPIC grout plan.

The physical properties, stress-strain response of the hydrostatic compression, triaxial compression and uniaxial strain tests on the various core samples and grout mixtures were performed jointly by Terra Tek, Inc. and the Waterways Experiment Station. The results of these tests are contained in Appendix A.

The Fenix and Scisson grouting report is given in Appendix C. The results of the mechanical tests and the physical properties of the core samples and grouts are given in Appendixes A and B.

The physical properties, triaxial and unconfined compression, and uniaxial strains are given in Table 2.4 and Appendix A.

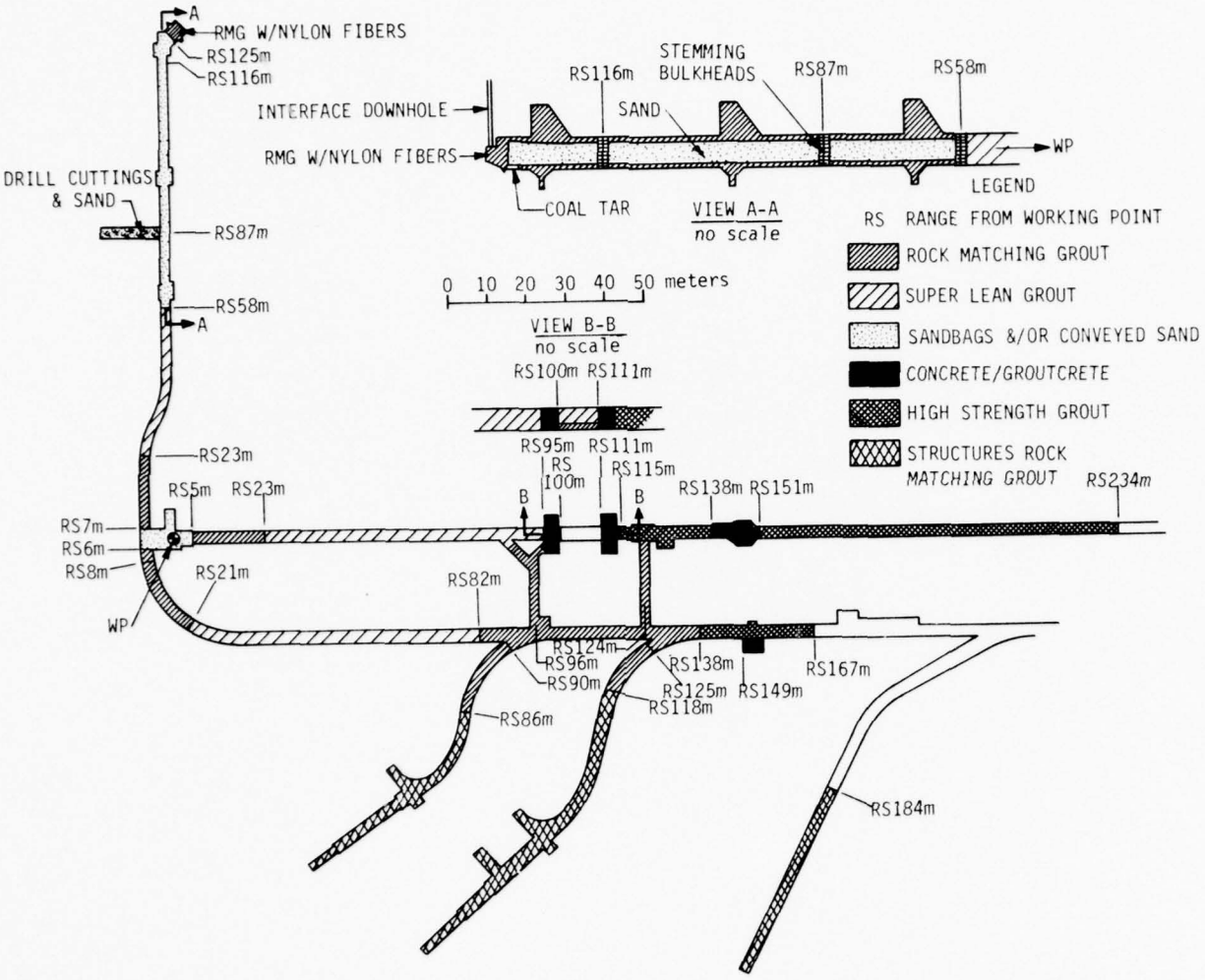

Figure 4.1 MIGHTY EPIC grout stemming plan.

APPENDIX A

TERRA TEK TR-76-63 MATERIAL PROPERTIES OF NEVADA TEST SITE TUFF AND GROUT WITH EMPHASIS ON THE MIGHTY EPIC EVENT

PREFACE

The authors would like to express their thanks for the guidance of Mr. J. W. LaComb and to Mr. C. N. Snow for his assistance with geology and core samples.

TABLE OF CONTENTS

INTRODUCTION

The Defense Nuclear Agency (DNA) nuclear test program at the Nevada Test Site requires, among many things, the mechanical and physical properties of the construction material and rock at the test location. The material properties are needed primarily for the purpose of evaluating the potential for successful stemming and containment of the nuclear tests. They are also used in modeling material behavior in subsequent ground motion calculations for predicting and evaluating experimental programs.

This report summarizes material evaluations conducted by Terra Tek over a period of 16 months (April 1975 through July 1976) for DNA Test Command. The primary task during this period was material evaluations for the Mighty Epic event (both preshot and postshot). Tuff, grout, sand, concrete, concrete-steel interfaces and steel were tested. Other material evaluations and analyses during this period were for 1) the "two-in-one concept" -- a proposed plan to use a common tunnel and equipment for two nuclear events, 2) determining the influence of fracturing on ultrasonic velocities to help explain field seismic and sonic velocity results, 3) obtaining the angles-of-internal-friction in the tuff as a function of confining pressure for use in material modeling, 4) determining and evaluating methods for extracting pore water for subsequent chemical analysis, 5) measuring the effect of hydrostatic pressure (i.e. grain size distributions, cohesion, etc.) on sand-water mixtures, 6) evaluating currently used and proposed methods for obtaining the elastic moduli needed to determine *in situ* stress from tuff overcore samples, and 7) evaluating the possibility of resaturating dry tuff core samples for obtaining material properties representative of the original saturated material and for evaluating the likelihood of water invasion into core samples during the field coring

process. During the contract period, reports were distributed on each of these tasks. All those reports are reproduced here as originally distributed. As an introduction a synopsis (in some cases, the abstract from the report) of the testing and analysis for each task is provided here.

Mighty Epic Event: The Mighty Epic event included, in addition to the standard "Line-of-Site-Pipe", a number of structures and an experiment to evaluate movement along a material discontinuity (this discontinuity has been referred in the past as the "interface"). The discontinuity was a change from tuff material to a much harder and competent palezoic material. The structures experiment required extensive tuff characterization, both for design of the experiments and to facilitate development of a grout which closely matched selected tuff properties. Other structures materials evaluated were concrete, concrete/steel and steel. For the interface experiment, direct shear tests were conducted to define the frictional properties. Magnetic characterization of core samples were also needed to assist in analyzing post-shot movement at the interface.

Reports describing the above work are:

Material Properties for Mighty Epic Interface Experiment, June 1975, TR 75-36

Some Comments on Mighty Epic Material Properties, August 1975, TR 75-42

Physical and Mechanical Properties of Several Grout Mixtures, August 1975, TR 75-45

Material Properties on Samples from Mighty Epic Drill Holes U12n.10 UG#4, U12n.10 UG#6a and U12n.10 UG#7, September 1975, TR 75-50

Some Material Properties on Core Samples from Several Drill Holes Relating to the Mighty Epic Event, November 1975, TR 75-64

Some Mechanical Properties of Concrete, Steel and Concrete-Steel Interfaces Used in Mighty Epic Structures, July 1976, TR 76-14

Characterization of Tuff and Development of Grouts for Mighty Epic Structures Program, April 1976, TR 76-21

Letters or data forwarded which were not contained in the above reports

The report entitled "Characterization of Tuff and Development of Grouts for Mighty Epic Structures Program" is a summary of much of the Mighty Epic testing and contains the average material properties of the structures region along with the properties of the tuff matching grout -- ME8-11.

Investigation of the Effect of Fracturing on the Ultrasonic Velocities in Ash-Fall Tuff: The effect of fracturing on ultrasonic velocities in rock have been investigated. The material was an ash-fall tuff taken from the Nevada Test Site, Area 12. Fractures were generated in uniaxial load (compression) tests and direct shear tests. The results, in general, show the same trend as reported in other rock types: i.e., a decrease in both the p-wave (longitudinal) and s-wave (shear) velocities resulting from fracture initiation, extention and growth. The maximum observed change for the p-wave was ~25 percent, and ~10 percent for the s-wave.

Comparison of Preshot and Postshot Material Properties at the Nevada Test Site for the "Two-In-One Concept": This concept is one of locating a nuclear event in the same main drift but several hundred feet in the portal direction from a previous event. The concept results in substantial cost savings through reuse of a considerable amount of equipment (gas seal doors, cable access drifts, etc.)

Early evaluation of the concept required a close look at the tuff properties as a function of preshot versus postshot status and as a function of distance from the working points (i.e. the properties of the preshot tuff, at say 300 feet, were compared with the properties of postshot tuff at 300

feet). This comparison was necessary to evaluate potential "second event" locations and insure that the material surrounding this "second event" were effective for stemming and containment.

Determination of the Angle-Of-Internal-Friction for NTS Tuffs: Discussions with Joe LaComb, DNA Field Command, and inquiries from those doing calculations for design for tunnel structures in the tuffs have led to consideration of "Angle-of-Internal-Friction Models". Intuitive reasoning as well as data available indicate the ambiguity related to any estimate of angle-of-internal-friction for the intact tuffs. This brief write-up is an attempt to clarify the angle-of-internal-friction model for the tuffs and to help suggest what tests might be most suited to provide an adequate model.

Water Extraction from Nevada Test Site Tuffs: The hydrology of the Rainier Mesa, specifically "T" tunnel area at the Nevada Test Site, is of interest to the nuclear test program. Terra Tek has been actively developing methods for extracting water from core samples for subsequent chemical and mineralogical analysis. The development of consistent water data is dependent upon both the method of water extraction and sanitary laboratory conditions. The extraction method is critical since the bounded waters within the tuff may be extracted at different energy levels.

Hydrostatic Response of a Water Saturated Sand: Mixtures of sand and water have a number of Nevada Test Site applications, the majority of which directly relate to the stemming and containment of nuclear tests. Specific applications required knowing the effect on the sand-water mixture of a hydrostatic pressure cycle.

Mixtures were subjected to a 4 kilobar hydrostatic pressure cycle followed by measurements of the sand grain size distribution and observations regarding the cohesion of the mixture (i.e. existence of "welding").

State of Stress Effects on Laboratory Determination of the Elastic Modulus of Stress-Relief Overcores: The U.S. Geological Survey has conducted *in situ* stress determinations under Rainier Mesa using the U.S. Bureau of Mines three-component borehole deformation overcore technique. The calculated *in situ* stress states are used to better quantify and understand containment phenomena. Since laboratory determined overcore elastic moduli are used for *in situ* stress calculations, a study of state of stress effects on the overcore elastic modulus was conducted. Normal tuff overcore laboratory testing has involved biaxial loading (radial pressurization with $\sigma_z = 0$) in which radial pressures of only 3.45 MPa (34.5 bars) were obtainable due to sample failure. Since Rainier Mesa *in situ* stresses have been calculated as being as high as 6.9 MPa (69 bars), testing techniques were evaluated which incorporated axial stresses to achieve 6.9 MPa radial pressure. Modulus errors caused by sample nonlinearity and a suggested laboratory technique are also discussed.

Specific Moisture Retention of Nevada Test Site Tuffs: Moisture was reintroduced into dry Nevada Test Site tuff core chips through placement in a high humidity (~95 to 100 percent) chamber at room temperature (~23°C) and atmospheric pressure (~650 mm). A minimum of 29 days was required for the dry samples to equal or exceed what was considered their *in situ* saturation levels (these *in situ* saturation levels were obtained from adjacent samples). Mechanical tests conducted subsequent to resaturation suggest that dried-resaturated samples can be used to obtain representative material properties for virgin saturated tuff.

Tuff samples, immediately sealed at the Nevada Test Site on removal from a core barrel, were subjected to the same environment to assist in analyzing the invasion of the drilling water. Test results to date are inconclusive.

Each report has been reproduced as originally distributed. Page numbers have been changed for continuity in this final report.

MIGHTY EPIC EVENT

Material Properties for Mighty Epic Interface Experiment

Some Comments on Mighty Epic Material Properties

Physical and Mechanical Properties of Several Grout Mixtures

Material Properties on Samples from Mighty Epic Drill Holes U12n.10 UG#4, U12n.10 UG#6a and U12n.10 UG#7

Some Material Properties on Core Samples from Several Drill Holes Relating to the Mighty Epic Event

Some Mechanical Properties of Concrete, Steel and Concrete-Steel Interfaces Used in Mighty Epic Structures

Characterization of Tuff and Development of Grouts for Mighty Epic Structures Program

Properties of U12n.10 MH#2 and MH#3 Core Samples

Miscellaneous Mighty Epic Properties

Progress Report One

MATERIAL PROPERTIES FOR MIGHTY EPIC INTERFACE EXPERIMENT

by

S. W. Butters
S. J. Green

Submitted to

Field Command
Defense Nuclear Agency
Nevada Test Site
Mercury, Nevada

Attn: Mr. J. W. LaComb

TR 75-36
June 1975

SUMMARY

Some physical and mechanical properties have been determined for material in the horizontal plane (along the LOS tunnel) and above and below the working point for the Mighty Epic Event in Area 12 at the Nevada Test Site. These tests were primarily used for site stemming and containment evaluation, and most of these data were included in a previous Terra Tek Report, TR 75-7 (January 1975).

At the meeting at the Nevada Test Site 16 June 1975, further material property tests were outlined to define better the "interface", and to determine the shear strength and the elastic constants (mainly velocities) for the material below the working point, down through the "interface" and on below. Once these data have been obtained, a better friction model for the interface and possible "layer configurations" to be used for calculations can be determined.

TABLE OF CONTENTS

LIST OF FIGURES

LIST OF TABLES

MATERIAL PROPERTY DATA AVAILABLE

Location of Drill Holes: A first set of data were generated primarily for exploratory stemming and containment site evaluation, while a second set of data were a preliminary evaluation of the material below the working point. The drill holes from which samples were obtained for the two sets of data were: (1) U12n.05 UG#4, U12n.10 UG#1 and UE12n #8, and (2) U12n.10 UG#2, U12n.10 UG#3 and UE12n #9, respectively. The approximate locations of these drill holes are indicated on the map of the Mighty Epic region in the "N" Tunnel complex of Area 12, as shown in Figure 1.[1]

The drill holes U12n.05 UG#4 and U12n.10 UG#1 are horizontal drill holes in the plane of the working point, and UE12n #8 and UE12n #9 are vertical drill holes form the mesa surface. The U12n.10 UG#2 and UG#3 drill holes were collared back from the working point in the main drift and extended downward to make contact with the beds below the working point. A drill hole designated U12n.10 UG#5 was drilled downward, from the bypass drift at a lesser angle than the UG#2 and UG#3 to give an indication of the layering below and past the working point. No physical or mechanical properties data have been generated to date from this drill hole.

Tests on Cores: The U12n.05 UG#4, U12n.10 UG#1 and UE12n #8 core samples were tested in September 1974, January 1975, and December 1973 respectively.[2] The UE12n #9, U12n.10 UG#2 and U12n.10 UG#3 core samples were all tested in May 1975.

Tests for this first set of data for the U12n.05 UG#4, U12n.10 UG#1 and UE12n #8 core samples include hydrostatic compression tests, uniaxial strain tests, ultrasonic velocity measurement and physical property measurements as shown in Figure 2 and Table 1. Tests for the second set of data

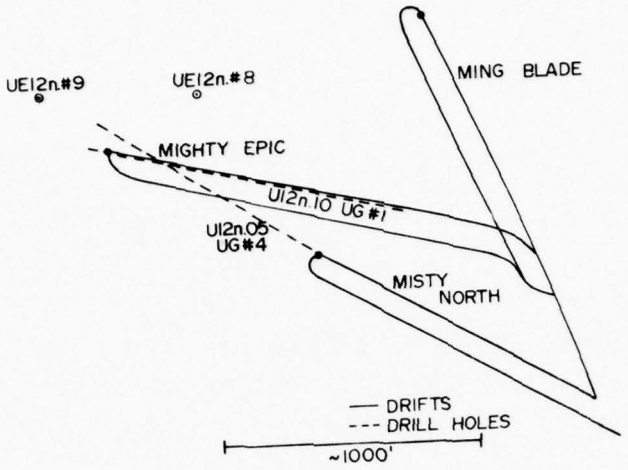

Figure 1a. Plan View of Mighty Epic Region, Area 12, "N" Tunnel Complex

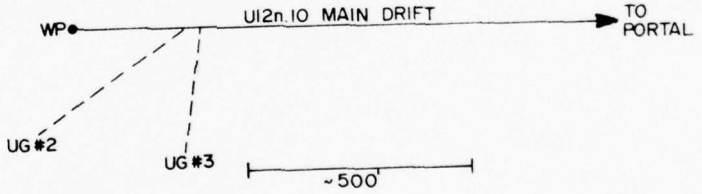

Figure 1b. Section View along the Mighty Epic Main Drift

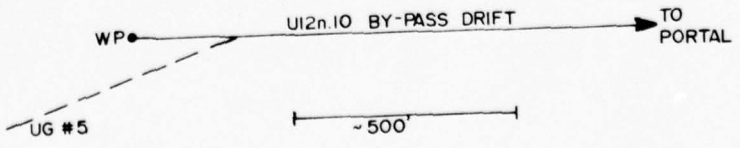

Figure 1c. Section View along Mighty Epic Bypass Drift

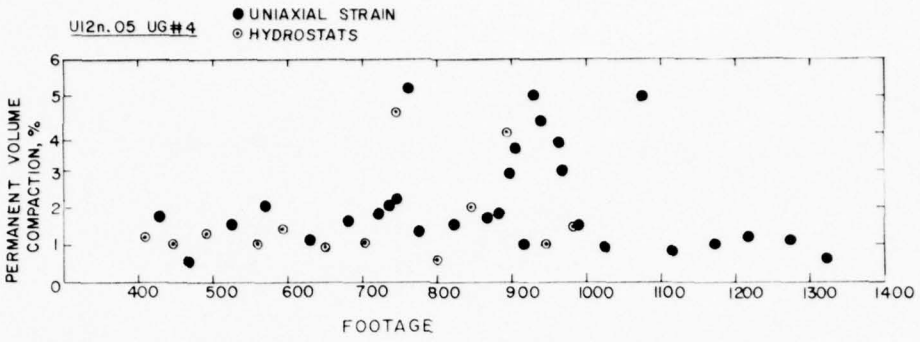

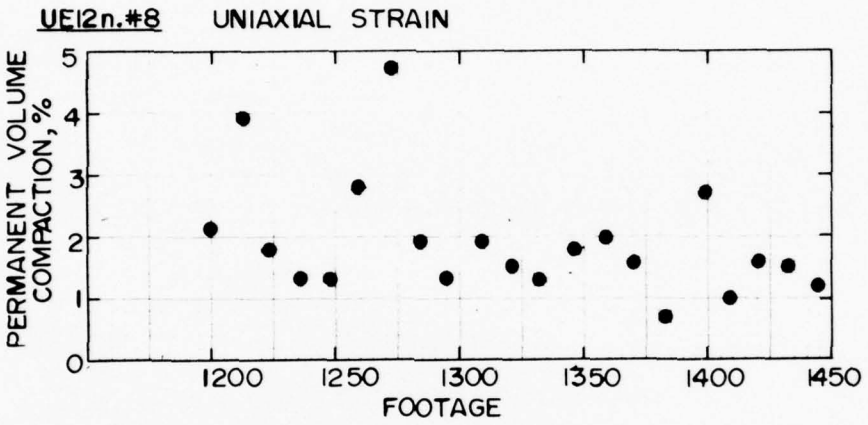

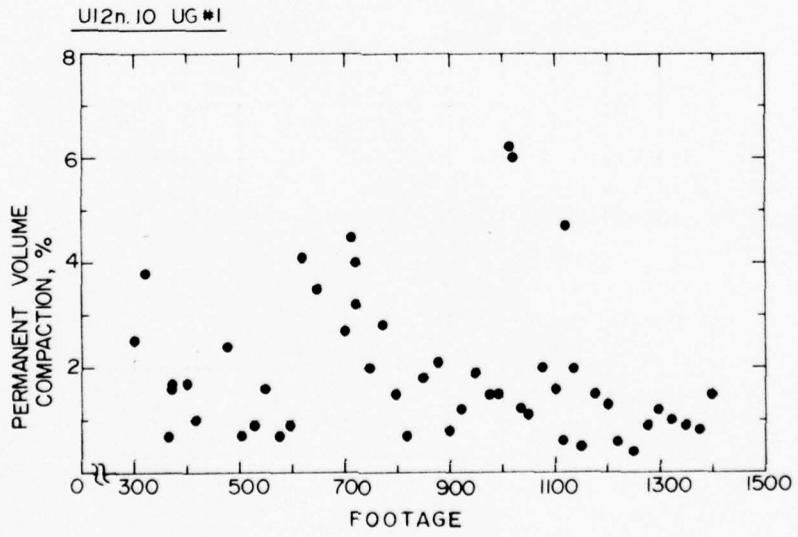

Figure 2. Tests for Stemming and Containment Evaluation

TABLE 1. TABULATED TEST DATA FOR STEMMING AND CONTAINMENT EVALUATION

DRILL HOLE FOOTAGE	DENSITY (gm/cc)			WATER BY WET WEIGHT (%)	POROSITY (%)	SATURATION (%)	CALC AIR VOIDS (%)	MEAS PERMANENT COMP (%)	VELOCITY (ft/sec)	
	AS-RECEIVED	DRY	GRAIN						LONG	SHEAR
UE12n #8										
1200	1.98	1.61	2.43	19	34	100	0.0	2.1	7,350	3,090
1212	1.89	1.59	2.43	16	34	86	4.8	3.4	11,260	5,260
1224	1.95	1.68	2.43	14	31	87	3.9	1.8	9,320	4,130
1236	1.96	1.62	2.35	17	31	100	0.0	1.1	10,340	4,390
1247	1.95	1.56	2.33	20	33	100	0.0	1.1	6,660	2,710
1259	1.84	1.48	2.39	19	38	94	2.2	2.8	10,290	5,210
1272	1.79	1.40	2.42	22	42	93	2.9	4.5	8,410	3,710
1294	1.87	1.52	2.36	18	35	98	0.9	1.9	10,630	5,810
1295	1.80	1.44	2.39	20	40	90	4.0	1.3	9,560	3,970
1309	1.88	1.50	2.42	20	38	100	0.0	1.9	9,090	3,900
1321	1.95	1.58	2.43	19	35	100	0.0	1.6	8,830	4,000
1333	2.04	1.71	2.45	16	30	100	0.0	0.8	8,130	3,410
1345	1.91	1.50	2.48	21	39	100	0.0	2.0	9,140	4,070
1358	1.97	1.47	2.40	21	39	100	0.0	2.0	10,270	4,720
1371	1.90	1.48	2.42	22	39	100	0.0	1.6	8,760	3,710
1383	1.84	1.46	2.43	21	40	95	1.6	0.7	11,168	5,270
1397	1.85	1.48	2.41	20	39	96	1.7	2.7	9,840	5,350
1409	1.92	1.58	2.40	18	34	99	0.2	2.0	9,450	4,660
1421	1.86	1.49	2.40	20	38	98	0.7	1.6	8,890	4,410
1433	1.93	1.60	2.42	17	34	98	0.6	1.5	9,220	3,800
1445	1.93	1.59	2.45	18	35	98	0.8	1.2	8,630	3,350

DRILL HOLE FOOTAGE	DENSITY (gm/cc)			WATER BY WET WEIGHT (%)	POROSITY (%)	SATURATION (%)	CALC AIR VOIDS (%)	MEAS PERMANENT COMP (%)	VELOCITY (ft/sec)	
	AS-RECEIVED	DRY	GRAIN						LONG	SHEAR
U12n.05 UG#4 Uniaxial Strain										
430	1.78	1.35	2.41	24	44	99	0.7	1.7	8600	4130
471	2.02	1.75	2.44	14	28	97	1.0	0.5	12200	5873
526	1.83	1.42	2.44	23	42	99	0.4	1.5	9360	4660
572	1.93	1.62	2.44	16	34	94	2.2	2.0	9350	4400
634	1.88	1.50	2.47	20	39	97	1.2	1.1	8630	3900
683	1.87	1.51	2.41	19	37	95	1.7	1.6	9420	4560
724	1.97	1.63	2.56	17	36	92	2.8	1.8	9420	3940
738	1.84	1.47	2.46	20	40	93	3.0	2.0	8460	4330
748	1.88	1.54	2.42	18	36	94	2.3	2.1	8200	3350
761	1.84	1.51	2.43	18	38	89	4.2	5.2	8660	4460
777	1.82	1.42	2.46	22	42	94	2.5	1.3	8630	4040
824	1.84	1.47	2.41	20	39	94	2.3	1.5	9840	5080
872	1.89	1.55	2.43	18	37	93	2.2	1.7	9300	4000
883	1.87	1.53	2.44	18	37	92	3.1	1.8	9640	4860
895	1.90	1.58	2.44	17	35	91	3.2	2.9	10170	4690
907	1.75	1.37	2.40	22	43	90	4.5	3.6	7510	2983
918	1.95	1.63	2.43	16	33	96	1.3	1.0	10830	6205
931	1.76	1.36	2.43	22	44	93	4.5	5.0	8590	4000
940	1.79	1.42	2.40	21	41	91	3.5	4.3	9940	5120
963	1.76	1.31	2.48	25	47	94	2.7	3.7	7410	3220
964	1.82	1.42	2.43	22	43	94	2.4	3.7	9550	4790
968	1.92	1.60	2.43	16	33	90	2.9	3.0	10370	5510
996	1.82	1.41	2.46	22	43	95	2.2	1.5	8960	4460
1023	2.01	1.71	2.45	14.9	30	99	0.2	0.9	9301	4458
1075	1.76	1.41	2.38	20.0	41	86	5.6	5.0	7850	3926
1119	1.95	1.63	2.43	16.4	33	97	1.0	0.8	10531	5768
1175	1.96	1.64	2.44	16.2	33	97	0.9	1.0	10499	6307
1219	1.91	1.56	2.43	18.0	36	96	1.1	1.2	9152	4864
1273	1.93	1.58	2.50	18.4	37	96	1.4	1.1	8847	4425
1322	1.96	1.67	2.43	15.0	32	94	2.0	0.6	10991	6103

DRILL HOLE FOOTAGE	DENSITY (gm/cc)			WATER BY WET WEIGHT (%)	POROSITY (%)	SATURATION (%)	CALC AIR VOIDS (%)	MEAS PERMANENT COMP (%)	VELOCITY (ft/sec)	
	AS-RECEIVED	DRY	GRAIN						LONG	SHEAR
U12n.10 UG #1										
301	1.88	1.68	2.42	19.9	38	99	0.5	2.5	10,010	3,440
324	1.83	1.45	2.42	20.8	40	95	1.9	3.8	5,540	2,660
367	2.00	1.69	2.47	15.7	32	99	0.2	0.7	10,240	5,120
374	1.90	1.52	2.45	14.6	38	99	0.3	0.7	8,690	2,920
375	1.91	1.53	2.46	19.3	37	99	0.5	1.6	8,270	3,220
406	1.89	1.49	2.49	21.0	40	99	0.3	1.7	7,540	2,160
419	1.96	1.66	2.47	15.3	33	92	2.7	1.0	8,100	2,890
478	1.94	1.61	2.46	17.1	34	97	1.2	2.4	9,740	5,080
507	1.95	1.61	2.45	17.3	34	98	0.6	0.7	10,600	5,740
527	1.93	1.58	2.47	18.1	36	96	1.3	0.9	11,740	6,820
551	1.88	1.54	2.46	18.1	38	93	3.5	1.6	8,100	4,040
578	1.99	1.64	2.53	17.5	35	99	0.4	0.3	10,890	5,510
598	1.97	1.64	2.50	16.5	35	94	2.2	0.9	8,560	3,970
619	1.78	1.35	2.49	24.2	46	94	2.9	4.1	9,280	4,200
651	1.90	1.56	2.48	17.9	37	91	3.5	1.6	8,760	3,870
676			2.49	17.8					---	---
703	1.82	1.39	2.45	23.3	43	98	1.0	2.7	10,300	4,660
715	1.77	1.40	2.40	21.2	42	90	4.2	4.5	9,385	4,509
722	1.86	1.51	2.42	18.5	38	97	1.4	3.2	8,570	3,810
725	1.81	1.43	2.48	20.9	42	90	4.4	4.0	9,280	4,690
748	1.85	1.42	2.52	23.3	44	99	0.6	2.0	8,530	3,870
775	1.87	1.44	2.56	23.0	44	98	0.9	2.8	10,420	6,170
799	2.02	1.68	2.55	16.8	34	99	0.3	1.5	9,640	4,920
824	2.08	1.78	2.57	14.6	31	99	0.3	0.7	11,880	6,720
849	1.91	1.53	2.49	19.8	38	99	0.8	1.8	8,990	3,900
875	1.84	1.39	2.57	24.7	46	99	0.5	2.1	9,840	3,840
901	1.92	1.52	2.56	21.0	41	99	0.4	0.8	9,450	4,400
926	1.95	1.58	2.52	19.4	37	99	0.3	1.2	8,630	3,900
950	1.88	1.55	2.48	17.4	36	97	3.3	1.9	10,170	5,180
975	1.88	1.49	2.51	21.2	41	98	0.9	1.5	8,690	3,610
993	1.93	1.58	2.46	18.3	36	99	0.4	1.5	8,804	4,319
995	1.80	1.46	2.41	19.1	40	87	5.3	---	9,510	4,530
1016	1.77	1.42	2.40	20.0	41	87	5.5	6.2	8,207	3,993
1024	1.82	1.47	2.45	19.3	40	88	4.9	6.0	8,270	3,870
1034	1.94	1.61	2.46	17.0	35	96	1.5	1.2	10,184	5,474
1050	1.87	1.48	2.49	20.9	40	97	1.4	1.1	8,230	3,800
1076	1.80	1.37	2.49	24.0	45	96	1.9	2.0	6,270	4,200
1103	1.96	1.57	2.57	19.9	39	99	0.2	1.6	9,550	4,720
1114	1.96	1.62	2.49	17.6	35	98	0.7	0.6	11,086	6,098
1126	1.76	1.38	2.43	21.6	43	88	5.4	4.7	11,350	4,260
1136	1.84	1.48	2.46	19.5	40	90	3.9	2.0	9,365	4,818
1149	1.97	1.65	2.45	16.9	33	96	1.3	0.5	11,150	6,330
1176	1.82	1.41	2.44	22.8	42	97	1.2	1.5	10,436	5,770
1201	1.90	1.53	2.46	19.5	38	97	1.0	1.3	11,290	6,360
1221	1.96	1.65	2.44	15.6	32	94	1.8	0.6	10,509	5,733
1225			2.49	24.1					---	---
1253	2.02	1.72	2.47	14.6	30	98	0.7	0.4	10,600	5,740
1276	1.85	1.44	2.49	22.2	42	98	0.8	0.9	9,310	5,150
1299	1.93	1.57	2.47	18.8	37	99	0.4	1.2	9,350	4,860

for the UE12n #9, U12n.10 UG#2 and U12n.10 UG#3 core samples include uniaxial strain tests, physical property measurements and ultrasonic velocity measurements. These data are shown in Figures 3 through 5 and Table 2.

Variation through Beds: Figures 3 through 5 have been plotted such that the variation in several of the material properties can be seen as a function of distance along the drill hole. The different lithological beds along the drill hole are estimated from inspection of the cores (3), and are shown as dashed lines on the figures. The descriptions of each "layer" were those used at the meeting on 16 June at NTS. The next section discusses the layers in more detail.

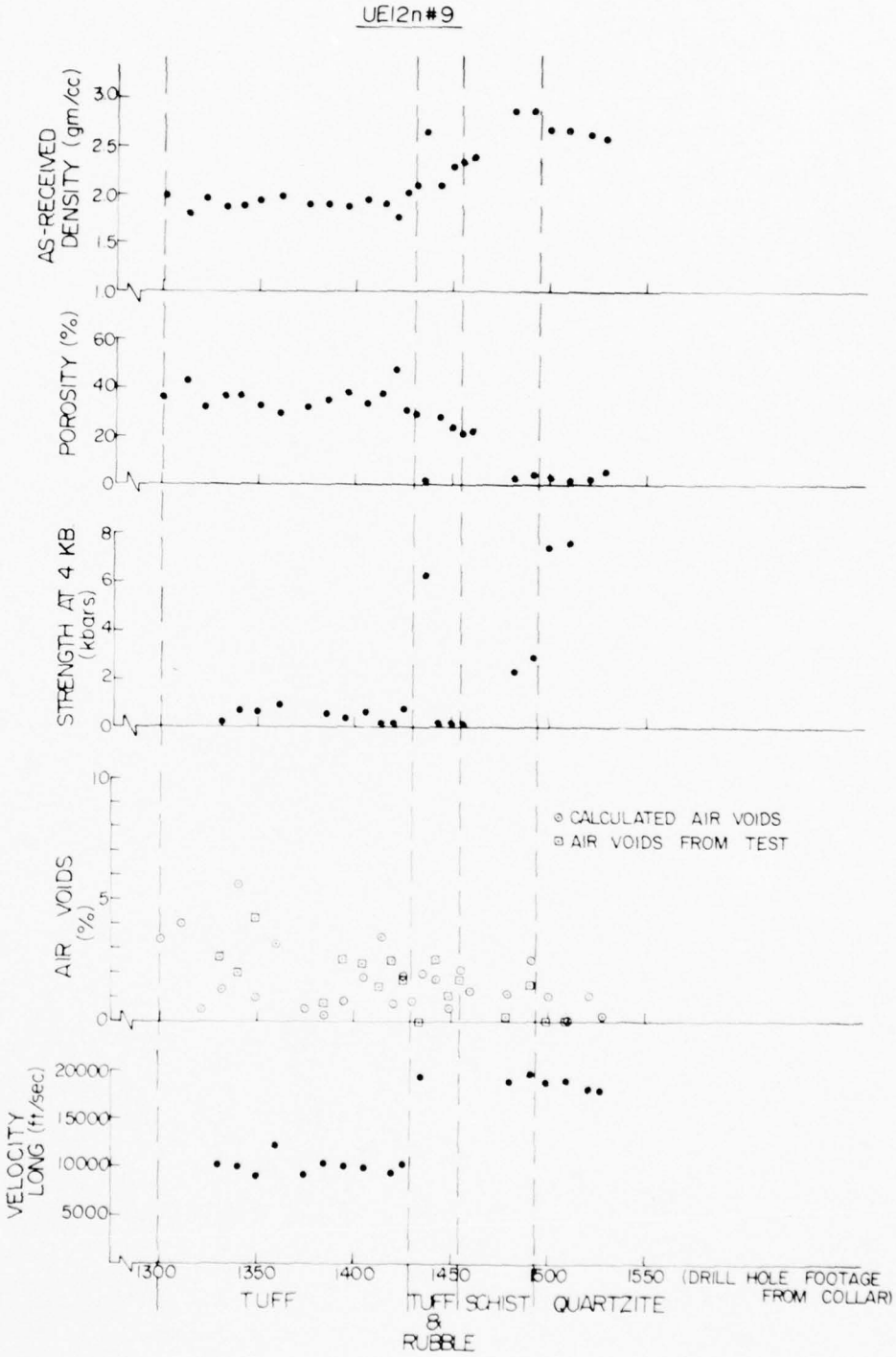

Figure 3. Physical and Mechanical Properties Versus Drill Hole Footage Showing Lithological Zones for the UE12n #9 Drill Hole

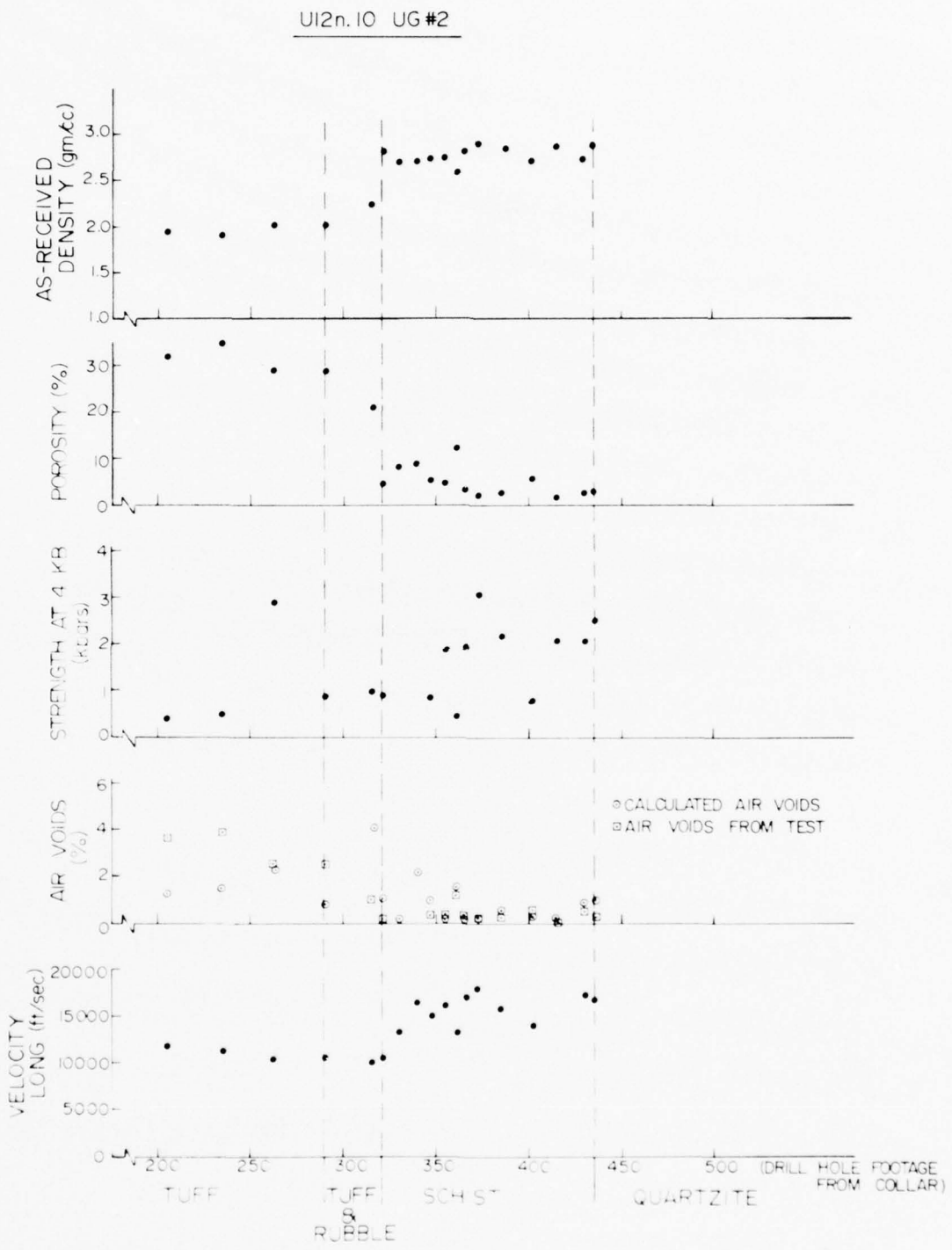

Figure 4. Physical and Mechanical Properties Versus Drill Hole Footage Showing Lithological Zones for the U12n.10 UG#2 Drill Hole

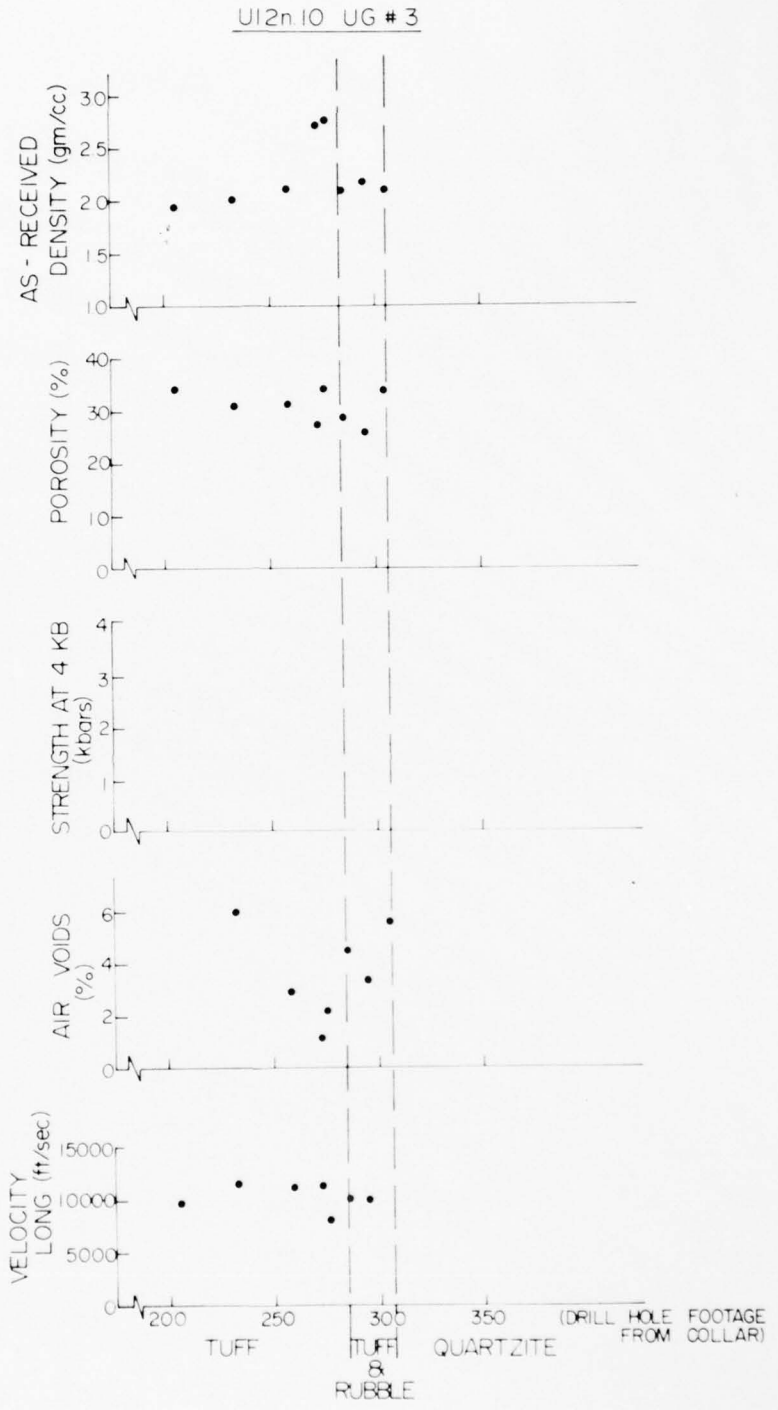

Figure 5. Physical and Mechanical Properties Versus Drill Hole Footage Showing Lithological Zones for the U12n.10 UG#3 Drill Hole

TABLE 2. TABULATED TEST DATA FOR PRELIMINARY EVALUATION.

UE12n #9

SAMPLE LOCATION (feet)		ROCK UNIT	DENSITY (g/cc)			POROSITY %	MOISTURE CONTENT % (wet wt.)	SATURATION %	AIR VOIDS %	PERMANENT DEFORMATION %		ULTRASONIC VELOCITY (ft/sec)		PERMEABILITY (darcies)	ATTERBERG LIMITS			STRENGTH AT 4 KB CONFINING PRESSURE
			As-Received	Dry	Grain					HYDRO	1-D	LONG	SHEAR		LL	PL	PI	
48		Tmr	2.23	2.07	2.58	17	7.4	96	0.7			11360	5683	0.01				
111		Tmr	1.65	1.33			19.9							0.97				
146		Tp	1.85	1.44	2.48	42	22.4	99	0.6					1.35				
193					2.43		22.5											
222			1.57	1.14	2.31	50	27.3	85	7.5		10.3			2.18				.09
255			1.70	1.30	2.34	44	23.1	88	5.1					0.67				
275			1.83	1.48	2.36	37	19.0	94	2.4					0.77				
304			1.74	1.42	2.37	38	15.9	72	10.6					0.27				
327			1.88	1.53	2.36	35	18.5	99	0.4		4.5	6630	2250	0.65				.24
350			1.59	1.21	2.36	49	24.1	79	10.3					1.51				
372			1.80	1.49	2.37	37	17.0	83	6.4		7.8			1.02				.26
396			1.72	1.30	2.39	46	24.8	93	3.1			7010	2440	1.46				
424			1.91	1.51	2.61	42	20.5	93	3.0					0.44				
451			1.55	1.12	2.35	53	23.1	83	8.8		5.4			1.11				.11
476			1.71	1.35	2.38	43	21.2	84	7.1		6.8			3.10				.14
510			1.89	1.58	2.39	34	16.5	93	2.5		3.5			0.89				.26
539			1.82	1.50	2.44	38	17.5	83	6.5					3.48				
564			1.86	1.49	2.38	37	20.0	99	0.2									
593			1.87	1.49	2.49	40	20.7	96	1.6					0.21				
616			1.64	1.11	2.46	55	32.6	98	1.0					0.22				
642			1.71	1.30	2.37	45	24.2	92	3.8					4.00				
665		Tts	1.52	1.01	2.30	56	33.5	90	5.4					0.21				
690		Tts	1.57	1.21	2.31	48	22.9	76	11.6					0.40				
716			1.36	0.95	2.30	59	30.7	71	17.1					0.78				
746			1.50	1.00	2.33	57	33.2	87	7.5					0.85				
766			1.54	1.06	2.31	54	31.3	89	5.9					0.39				
790			1.61	1.19	2.39	50	26.1	94	3.1			5430	2320	0.39				
817			1.83	1.39	2.47	43	23.7	99	0.1			6170		0.20				
844			1.77	1.31	2.45	47	26.0	98	0.8					0.80				
899			1.79	1.42	2.49	43	20.9	87	5.5			10350	4490	0.36				
949			1.55	1.20	2.39	50	22.9	72	14.2					0.27				
1000			1.53	1.07	2.41	56	30.6	84	8.9			6610	1960	0.41				
1050			1.80	1.40	2.45	43	22.2	94	2.7			12090	6050	0.23				
1106			1.22	1.62	2.50	35	17.3	93	1.7			9220	4670	0.01				
1154		Tcy	1.78	1.51	2.43	38	15.4	72	10.5			8000	5440	0.23				
1205			1.82	1.37	2.52	46	24.7	98	0.7									
1253			1.93	1.69	2.47	32	14.9	94	2.1			8980	4240	0.01				
1300		Tcy	1.88	1.65	2.57	36	16.4	91	3.3					6.70				
1311			1.80	1.42	2.46	43	21.7	92	4.0									
1321			1.95	1.63	2.40	32	16.3	98	0.5									
1331			1.87	1.51	2.40	37	14.1	97	1.3		2.60	10160	5270					.19
1340			1.87	1.55	2.46	37	16.7	85	5.6		1.95	10350	5700					.68
1349			1.95	1.63	2.44	33	16.7	97	0.9		4.15	9060	4360					.62
1360			1.99	1.73	2.47	30	13.2	88	3.1		3.75	12200	6990					.93
1374			1.94	1.62	2.38	32	15.9	98	0.5			9230	4630					
1385			1.94	1.59	2.44	35	18.0	99	0.2		.70	10440	5510					.55
1395			1.88	1.51	2.43	38	19.7	98	0.8		2.57	10020	5000					.39
1405			1.94	1.62	2.44	34	16.4	95	1.8		2.35	10010	5470					.66
1413			1.89	1.54	2.49	38	18.3	91	3.4		1.40							.09
1419			1.76	1.28	2.48	48	27.1	99	0.7		2.50	9330	4120					.11
1425			2.02	1.73	2.51	31	14.6	94	1.8		1.60	10270	5140					.72
1430			2.11	1.81	2.59	30	13.9	97	0.8									
1436		Tuff&	2.66	2.66	2.72	2	00.2		1.9		0	19370	12493					6.28
1442		Rubble	2.10	1.84	2.54	28	12.4	94	1.7		2.50							.16
1448			2.30	2.07	2.72	24	10.2	97	0.5		1.05							.19
1454			2.35	2.17	2.73	21	7.9	90	2.1		1.75							.10
1460		Schist	2.39	2.18	2.82	23	9.0	95	1.2									
1467		(Ewc)			2.88		8.1											
1481			2.88	2.86	2.95	3	0.63	60	1.1		.20	18720	11920					2.28
1491			2.89	2.87	2.99	4	0.44	36	2.5		.15	19600	11400					2.86
1498		Dolie-	2.68	2.65	2.75	3	0.93	70	1.0		0	18770	12470					7.40
1509		Orite	2.67	2.66	2.69	1	0.38	101	0		0	18920	12730					7.56
1521		(pEs)	2.64	2.63	2.69	2	0.37	60	1.0			17980	10780					
1527			2.58	2.53	2.67	5	1.89	95	0.2			17920	11320					

SAMPLE LOCATION (feet)		ROCK UNIT	DENSITY (g/cc)			POROSITY %	MOISTURE CONTENT % (wet wt.)	SATURATION %	AIR VOIDS %	PERMANENT DEFORMATION %		ULTRASONIC VELOCITY (ft/sec)		PERMEABILITY (darcies)	ATTERBERG LIMITS			STRENGTH AT 4 KB CONFINING PRESSURE
			As-Received	Dry	Grain					HYDRO	1-D	LONG	SHEAR		LL	PL	PI	
29		Tts	1.85	1.50	2.42	38	19.0	92	2.9			8810	4270					
62		Tbt	2.03	1.79	2.39	25	11.9	95	1.1			11280	6580					
90		Tts	1.96	1.62	2.40	35	17.1	97	1.1			8090	4320					
127			2.00	1.69	2.47	32	15.7	99	0.3			10360	4920					
152			1.88	1.53	2.45	37	18.4	93	2.6			8540	3960					
170			2.00	1.65	2.57	36	17.4	97	1.0			9580	3970					
205			1.96	1.68	2.54	34	14.4	84	5.6			9860	4050					
233		Tts	2.02	1.77	2.55	31	12.1	80	5.0			11540	6230					
250			2.13	1.85	2.68	31	13.3	91	2.9			11240	5680					
272			2.23	1.97	2.69	27	11.6	96	1.1			11440	5930					
276			2.03	1.71	2.60	34	15.8	94	2.2			8230	3700					
286			2.11	1.86	2.63	29	11.7	84	4.5			10270	5290					
294		Tuff&	2.18	1.95	2.64	26	10.4	87	3.4			10210	5140					
305		Rubble	2.12	1.84	2.77	34	13.2	83	5.6									

TABLE 2 (CONT)

U12n.10 UG#2

SAMPLE LOCATION (feet) COREA	e	ROCK UNIT	DENSITY gm/cc As-Received	Dry	Grain	POROSITY %	MOISTURE CONTENT % (Wet Wt.)	SATURATION %	AIR VOIDS %	PERMANENT COMPACTION % HYDRO	I-D	ULTRASONIC VELOCITY ft./sec. LONG	SHEAR	PERMEABILITY (darcies)	ATTERBERG LIMITS LL	PL	PI	STRENGTH AT 4 KB CONFINING PRESSURE
29		Tt_3	1.94	1.64	2.50	35	15.6	87	4.4		3.00	9020	4040					0.42
71		Tbt	1.97	1.73	2.43	29	12.0	82	5.2		0.50	12200	6850					2.50
111		Tt_2	1.90	1.55	2.46	37	18.4	94	2.1		1.60	8910	3470					0.36
141		|	1.94	1.58	2.51	37	18.7	98	0.7		3.00	10650	5180					
170		|	2.15	1.98	2.46	20	8.1	88	2.4		0.70	13450	7920					1.65
206		|	1.96	1.65	2.44	32	15.7	96	1.3		3.60	11830	6910					0.41
236		|	1.93	1.60	2.45	35	17.1	96	1.5		3.90	11340	5420					0.50
262		|	2.01	1.74	2.46	29	13.3	92	2.4		2.50	10470	4810					2.90
290		Tt_1	2.03	1.75	2.47	29	13.8	97	0.8		0.50	10670	6510					0.92
316		Tuff& Rubble	2.26	2.08	2.65	21.0	7.8	81	4.1		1.00	10150	4390					1.00
321		|	2.82	2.79	2.92	4.4	1.2	75	1.1		0.15	16380	9090					0.93
330		schist	2.71	2.63	2.86	8.0	2.9	98	0.2			13410	5620					
339		(Ewc)	2.73	2.66	2.91	8.7	2.4	75	2.2			16640	9080					
347		|	2.75	2.71	2.86	5.0	1.5	80	1.0		0.35	15010	9010					0.90
355		|	2.76	2.72	2.85	4.7	0.6	96	0.2		0.25	16170	9230					1.90
361		|	2.61	2.51	2.85	12.0	4.1	88	1.6		1.20	13470	8770					0.47
366		|	2.83	2.80	2.89	3.0	1.0	98	0.1		0.20	17340	10160					1.95
373		|	2.91	2.89	2.95	2.0	0.6	88	0.2		0.15	18040	9890					3.10
385		|	2.86	2.84	2.91	2.6	0.7	77	0.6		0.25	15870	8910					2.20
401		|	2.73	2.67	2.84	5.7	2.0	95	0.3		0.50	14130	7290					0.80
414		|	2.88	2.86	2.91	1.7	0.6	91	0.2		0.07	17490	9920					2.10
430		|	2.75	2.73	2.91	2.6	0.6	64	0.9		0.05	17560	10170					2.10
435		|	2.89	2.87	2.96	2.8	0.6	62	1.0		0.20	16890	9050					2.52
481		Quart-zite (ees)			2.94													

U12n.10 UG#3

29		Tt_3	1.85	1.50	2.42	38	19.0	92	2.9			8810	4270					
62		Tbt	2.03	1.79	2.39	25	11.9	95	1.1			11280	6580					
90		Tt_2	1.96	1.62	2.48	35	17.1	97	1.1			8090	4320					
122		|	2.00	1.69	2.47	32	15.7	99	0.3			10360	4920					
152		|	1.88	1.53	2.45	37	18.4	93	2.6			8540	3960					
170		|	2.00	1.65	2.57	36	17.4	97	1.0			9580	3920					
205		|	1.96	1.68	2.54	34	14.4	84	5.6			9860	4050					
233		Tt_1	2.02	1.77	2.55	31	12.1	80	6.0			11540	6230					
258		|	2.13	1.85	2.68	31	13.3	91	2.9			11240	5680					
272		|	2.23	1.97	2.69	27	11.6	96	1.1			11440	5930					
276		|	2.03	1.71	2.60	34	15.8	94	2.2			8230	3700					
286		|	2.11	1.86	2.63	29	11.7	84	4.5			10270	5200					
294		Tuff&	2.18	1.95	2.64	26	10.4	87	3.4			10210	5140					
305		Rubble	2.12	1.84	2.77	34	13.2	83	5.6									

BEST ESTIMATE OF GEOLOGIC CONFIGURATION

The geologic materials present below the working point, as indicated earlier in Figures 3 through 5, are tuff or tuffaceous sandstone (Tt_2), tuff and rubble, micacious schist (ϵwc) and sterling quartzite ($p\epsilon s$).[3] The tuff is a competent material with few fractures and little or no variation with depth. The tuff and rubble zone is a tuffaceous sandstone containing rubble, from millimeter to meter size, of quartzite and schist fragments. The micacious schist layer is composed of an upper layer (approximately 10 to 15 feet) of highly weathered and fractured schist with reddish, silt-like material filling the cracks while the lower portion is much more competent and contains some tight fractures. The quartzite zone contains a considerable amount of fracturing, but most are considered tight with little or no filler material.

A plan view of the "Mighty Epic" site, Figure 6, shows the location and orientation of the two cross-sections shown in Figures 7 and 8. These

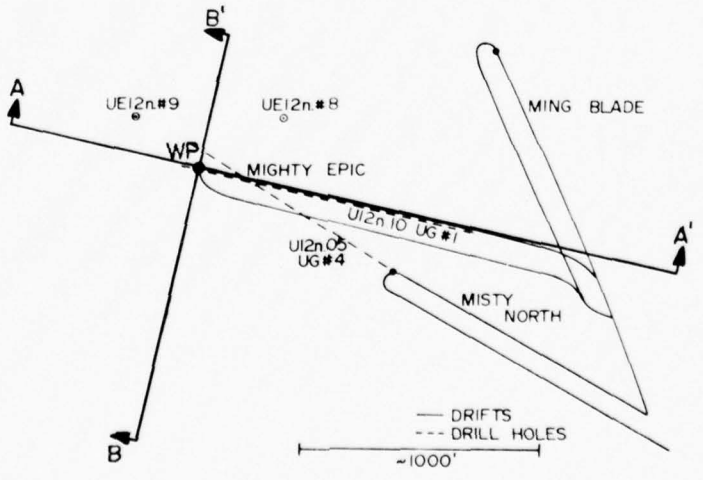

Figure 6. Plan View of Mighty Epic Site Showing Location of Cross-Sections

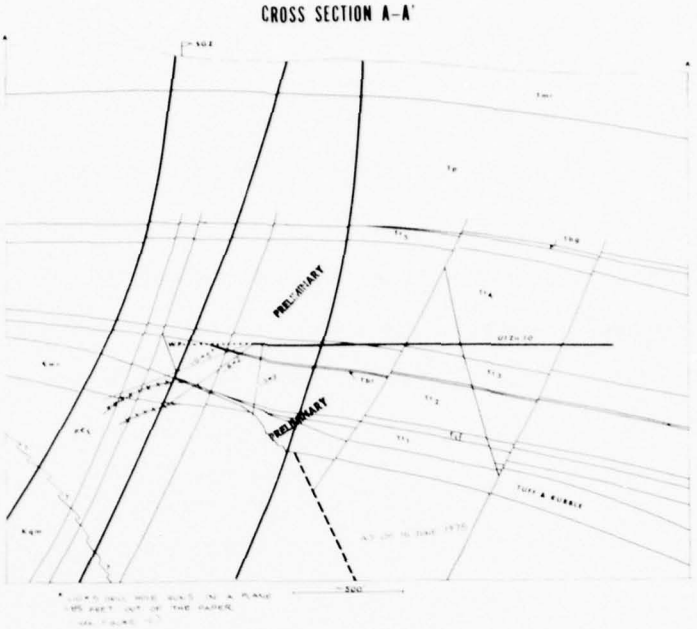

Figure 7. Geology Shown in Cross-Section along the Mighty Epic Main Drift (Reference 4)

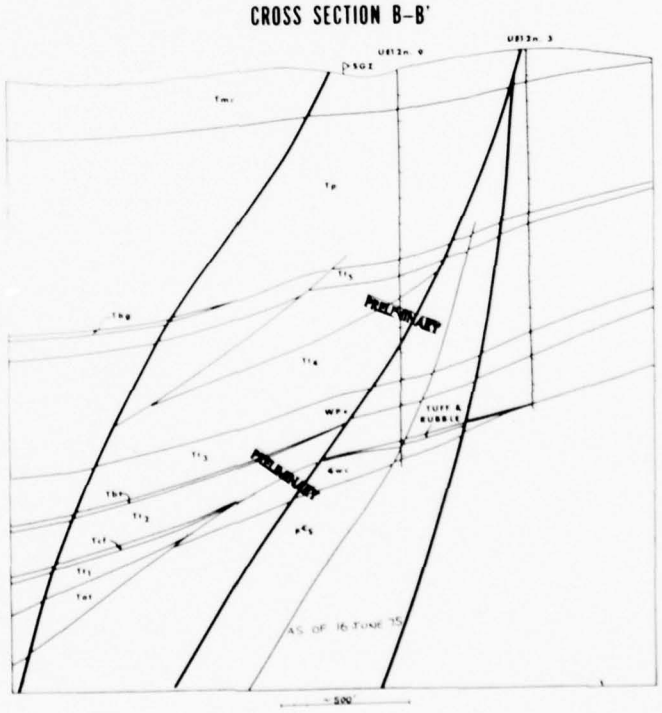

Figure 8. Geology Shown in Cross-Section Perpendicular to Mighty Epic Main Drift and through the Working Point (Reference 4)

cross-sections were produced by United States Geological Survey[4] and were preliminary as of 16 June 1975. More recent data from an exploratory drill hole,[4] U12n.10 UG#5, suggests that the schist and quartzite layers dip to the north (approximately) -- see dashed and crossed line in Figure 7 -- contrary to what was initially presented.

MATERIAL PROPERTY DATA NEEDED FOR INTERFACE CALCULATION

Data Necessary: The purpose of the laboratory tests is to define the mechanical and physical properties of the various rock units (tuff, tuff and rubble, etc.) to then allow a recommendation of a layer configuration such as shown in Figure 9. The laboratory tests necessary on samples from each of the rock units are hydrostatic, triaxial compression, and possibly other load path tests, ultrasonic velocity measurements, and physical property measurements including densities and porosity. For the "interface", different tests will be needed to define a friction model, including direct-shear tests. Some of these data have already been generated. Further tests are necessary, however, to define the average *in situ* properties, especially in the case of the tuff and rubble and the upper schist zone. The tests will require special care in preparing test samples from the "worst" to the "best" material to subsequently define the average and the lower and upper bounds of the material properties.

Cores Required: A survey was made to determine what portion of the original core samples received at Terra Tek were available for added testing. Table 3 gives a list of this information. There are adequate core samples in the tuff, lower schist and the quartzite layers, but essentially no samples in the "tuff and rubble" and the upper schist layers. A minimum of three 12-inch long core samples in each of these two regions are considered necessary to characterize the material.

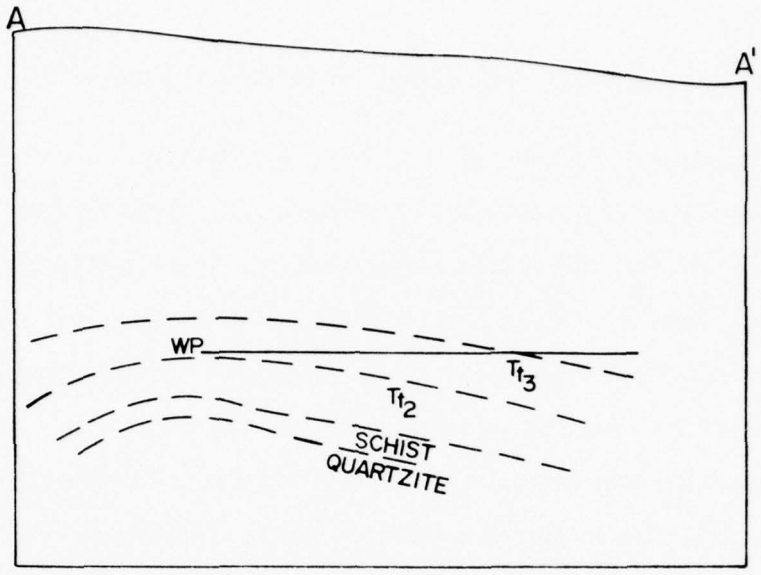

Figure 9a. Anticipated Layer Configuration for a Section along the Mighty Epic Main Drift

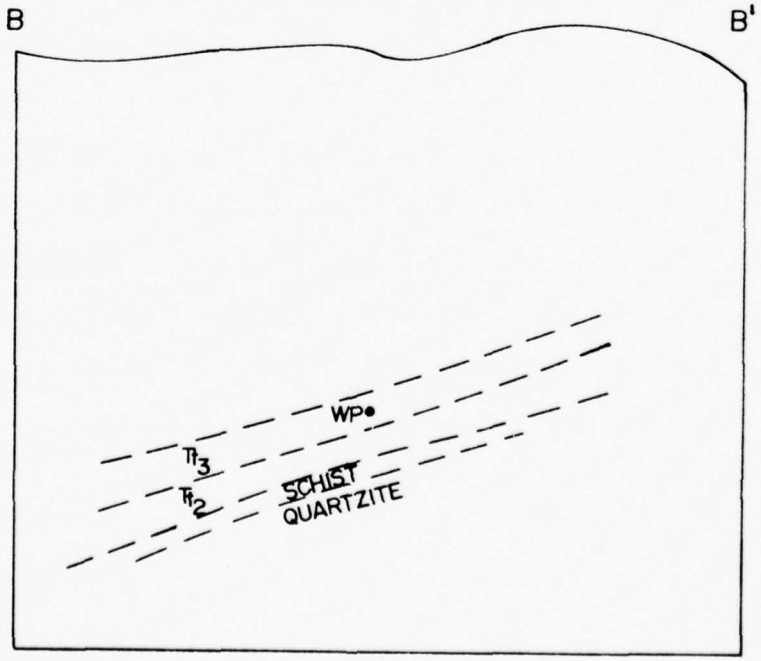

Figure 9b. Anticipated Layer Configuration for a Section through the Working Point and Perpendicular to the Mighty Epic Main Drift

TABLE 3. TERRA TEK CORE SAMPLE INVENTORY

Drill Hole	Rock Unit	Drill Hole Footage (feet)	Length (inches)	Number of Test Samples
U#12N #9	Tuff &	1436	2	none
	Rubble	1442	0	none
	↓	1454	2	none
	Schist	1481	4	1
	|	1491	11	4
	Paleo-zoic	1509	2	none
U12n.10 UG#2	Tt_2	290	11	4
	Tuff &	316	3	1
	Rubble	321	4	none
	Schist	330	0	none
	|	339	6	2
	|	347	2	none
	|	355	2	none
	|	361	7	2
	|	366	7	2
	|	374	6	2
	|	385	5	2
	|	402	3	1
	|	414	5	2
	|	431	0	none
	|	435	5	2
U12n.10 UG#3	Tt_1	259	8	3
	|	273	7	2
	|	277	9	3
	|	286	12	4
	Tuff &	295	7	2
	Rubble	305	5	1

REFERENCES

1. Communication with Cliff Snow, Nevada Test Site, Mercury, Nevada, January 1975-June 1975.

2. S. W. Butters, A. H. Jones, S. J. Green, "Properties of Quartzite from Area 12 of the Nevada Test Site", Terra Tek Report TR 75-7, January 1975.

3. Data provided by G. Fairier, United States Geological Survey; and J. W. LaComb, Nevada Test Site; May 1975.

4. Meeting at Nevada Test Site, Mercury, Nevada, 16 June 1975.

SOME COMMENTS ON

MIGHTY EPIC MATERIAL PROPERTIES

S. J. Green
S. W. Butters
J. N. Johnson
A. H. Jones

Submitted to:

Field Command
Defense Nuclear Agency
Nevada Test Site

Attn: Mr. Joseph LaComb

Contract DNA 001-75-C-0260

From

Terra Tek, Inc.
420 Wakara Way
Salt Lake City, Utah 84108

TR 75-42
August 1975

PREFACE

Some comments are made with regard to the Mighty Epic site material properties and to the associated structures calculational effort. These comments are made after meetings at NVOO on August 1, at Headquarters, DNA, August 8, and after discussions with Cliff McFarland and Kent Goering on August 12.

GENERAL DISCUSSION

Discussions between Ivan Sandler and Jim Johnson led to the presentation given by Ivan Sandler at the DNA meeting on August 8. The discussions between Jim and Ivan were conducted following the general ground rule that a "PW Capped Model" would be used to fit the Mighty Epic site tuffs for the "structure calculations". During the discussions between Jim and Ivan, representative stress-strain curves available on tunnel-bed tuffs from other sites were used for reference in the formulation of the cap model[1]. Jim indicated that the Mighty Epic site had not yet been characterized and that more test data would be passed on to Ivan as they became available.

The cap model was developed knowing that certain phenomena, particularly those occurring after reaching the failure surface, would not be handled correctly. For example, the model was not intended to fit the apparent loss of strength which occurs as a test sample is unloaded via a constant axial strain path[2]. (This is known to be an effect caused by the pore pressure[3].) Secondly, it was intended that as more material property data for the Mighty Epic site became available, the parameters in the cap model would be readjusted to best represent the average properties of the site over the region of interest.

There are known phenomena that the "cap model formulated" does not fit, or handle properly. These include:

-- details of the elastic-limit where crush-up begins[4], which is complicated here by not knowing the *in situ* stress

-- the difference between the apparent elastic constants obtained from the seismic velocities and from the slopes of the laboratory stress-strain curves[5], i.e. the elastic constants obtained from the [longitudinal] seismic velocity and guessing the shear-wave velocity are "faired" into the elastic constants obtained from the slopes of the stress-strain curves

-- pore pressure effects are not accounted for adequately[2,3]

-- the laboratory stress-strain curves are not fit beyond an initial loading (and to some extent unloaded) cycle[2,6]

-- the tensile and extension strength is not adequately handled[7]

The reason for not handling the above phenomena is probably due to a lack of material property data, rather than to any "shortcoming" of the cap model.

Some material property data on the Mighty Epic site has been presented previously in Terra Tek reports[8,9]. Surprisingly, some cores from the region of the structures experiments exhibit quite high shear strength, up to 1.0 - 1.5 kilobars stress difference at multi-kilobar confining pressures; typical tunnel-bed tuffs show stress difference of about 0.3 kilobars at 1 kilobar confining pressure[9]. It is not clear why so many cores exhibit this high strength; Joe LaComb does not seem concerned with this, and I believe he feels that there may be relatively "thin" beds of this strong tuff.

At the NVOO meeting, some data were presented by Joe LaComb suggesting a low seismic velocity over parts of the Mighty Epic site. I believe Joe attributes this to stress relaxation surrounding the main and structures experiment tunnels[10]. Joe indicated he intends to conduct additional seismic surveys as well as hydraulic-fracturing and over-coring experiments to obtain more information about the *in situ* stress. The exact program he was going to conduct was not clear from the NVOO meeting, and no subsequent discussion was held. If this relaxation phenomenon is correct then the stresses around the structures tunnel is unknown. The *in situ* stress a few feet away from the scaled structures will not be well defined.

The "pressure range" for which the structures calculations will be most sensitive to the material properties (right around the structure) appears to be the following. For the spherical structures, collapse will likely occur at high pressures (maybe one kilobar) if at all; for the SRI structures, the porous concrete will collapse at stresses as low as about 0.1 kilobar (based on discussions at NVOO). Therefore, "more detailed" strength of the tuff and the grout around the structures should be obtained over these pressure ranges.

Strength of the grout (to be used around the structures) is such that it will not match the strength of the tuff over pressure ranges from 0.1 to 1.0 kilobars[11,12]. That is, if the angle of internal friction

of the grout is matched to that of the tuff in the zero to one or two-hundred bar pressure region, then the strength of the grout at higher confining pressures will be 1/2 to 1/3 that of the tuff (assuming the tuff strength is about 0.3 kilobars stress difference). On the other hand, if the angle of internal friction of the grout matches the tuff at the higher confining pressures, i.e. 0.5 - 1.0 kilobars pressure, then the strength of the grout at low pressure (one hundred bars) will be much greater than the tuff.

The differences in strength was discussed at the NVOO meeting, and it was Joe's opinion (I believe) that an economical (and pumpable) grout should be used to reasonably match the tuff. The strength of whatever grout used would be determined, and no further effort would be conducted to produce a "tuff matching" grout.

It is our feeling that because of the high water content in the grouts, the micro-mechanisms for deformation are different than in the tuff. In the tuffs, for example, we believe that through-going fracture-planes occur and sliding on the fracture-plane results. In the grout, a general collapse of the sample occurs without producing a through-going fracture-plane. This difference in micro-mechanisms leads us to believe that it is unlikely that pumpable grouts (50% water or thereabouts) can ever be made to match the tuff's strength properties over all pressure ranges.

Concretes used in the structures will undoubtedly behave as other cement-type materials do--reference, for example, the previous Terra Tek report on plain concrete[13]. The concretes will undoubtedly show increase in strength with confining pressure, collapse of the porous matrix, and complex post-maximum stress behavior. Furthermore, the concretes are likely to be strain-rate sensitive, exhibiting maybe a factor of two increase in strength for rapid loading as opposed to standard testing rate loadings[14].

RECOMMENDATIONS

Terra Tek recommends the following with respect to the Mighty Epic Experiment materials characterization:

1. Some added tests should be performed to better characterize the tuffs from the working point out to the structures, and particularly in the regions of a few feet around the structures tunnels. These tests would determine the failure envelope and the stress-strain response up to about 1 kilobar.

2. For any calculations, the most representative material property data should be used to formulate the parameters in the cap model. This will probably not cost any more, and will provide the best material properties for the Mighty Epic site.

3. The grout used around the structures should be characterized to the extent of determining the failure envelope and the stress-strain response to selected loadings up to about 1 kilobar. This will provide data to indicate the difference between the grout and the tuff over pressure ranges up to about 1 kilobar.

4. The concrete used in the different structures should be characterized to the extent of determining the failure envelope, the stress-strain response, and some limited information on its dynamic (rapid loading) response.

5. Some information should be obtained on the "bond strength factor" for the concrete-to-steel. This can be done by running one or two direct shear tests where concretes used in the structures are sheared along steel plates - i.e., a direct shear test at several normal stresses[15]. It is not suggested that an extensive program be conducted, but that some indication of bond strength be obtained to serve as guidance for the calculators.

6. Some added material property tests are still needed for the "interface" calculation, and those proposed in Terra Tek report TR 75-36 should be performed as cores become available.

REFERENCES

1. S. J. Green, S. W. Butters, and R. M. Griffin, "High Pressure Mechanical Properties of the U12n.05 and U12t.02 Test Sites," Terra Tek Report TR 72-19, July 1972.

2. S. W. Butters, S. J. Green, and A. H. Jones, "Laboratory Tests on Rocks to Simulate Shock Wave Load-Unload From a Nuclear Explosion," Terra Tek Report TR 72-82, May 1974.

3. J. N. Johnson, S. W. Butters, W. F. Brace, A. H. Jones, and S. J. Green, "Plasticity Theory for Partially and Fully Saturated Porous Geological Materials," Terra Tek Report TR 74-53, October 1974.

4. S. W. Butters, "Selected Tests for Teleseismic Program," July 1975.

5. S. W. Butters, "Determination of Elastic Constants," Terra Tek Research Task Report, May 1975, and L. M. Barker, R. Lingle, and R. R. Hendrickson, "Interferometric Measurement of Transverse Strain for Determination of Low-Pressure Elastic Moduli of Rocks," Terra Tek Report TR 75-30, June 1975.

6. R. J. Reid, "Recoverable Dilatancy on Tuffs and Sandstones, February 1973, and S. J. Green, S. W. Butters, and A. H. Jones, "Recoverable Dilatancy Exhibited by Rocks 'Transactions, American Geophysical Union,'" Vol. 54, Number 4, April 1973.

7. S. W. Butters, J. N. Johnson, H. S. Swolfs, and A. H. Jones, "Modeling and Properties for Welded Tuff from Mt. Helen - Sandia Test Range, Nevada," Terra Tek Report 75-9, January 1975.

8. S. W. Butters, A. H. Jones, and S. J. Green, "Properties of Quartzite from Area 12 of the Nevada Test Site," Terra Tek Report TR 75-7, January 1975.

9. S. W. Butters and S. J. Green, "Progress Report One - Material Properties for Mighty Epic Interface Experiment," Terra Tek Report TR 75-36, June 1975, and Terra Tek letter, subject: "Response to Request for Properties for Tuff Surrounding the Mighty Epic Working Point," dated February 5, 1975, from S. W. Butters to Jim Drake.

10. R. Lingle, R. S. Rosso and L. M. Buchholdt, "An Investigation to Determine the Effect of Fracture on the Ultrasonic Velocities in Ash-Fall Tuff," Terra Tek Report 75-20, May 1975.

11. W. F. Brace, S. J. Green, A. H. Jones, and S. W. Butters, "Determination of the Angle of Internal Friction," Terra Tek Report TR 75-38, July 1975.

12. S. W. Butters, J. N. Johnson, and S. J. Green, "Mechanical Behavior of NTS Grout," Terra Tek Report TR 74-40, August 1974.

13. S. J. Green, "Final Report - Constitutive Relations for Concrete at Intermediate Pressure Levels," Terra Tek Report 71-34, October 1971.

14. H. E. Read and C. J. Maiden, "The Dynamic Behavior of Concrete," Systems, Science and Software Report 3SR-707, August 1971.

15. H. R. Pratt and A. D. Black, "Strength, Deformation and Friction of *In Situ* Rock," Terra Tek Report TR 73-68, December 1973; and R. S. Rosso, "Rock Strength and Joint Property Data for the Mahoning Dam Site," Terra Tek Report TR 75-34, June 1975.

PHYSICAL AND MECHANICAL PROPERTIES OF SEVERAL GROUT MIXTURES

By

S. W. Butters
A. H. Jones
S. J. Green

Submitted to:

Field Command
Defense Nuclear Agency
Nevada Test Site
Mercury, Nevada

Attn: Mr. J. W. LaComb

TR 75-45
August 1975

SUMMARY

Physical and mechanical properties tests have been conducted on several batches of grout supplied by Waterways Experiment Station. The grouts are used for gage implacement and containment of structures experiments during nuclear events at the Nevada Test Site and the grout properties are required to insure the proper grout selection. The grouts were designated HPRM-1, HPRM-2, HPRM-3, HPRM-4, HPRM-5, HPSL-16, HPNS-1 and HPNS-3C.

The properties determined for the grouts at 14, 28 and 56 day age are: physical properties (densities, porosities, water content, etc.), ultrasonic velocities and mechanical properties (shear strength, stress-strain response) from triaxial compression and uniaxial strain tests. The entire test program is not complete and the data reported is preliminary.

The data is reported in the form of tables which contain the physical properties and velocities at each of the three ages (with the exception of the HPNS-3C) and plots showing the shear strength as a function of confining pressure and the permanent compaction resulting from uniaxial strain load-unload tests.

Table 1: Physical Properties and Ultrasonic Velocities at 14 Day Age.

DRILL HOLE FOOTAGE	DENSITY (gm/cc)			WATER BY WET WEIGHT (%)	POROSITY (%)	SATURATION (%)	CALC AIR VOIDS (%)	MEAS PERMANENT COMP. (%)		VELOCITY (ft/sec)	
	AS-RECEIVED	DRY	GRAIN							LONG	SHEAR
Grout 14 Day								Hyd.	1-D		
HPRM-1	2.06	1.65	2.97	20.1	44	93	3.0	2.1	2.3	9478	5274
HPRM-2	2.04	1.64	3.01	19.8	46	89	5.1	2.2	2.25	9166	5022
HPRM-3	2.07	1.58	3.11	23.6	49	99	0.5	1.5	1.6	8366	4472
HPRM-4	2.01	1.55	3.06	22.9	49	94	3.2	3.1	3.5	9084	4640
HPRM-5	1.92	1.46	3.02	23.9	52	88	5.9	3.5	4.0	7910	3753
HPSL-16	1.86	1.37	2.94	26.5	54	92	4.3	2.4	2.5	6579	2459
HPNS-1	2.04	1.51	3.35	25.9	55	96	2.05	1.8	1.8	7213	3427
HPRM-3C	2.10	1.71		18.9				2.4	2.6	9850	5333

Table 2: Physical Properties and Ultrasonic Velocities at 28 Day Age.

DRILL HOLE FOOTAGE	DENSITY (gm/cc)			WATER BY WET WEIGHT (%)	POROSITY (%)	SATURATION (%)	CALC AIR VOIDS (%)	MEAS PERMANENT COMP. (%)		VELOCITY (ft/sec)	
	AS-RECEIVED	DRY	GRAIN							LONG	SHEAR
Grout 28 Day								Hyd.	1-D		
HPRM-1	2.02	1.56	2.97	22.9	48	97	1.3	2.2	2.8	10,259	5696
HPRM-2	2.04	1.61	3.01	21.0	46	93	3.3	1.7	2.7	11,591	6363
HPRM-3	2.08	1.61	3.11	22.7	48	98	1.0	1.5	1.9	8,871	4695
HPRM-4	1.98	1.53	3.06	22.9	50	91	4.5	3.5	3.9	9,058	4678
HPRM-5	1.94	1.45	3.02	27.4	52	95	2.6	2.9	3.0	7,707	3796
HPSL-16	1.86	1.36	2.94	27.0	54	93	3.7	2.4	2.7	6,303	2717
HPNS-1	2.05	1.51	3.35	26.7	55	99	0.2	2.0	2.5	7,519	3619

Table 3: Physical Properties and Ultrasonic Velocities at 56 Day Age.

DRILL HOLE FOOTAGE	DENSITY (gm/cc)			WATER BY WET WEIGHT (%)	POROSITY (%)	SATURATION (%)	CALC AIR VOIDS (%)	MEAS PERMANENT COMP. (%)		VELOCITY (ft/sec)	
	AS-RECEIVED	DRY	GRAIN							LONG	SHEAR
Grout 56 Day								Hyd.	1-D		
HPRM-1	2.05	1.63	2.97	20.5	45	93	3.2	2.5	3.0	10,269	5,545
HPRM-2	2.02	1.57	3.01	22.4	48	94	2.7	1.5	2.9	11,591	6,368
HPRM-3	2.10	1.65	3.11	21.2	47	95	2.5	1.6	2.5	9,672	5,230
HPRM-4	1.96	1.49	3.06	24.1	51	92	4.3	4.3	4.4	8,215	3,976
HPRM-5	1.97	1.48	3.02	24.8	51	96	2.0	2.5	2.7	8,064	4,117
HPSL-16	1.85	1.34	2.94	27.4	54	93	3.6	2.3	3.0	8,291	3,819
HPNS-1	2.09	1.58	3.35	24.2	53	96	2.2	2.1	2.6	8,015	4,006

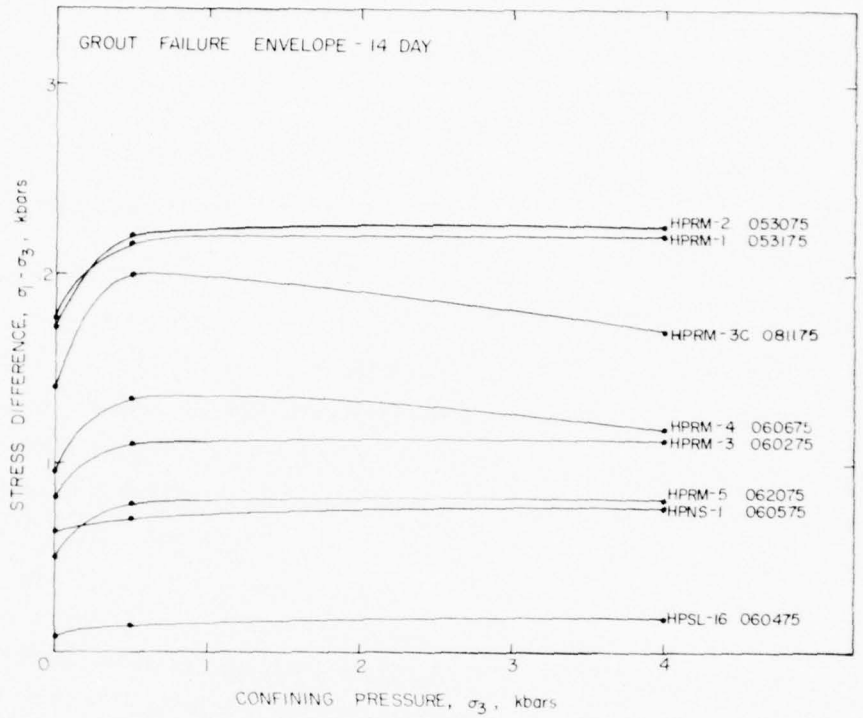

Figure 1: Failure Envelope at 14 Day Age

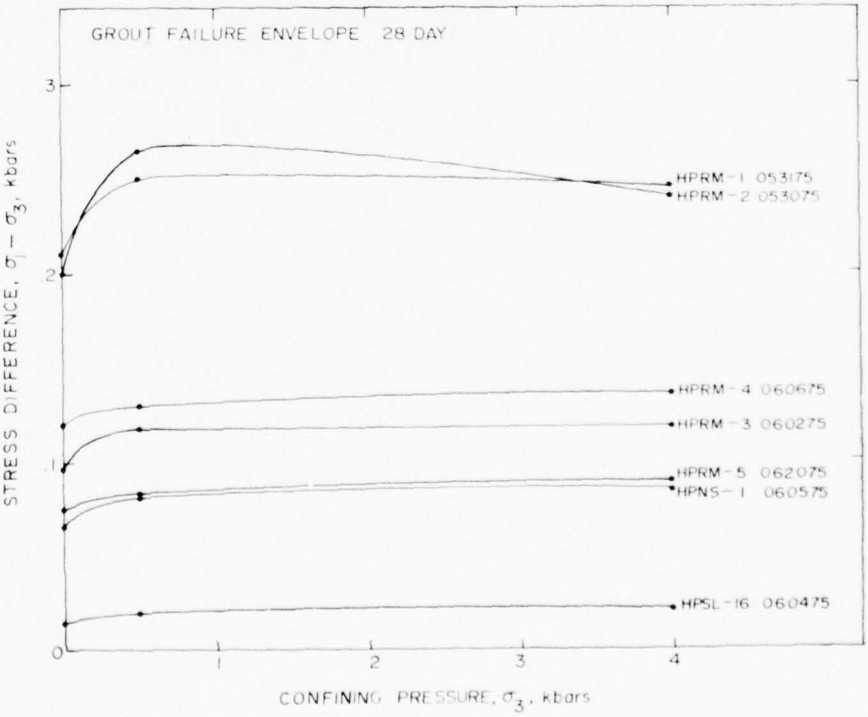

Figure 2: Failure Envelope at 28 Day Age

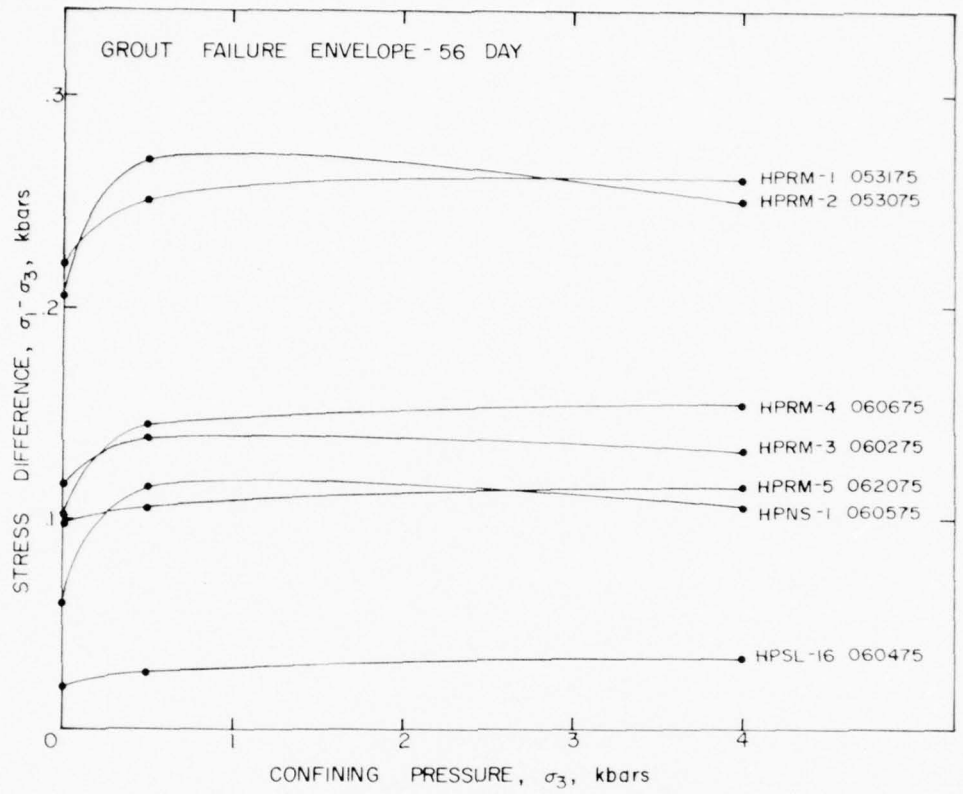

Figure 3: Failure Envelope at 56 Day Age

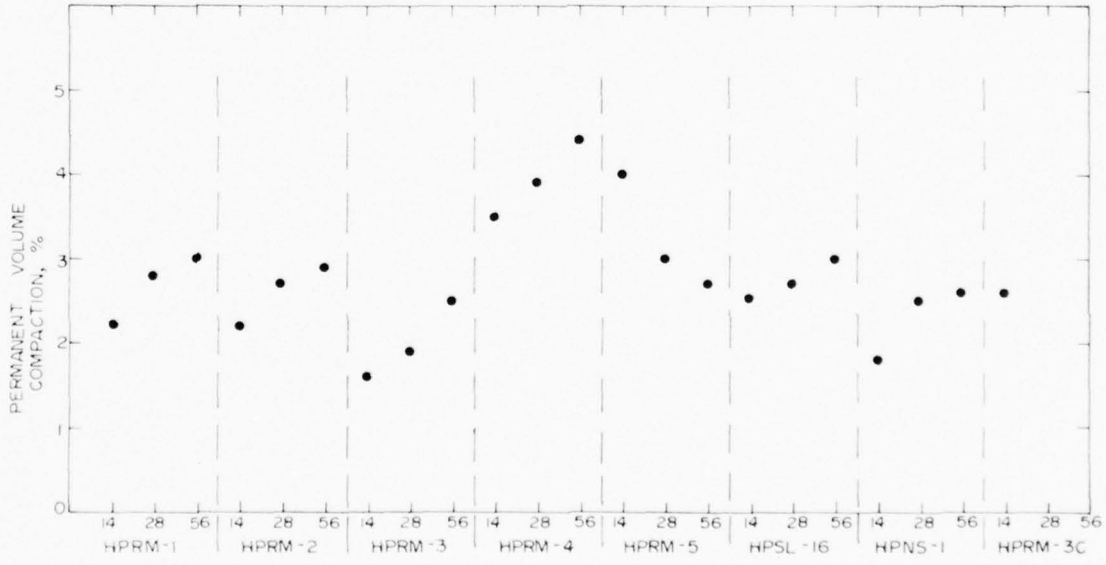

Figure 4: Permanent Volume Compaction
from Uniaxial Strain Tests

PROGRESS REPORT III

MATERIAL PROPERTIES ON SAMPLES FROM MIGHTY EPIC

DRILL HOLES U12n.10 UG #4, U12n.10 UG #6a and U12n.10 UG #7

by

S. W. Butters
A. H. Jones
S. J. Green

Submitted to

Commander, Field Command
Defense Nuclear Agency
Albuquerque, New Mexico

Attn: Mr. J. W. LaComb
Mercury, Nevada

Contract Number DNA001-75-C-0260

Terra Tek, Inc.
University Research Park
420 Wakara Way
Salt Lake City, Utah 84108

TR 75-50
September 1975

PREFACE

Mighty Epic pretest planning require material properties for both shock wave propagation and rock/structural interaction calculations. In response to this requirement, Terra Tek has performed testing and reported properties in the following reports:

Progress Report I - Material Properties for the Mighty Epic Interface Experiment TR 75-36

Determination of Coefficient of Internal Friction TR 75-38

Some Comments on the Mighty Epic Material Properties TR 75-42

Physical and Mechanical Properties of Several Grout Mixtures (Preliminary) TR 75-45

Testing is continuing and properties from the U12n.10 UG #4, U12n.10 UG #6a and U12n.10 UG #7 core samples are included herein.

TABLE OF CONTENTS

LIST OF FIGURES

LIST OF TABLES

INTRODUCTION

Material properties have been determined on core samples from three drill holes in the Mighty Epic region at the Nevada Test Site, Mercury, Nevada. The testing was conducted on core samples from drill holes U12n.10 UG #4 and U12n.10 UG #6a, which are both located in the structures area as shown in Figure 1, and U12n.10 UG #7 which is in between the bypass drift and the main drift and was drilled toward the working point. All three of the drill holes are in the horizontal plane of the working point.

The material properties measured are physical properties (as-received density, dry density, percentage water and etc.) and longitudinal and shear velocities. In addition to tests for measuring the permanent volume compaction resulting from compaction in uniaxial strain to 4 kilobars lateral stress, further mechanical characterizations were obtained through triaxial compression tests. The confining pressures ranged from 0 (unconfined compression) to 4 kilobars but concentrating on the 0 to 500 bars range.

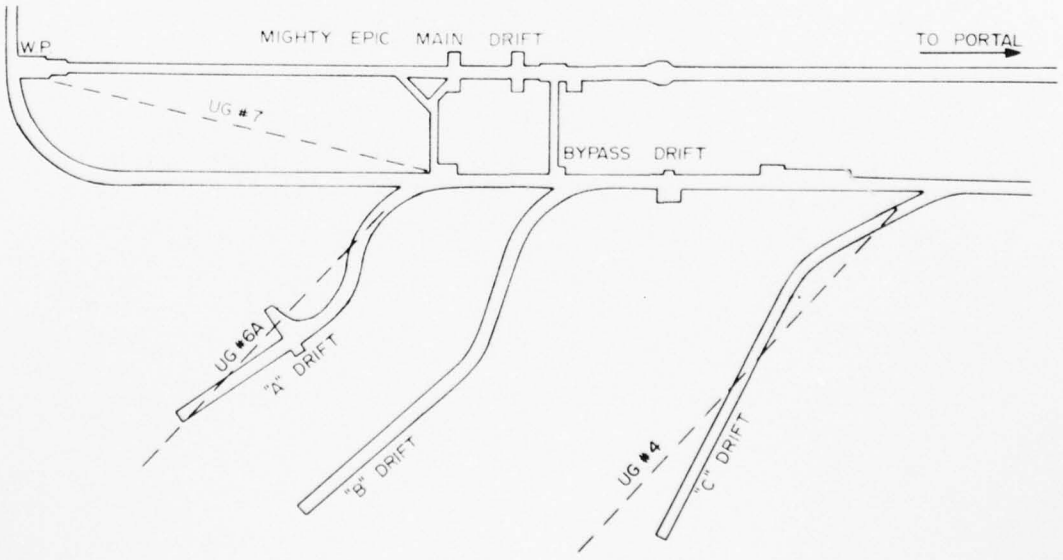

Figure 1. Plan View of the Mighty Epic Tunnels and Selected Drill Holes

TEST RESULTS

The U12n.10 UG #4, U12n.10 UG #6a and U12n.10 UG #7 drill hole samples physical properties, permanent volume compaction and ultrasonic velocities are listed in Tables 1, 2, and 3 respectively. Selected physical and mechanical properties have been plotted vs. the drill hole footage for each of the three drill holes in Figures 2, 3 and 4. The data has been plotted in this manner with the intent of indicating average properties (dashed line) and the amount of scatter in these properties as a function of drill hole footage.

Individual test curves plotted as axial stress vs. volume change and stress difference vs. confining pressure are contained in the appendix. Uniaxial strain tests curves for samples from drill holes U12n.10 UG #4 and U12n.10 UG #6a were plotted as axial stress vs. volume change such that the constrained modulus could be scaled from the slopes of the curves. The U12n.10 UG #7 test data is plotted in the usual manner -- mean normal stress vs. volume change.

The detailed triaxial compression tests on samples 257 feet from U12n.10 UG #4 and on the sample at 116 feet from U12n.10 UG #6a are shown in Figures 5 and 6. These results are plotted as stress difference vs. confining pressure through the confining pressure range of 0 to 100 bars. The same data is extended out to a confining pressure of 4 kilobars in Figure 7 and plotted as stress difference vs. axial shortening in Figure 8 for the test at a confining pressure of 50 bars.

Table 1. Physical Properties, Permanent Volume Compaction and Ultrasonic Velocities on Core Samples from U12n.10 UG #4

DRILL HOLE FOOTAGE	DENSITY (gm/cc) AS-RECEIVED	DRY	GRAIN	WATER BY WET WEIGHT (%)	POROSITY (%)	SATURATION (%)	CALC AIR VOIDS (%)	MEAS PERMANENT COMP (%)	VELOCITY (ft/sec) LONG	SHEAR
U12n.10 UG #4								Hyd. 1-0		
227	1.86	1.52	2.44	18.6	38	91	3.2	1.4	9,469	4596
251	1.99	1.69	2.41	14.8	30	98	0.5	1.3	10,751	5761
254	1.95	1.65	2.39	15.4	31	96	1.3	1.8	10,009	5095
257	1.89	1.54	2.42	18.4	36	95	1.8			
263	1.97	1.65	2.50	16.2	34	94	1.9		9,694	4094
282	1.96	1.64	2.45	16.3	33	97	0.9	1.3	9,370	4104
307	2.01	1.73	2.41	14.0	28	99	0.2	0.9	9,557	6555
327	1.78	1.42	2.38	20.0	40	88	4.8		13,061	5154
331	1.74	1.37	2.36	21.2	42	88	5.2	3.2	10,548	4695
336	1.77	1.42	2.39	20.1	41	87	5.3	3.5	13,205	7523
339	1.77	1.38	2.38	22.1	42	93	2.7			

Table 2. Physical Properties, Permanent Volume Compaction and Ultrasonic Velocities on Core Samples from U12n.10 UG #6a

DRILL HOLE FOOTAGE	DENSITY (gm/cc) AS-RECEIVED	DRY	GRAIN	WATER BY WET WEIGHT (%)	POROSITY (%)	SATURATION (%)	CALC AIR VOIDS (%)	MEAS PERMANENT COMP (%)	VELOCITY (ft/sec) LONG	SHEAR
U12n.10 UG #6A								Hyd. 1-0		
84	1.99	1.69	2.43	14.8	30	97	0.8	1.1	10,200	4809
109	1.97	1.69	2.35	14.0	28	98	0.7	0.7	11,227	5675
113	1.93	1.59	2.41	17.4	34	99	0.4		9,226	4505
116	1.98	1.72	2.38	12.9	28	93	1.9			
136	1.93	1.60	2.42	17.1	34	97	1.0	1.0	9,822	4563
163	1.97	1.68	2.41	15.0	31	97	1.0	1.1	10,305	4737
189	1.94	1.65	2.38	14.9	31	95	1.6	1.1	9,947	4895
192	2.01	1.80	2.35	10.4	23	90	2.4	0.8	11,683	6046
216	2.03	1.82	2.34	10.2	22	95	1.1	0.6	12,342	7306
220	1.96	1.65	2.41	15.6	31	97	1.1		10,561	4859
231	2.01	1.75	2.41	13.0	27	96	1.1			
247	2.00	1.75	2.35	12.4	25	98	0.6	0.6	13,094	7549

Table 3. Physical Properties, Permanent Volume Compaction and Ultrasonic Velocities on Core Samples from U12n.10 UG #7

DRILL HOLE FOOTAGE	DENSITY (gm/cc) AS-RECEIVED	DRY	GRAIN	WATER BY WET WEIGHT (%)	POROSITY (%)	SATURATION (%)	CALC AIR VOIDS (%)	MEAS PERMANENT COMP (%)	VELOCITY (ft/sec) LONG	SHEAR
U12n.10 UG#7										
3	1.87	1.53	2.33	18.0	35	95	1.7	1.4	9478	4888
76	1.98	1.68	2.42	15.4	30	95	2.1	2.9	10377	5446
96	1.80	1.41	2.46	21.7	43	95	1.7	3.2	7287	3078
73	1.90	1.58	2.43	17.4	35	97	1.2	1.5	10423	5470
98			2.37	19.3					12566	6276
99	1.91	1.61	2.35	15.7	33	95	1.9	1.5	9798	4370
124	1.86	1.51	2.36	18.6	37	98	0.7	2.3	9039	4416
149	1.97	1.68	2.39	14.7	30	97	1.0	0.4	10847	5269
150	1.97	1.69	2.43	14.5	30	96	1.1	0.9	10651	5620
162	1.88	1.53	2.36	18.6	38	98	0.8	1.5	9849	4444
180	1.94	1.62	2.43	15.6	33	97	1.0	0.7	10413	5479
197	1.99	1.71	2.43	14.1	30	95	1.6	1.9	9311	4065
208	2.01	1.73	2.44	13.8	29	96	1.3	1.1	9632	3916
226	1.97	1.69	2.34	14.7	30	99	0.3	0.7	12510	6309
232	1.88	1.52	2.46	19.6	38	97	0.9	2.2	8547	3826
239	1.78	1.48	2.45	17.7	35	79	8.1	6.9	12520	4692
241	1.84	1.55	2.46	18.0	37	91	3.4	4.4	9266	4183
256	1.96	1.67	2.48	16.4	34	95	2.4	1.5	9833	4518
270	1.95	1.62	2.47	17.1	35	96	2.0		9623	4489
271	1.96	1.64	2.46	16.2	33	95	1.6	2.3	8937	4111
281	1.91	1.56	2.48	18.6	37	95	1.9	2.2	9537	4573
286	1.89	1.55	2.52	17.9	36	89	4.1	3.0	10410	5070
298	1.91	1.58	2.40	17.3	34	96	1.5	1.8	10272	4665
309	1.99	1.70	2.44	14.7	31	96	1.0	1.5	11099	5640

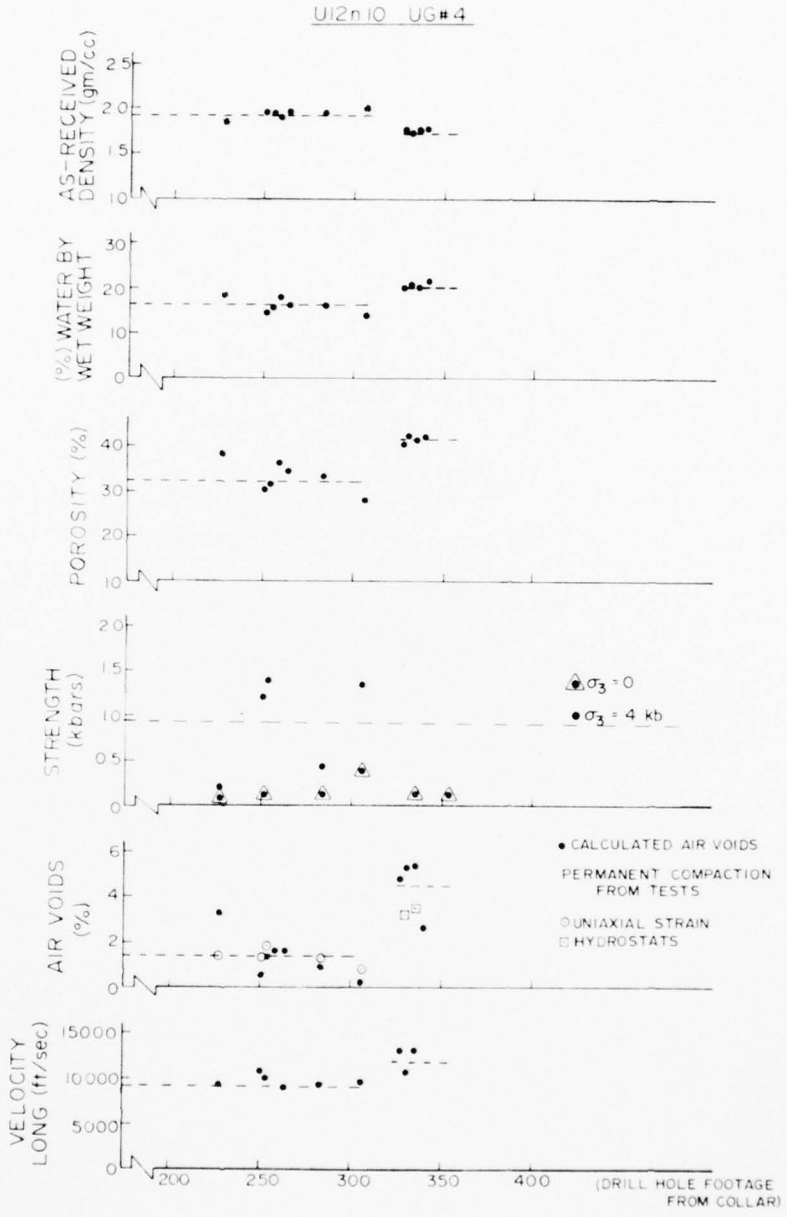

Figure 2. Selected Data from U12n.10 UG #4 Drill Hole Samples vs. the Footage Along the Drill Hole

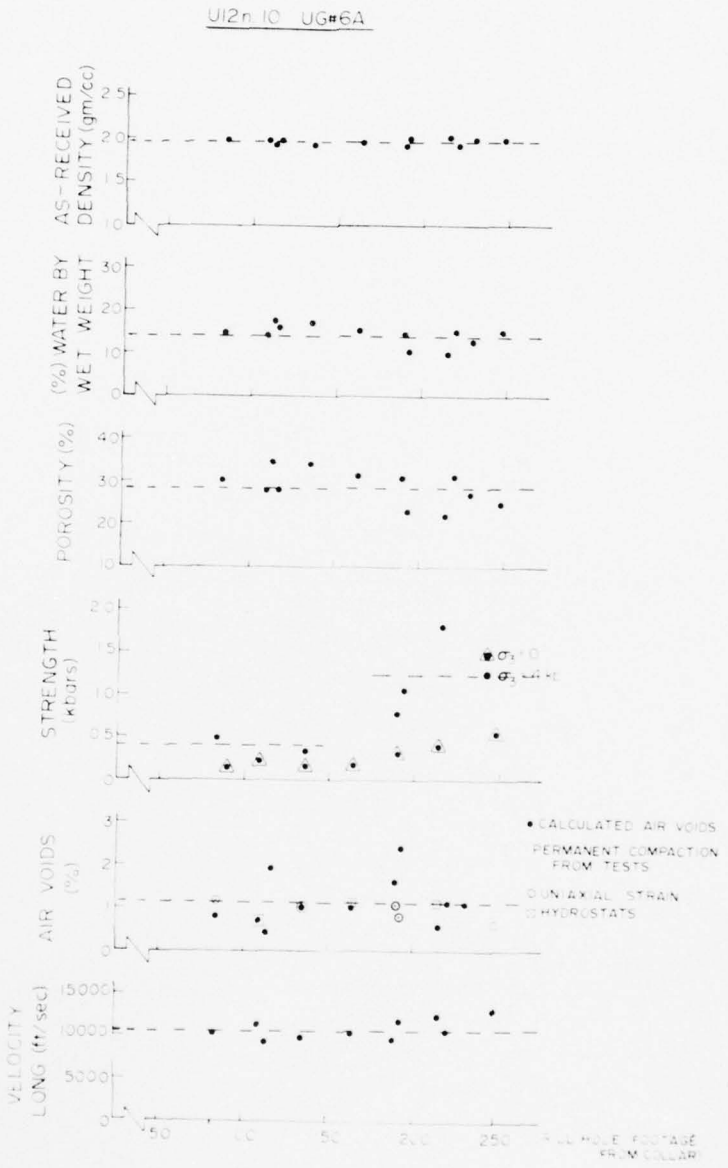

Figure 3. Selected Data from U12n.10 UG #6a Drill Hole Samples vs. the Footage Along the Drill Hole

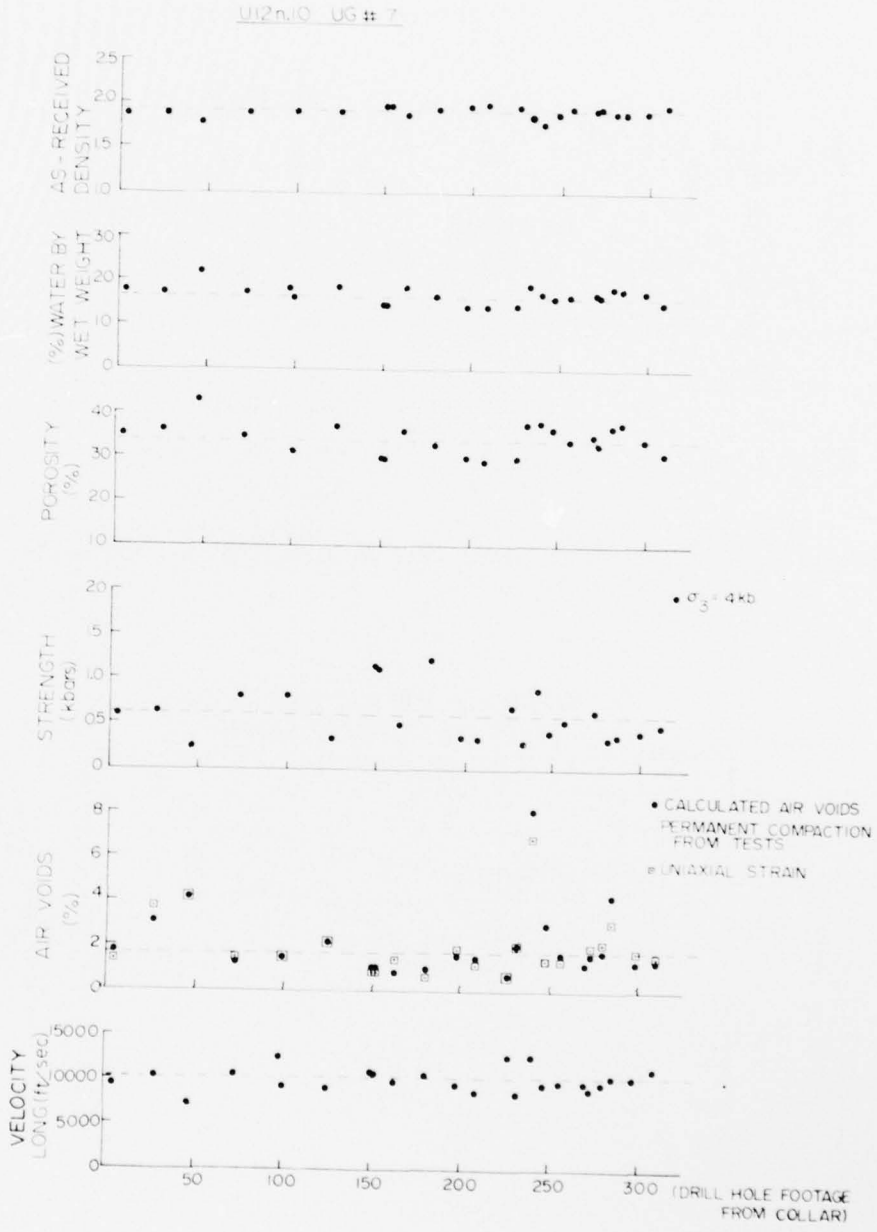

Figure 4. Selected Data from U12n.10 UG #7 Drill Hole Samples vs. the Footage Along the Drill Hole

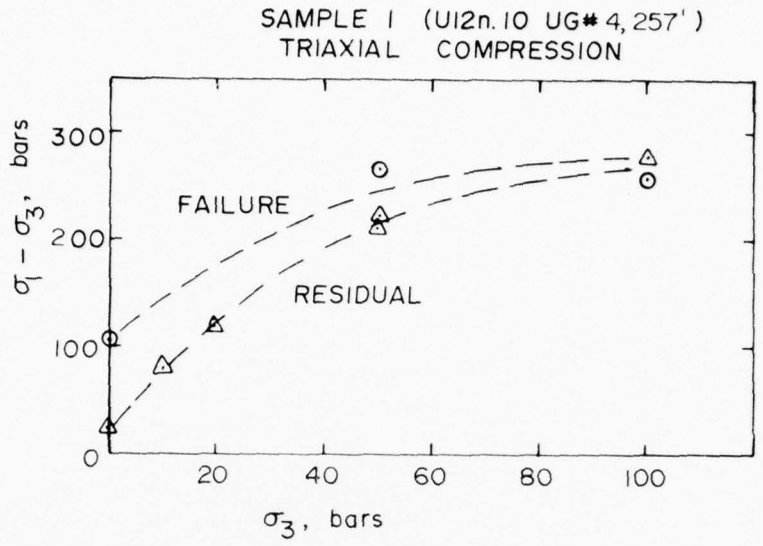

Figure 5. Triaxial Compression Test on U12n.10 UG #4,257' Sample

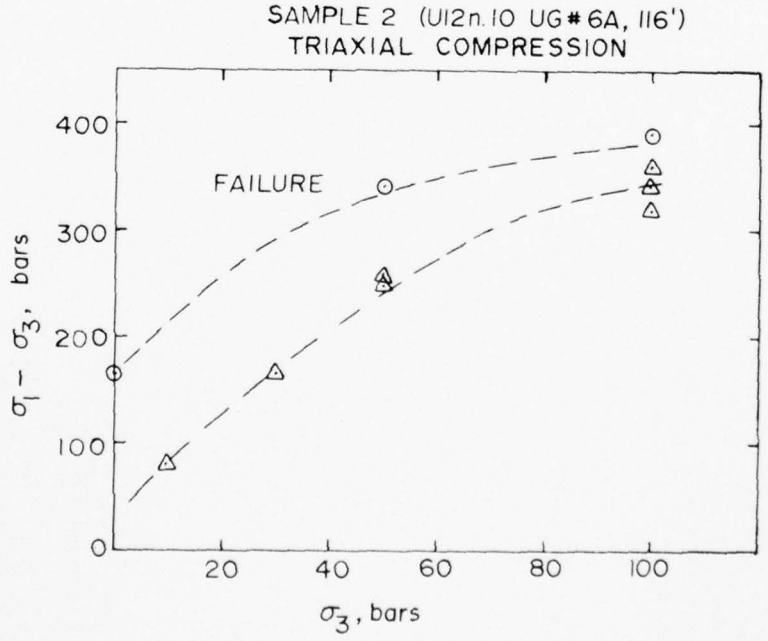

Figure 6. Triaxial Compression Test on U12n.10 UG #6a 116' Sample

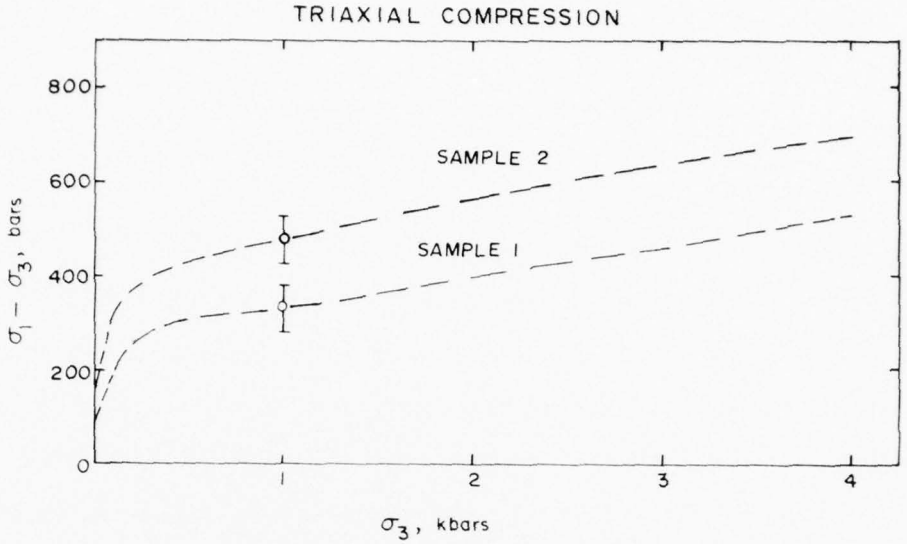

Figure 7. Triaxial Compression Test on U12n.10 UG #4 and U12n.10 UG #6a Samples

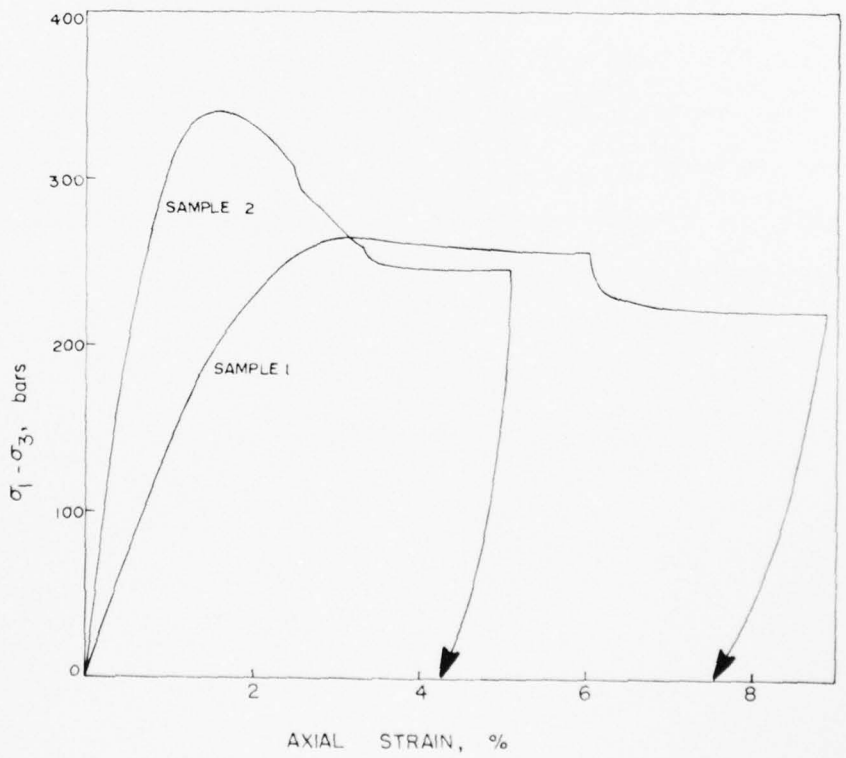

Figure 8. Stress-Strain Response on U12n.10 UG #4 and U12n.10 UG #6a Samples at a Confining Pressure of 50 Bars

DISCUSSION

The material properties show trends expected as the various lithological beds are penetrated by the drill holes. However, the Mighty Epic regions portrayed by the UG #4, UG #6a and UG #7 drill holes, on the average, indicate higher as-received densities, shear strengths and ultrasonic velocities (Figures 2, 3 and 4) than "typical" ash fall tuff [1,2]. The porosities, air void contents and water contents are about the same.

The triaxial compression tests on the two samples from UG #4 and UG #6a (Figures 5-8) were for the purpose of estimating the tuff failure envelope for comparison to grout mixtures. The difficulties in producing a "tuff matching" grout is in matching the failure envelope over a range of pressure. The grout tends to show lower strength increase with pressure than the tuff.

Additional triaxial compression tests are planned on selected samples to further characterize the tuff material in the immediate vicinity of the structures experiments.

REFERENCES

1. Butters, S. W., Nielsen, R. N., Jones, A. H., Green, S. J., "Mechanical & Physical Properties of Nevada Test Site Tuffs and Grouts from Exploratory Drill Holes", Terra Tek Report TR 73-69, December, 1973.

2. Butters, S. W., Johnson, J. N., Green, S. J., "The Mechanical Behavior of NTS Grout", Terra Tek Report TR 74-40, August, 1974.

APPENDIX

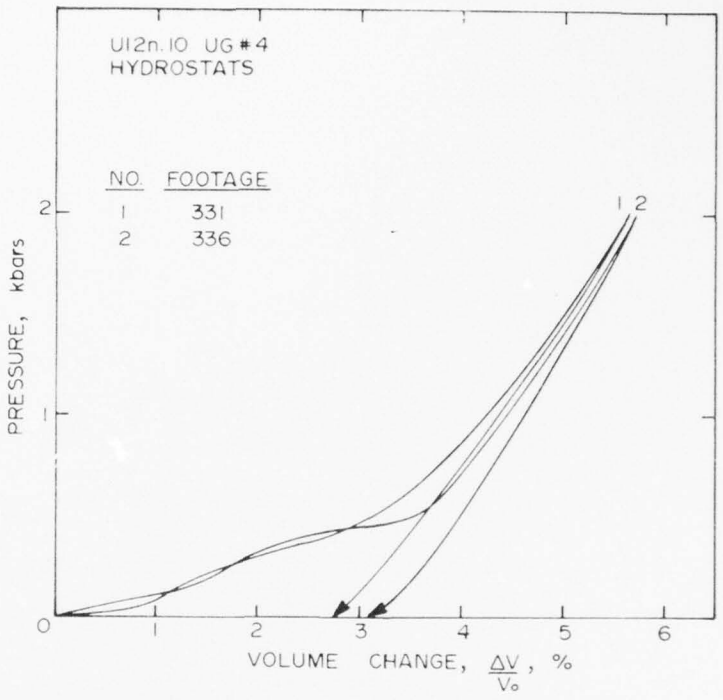

Hydrostatic Compression, U12n.10 UG #4

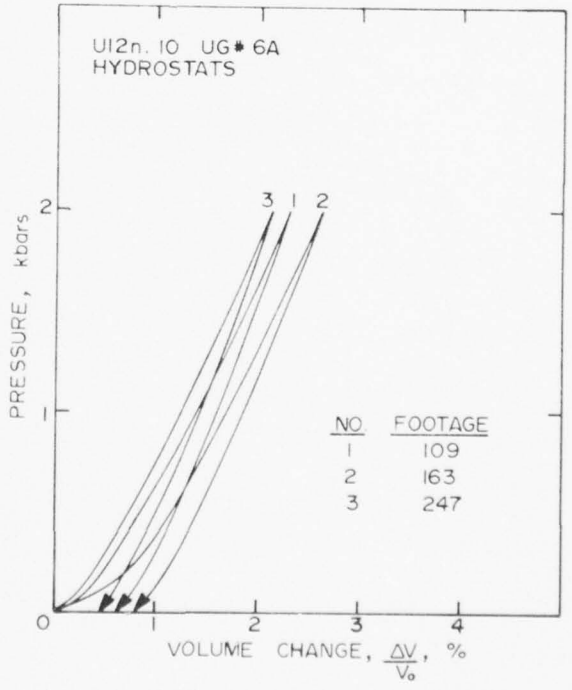

Hydrostatic Compression, U12n.10 UG #6a

AD-A048 165 DEFENSE NUCLEAR AGENCY WASHINGTON D C F/G 18/3
HUSSAR SWORD SERIES. MIGHTY EPIC EVENT, CONSOLIDATED MIGHTY EPI--ETC(U)
APR 77 H L PIPER

UNCLASSIFIED DNA-POR-6962 ERDA-WT-6962 NL

2 OF 3
ADA
048165

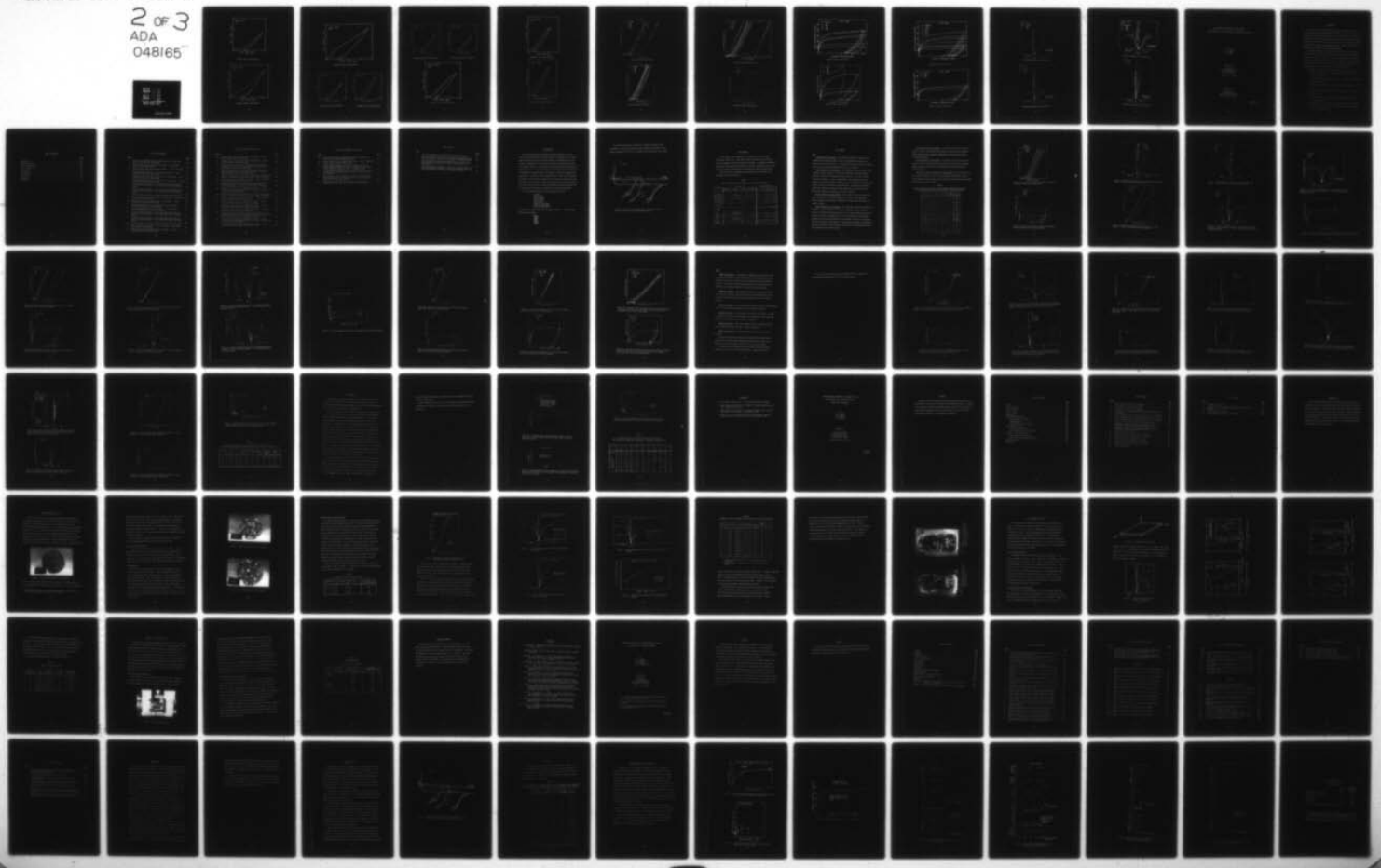

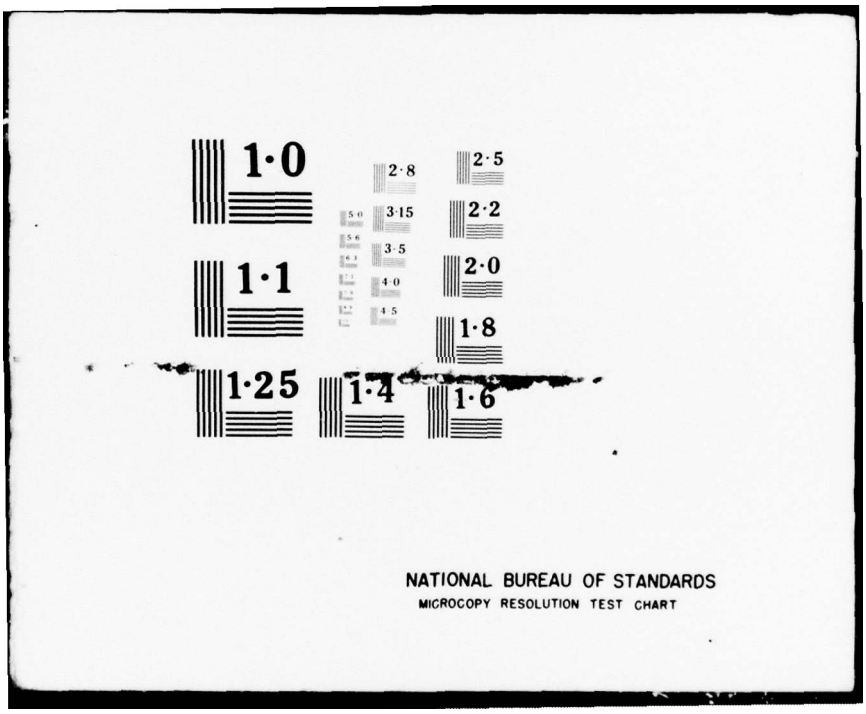
1·0
1·1
1·25
1·4
1·6
1·8
2·0
2·2
2·5
2·8
3·15
3·5
4·0
4·5
5·0
5·6
6·3
NATIONAL BUREAU OF STANDARDS
MICROCOPY RESOLUTION TEST CHART

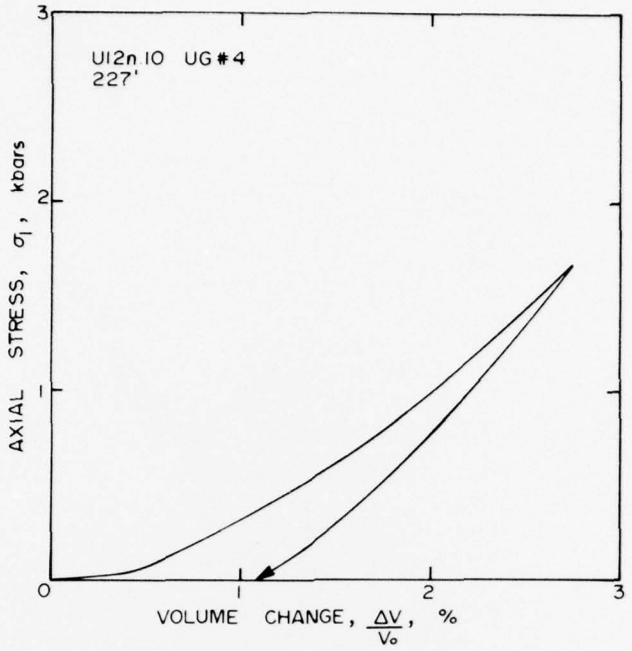

Uniaxial Strain, U12n.10 UG #4

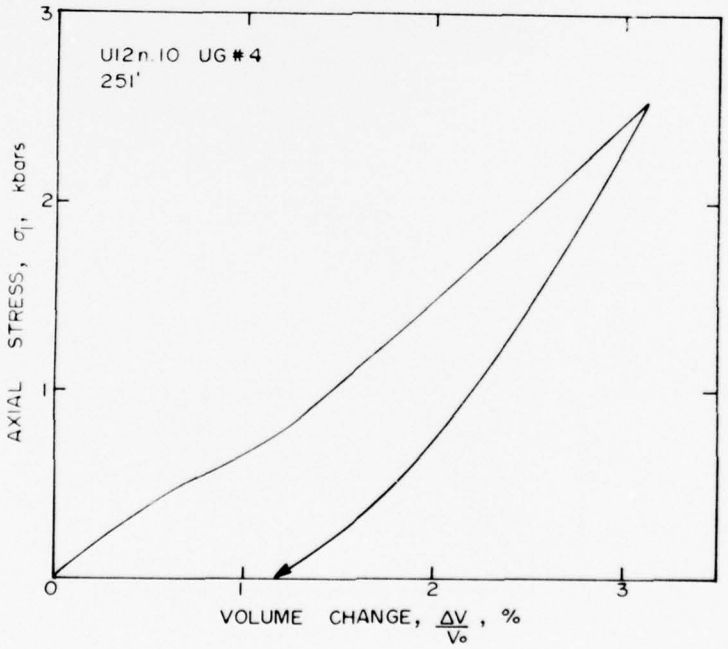

Uniaxial Strain, U12n.10 UG #4

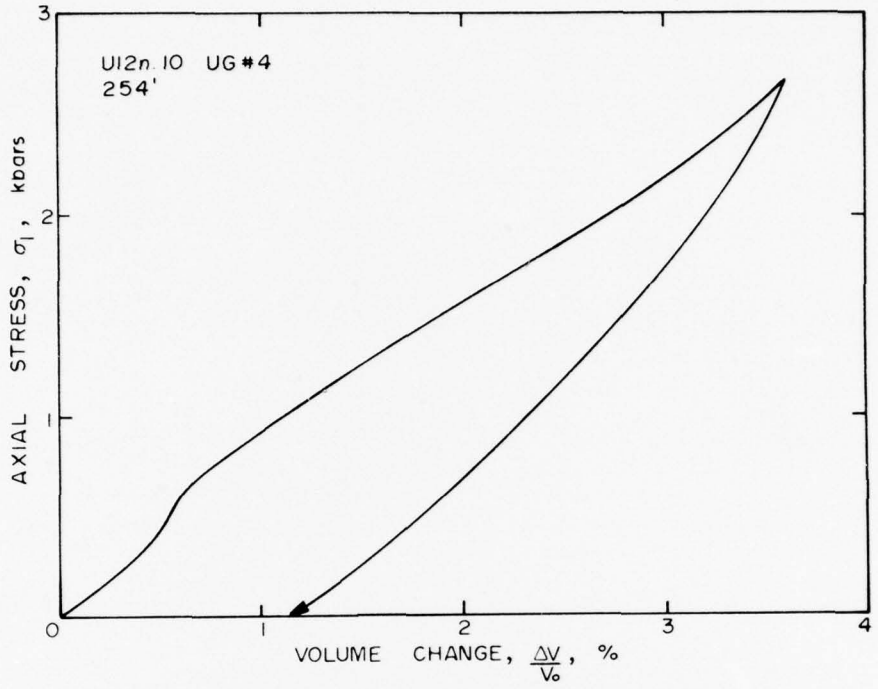

Uniaxial Strain, U12n.10 UG #4

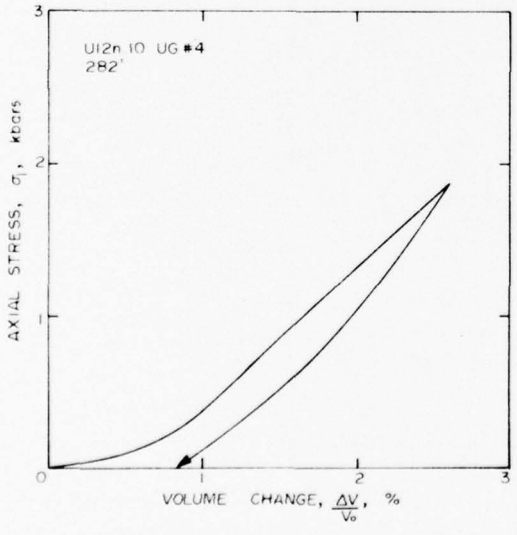

Uniaxial Strain, U12n.10 UG #4

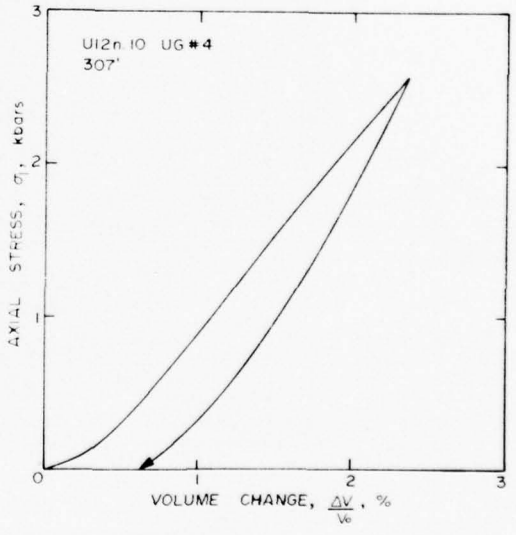

Uniaxial Strain, U12n.10 UG #4

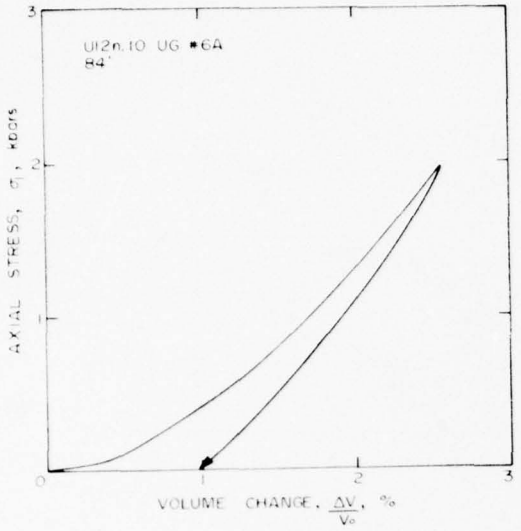

Uniaxial Strain, U12n.10 UG #6a

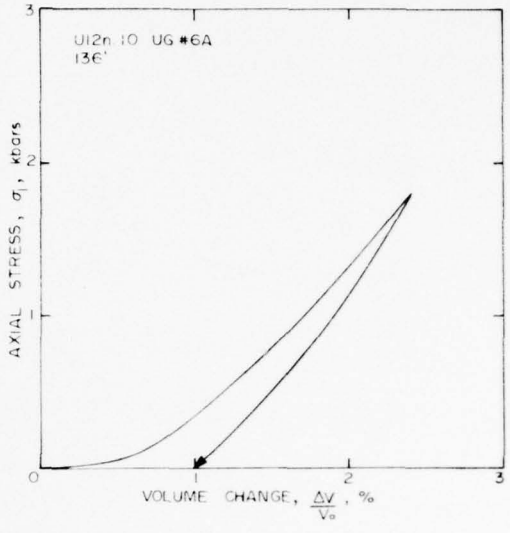

Uniaxial Strain, U12n.10 UG #6a

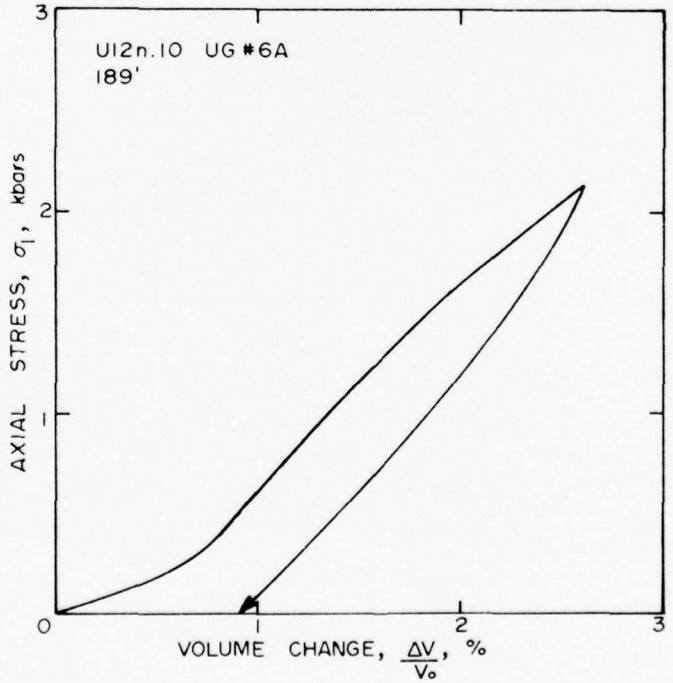

Uniaxial Strain, U12n.10 UG #6a

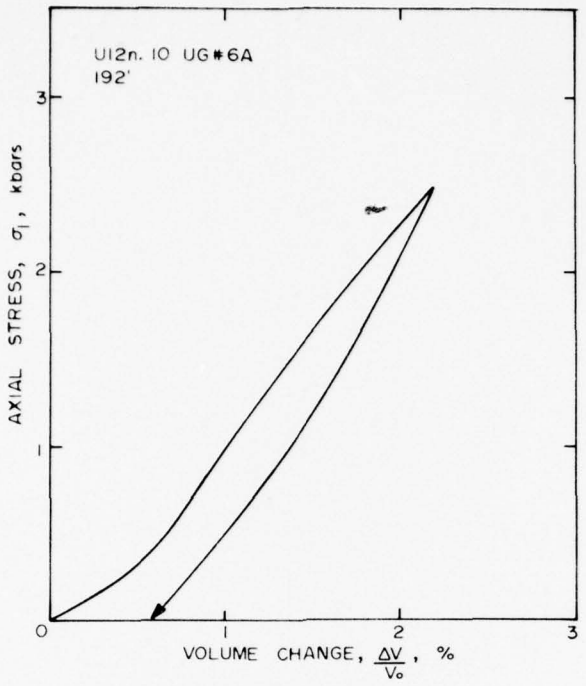

Uniaxial Strain, U12n.10 UG #6a

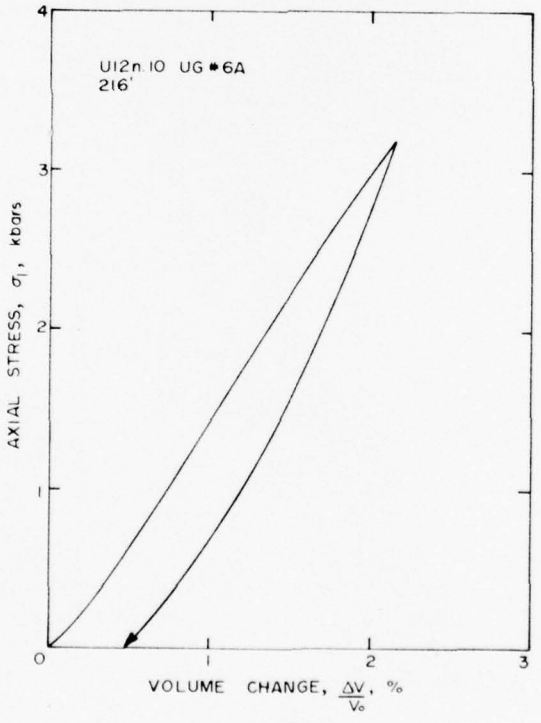

Uniaxial Strain, U12n.10 UG #6a

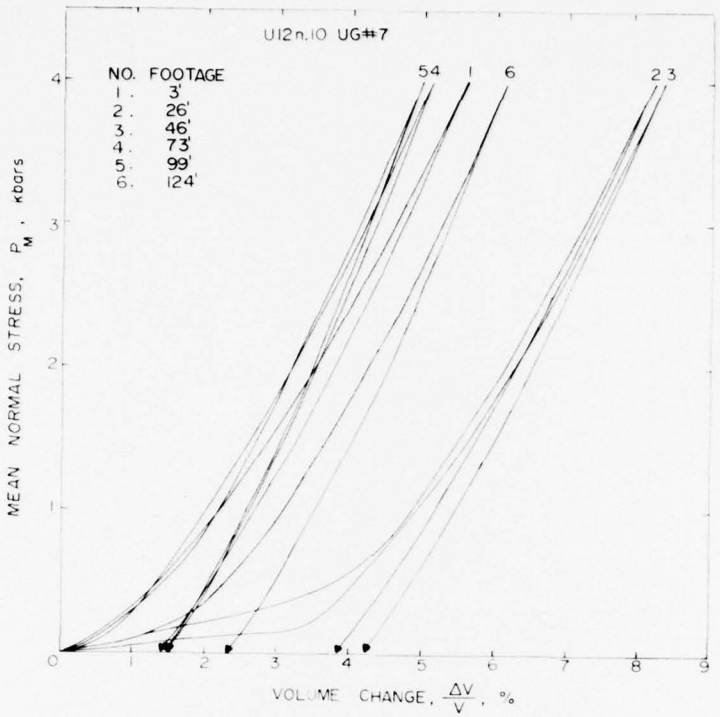

Uniaxial Strain, U12n.10 UG #7

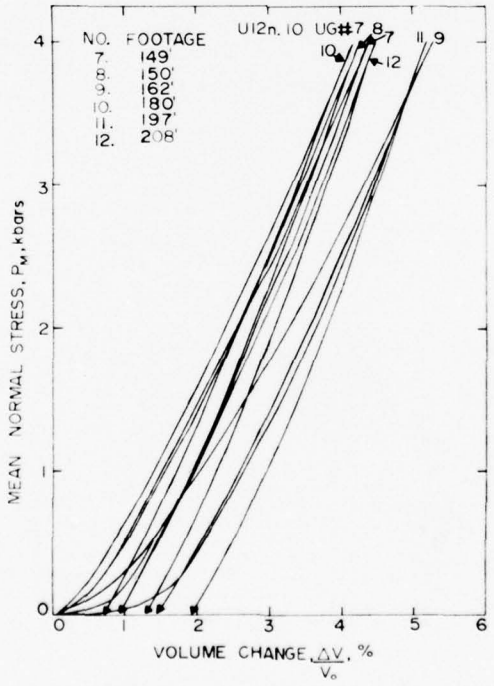

Uniaxial Strain, U12n.10 UG #7

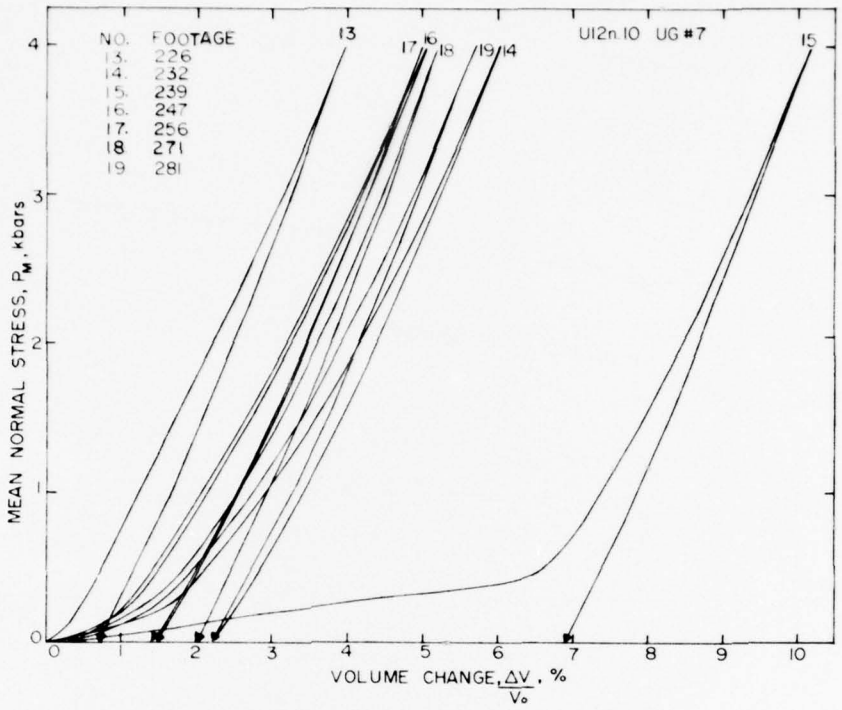

Uniaxial Strain, U12n.10 UG #7

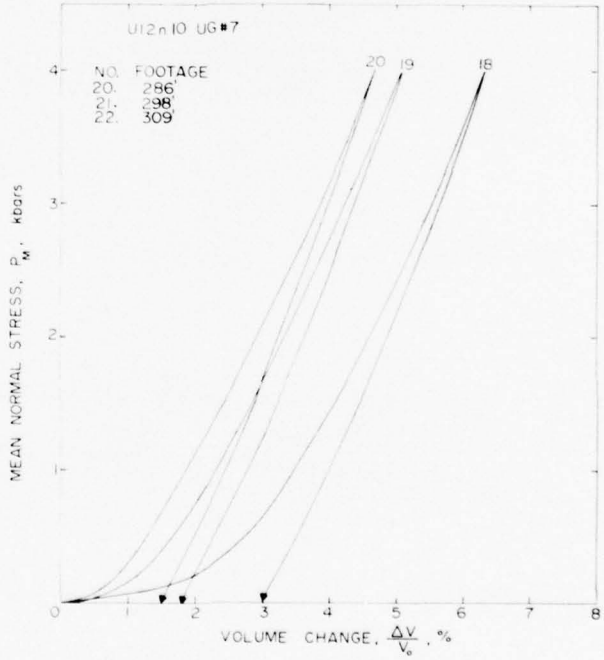

Uniaxial Strain, U12n.10 UG #7

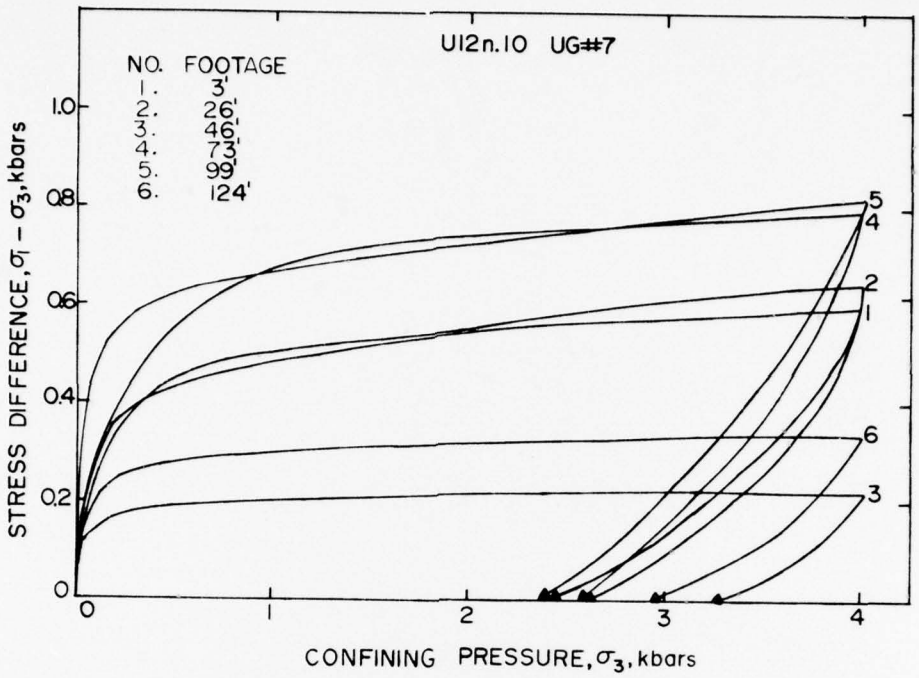

Uniaxial Strain, U12n.10 UG #7

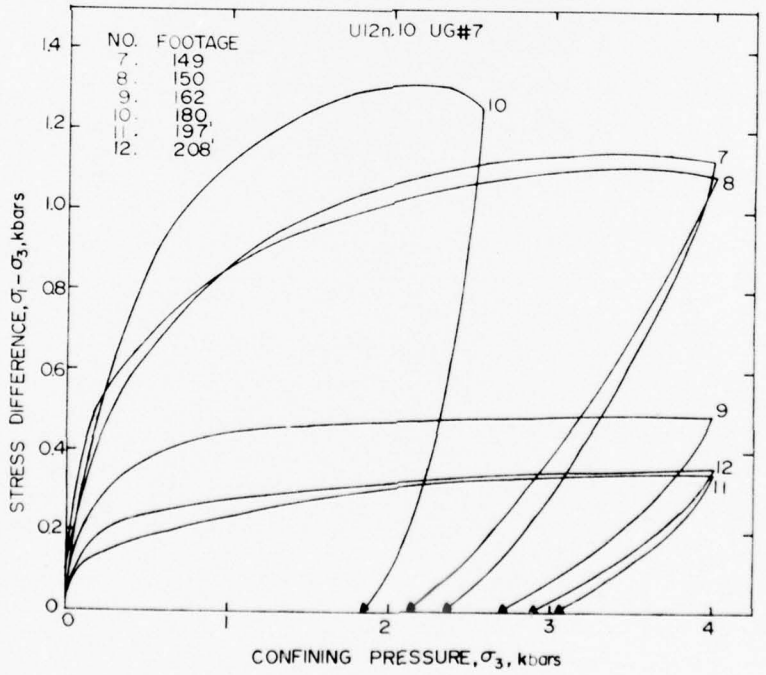

Uniaxial Strain, U12n.10 UG #7

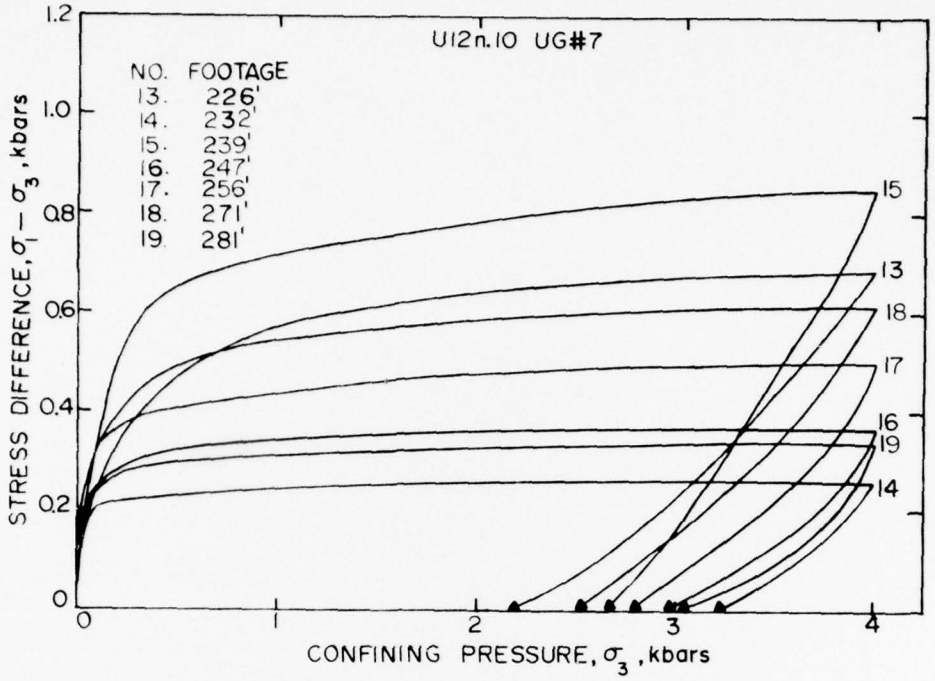

Uniaxial Strain, U12n.10 UG #7

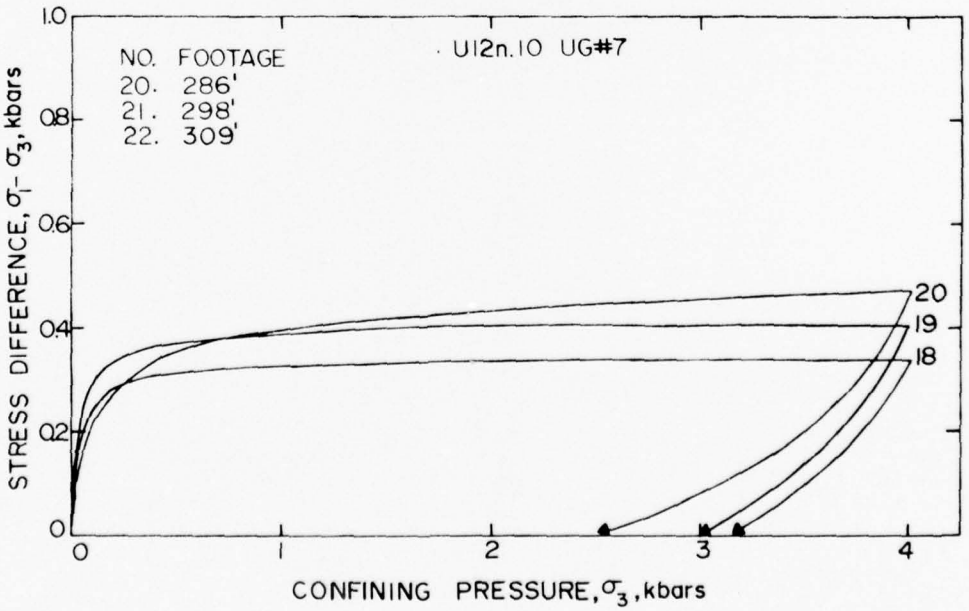

Uniaxial Strain, U12n.10 UG #7

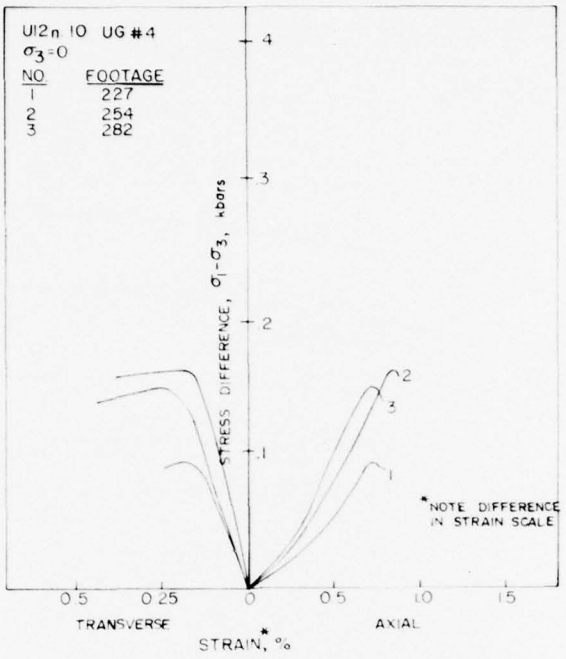

Unconfined Compression, U12n.10 UG #4

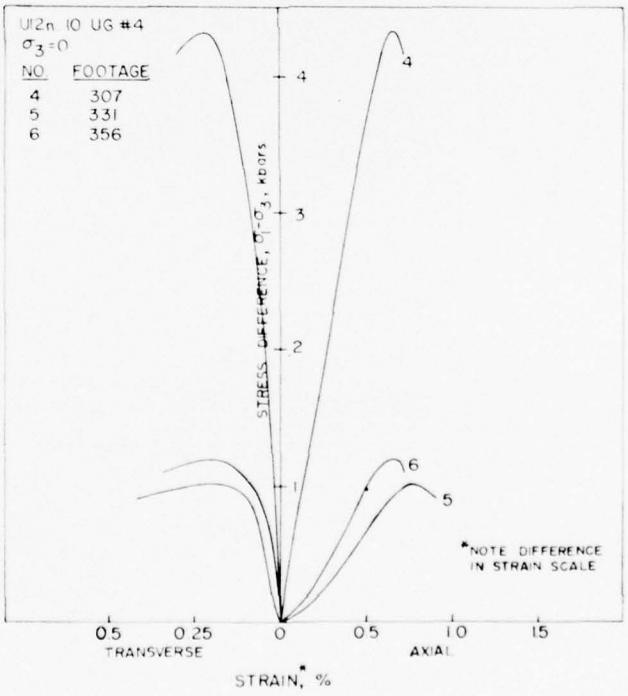

Unconfined Compression, U12n.10 UG #4

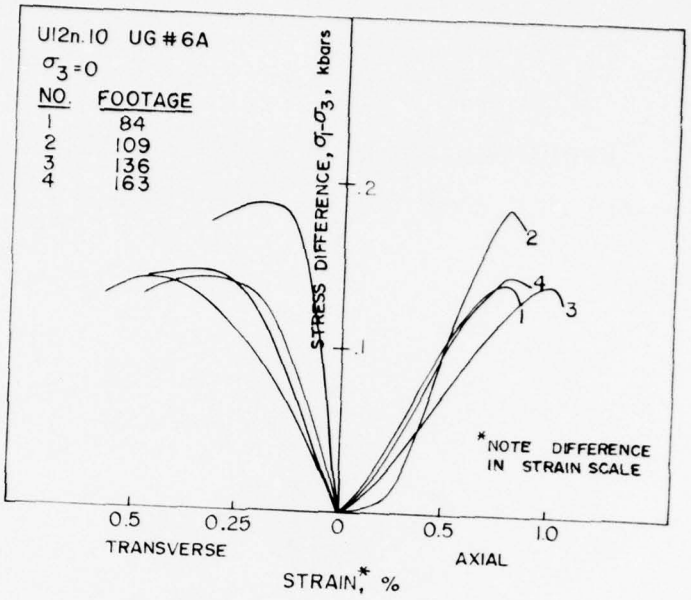

Unconfined Compression, U12n.10 UG #6a

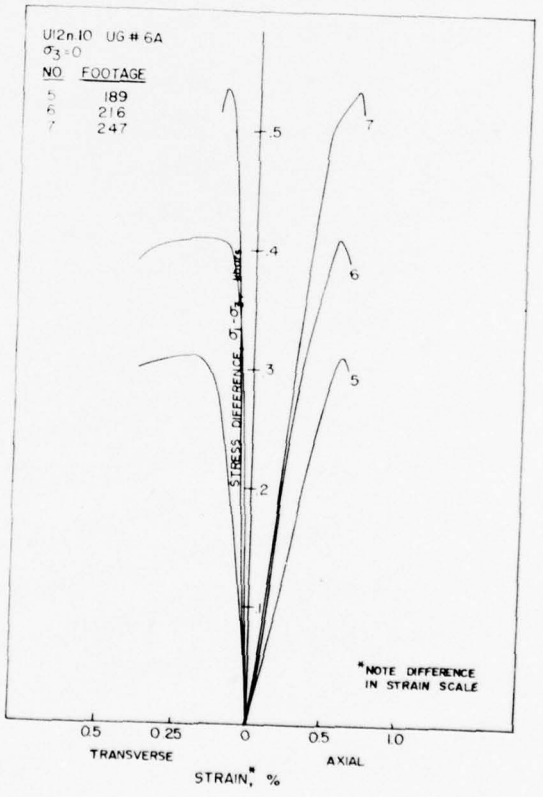

Unconfined Compression, U12n.10 UG #6a

SOME MATERIAL PROPERTIES ON CORE SAMPLES FROM SEVERAL DRILL HOLES RELATING TO THE MIGHTY EPIC EVENT

by

S. W. Butters
A. H. Jones
S. J. Green

Submitted to

Commander
Defense Nuclear Agency
Field Command
Mercury, NV 89023

Attn: J. W. LaComb

Submitted by

Terra Tek, Inc.
420 Wakara Way
University Research Park
Salt Lake City, UT 84108

TR 75-64
November 1975

BACKGROUND

In preparation for the Mighty Epic event at the Nevada Test Site, several studies have required material properties for the surrounding rock media (tuff) and several grout mixtures. The tuff material properties determined thus far have been from several drill holes[1] beginning with initial exploratory drill holes to more recent drill holes in the immediate vicinity of the working point and the structures studies. Material properties of several grout mixtures[2] have also been determined.

The material properties determined have been physical properties (as-received density, dry density, grain density, percentage water, porosity, saturation and air void content), mechanical properties (shear strength as a function of confining pressure), ultrasonic longitudinal and shear velocities and other properties such as the air void content estimated from the permanent compaction of the uniaxial strain load-unload tests.

The Mighty Epic related reports distributed to date are as follows:

1. Properties of Quartzite from Area 12 of the Nevada Test Site, TR 75-7, January, 1975.
2. Progress Report I - Material Properties for Mighty Epic Experiment, TR 75-36, June, 1975.
3. Determination of the Angle of Internal Friction, TR 75-38, July, 1975.
4. Progress Report II - Mighty Epic Material Properties, TR 75-42, August, 1975.
5. Physical and Mechanical Properties of Several Grout Mixtures, TR 75-45, August, 1975.
6. Progress Report III - Material Properties on Samples from Mighty Epic Drill Holes U12n.10 UG#4, U12n.10 UG#6a and U12n.10 UG#7, TR 75-50, September, 1975.

TABLE OF CONTENTS

LIST OF ILLUSTRATIONS

LIST OF ILLUSTRATIONS (Continued)

LIST OF ILLUSTRATIONS (Continued)

LIST OF TABLES

INTRODUCTION

As a continuing effort to determine material properties for site evaluation and development of material models for subsequent use in ground motion calculations, tests have been conducted to determine physical and mechanical properties of tuff and grout relating to the Mighty Epic event at the Nevada Test Site. The purpose of the laboratory testing program has been several fold: 1) initial evaluation of the global material properties, 2) development of material models for purposes of predicting stemming and containment, 3) prediction of the response across a soft to hard interface, 4) determine if the material properties are a function of distance from the tunnel wall (this question is related to the seismic velocities obtained in the field) and 5) to insure a proper match between the tuff properties and the emplaced grout properties surrounding the structures experiments.

Core samples were tested from the following drill holes:

UE12n#9
U12n.10 UG#7
U12n.10 ISS#1
U12n.10 ISS#5
U12n.10 HF#2
U12n.10 HF#4
U12n.10 A Structures
U12n.10 B Structures
U12n.10 C Structures

The locations of these drill holes are shown in Figure 1. Grout mixtures tested were designated:

ME801
ME802
ME804
ME805
ME806
ME8011

The tuff and grout data are reported in tabular and graphic form followed by a discussion which specifically addresses the question of the material properties of the tuff as compared to the properties of the grouts.

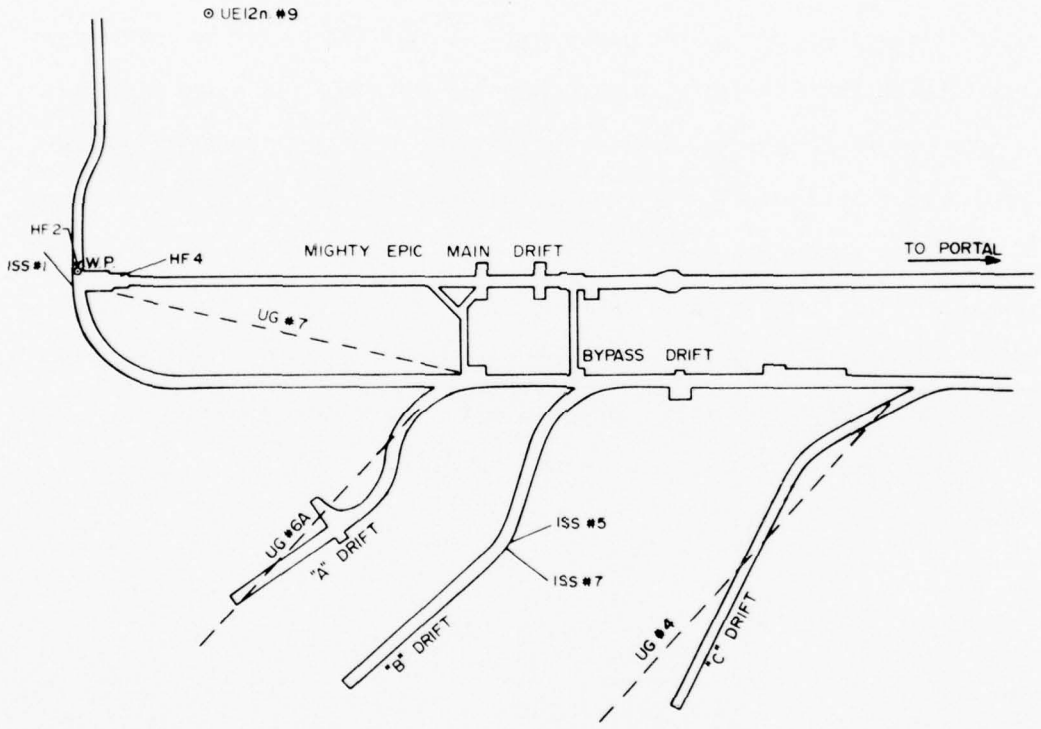

Figure 1: Plan view of the Mighty Epic area showing the drill holes from which core samples have been tested.

TEST PROGRAM

As discussed in the introduction, the purpose of the core sample testing was several fold. The types of tests, therefore, varied according to the purpose for which the data was intended. For example, the U12n.10 ISS#5 drill hole samples were subjected to triaxial compression tests since the shear strength of the material is important for the structural tests.

The types of tests conducted on the subject drill hole samples and the grout are listed in Table 1.

TABLE 1

Terra Tek Laboratory Test Program on Tuff and Grout Samples

DRILL HOLE	MECHANICAL TESTS				PHYSICAL PROPERTIES
TUFF	HYDROSTATIC COMPRESSION	TRIAXIAL COMPRESSION	UNIAXIAL STRAIN	ULTRASONIC VELOCITIES	AS REC, DRY AND GRAIN DENSITIES
UE12n#9		σ_3=0	X	X	X
U12n.10 UG#7	X	σ_3=0,0.5,4 kb		X	X
U12n.10 ISS#1			X	X	X
U12n.10 ISS#5	X	σ_3=0,0.5,4 kb		X	X
U12n.10 HF#2			X	X	X
U12n.10 HF#4			X	X	X
U12n.10 A,B,C structures			X	X	X
GROUT					
ME801	X	σ_3=0,0.1,0.25, 0.5,4 kb	X	X	X
ME802	X	σ_3=0,0.5,4 kb	X	X	X
ME804	X			X	X
ME805	X	σ_3=0.05,0.1, 0.5,1.0,4 kb		X	X
ME806	X			X	X
ME8011			X	X	X

TEST RESULTS

TUFF

UE12n#9 Drill Hole Samples: The physical properties, uniaxial strain permanent volume compaction and ultrasonic longitudinal and shear wave velocities are listed in Table 2. The uniaxial strain test curves are shown in Figure 2 and the unconfined compression results in Figure 3.

U12n.10 UG#7 Drill Hole Samples: The hydrostatic pressure-volume strain response is shown in Figure 4. The stress difference versus individual strains for the triaxial compression at pressures of 0, 0.5 and 4 kilobars are shown in Figures 5, 6 and 7, respectively. The strength of the core samples at these three confining pressure states are replotted in Figure 8 and indicate the failure surface for these materials. The physical properties, hydrostatic compression permanent volume compaction and ultrasonic longitudinal and shear wave velocities are listed in Table 2.

U12n.10 ISS#1 Drill Hole Samples: The uniaxial strain test curves are shown in Figure 9. The physical properties, uniaxial strain permanent volume compaction and ultrasonic longitudinal and shear wave velocities are listed in Table 2.

U12n.10 ISS#5 Drill Hole Samples: The hydrostatic pressure--volume strain response is shown in Figure 10. The stress difference versus individual strains for constant confining pressures of 0, 0.5 and 4 kilobars are shown in Figures 11, 12 and 13, respectively. Again the maximum stress differences obtained at these confining pressures are replotted in Figure 14 to indicate the failure surface for the material. The physical properties, the hydrostatic compression permanent volume compaction and ultrasonic longitudinal and shear wave velocities are listed in Table 2.

U12n.10 HF#2 Drill Hole Samples: The uniaxial strain test curves are shown in Figure 15 and the physical properties, uniaxial strain permanent volume compaction and ultrasonic longitudinal and shear wave velocities are listed in Table 2.

U12n.10 HF#4 Drill Hole Samples: The uniaxial strain test curves are shown in Figure 16 and the physical properties, uniaxial strain permanent volume compaction and ultrasonic longitudinal and shear velocities are listed in Table 2.

U12n.10 A, B and C Structures Drill Hole Samples: The uniaxial strain test curves are shown in Figure 17 and the physical properties, uniaxial strain permanent volume compaction and ultrasonic longitudinal and shear wave velocities are listed in Table 2.

TABLE 2

Physical Properties, Uniaxial Strain Permanent Volume Compaction and Ultrasonic Wave Velocities on Individual Tuff Samples Tested

DRILL HOLE FOOTAGE	DENSITY gm/cc			% WATER BY WET WEIGHT	POROSITY %	SATURATION %	% CALC AIR VOIDS	% MEAS PERMANENT COMP	VELOCITY ft/sec	
	AS RECEIVED	DRY	GRAIN						LONG	SHEAR
UE12n #9										
1130	1.77	1.37	2.39	22.6	43	93	2.9	2.8	9469	4226
1170	1.85	1.47	2.43	20.5	40	95	1.6	1.3	9459	4813
1224	1.82	1.41	2.44	22.0	42	95	2.0	2.2	10696	5794
1276	1.95	1.62	2.45	17.0	34	98	0.6	1.9	10217	4764
U12n.10 UG#7										
169	1.88	1.52	2.45	19.2	38	95	1.9		8668	4193
211	1.93	1.62	2.47	16.7	34	95	1.8		9482	4396
262	1.94	1.61	2.45	16.9	34	96	1.3		10003	4770
U12n.10 HF2										
9	2.04	1.77	2.44	13.1	27	97	0.8	0.6	12064	6483
16	2.08	1.83	2.46	12.4	27	97	0.7	0.8	10253	4587
29	1.91	1.58	2.43	17.4	35	95	1.8	1.2	10833	5371
U12n.10 HF4										
15	1.94	1.61	2.44	16.9	34	97	1.1	1.1	10249	4997
22	1.95	1.64	2.42	15.7	32	96	1.6	1.2	10308	5016
26	1.96	1.64	2.43	16.2	33	97	0.9	1.0	9980	4793
U12n.10 TSS#1										
5	1.96	1.64	2.44	16.6	33	99	0.4	0.6	11923	6752
19	1.95	1.63	2.43	16.2	33	96	1.4	1.3	11204	5892
20	1.99	1.62	2.46	17.0	34	98	0.8	0.8	11394	5981
27	1.85	1.51	2.42	18.4	38	91	3.4	3.5	9446	4758
28	1.80	1.44	2.42	21.2	41	93	4.2	4.8	9829	4393
U12n.10 TSS#5										
9	1.91	1.55	2.48	18.5	37	94	2.1		8960	4070
11	1.93	1.63	2.36	15.4	37	97	1.3		10760	4970
17	1.91	1.59	2.40	16.8	33	96	1.4		9380	4280
26	1.88	1.52	2.40	19.0	36	98	0.7		9390	4170
28	1.93	1.63	2.36	15.5	31	96	1.1		10190	4900
U12n.10 A Structure										
31	1.92	1.61	2.39	16.2	33	94	1.9	0.9	11206	6162
B Structure										
25	1.91	1.56	2.44	18.5	36	97	0.9	0.8	9567	4512
C Structure										
30	1.84	1.44	2.46	22.0	41	98	0.9	0.6	10801	5382

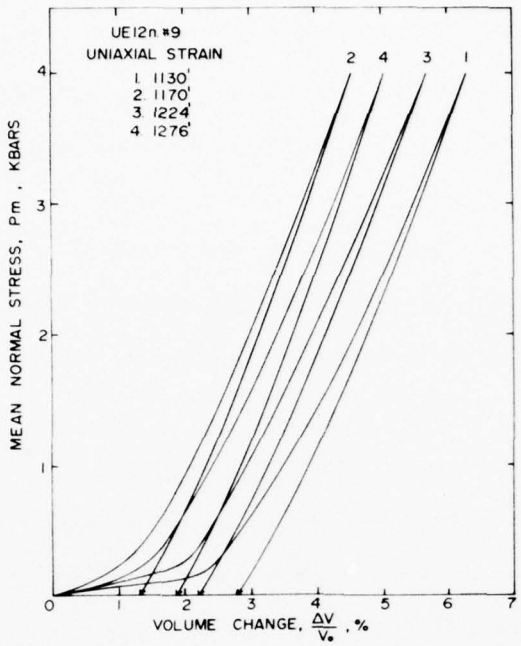

Figure 2a: Uniaxial strain tests on UE12n#9 core samples -- mean normal stress versus volume change.

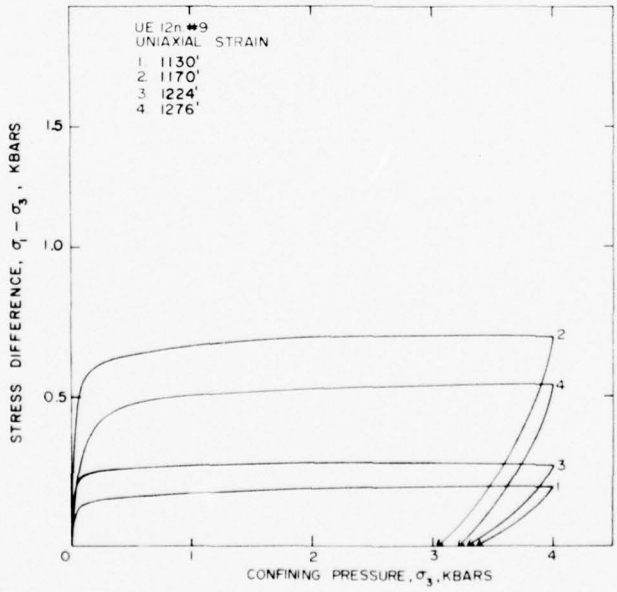

Figure 2b: Uniaxial strain tests on UE12n#9 core samples -- stress difference versus confining pressure.

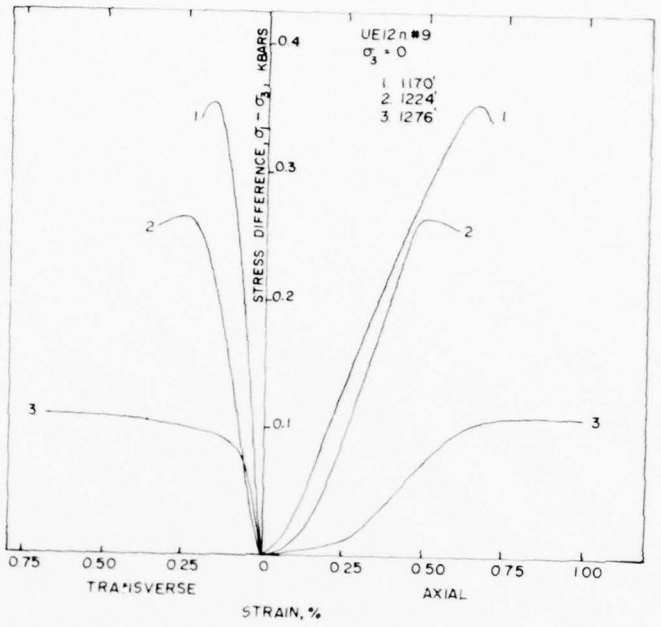

Figure 3: Unconfined compression tests on UE12n#9 core samples -- stress difference versus individual strains.

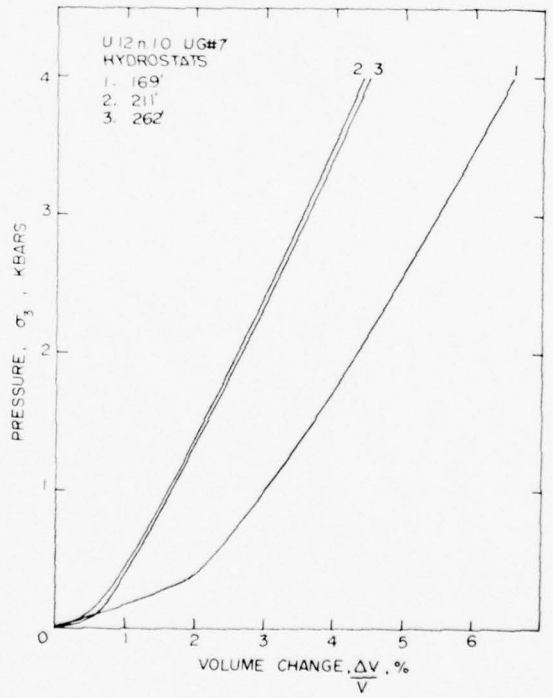

Figure 4: Hydrostatic compression test on U12n.10 UG#7 core samples -- confining pressure versus volume change.

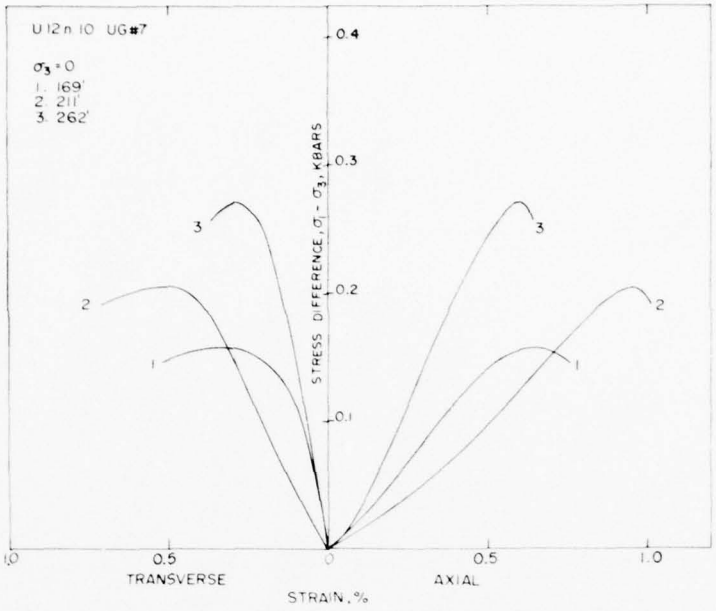

Figure 5: Unconfined compression tests on U12n.10 UG#7 core samples -- stress difference versus individual strains.

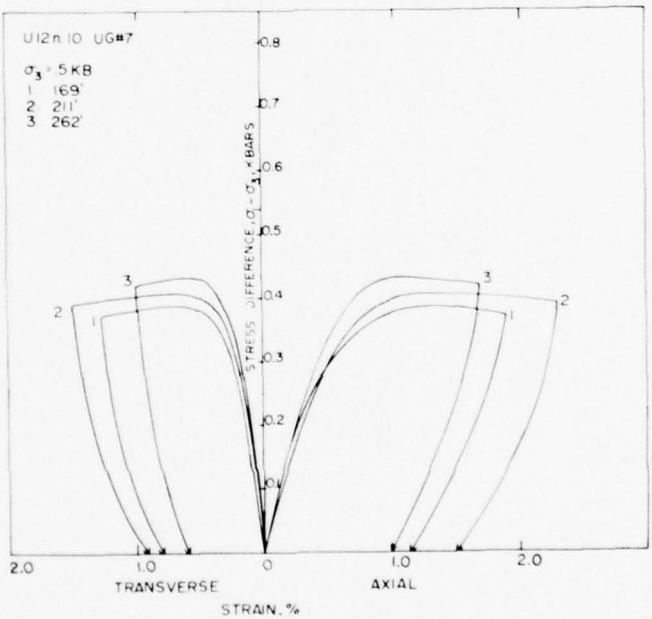

Figure 6: Triaxial compression tests at 0.5 kilobars confining pressure on U12n.10 UG#7 core samples -- stress difference versus individual strains.

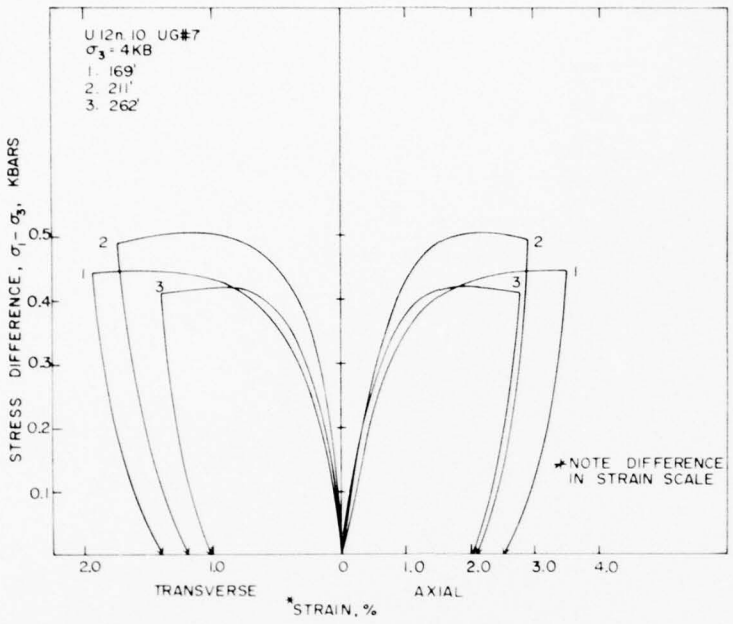

Figure 7: Triaxial compression tests at 4.0 kilobars confining pressure on U12n.10 UG#7 core samples -- stress difference versus individual strains.

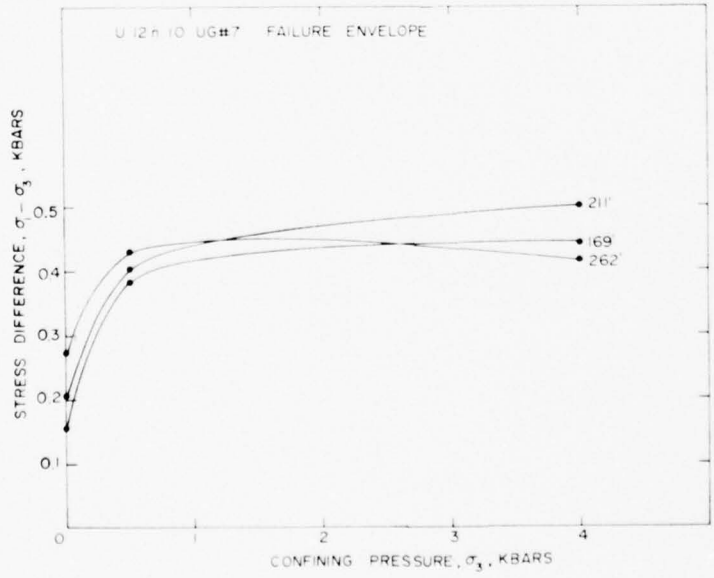

Figure 8: Failure envelope from triaxial compression tests on U12n.10 UG#7.

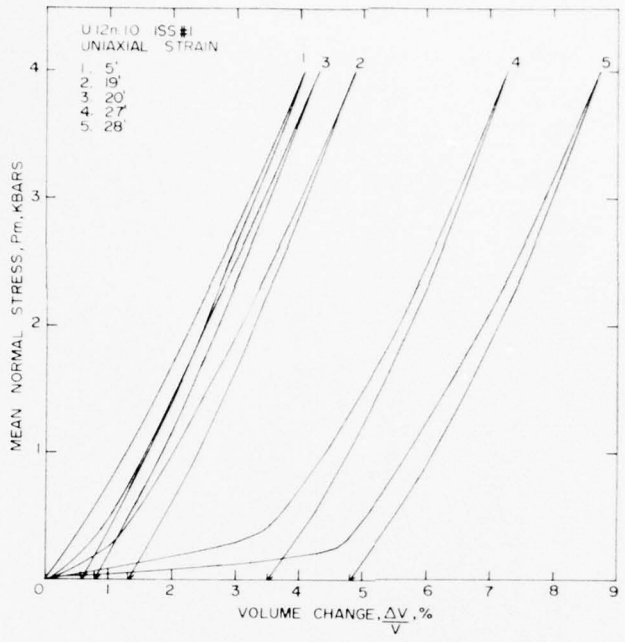

Figure 9a: Uniaxial strain tests on U12n.10 ISS#1 core samples -- mean normal stress versus volume change.

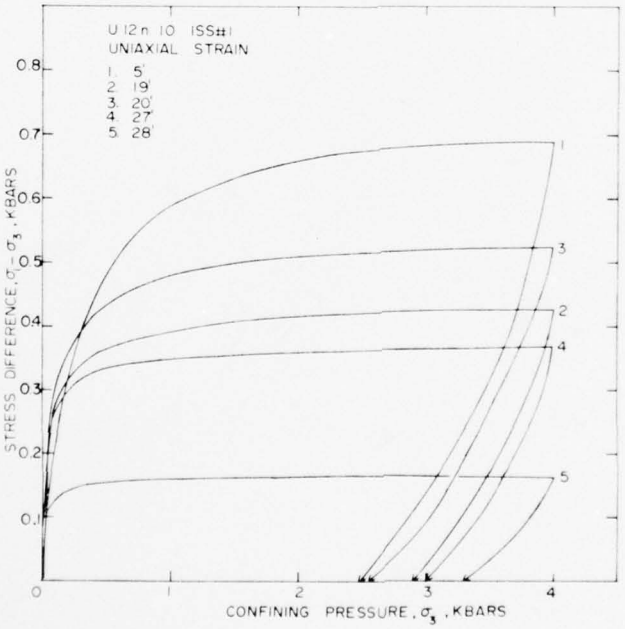

Figure 9b: Uniaxial strain tests on U12n.10 ISS#1 core samples -- stress difference versus confining pressure.

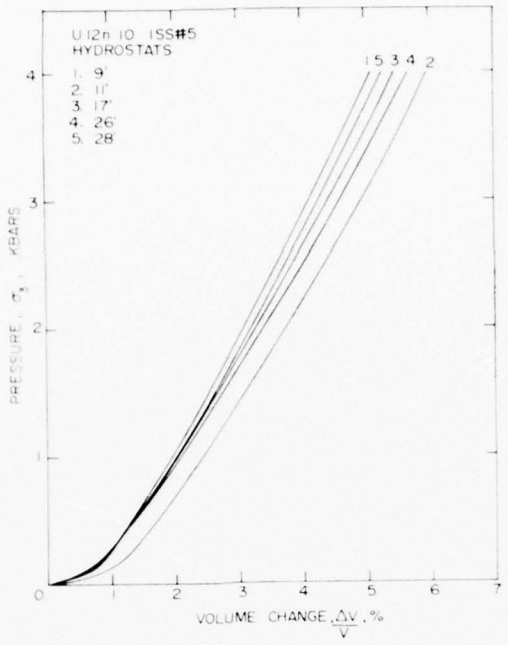

Figure 10: Hydrostatic compression tests on U12n.10 ISS#5 core samples -- confining pressure versus volume change.

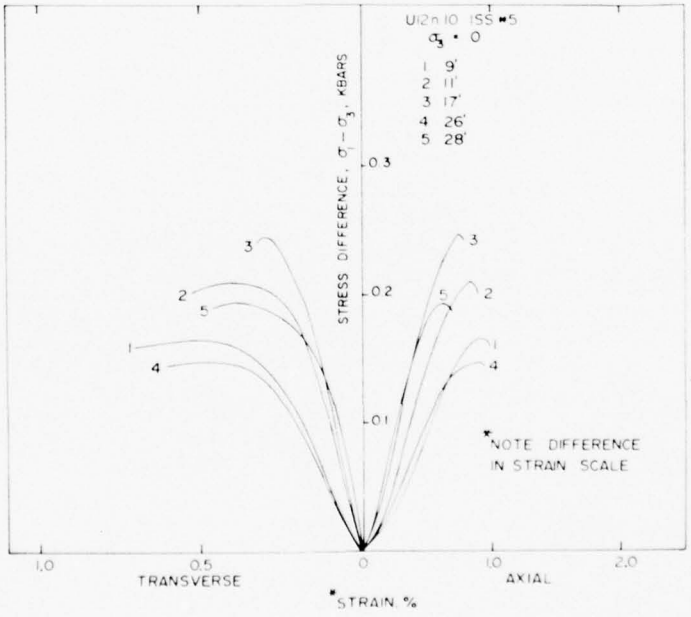

Figure 11: Unconfined compression tests on U12n.10 ISS#5 core samples -- stress difference versus individual strains.

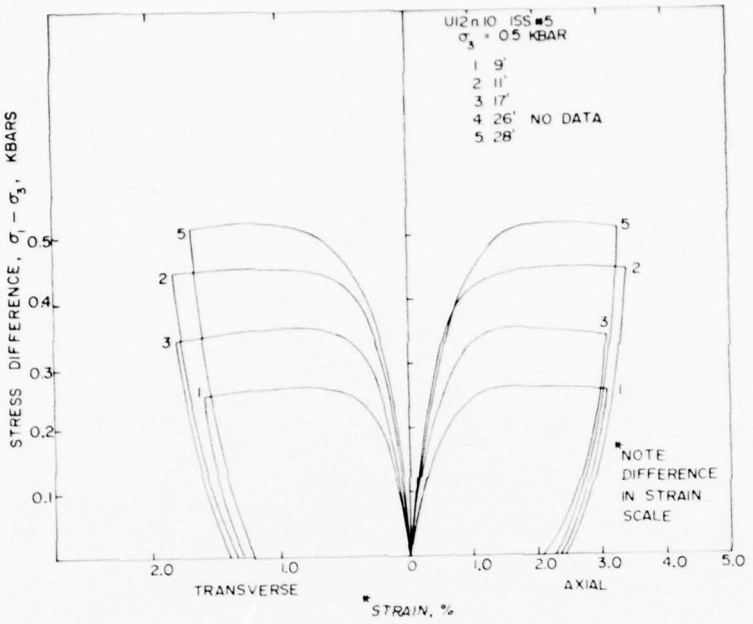

Figure 12: Triaxial compression tests at 0.5 kilobars confining pressure on U12n.10 ISS#5 core samples -- stress difference versus individual strains.

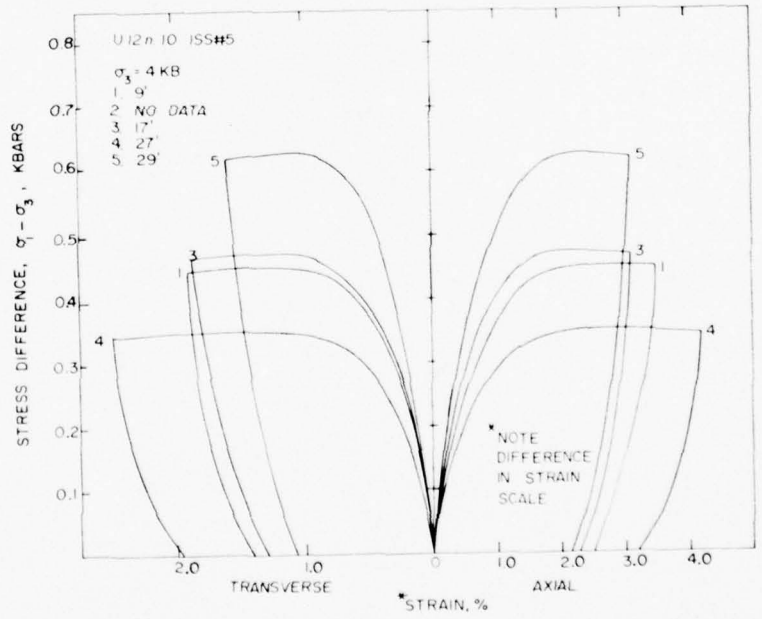

Figure 13: Triaxial compression tests at 4.0 kilobars confining pressure on U12n.10 ISS#5 core samples -- stress difference versus individual strains.

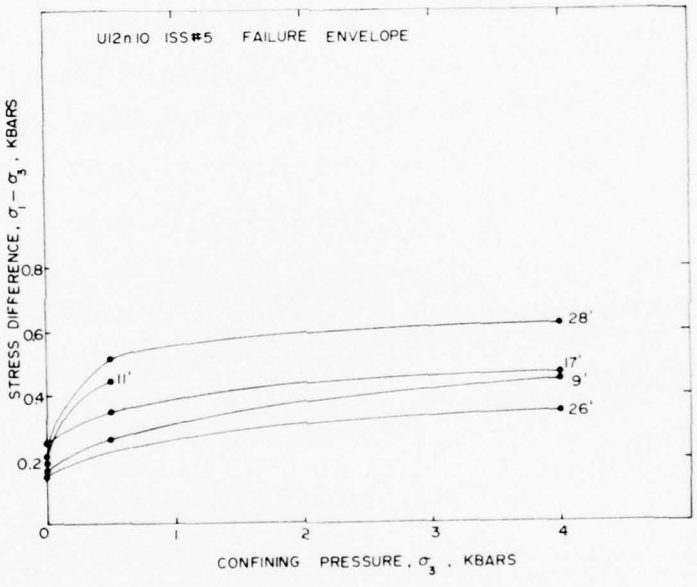

Figure 14. Failure envelope from triaxial compression tests on U12n.10 ISS#5.

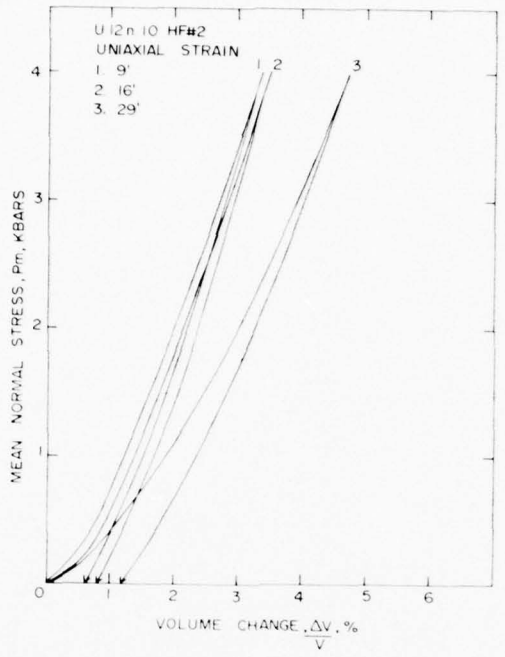

Figure 15a: Uniaxial strain tests on U12n.10 HF#2 core samples -- mean normal stress versus volume change.

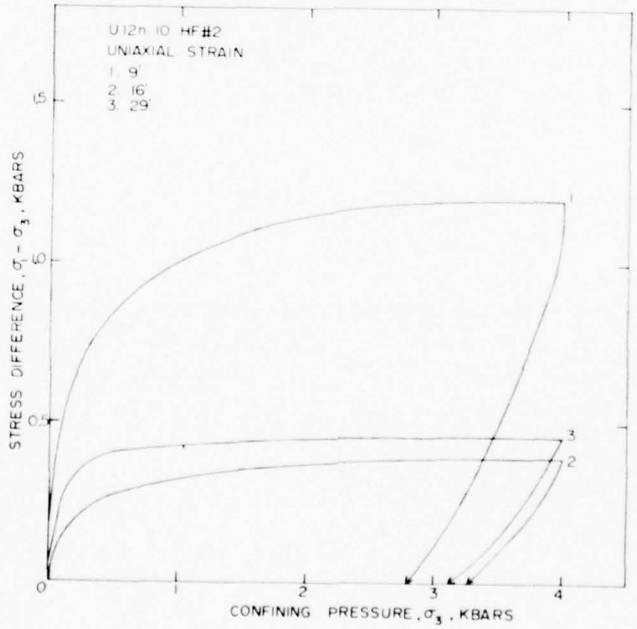

Figure 15b: Uniaxial strain tests on U12n.10 HF#2 core samples -- stress difference versus confining pressure.

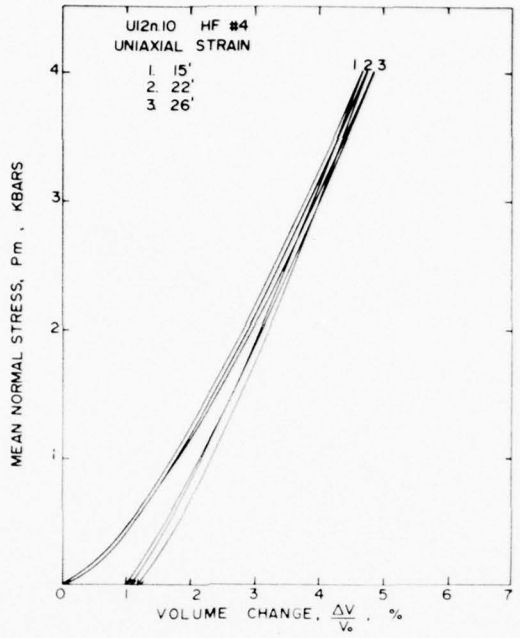

Figure 16a: Uniaxial strain tests on U12n.10 HF#4 core samples -- mean normal stress versus volume change.

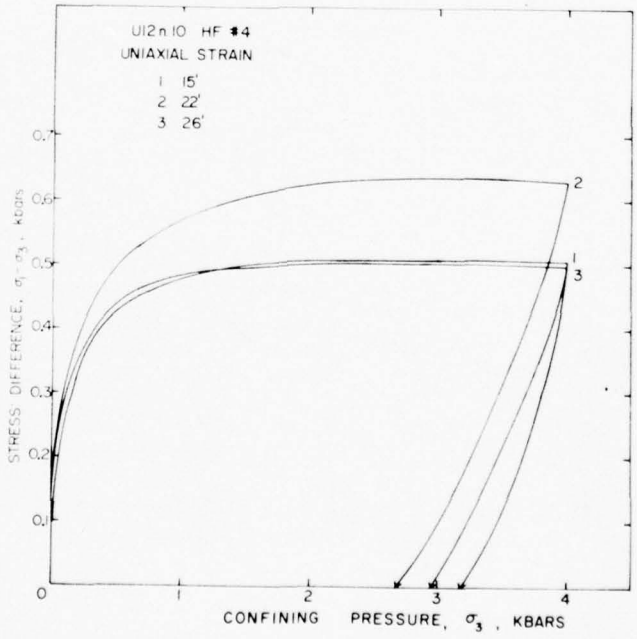

Figure 16b: Uniaxial strain tests on U12n.10 HF#4 core samples -- stress difference versus confining pressure.

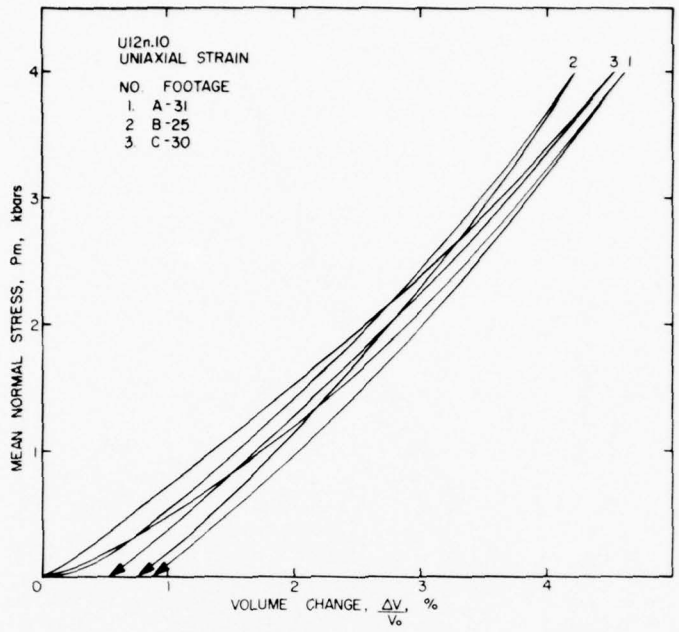

Figure 17a: Uniaxial strain tests on U12n.10 A Structures (31 feet), B Structures (25 feet) and C Structures (30 feet) core samples -- mean normal stress versus volume change.

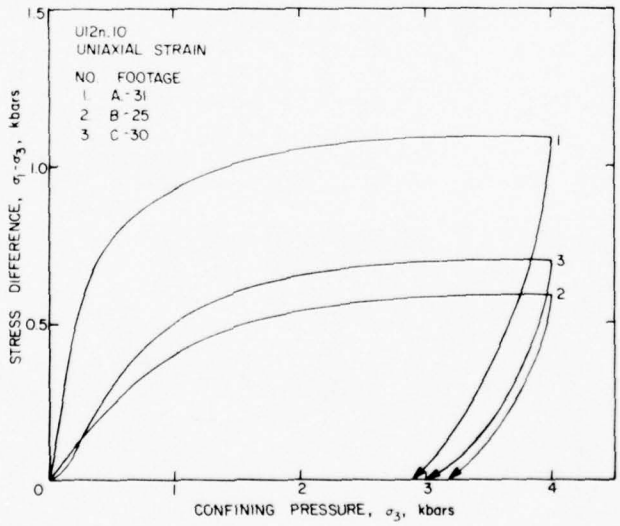

Figure 17b: Uniaxial strain tests on U12n.10 A Structures (31 feet), B Structures (25 feet) and C Structures (30 feet) core samples -- stress difference versus confining pressure.

GROUT

ME8Ø1 Grout Samples: The hydrostatic compression and uniaxial strain test curves are shown in Figure 18 while the stress difference versus the individual strain curves for the triaxial compression tests are shown in Figure 19. The failure surfaces based on the triaxial test data for the different grouts tested are shown at the end of this grout section.

ME8Ø2 Grout Samples: The hydrostatic compression and uniaxial strain test curves are shown in Figure 20 while the stress difference versus the individual strain curves for the triaxial compression tests are shown in Figure 21.

ME8Ø4 Grout Samples: The stress difference versus the axial and transverse strains for the unconfined compression test is shown in Figure 22.

ME8Ø5 Grout Samples: The hydrostatic compression test result is shown in Figure 23 while the stress difference versus individual strain curves for the triaxial compression tests are shown in Figure 24.

ME8Ø6 Grout Samples: The stress difference versus individual strains for the unconfined compression tests is shown in Figure 25.

ME8Ø11 Grout Samples: The uniaxial strain test curves are shown in Figure 26.

The physical properties, hydrostatic compression and uniaxial strain permanent volume compactions and ultrasonic longitudinal and shear wave velocities are listed in Table 3 for all of the six grout mixtures.

The maximum stress difference (failure surface) during the triaxial compression tests on the various grout mixtures is shown in Figure 27.

As a note, the grout data shown was obtained from tests conducted at the fourteen day aging point of all of the grout mixtures.

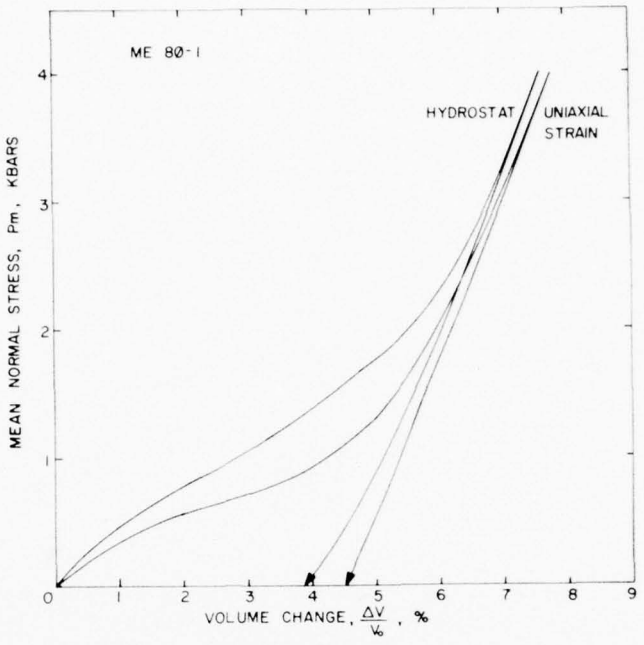

Figure 18a: Hydrostatic compression and uniaxial strain tests on ME801 grout samples -- mean normal stress versus volume change (14 day age).

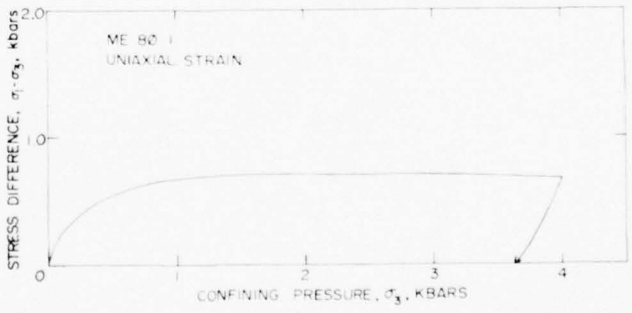

Figure 18b: Uniaxial strain test on ME801 grout sample -- stress difference versus confining pressure (14 day age).

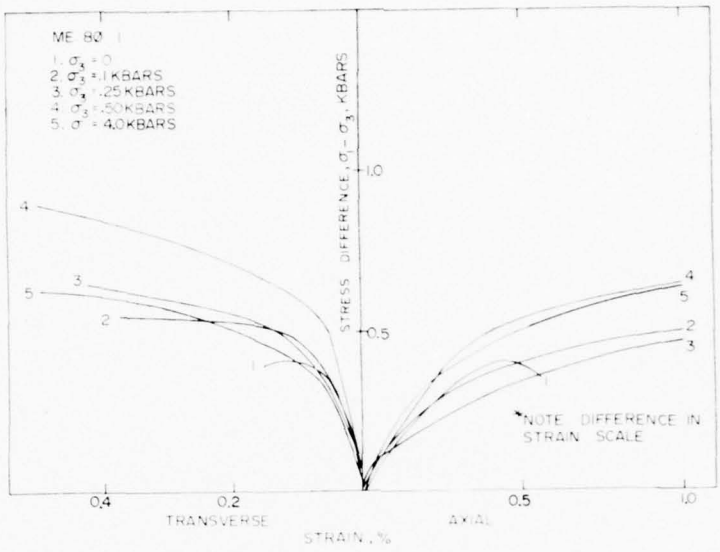

Figure 19a: Low stress-strain portion of the triaxial compression tests on ME80l grout samples -- stress difference versus individual strains (14 day age), see Figure 19b for entire test curves.

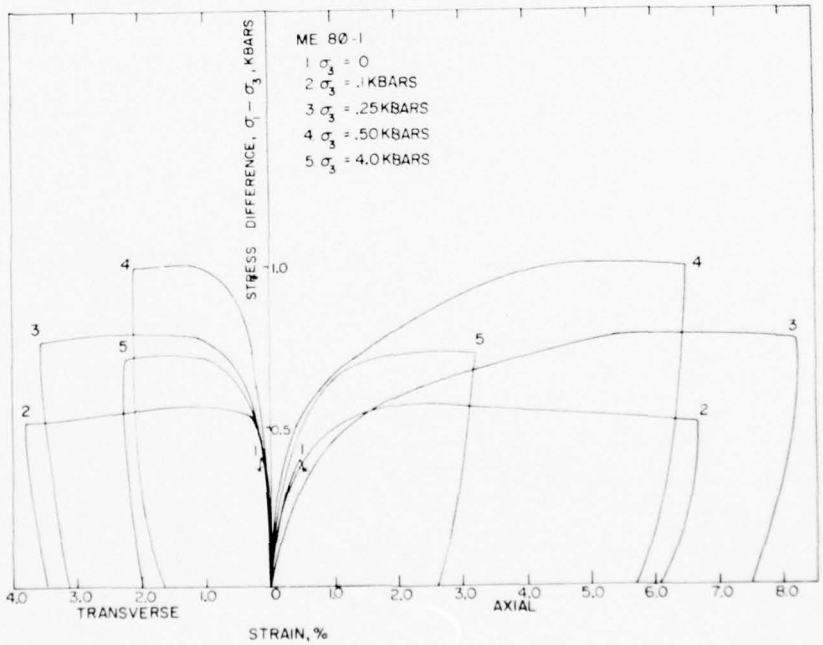

Figure 19b: Triaxial compression tests on ME80l grout samples -- stress difference versus individual strains (14 day age), see Figure 19a for low stress-strain response.

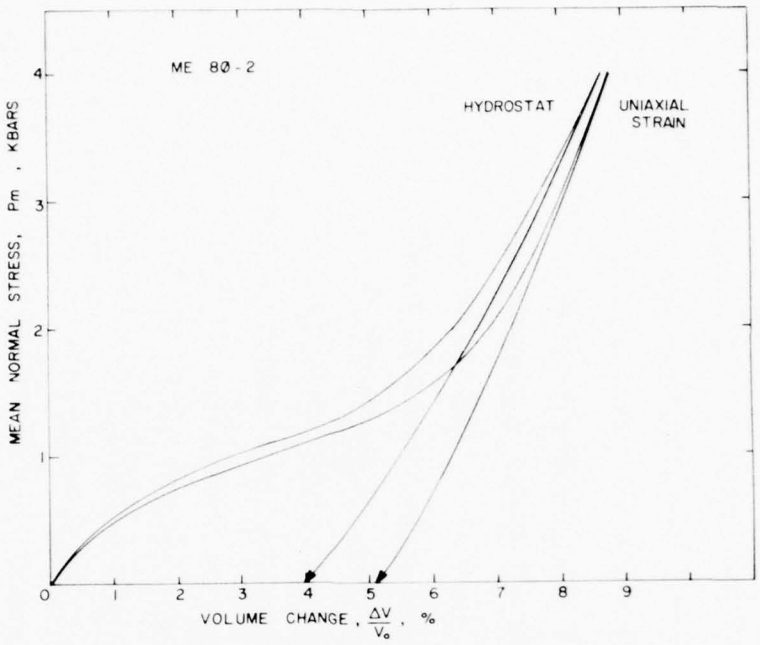

Figure 20a: Hydrostatic compression and uniaxial strain tests on ME8Ø2 grout samples -- mean normal stress versus volume change (14 day age).

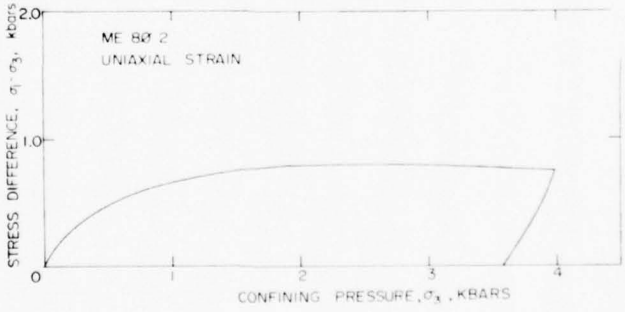

Figure 20b: Uniaxial strain test on ME8Ø2 grout sample -- stress difference versus confining pressure (14 day age).

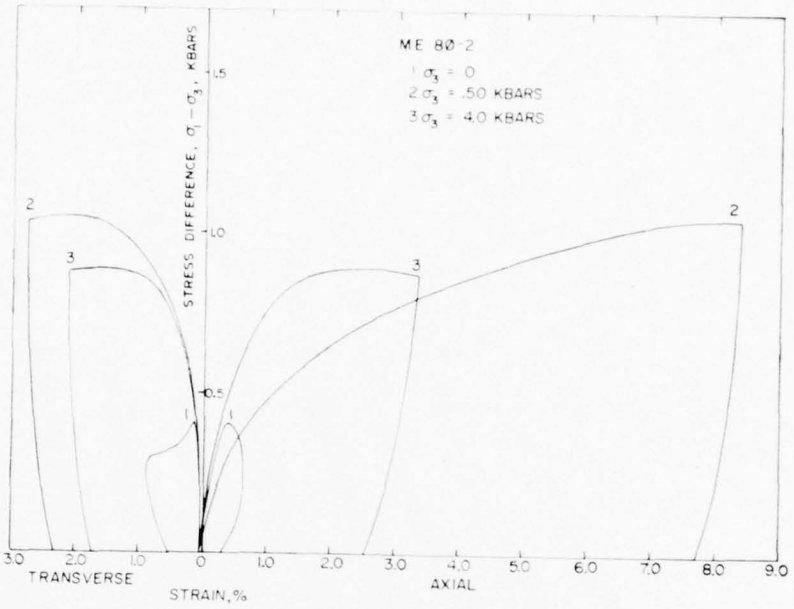

Figure 21: Triaxial compression tests on ME802 grout sample -- stress difference versus individual strains (14 day age).

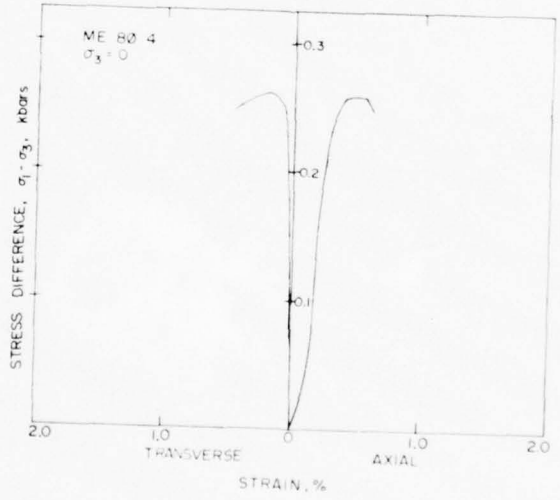

Figure 22: Unconfined compression test on ME804 grout sample -- stress difference versus individual strains (14 day age).

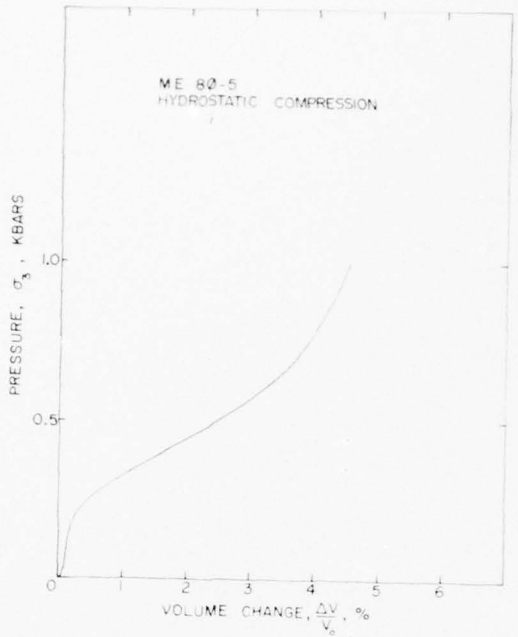

Figure 23: Hydrostatic compression test on ME8Ø5 grout sample -- confining pressure versus volume change (14 day age).

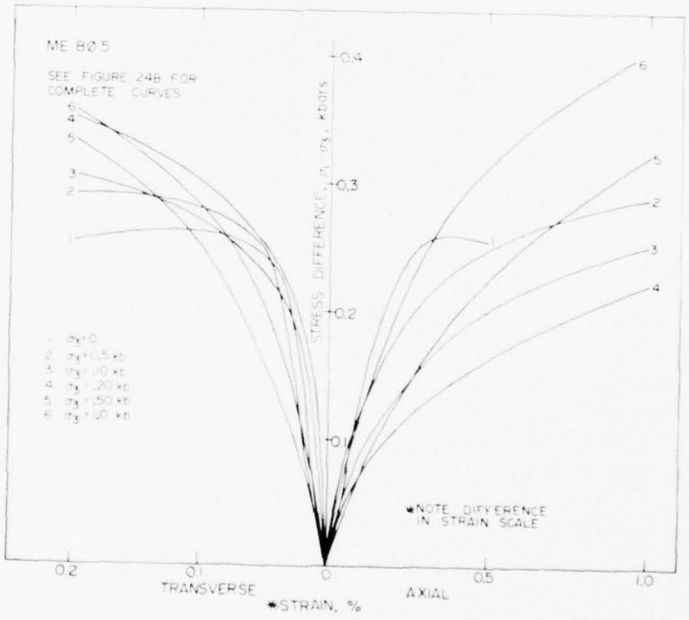

Figure 24a: Low stress-strain portion of the triaxial compression tests on ME8Ø5 grout samples -- stress difference versus individual strains (14 day age), see Figure 24b for entire test curves.

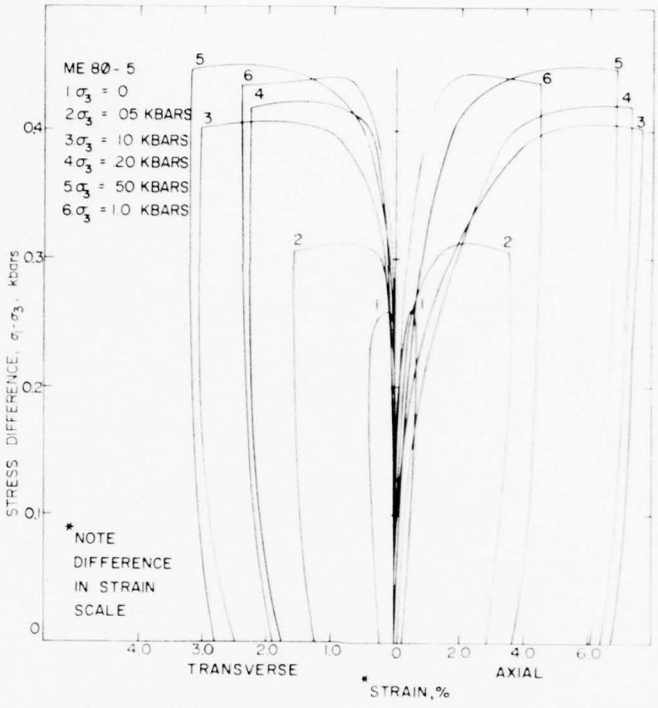

Figure 24b: Triaxial compression tests on ME805 grout samples -- stress difference versus individual strains (14 day age), see Figure 24a for low stress-strain response.

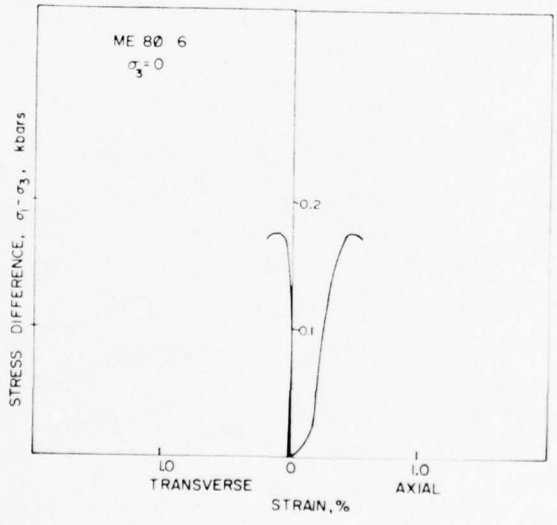

Figure 25: Unconfined compression tests on ME806 grout sample -- stress difference versus individual strains (14 day age).

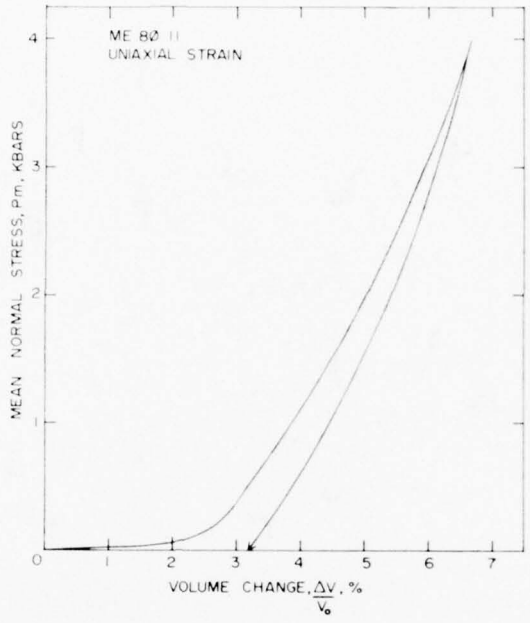

Figure 26a: Uniaxial strain tests on ME8Ø11 grout sample -- mean normal stress versus volume change (14 day age).

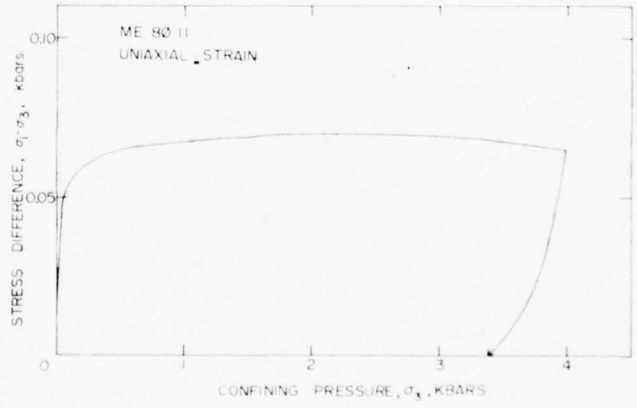

Figure 26b: Uniaxial strain tests on ME8Ø11 grout sample --stress difference versus confining pressure (14 day age).

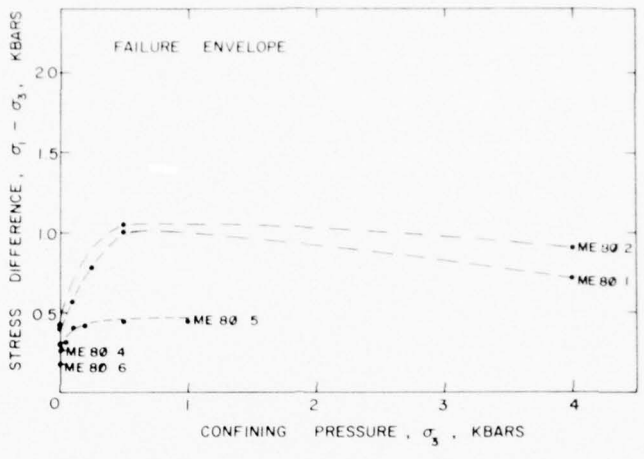

Figure 27: Failure envelope based on the triaxial compression tests on ME801, ME802 and ME305 grout samples (14 day age). Also shown is the unconfined compression tests on ME804 and ME806.

TABLE 3

Physical Properties, Hydrostatic Compression and Uniaxial Strain Permanent Volume Compaction and Ultrasonic Wave Velocities on Grout Samples

DRILL HOLE FOOTAGE	DENSITY gm/cc			% WATER BY WET WEIGHT	POROSITY %	SATURATION %	% CALC. AIR VOIDS	% MEAS. PERMANENT COMP.		VELOCITY ft/sec	
	AS-RECEIVED	DRY	GRAIN					Hyd.	1-D	LONG	SHEAR
ME801	1.95	1.61	2.57	17.4	38	90	3.7	3.9	4.5	12670	7402
ME802	1.89	1.57	2.54	17.0	38	84	6.1	4.0	5.1	12864	7188
ME804	1.91	1.56	2.52	18.5	38	92	2.9				
ME805	1.97	1.67	2.53	15.5	34	89	3.7			12700	7100
ME806	2.01	1.74	2.50	13.6	31	90	3.2				
ME811	2.05	1.77	2.53	13.7	30	93	2.0		3.4	9420	4272

DISCUSSION

The matching of the grout properties to the properties of the tuff in the structural test area is essential to the structures program. A good match would eliminate many pre-shot and most likely post-shot questions about the effect of differences in the properties.

In order to achieve a match, it was first necessary to characterize the tuff in the structures area. Up to the time that the match question arose, a number of exploratory tests had been conducted. These tests included uniaxial strain, physical property measurements and ultrasonic velocities. From these data, one could obtain absolute values for most of the important properties with the exception of the shear strength of the material (failure envelope). The failure envelope may be estimated from the stress-stress response of the uniaxial strain test. Therefore, the stress-stress curves for forty uniaxial strain tests were averaged. From these averages, failure envelopes were estimated (from experience, the stress-stress curve is assumed to be a lower bound) as reported in a letter to Mr. J. W. LaComb, 29 August, 1975, and shown in Figure 28. The estimated failure envelopes, admittedly, do not give the exact shape and can vary in magnitude, but they provided an early strength estimate in order that the process of matching a grout to the tuff could begin.

Failure envelopes from triaxial compression tests have since been obtained for the tuff from the structures test area (Figure 14). With this recent data, the early strength estimates and comparative triaxial compression data on U12n.10 ISS#7 from WES[4], a representative failure envelope of the tuff in the structures area was approximated by the author and Mr. R. L. Stowe (WES), Figure 29. This failure envelope is shown again in

Figure 30 along with the failure surfaces of some of the Mighty Epic grout mixtures tested to date.

Other properties of the tuff in the structures area have been averaged and the data is listed in Table 4, again with the grout properties for comparison.

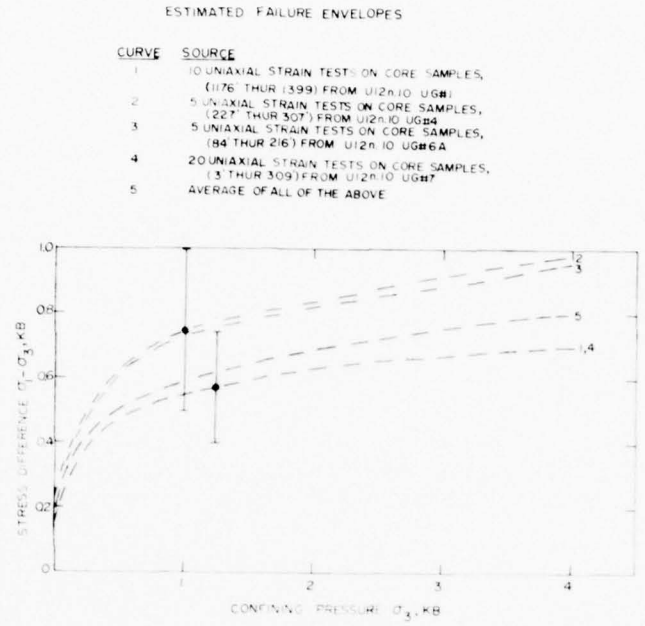

Figure 28: Estimated failure envelopes based on uniaxial strain test results on core samples from U12n.10 UG#4, UG#6a, ISS#5 and ISS#7 drill holes[3].

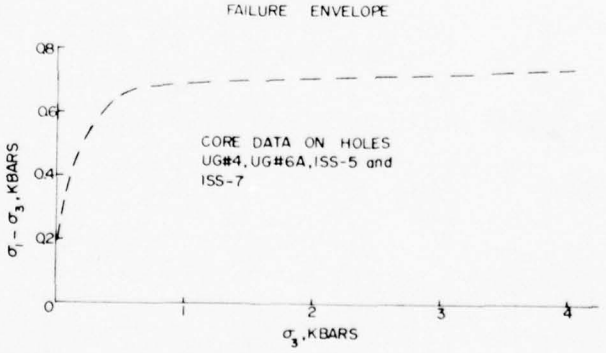

Figure 29: Representative failure envelope for the tuff in the Structures area, based on uniaxial strain tests and triaxial compression test data from Terra Tek and WES[4].

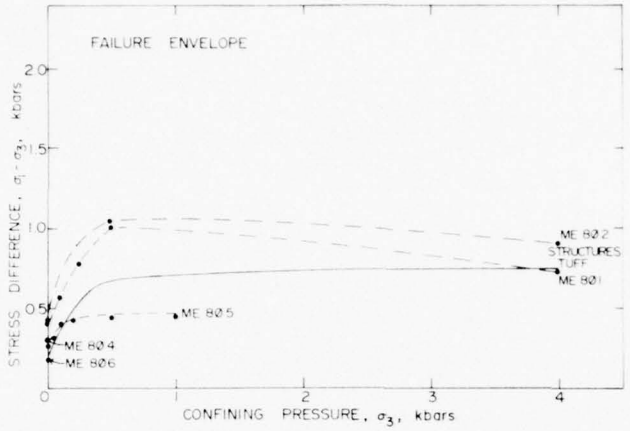

Figure 30: Combined structures tuff failure envelope and grout failure envelopes shown in Figure 29 and Figure 27, respectively.

TABLE 4

Average Structures Tuff Physical Properties, Permanent Compaction and Ultrasonic Wave Velocities. Also listed for comparison is the physical properties of the grout as reported in Table 3.

Drill Hole Footage	Density gm/cc As-Received	Dry	Grain	% Water By Wet Weight	Porosity %	Saturation %	% Calc. Air Voids	% Meas. Permanent Comp.	Velocity ft/sec Long	Shear
STRUCTURES TUFF	1.97 ±0.04*	1.67 ±0.08	2.40 ±0.04	15 ±2	29 ±8	96 ±2	1.2 ±0.7	1.1 ±0.3	10,400 ±1100	5300 ±1100
GROUT								Hyd. 1-D		
ME801	1.95	1.61	2.57	17.4	38	90	3.7	3.9 4.5	12670	7402
ME802	1.89	1.57	2.54	17.0	38	84	6.1	4.0 5.1	12864	7188
ME804	1.91	1.56	2.52	18.5	38	92	2.9			
ME805	1.97	1.67	2.53	15.5	34	89	3.7		12700	7100
ME806	2.01	1.74	2.50	13.6	31	90	3.2			
ME8011	2.05	1.77	2.53	13.7	30	93	2.0	3.2	9420	4272

* ± values represent one standard deviation.

REFERENCES

1. Core samples supplied by Mr. J. W. LaComb, DNA, Mercury, Nevada.

2. Grout samples supplied by Mr. R. Bendenelli, Waterways Experiment Station, Vicksburg, Mississippi.

3. Letter from S. W. Butters to J. W. LaComb, 29 August, 1975, subject -- "Estimated Failure Envelopes on Mighty Epic Tuff".

4. Stowe, R. L., "Triaxial Test Results of Tuff and Grout", Waterways Experiment Station, Vicksburg, Mississippi, September, 1975.

SOME MECHANICAL PROPERTIES OF CONCRETE, STEEL AND CONCRETE-STEEL INTERFACES USED IN MIGHTY EPIC STRUCTURES

by

R. K. Dropek
D. O. Enniss
R. S. Rosso
S. W. Butters

Submitted to

Mr. J. W. LaComb
Defense Nuclear Agency
Nevada Test Site
Mercury, Nevada 89023

Contract DNA 001-75-C-0260

TR 76-14
July 1976

PREFACE

Concrete and steel structure response was predicted and measured for the Mighty Epic nuclear test in Area 12 of the Nevada Test Site. In support of this analysis Terra Tek determined material properties of the steel and three types of concrete as well as the coefficient of friction for the steel-concrete interface. Test results are presented.

TABLE OF CONTENTS

LIST OF FIGURES

LIST OF TABLES

INTRODUCTION

One of the experiments planned for the Mighty Epic event in Area 12, Nevada Test Site was to evaluate the effects of shock loading on concrete and steel structures. Experimental analysis required mechanical properties for the concrete, steel and concrete-steel interfaces. Concrete properties were determined through uniaxial and triaxial compression tests at quasi-static loading rates. Steel samples were tested in uniaxial tension and compression while the coefficient of friction for the concrete interfaces were determined in direct shear tests.

CONCRETE MECHANICAL TESTS

Concrete samples used in this study were obtained from two sources. Lasker Boiler and Engineering Corporation of Chicago, Illinois supplied 30 standard cylindrical test samples 15.2 cm. diameter by 30.5 cm. long. This concrete was designated LBC-5.5 ksi (i.e., anticipated 28 day unconfined strength of 5.5 ksi). The average water-cement ratio was 0.36:1*; the mean coarse aggregate size was 1.9 cm. and comprised about 45 percent of the concrete by weight (see Figure 1).[1] The second concrete source was Lockheed Shipbuilding and Construction Company, Seattle, Washington from which 60 standard cylindrical samples, 15.2 cm. diameter by 30.5 cm. long were obtained.

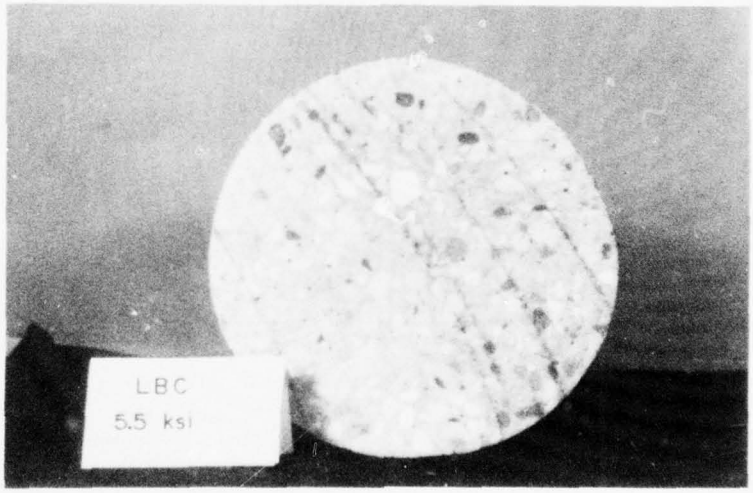

Figure 1. Cross section of LBC-5.5 ksi concrete.

These 60 cylinders were subdivided into two groups: 30 cylinders were a 5.5 ksi mix design while the remaining 30 cylinders were of a 7.2 ksi mix design.

---

* The water-cement ratio is here defined as the weight of water divided by the weight of cement per cubic yard of concrete.

These cylinders were designated as LH-5.5 ksi and LH-7.2 ksi, respectively, indicating a 5.5 ksi and 7.2 ksi 28 day unconfined compressive strength. Both concretes had a mean coarse aggregate size of 1.3 cm. The LH-5.5 ksi concrete had a water-cement ratio of 0.39:1 and was 56 percent coarse aggregate by weight as shown in Figure 2. The LH-7.2 ksi concrete had a water-cement ratio of 0.44:1 and was 14.5 percent coarse aggregate by weight as shown in Figure 3.[2]

The cylinders were shipped sealed to preserve moisture. Mechanical testing commenced approximately 2 months after the pour date.

Concrete Sample Preparation

Concrete test sample ends were ground parallel to within ± .005 cm. Samples designated for triaxial compression testing were examined for subsurface cavities which might collapse during pressurization. These cavities were filled with a grout and subsequently jacketed with polyurethane. Steel endcaps were attached with rubber tape and stainless steel lockwire.

Instrumentation

Both axial and lateral stresses and strains were measured. Axial stress was measured to within 6 bars. A 350 ohm manganin wire pressure coil was used to obtain the confining pressure. Pressure coil readings were accurate to within 2 bars. Confining pressure was also monitored with a Heise pressure gauge. Axial and lateral strains were obtained using strain gauged cantilever systems and calibrated to be accurate within .006 percent strain and .003 percent strain, respectively. A more detailed description of the transducer systems may be found in Reference 3. During testing, data was recorded using a PDP Lab 11 computer in conjunction with x-y recorders.

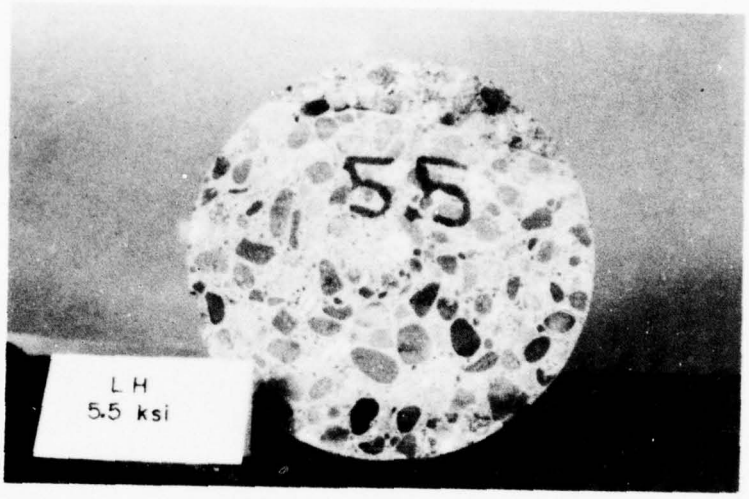

Figure 2. Cross section of LH-5.5 Ksi concrete.

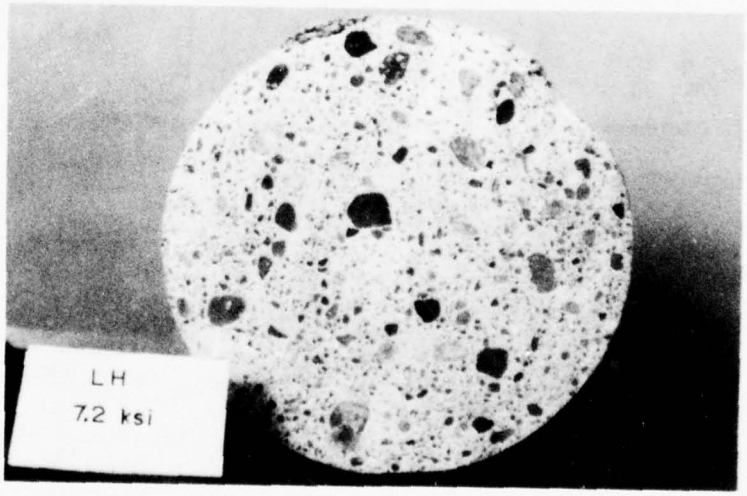

Figure 3. Cross section of LH-7.2 Ksi concrete.

Concrete Results and Conclusions

The general shape and character of the stress-strain triaxial compression curves agree with other published results.[4-7] The initial non-linear portion of the stress-strain curves for both the hydrostatic and unconfined tests have been shown to occur if microcracks exist in the concrete.[8] Microcracks may have resulted from excessive mortar shrinkage due to excess water or by separation of the aggregate and matrix due to temperature fluctuations. In addition, the handling and transportation of "green" concrete may have an effect on microcracking. This initial nonlinear portion was followed by a linear region up to about 50 percent of the failure strength for the unconfined tests. A third stage during unconfined testing was then observed which showed nonlinear stress-strain response to failure. After the initial nonlinear foot, the hydrostatic loading curves also showed fairly linear response up to about 500 bars confining pressure after which a second nonlinear confining pressure-volume strain region occurred.

Table I lists the bulk modulus determined from hydrostatic loading of the concrete as shown in Figure 4. The bulk moduli in Table I were determined using a secant slope from 0 to 0.55 kilobars.

TABLE I

Bulk Moduli for the Three Concretes

Concrete Type	Hydrostatic Stress Range, bars	Bulk Modulus, Kb (0 to 552 bars)
LBC - 5.5 ksi	0 to 552	110
LH - 5.5 ksi	0 to 552	138
LH - 7.2 ksi	0 to 552	96

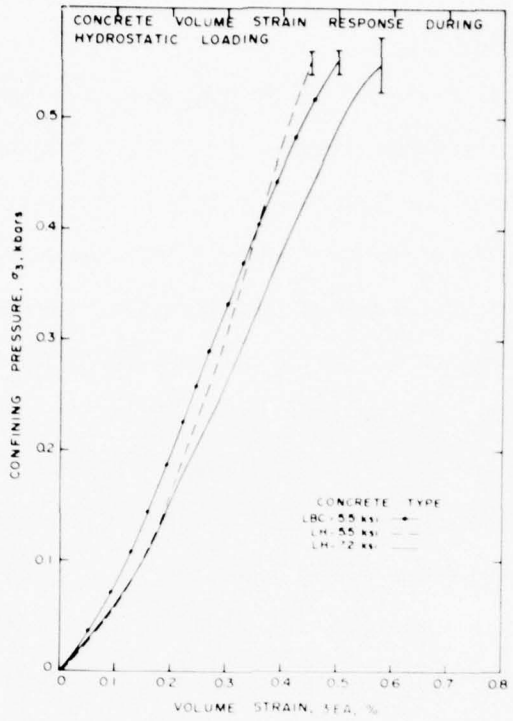

Figure 4. Hydrostatic pressure versus volume strain for the three types of concrete.

Table II lists triaxial compression test results. Published values for the Young's modulus range from 200 to 400 kilobars depending upon concrete mix design, while reported values for Poisson's ratio average about 0.2.[9,10] The values reported herein are consistent with those previously reported data.

Figures 5, 6, and 7 show the triaxial stress-strain data for the three concrete types. The maximum stress difference attained during triaxial compression testing was interpreted as the ultimate stress. Obtaining reliable stress-strain data beyond the ultimate stress was often not possible due to catastrophic sample failure which resulted in exceeded data acquisition capabilities. Thus, the arrows indicate the direction taken

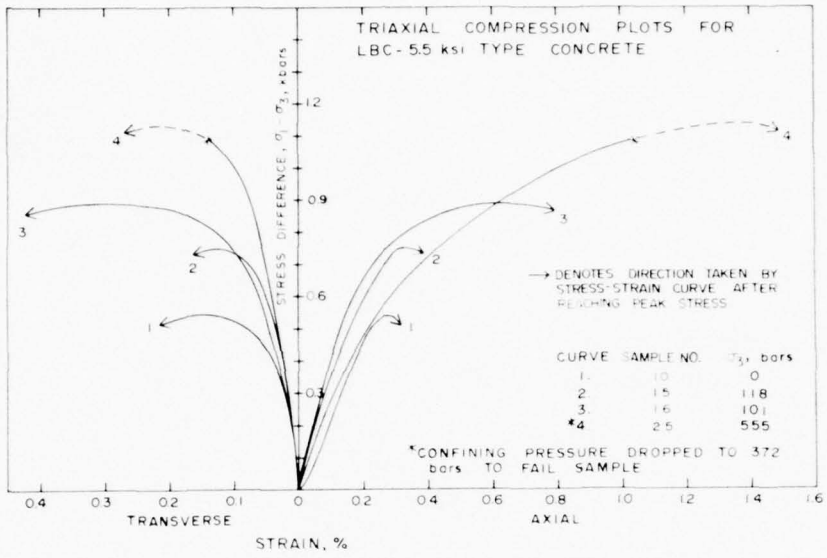

Figure 5. Stress difference versus strain plots for LBC-5.5 ksi concrete.

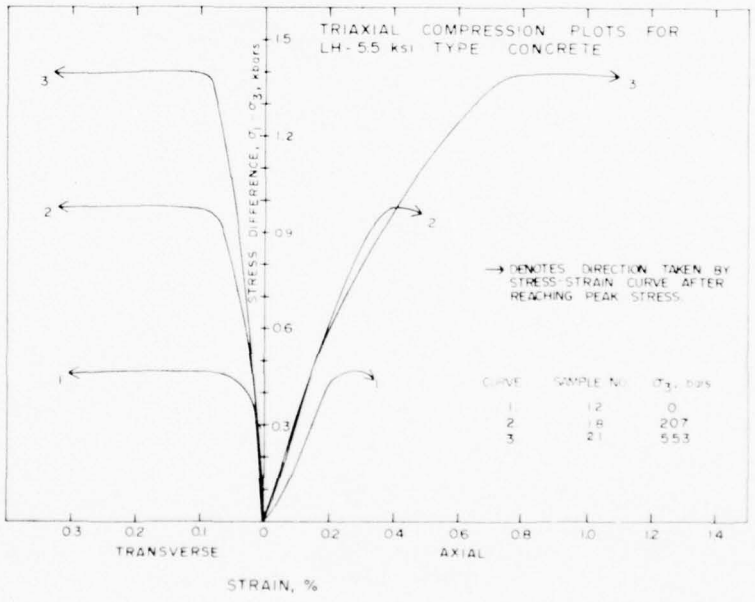

Figure 6. Stress difference versus strain plots for LH-5.5 ksi concrete.

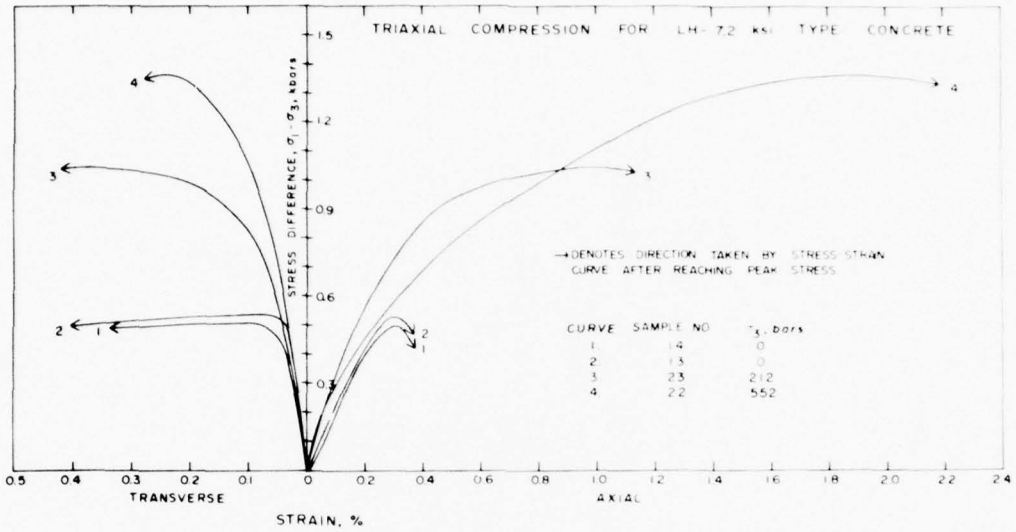

Figure 7. Stress difference versus strain plots for LH-7.2 ksi concrete.

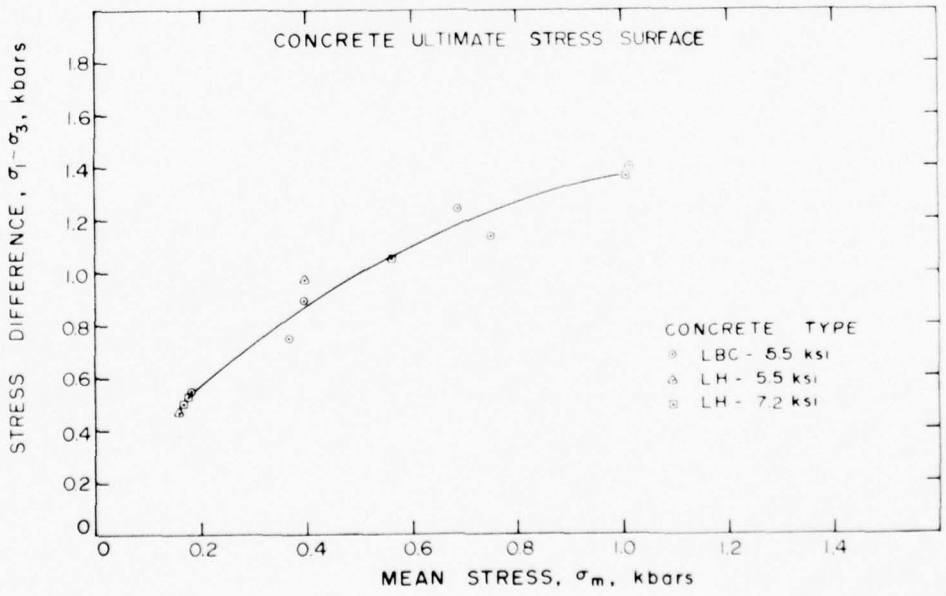

Figure 8. Ultimate stress surface for the three concrete types.

TABLE II

Summary of Triaxial Compression Test Results for the Three Concretes

Sample	Concrete Type	Test Type	Ultimate Stresses, bars			Young's Modulus, Kb	Poisson's Ratio
			σ_3	$\sigma_1-\sigma_3$	σ_{mean}		
10	LBC-5.5	Unconfined	0	546	182	260*	0.12
16	LBC-5.5	Triaxial	101	888	397	445	0.33
15	LBC-5.5	Triaxial	118	750	368	400	0.20
17	LBC-5.5	Triaxial	276	1240	690	---	----
25	LBC-5.5	Triaxial	372	1138**	751	300	0.14
12	LH-5.5	Unconfined	0	470	157	260*	0.08
18	LH-5.5	Triaxial	207	976	395	320	0.13
21	LH-5.5	Triaxial	552	1395	1018	330	0.13
13	LH-7.2	Unconfined	0	528	176	210*	0.10
14	LH-7.2	Unconfined	0	500	167	230*	0.15
23	LH-7.2	Triaxial	212	1055	564	345	0.23
22	LH-7.2	Triaxial	552	1366	1007	345	0.20

* Scaled on linear portion of curve, (i.e., does not include the "foot on the curve).

** Confining pressure, σ_3, lowered from 552 to 372 bars to achieve sample failure.

by the stress-strain curve after attaining ultimate stress. Figure 8 shows the ultimate stress surface determined from the ultimate stress for each sample. A general trend of increasing ultimate stress with increasing mean stress was observed for the three concrete types. However, little difference in ultimate stress between concrete types was observed.

The brittle-ductile transition for the three concretes appears to be between 100 and 500 bars confining pressure as exemplified by the large compressive strains above 500 bars confining pressure. Ductile behavior was defined as axial strain greater than 1 percent. Other

investigators have observed the brittle-ductile transition to occur at about 150 to 200 bars confining pressure for a concrete mix having a water to cement ratio of 0.6:1 and a maximum aggregate size of 1.0 cm. Figures 9 and 10 show the recovered samples (numbers 23 and 25) after triaxial testing at confining pressures of 212 and 552 bars, respectively. The figures show a more localized failure zone at 212 bars confining pressure as compared to a more generalized (diffuse) failure at 552 bars confining pressure. A more generalized failure suggests increased ductility.

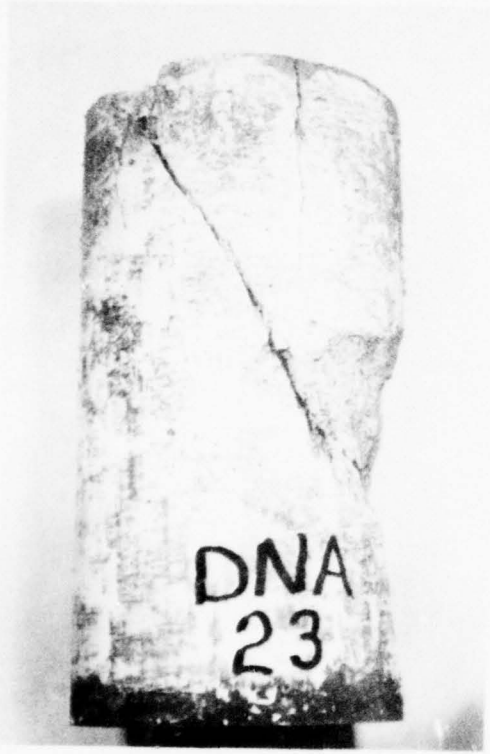

Figure 9. Photograph of sample 23 showing failure mode. Sample was triaxially tested at 212 bars confining pressure.

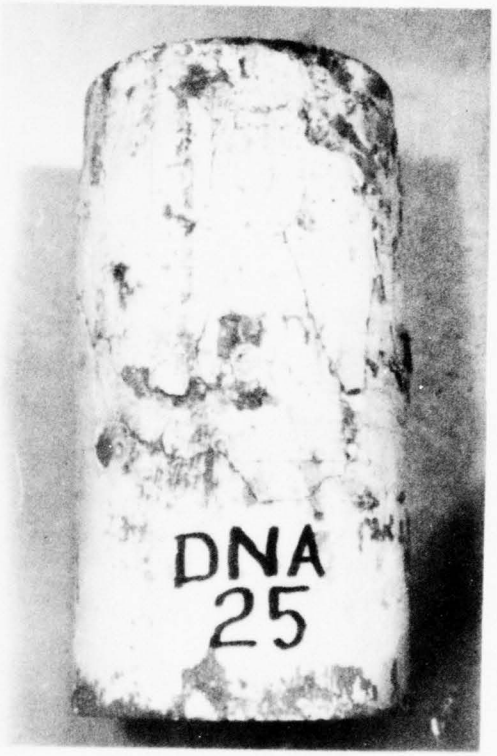

Figure 10. Photograph of sample 25 showing failure mode. Sample was triaxially tested at 552 bars confining pressure.

STEEL MECHANICAL TESTS[11]

The steel used in the Mighty Epic structures was an ASTM A36 mild steel. A sample of this steel was supplied to Terra Tek in the form of a plate, 30 cm. x 30 cm. x 1.9 cm., by Lasker Boiler and Engineering Corp. of Chicago, Illinois. Tensile and compressive tests were performed to determine the mechanical properties of the steel. Test samples were obtained from two orthogonal directions in the plane of the plate and one direction normal to the plane of the plate in order to check for anisotropy. The orthogonal directions were artibrarily selected since rolling directions were not specified by the contractor.

Steel Sample Preparation

The samples tested under the tensile load were cylindrical, 0.635 ± .013 cm. diameter, and 2.54 ± .013 cm. gage length. The samples for compressive testing were also cylindrical, 0.953 ± .013 cm. diameter, and 1.905 ± .013 cm. total length. Sample ends were prepared parallel to within ± .0003 cm. Axiality of the test specimen with the loading piston was within ± .01 cm. For both tensile and compression specimens, two strain gauges were bonded directly to the sample to monitor the axial and transverse strains. The strain gauges used were accurate to ± .005 percent strain. All sample preparation was done in accordance with ASTM Standards E8-65T and E9-61. All loadings were applied quasi-statically.

Steel Test Results and Conclusions

In order to clarify the designation of the test samples, the plate orientation shown in Figure 11 was selected. Tensile and compressive tests were performed on samples from both the "x" and "y" directions. Samples from the "z" direction were tested in compression only since the 3/4 inch

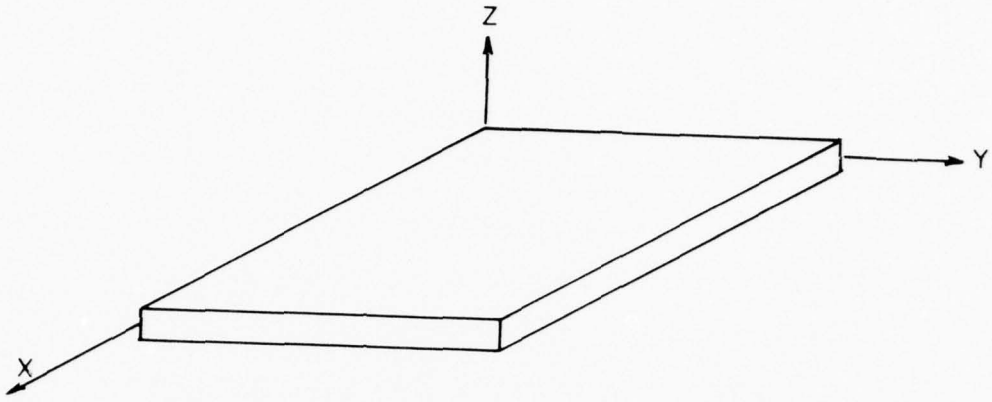

Figure 11. Orientation of steel plate.

thickness did not allow adequate length for a tensile sample. The stress-strain curves for various sample orientations are contained in Figures 12 through 16. In each case the test is designated by the direction of the samples longitudinal axis and the type of loading, i.e., XC indicates X direction, compressive loading.

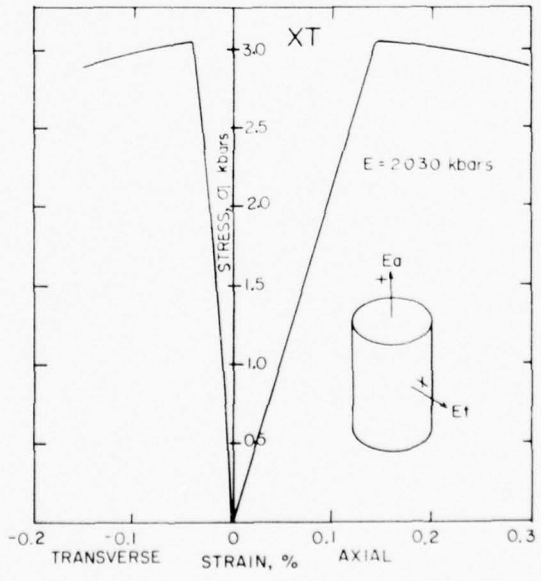

Figure 12. Tensile stress-strain steel sample, X direction.

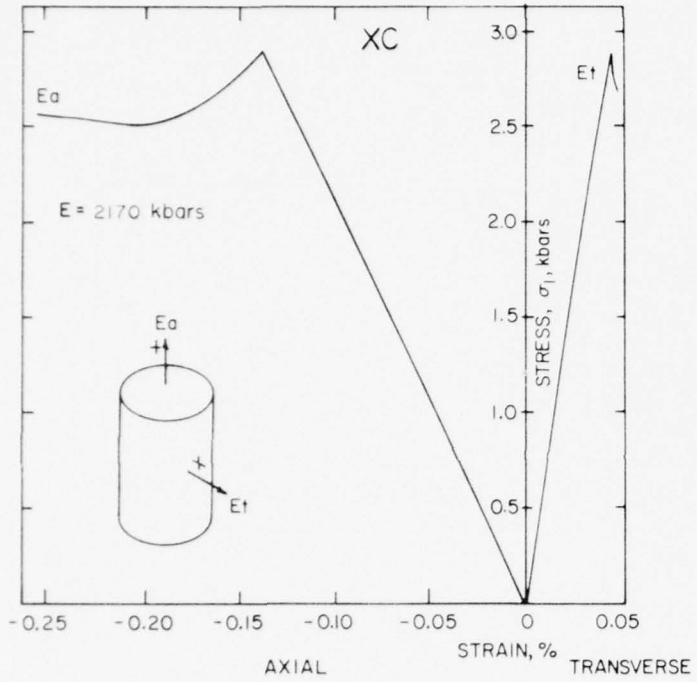

Figure 13. Compressive tests on steel sample, X direction.

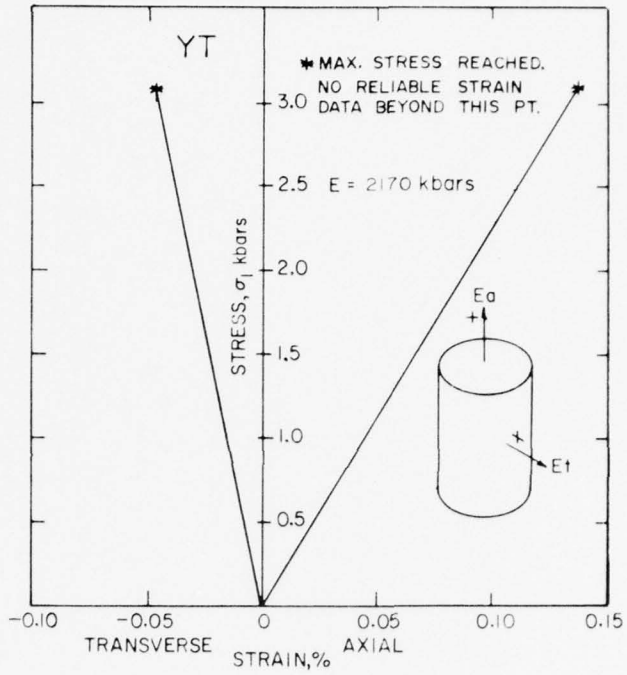

Figure 14. Tensile test on steel sample, Y direction.

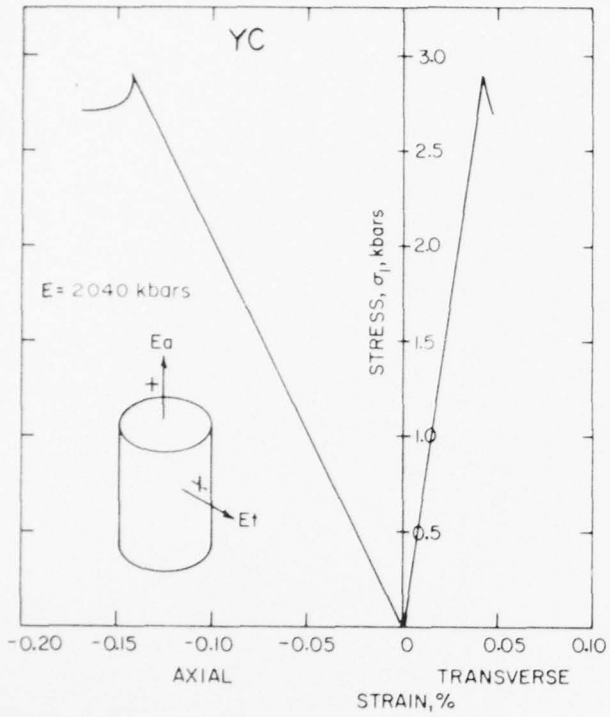

Figure 15. Compressive test on steel sample, Y direction.

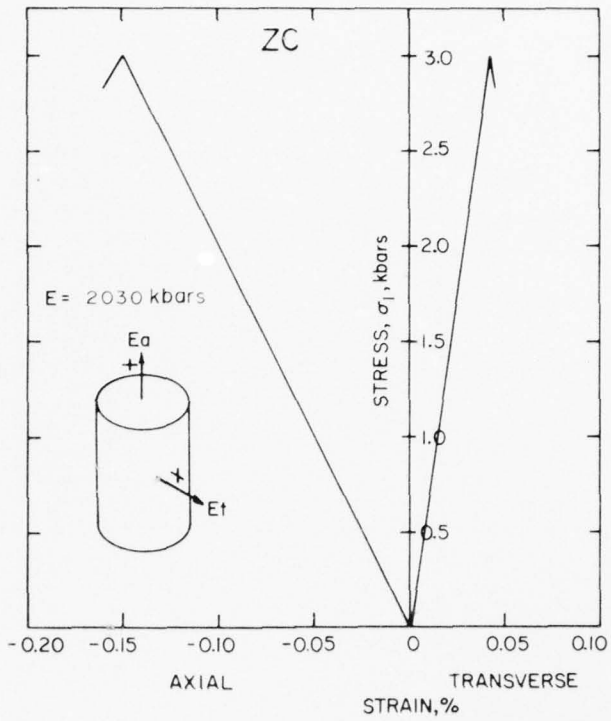

Figure 16. Compressive test on steel sample, Z direction.

All samples demonstrated a linear elastic region and a well defined yield point. The mean upper yield point observed during the loading was 2.96 ± 0.06 kbars. The mean Young's modulus measured was 2.090 ± 0.075 Mbars with a mean Poisson's ratio of 0.285 ± 0.015. The variation in behavior for the different orientations is due most likely to the small sample population tested rather than to some anisotropic nature of the plate.

A summary of the steel behavior is contained in Table III.

TABLE III

Summary of Steel Test Data

Test Designation	Test Type	Young's Modulus	Poisson's Ratio	Upper Yield Strength
XT	Tensile	2030 Kb	0.27	2.96 Kb
YT	Tensile	2170 Kb	0.31	3.03 Kb
XC	Compressive	2170 Kb	0.29	2.88 Kb
YC	Compressive	2040 Kb	0.28	2.93 Kb
ZC	Compressive	2030 Kb	0.27	3.02 Kb

CONCRETE - STEEL SHEAR TESTS

Lasker Boiler and Construction Company supplied ten 10.2 cm. cubes for testing the frictional properties of the concrete - steel interface. Samples were designated according to structure in which the concrete and steel were used, i.e., C-Y-13, C-X-5, etc. The cubes were composed of a 10.2 cm. x 10.2 cm. x 5.1 cm. thick steel plate upon which a 10.2 cm. x 10.2 cm. x 5.1 cm. thick piece of concrete was cast. The concrete and steel used in making the direct shear cubes was of the same batch and/or type as concrete (LBC-5.5 ksi) and steel previously reported herein. The cubes were placed into a water bath upon arrival at Terra Tek in order to promote curing and approximate Nevada Test Site tunnel humidity.

Apparatus and Instrumentation

Direct shear tests were performed in the machine shown in Figure 17. The normal load was applied with a servo-controlled actuator operating in the load feedback mode. The shear was applied by a servo-controlled

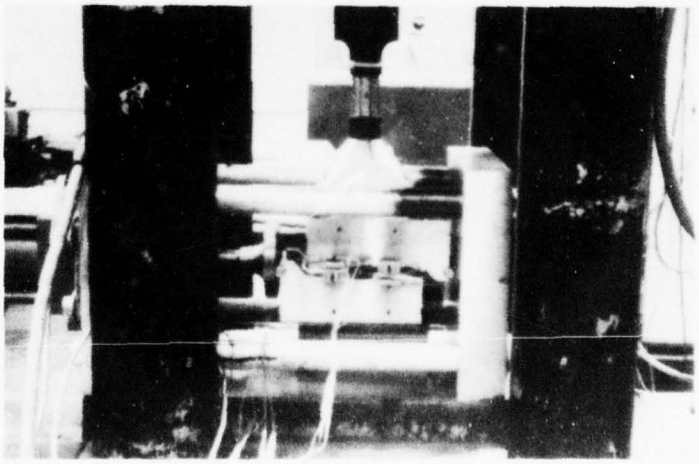

Figure 17. Direct shear machine.

actuator operating in the displacement feedback mode at a rate of 0.001 cm/sec. Both the normal and shear loads were measured directly by load cells placed in line with the actuators. Frictional load contribution due to the shear box was minimized by incorporating ball bearings and hardened steel bearing surfaces. Although the coefficient of friction for this bearing proved to be dependent upon normal load negligible errors were incurred. For a normal stress of 70 bars, the friction coefficient was .009 and at a normal stress of 700 bars it was .002. Through calibration, horizontal and vertical loads were determined to be accruate to within ± 0.25 bars. Transducers mounted on the shear boxes measured the relative horizontal displacement of the two boxes to within ± .015 cm. The direct shear specimens were held in place in the shear boxes using a grout, Ultra-Cal 30.

Direct Shear Results and Conclusions

Table IV lists the direct shear data for the three cubes. Sample C-Y-13 "stub" showed no breakdown shear stress and gave an average friction coefficient of 0.53. Sample C-Y-13 "sphere" showed an initial breakdown shear stress of 28.1 bars dropping to a residual shear stress of 25.2 bars giving initial and residual friction coefficients of .80 and .73, respectively. Sample C-X-5 showed no significant breakdown stress and gave an average friction coefficient of 0.70. Note that the terms "stub" and "sphere" indicate the type of structure in which the concrete was used.

The coefficient range 0.69 to 0.73 listed in Table IV should be considered the representative coefficient of friction since the sample C-Y-13 "stub" had become unbonded at the concrete-steel interface prior to testing. The authors feel this unbonding could have affected the data via some mechanism such as drying of the surfaces.

TABLE IV

DIRECT SHEAR DATA

(LBC - 5.5 ksi concrete)

Sample	Shear Rate 10^{-3} cm/sec	Normal Stress, bars (to shear plane)	Residual Friction Coefficient μ
C-Y-13 "stub"	1	34.5	.53
	1	68.3	.52
	1	101.4	.53
C-Y-13 "sphere"	1	34.5	.73
C-X-5	1	34.5	.69
	1	71.0	.70

CONCLUDING REMARKS

The concrete and steel mechanical tests showed behavior consistent with previously published results. Young's modulus and Poisson's ratio for the concrete averaged 310 kilobars and 0.17, respectively. The average bulk modulus for the three concrete types was 115 kilobars. The steel samples gave an average Young's modulus and Poisson's ratio of 2090 kilobars and 0.28, respectively. The direct shear tests showed that a coefficient of friction of 0.70 best represented the concrete-steel interface.

REFERENCES

1. Brumfield, M., 1976, Personal Communication, Carol Construction Company, Chicago, Illinois.

2. Merwood, D, 1976, Personal Communication, Concrete Technology, Tacoma, Washington.

3. Johnson, J. N., Dropek, R. K., 1975, "Measurements and Analysis of Pore Pressure Effects in the Inelastic Deformation of Rocks," Terra Tek, Inc., Technical Report TR 75-29.

4. Gardner, N. J., 1969, "Triaxial Behavior of Concrete," American Concrete Institute Journal, Proceedings, Vol. 66, No. 2, pp. 136-146.

5. Hatano, T., 1969, "Theory of Failure of Concrete and Similar Brittle Solid on the Basis of Strain," International Journal of Fracture Mechanics, Vol. 5, No. 1, pp. 73-79.

6. Kupfer, H. B., Gerstle, K. H., 1973, "Behavior of Concrete Under Biaxial Stresses," Journal of the Engineering Mechanics Division, ASCE Proceedings, EM-4, pp. 853-866.

7. Ishai, O., 1965, "The Time-Dependent Deformational Behavior of Cement Paste, Mortar and Concrete," The Structure of Concrete, Cement and Concrete Association Proceedings, September 1965, pp. 345-364.

8. Glucklich, J., 1965, "The Effect of Microcracking on Time-Dependent Deformations and the Long Term Strength of Concrete," The Structure of Concrete, Cement and Concrete Association Proceedings, September 1965, pp. 176-189.

9. Liu, T. C. Y., Nielson, A. H., Slate, F. O., 1972, "Biaxial Stress Strain Relations for Concrete," Journal of Structural Division, ASCE Proceedings, ST. 5, pp. 1025-1034.

10. Green, S. J., Swanson, S. R., 1973, "Static Constitutive Relations for Concrete," Air Force Weapons Laboratory Technical Report AFWL-TR-72-244.

11. Enniss, D. O., Butters, S. W., 1976, "Mechanical Behavior of Steel Used for Mighty Epic Structures," Terra Tek, Inc., Technical Report TR 76-38.

CHARACTERIZATION OF TUFF AND DEVELOPMENT OF GROUTS FOR MIGHTY EPIC STRUCTURES PROGRAM

by

S. W. Butters
R. L. Stowe*
J. W. LaComb**
R. A. Bendinelli***

Submitted to

Commander
Field Command
Defense Nuclear Agency
Albuquerque, New Mexico

Attn: J. W. LaComb

* R. L. Stowe, Concrete and Rock Properties Branch, Waterways Experiment Station, Vicksburg, Miss.

** J. W. LaComb, Civil Engineering, Nevada Test Site, Mercury, Nevada

*** R. A. Bendinelli, Grouting Branch, Waterways Experiment Station, Vicksburg, Miss.

TR 76-21
April 1976

SUMMARY

A Defense Nuclear Agency program at the Nevada Test Site to study the effect of shock waves -- both magnitude and direction -- on structures of varying configurations and designs required a complete characterization of the material (tuff and grout) surrounding the structures. It was also desired that the grout properties be similar to the tuff properties.

Tuff surrounding the structures was characterized through mechanical and physical properties measurements performed at Waterways Experiment Station (WES) and Terra Tek, Inc. Subsequent grout development then performed at the Grouting Branch of the Concrete Laboratory at WES with mechanical testing by both the Rock Properties Branch of the Concrete Laboratory at WES and Terra Tek, Inc. As samples from each mixture were tested, new mixtures were designed. Approximately twenty mixtures were analyzed before final grout selection, ME8-11. This ME8-11 grout was implaced in the structures drifts in preparation for the Mighty Epic event.

PREFACE

The authors would like to express their appreciation for the excellent and expedient laboratory support by the Grouting and Rock Properties Branches of Waterways Experiment Station and by Terra Tek.

TABLE OF CONTENTS

LIST OF ILLUSTRATIONS

LIST OF ILLUSTRATIONS (Continued)

LIST OF ILLUSTRATIONS (Continued)

APPENDIX B

LIST OF ILLUSTRATIONS (Continued)

LIST OF TABLES

INTRODUCTION

Line of Site (LOS) pipe emplacement for nuclear test programs utilize substantial amounts of grout materials. Different functional roles require different grout mixtures. For example, grouts have been designed to attenuate energy via high gas-filled porosity, to protect structures via the shear strength, to flow via the ductility, etc. It has proved difficult to obtain a single mixture with a combination of select properties. For example, to strengthen grout, the water content is decreased, this would, if saturation remained constant, result in a higher density, higher sound speeds, and a less workable mixture. A more detailed description of the dependence of properties on each other is included in the text.

Stringent requirements for grout properties was necessary for the Mighty Epic structures program at the Nevada Test Site Area 12. The grout and tuff properties were required pre-test for 1) evaluating pre-test static design methods, 2) determination of active instrumentation response for the structures in the nuclear test and 3) providing a basis for interpreting the Mighty Epic test data. To meet these objectives it was necessary to characterize the grout material and to match the grout properties very closely with those of the parent material-tuff.

Matching grout properties to that of the tuff required, first of all, the properties of the tuff. Material properties of primary importance were the shear strength, the air void content, the as-received density and the longitudinal pulse velocity. Waterways Experiment Station[1] (WES) and Terra Tek, were responsible for determining these properties.

Once an adequate tuff description was available, progress began on developing a matching grout. This process involved varying the constituents

of the grout mixtures by WES[2] and NTS[3] personnel. Each mixture was then tested by WES or Terra Tek to determine its' properties. Two major concerns during this process, in addition to matching the tuff properties, were maintaining a pumpable grout and insuring a low temperature rise during curing.

This report contains the test results from which the average properties of the tuff were obtained, a description of the grout constituents, the grout tests conducted, and the eventual verification of the grout mix properties actually implaced in the structures drifts.

STRUCTURES TUFF

The Mighty Epic program is planned for the "n" tunnel complex, Area 12. Material properties data were available from other events in the immediate vicinity, namely, Misty North and Ming Blade. The tuff that had been tested, however, was from a considerable number of different rock units ("tunnel beds"). Additionally, most of the tests previously conducted were primarily for siting purposes and the tuffs were incompletely characterized. It was, therefore, necessary to conduct select tests on cores specifically from the structures area.

The structures drifts relative to the Mighty Epic working point are shown in Figure 1. The structures are in the same horizontal plane of the working point, are designated "A", "B" and "C" and are contained within tunnel bed units 3BC, 3D, 4AB and 4CD.

Core holes U12n.10 UG#4 and UG#6a were drilled into the area prior to mining the drifts. The core samples from these holes were initially used for core testing to determine the suitability of the area for structures implacement. This data provided a generalized overview of the nature of the tuff in the structures area -- air void contents, densities, sound speeds and estimates of the strength of the material. These early estimates, especially on the strength of the tuff, were necessary to initiate a matching grout mixture development.

After completion of mining the structures drifts, core samples were obtained from the ISS #5 and ISS #7 drill holes and the A, B and C Structures areas. Along with samples remaining from the UG#4 and UG#6A holes, a number of triaxial compression tests were conducted to define the tuff failure envelope (maximum stress difference at varying confining pressures).

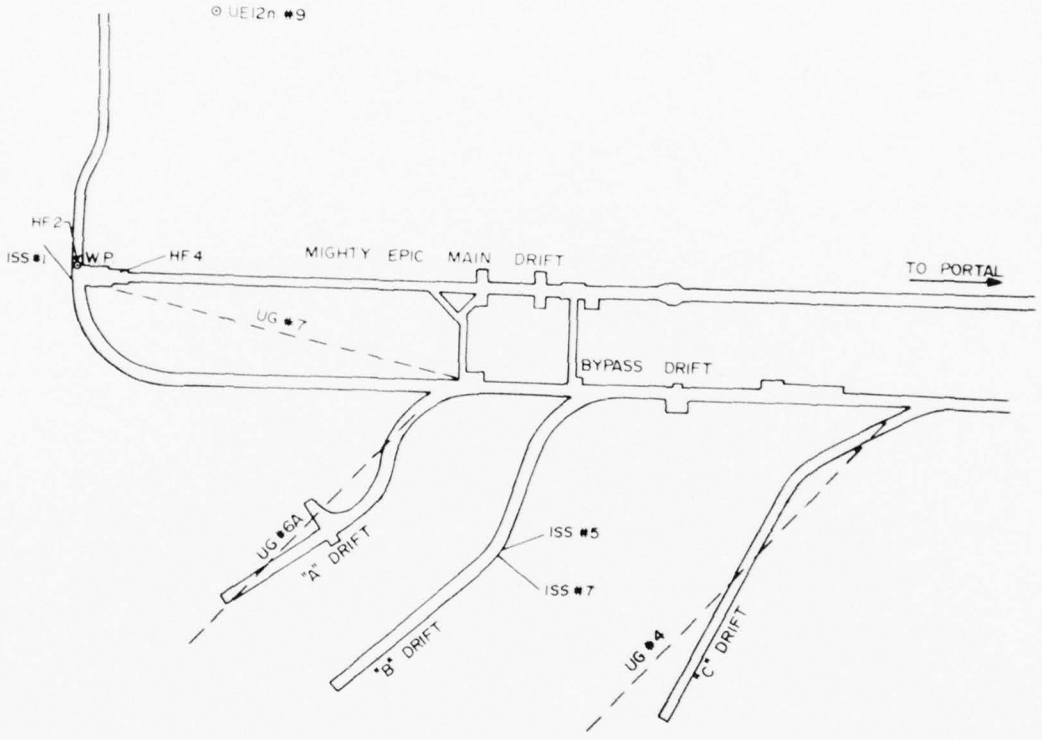

Figure 1. Plan View of the Mighty Epic Area Showing A, B, and C Structures Drifts and the Related Drill Holes.

TEST DATA

In many cases, the WES and Terra Tek data have been combined. This was done in order to use all data in establishing average properties. Selected properties are listed in Table 1 while the stress-strain response of the hydrostatic compression, triaxial compression and uniaxial strain tests are contained in Appendix A.

TABLE 1

PHYSICAL PROPERTIES, ULTRASONIC VELOCITIES AND PERMANENT VOLUME COMPACTION ON U12n.10 UG#4, UG#6a, ISS#5 AND A, B, AND C STRUCTURES DRIFT SAMPLES

DRILL HOLE FOOTAGE	DENSITY (gm/cc) AS-RECEIVED	DRY	GRAIN	WATER BY WET WEIGHT (%)	POROSITY (%)	SATURATION (%)	CALC AIR VOIDS (%)	MEAS PERMANENT COMP (%)	VELOCITY (ft/sec) LONG	SHEAR
U12n.10 UG#4								Hydr. 1-0		
227	1.88	1.62	2.64	16.6	39	97	3.0	1.4	9,449	4596
251	1.94	1.69	2.41	14.8	30	95	0.5	0.3	10,751	5761
255	1.95	1.65	2.39	15.4	31	96	1.3	0.8	10,309	5095
257	1.89	1.64	2.43	15.4	34	95	1.6			
263	1.97	1.65	2.60	16.2	36	94	1.9		9,696	4094
267	1.96	1.64	2.39	16.3	31	97	0.9	0.3	9,370	4104
307	2.01	1.73	2.41	14.0	28	99	0.2	0.9	9,657	6555
327	1.76	1.42	2.38	20.3	40	98	4.8		13,061	5154
335	1.74	1.37	2.36	21.2	42	98	5.3	3.2	10,548	4695
338	1.77	1.42	2.39	20.3	41	97	5.3	3.6	13,205	7523
339	1.77	1.38	2.38	22.1	42	93	2.7			
U12n.10 UG#6A										
84	1.93	1.69	2.43	14.8	30	97	0.8	1.1	10,200	4809
109	1.93	1.69	2.36	14.0	28	98	0.2	0.2	11,127	5675
113	1.83	1.58	2.41	17.4	34	99	0.4		9,206	4505
116	1.88	1.72	2.38	12.9	28	93	1.9			
136	1.93	1.65	2.42	17.1	34	97	1.0	1.0	9,822	4663
143	1.92	1.68	2.41	15.0	31	97	1.0	1.1	10,305	4737
169	1.93	1.65	2.38	14.9	31	95	1.6	1.1	9,947	4895
192	2.01	1.80	2.35	10.4	23	90	2.4	0.8	11,683	6046
216	2.03	1.82	2.34	10.2	22	95	1.1	0.6	12,342	7306
220	1.96	1.65	2.41	15.6	31	97	1.1		10,561	4859
231	2.01	1.75	2.41	13.0	27	96	1.1			
240	2.06	1.75	2.35	17.4	25	99	0.6	0.6	13,094	7649
U12n.10 USS#5										
9	1.91	1.59	2.48	18.5	37	94	2.1		8,960	4070
11	1.93	1.63	2.36	15.4	31	97	1.1		10,760	4970
12	1.91	1.58	2.41	16.0	33	96	1.5		9,380	4280
26	1.96	1.57	2.45	19.0	36	98	0.7		9,190	4170
28	1.93	1.63	2.36	15.5	31	96	1.1		10,190	4900
U12n.10 A Structure										
30	1.92	1.67	2.38	14.7	33	94	1.9	0.9	11,206	6182
B Structure										
25	1.91	1.56	2.45	18.5	36	97	0.9	0.8	9,567	4412
C Structure										
30	1.84	1.44	2.46	22.0	41	98	0.9	0.6	10,801	5382

AVERAGE STRUCTURES TUFF PROPERTIES

As stated earlier, a preliminary estimate of the tuff strength was required for the grout development. To provide this estimate, the UG#4 and UG#6a uniaxial strain test stress-stress curves (Appendix A) were averaged, see Figure 2. These curves, from past experience, are known to be a lower bound to the failure envelope produced by the triaxial compression tests. It should be emphasized that these average uniaxial strain test stress-stress curves do not define the magnitude or shape of the failure envelope but will provide a lower bound. The uniaxial strain test data suggested that the shear strength for the tuff in the structures area was about twice as strong as that of the "average" area 12 tuff[4]. Subsequent triaxial compression tests produced the failure points shown in Figure 3. These limited data provided the necessary failure envelope detail, see Figure 4.

The other properties of the tuff determined from the testing are summarized in Figures 5 through 8 as a function of distance along the drill hole. The average and standard deviation for these properties are listed in Table 2.

The tuff in the structures area and, in general, the Mighty Epic area has higher shear strength, higher density and higher sound speeds than the typical 12 tuff. The water content is lower for the structures tuff while the air void content is approximately the same.

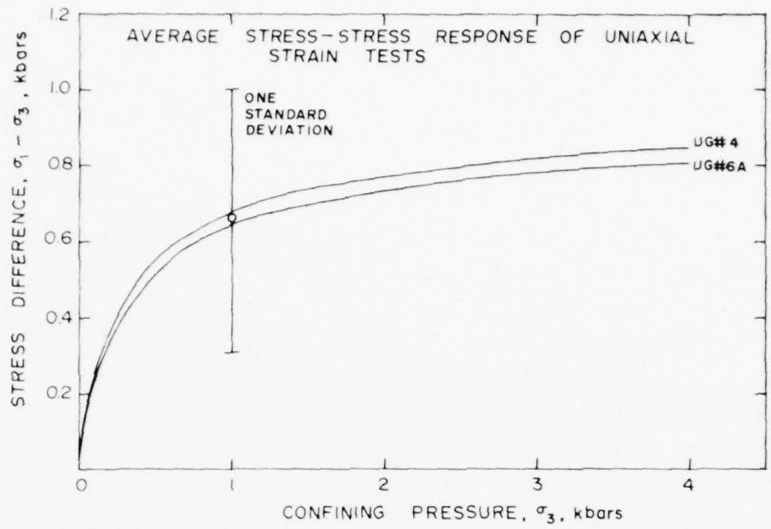

Figure 2. Average Stress-Stress Response of Uniaxial Strain Tests on U12n.10 UG#4 and UG#6a Core Samples (TTI).

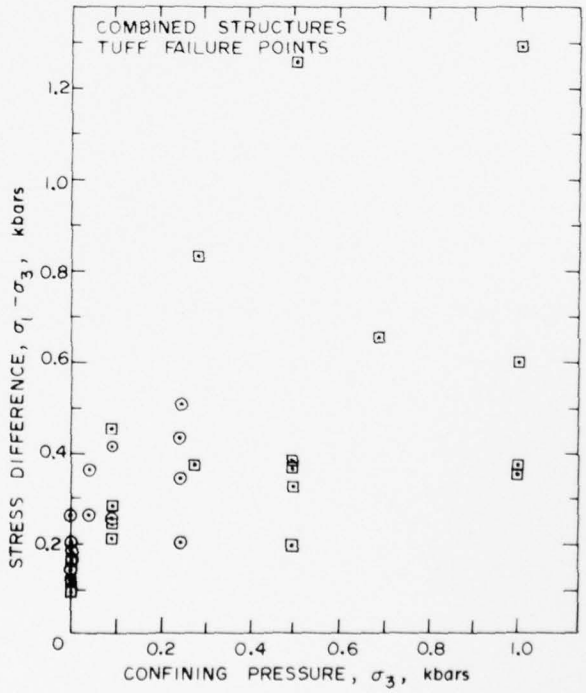

Figure 3. Combined Failure Data from U12n.10 UG#4, UG#6a, ISS#5 and ISS#7 Core Samples.

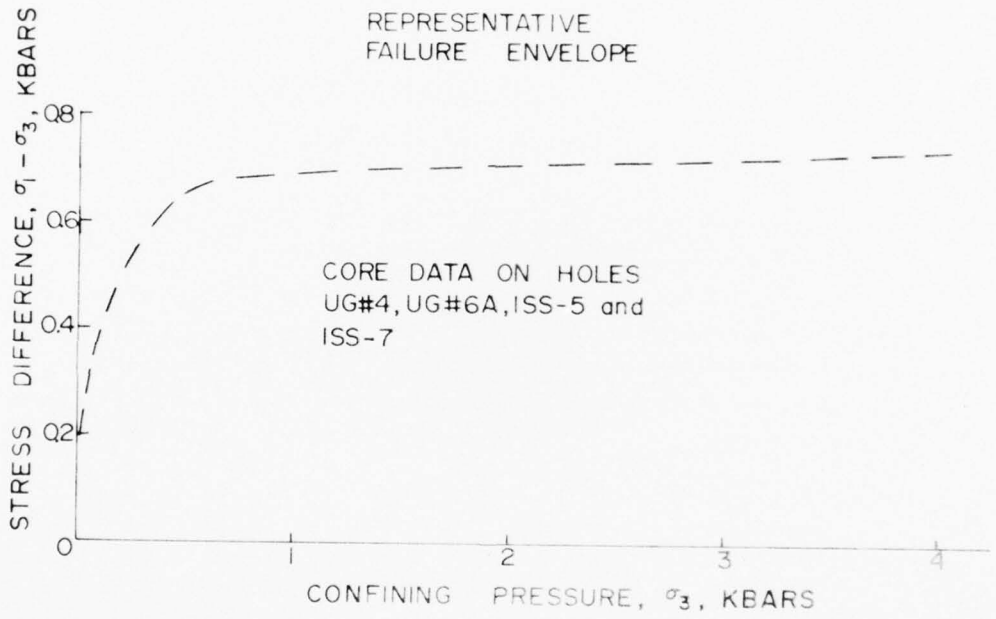

Figure 4. Structures Tuff Representative Failure Envelope.

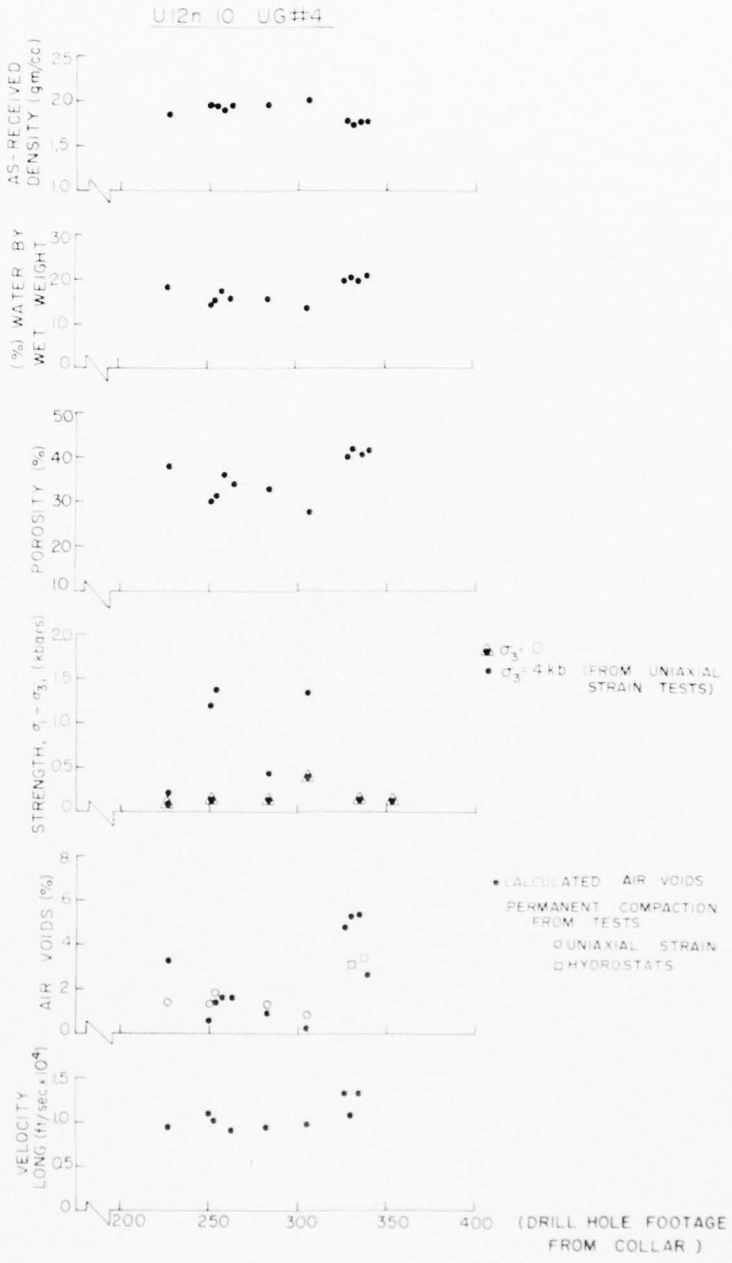

Figure 5. U12n.10 UG#4 Selected Properties as a Function of Drill Hole Footage.

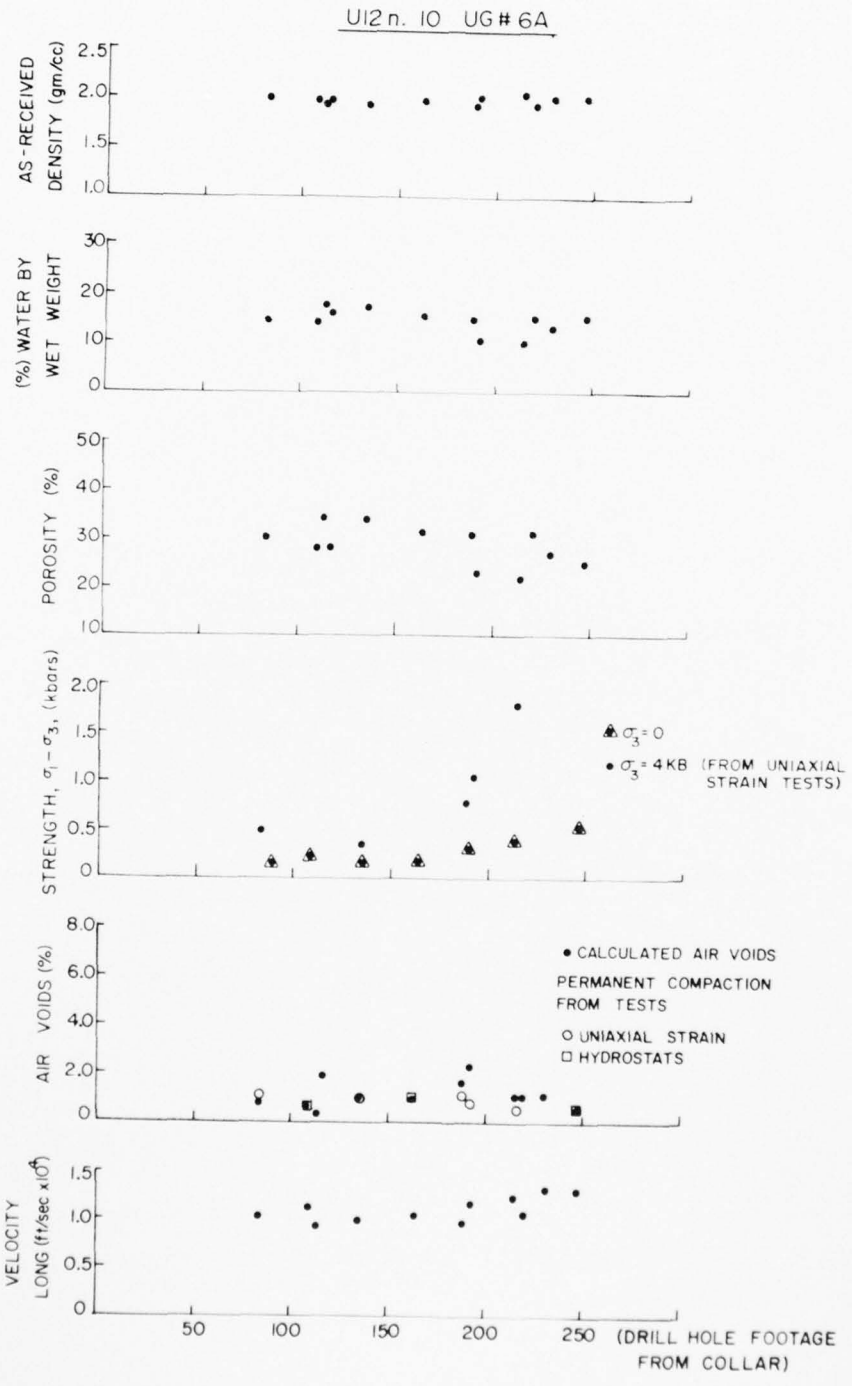

Figure 6. U12n.10 UG#6a Selected Properties as a Function of Drill Hole Footage.

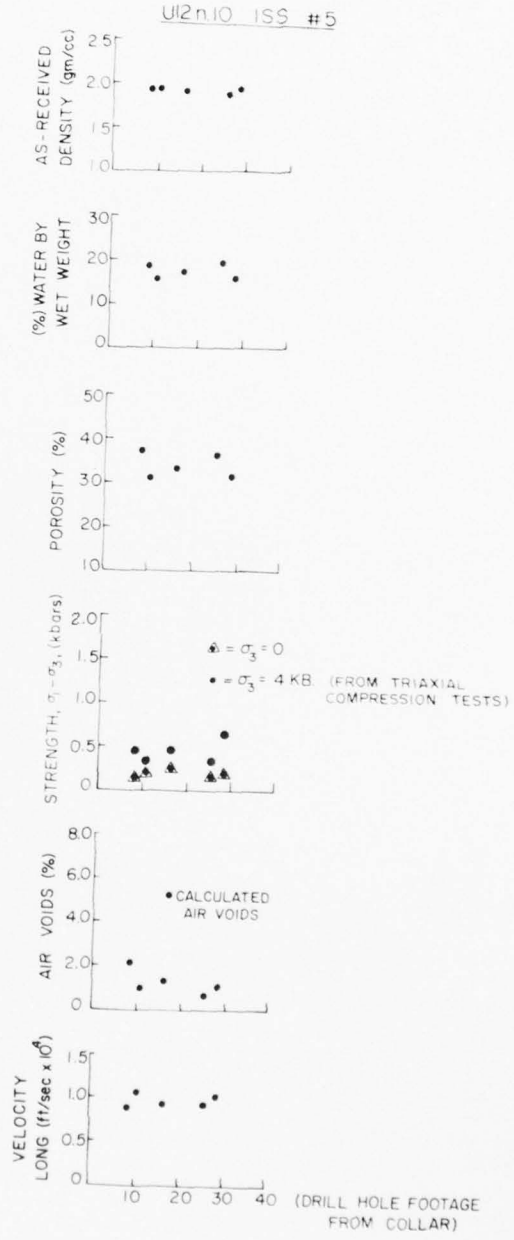

Figure 7. U12n.10 ISS#5 Selected Properties as a Function of Drill Hole Footage.

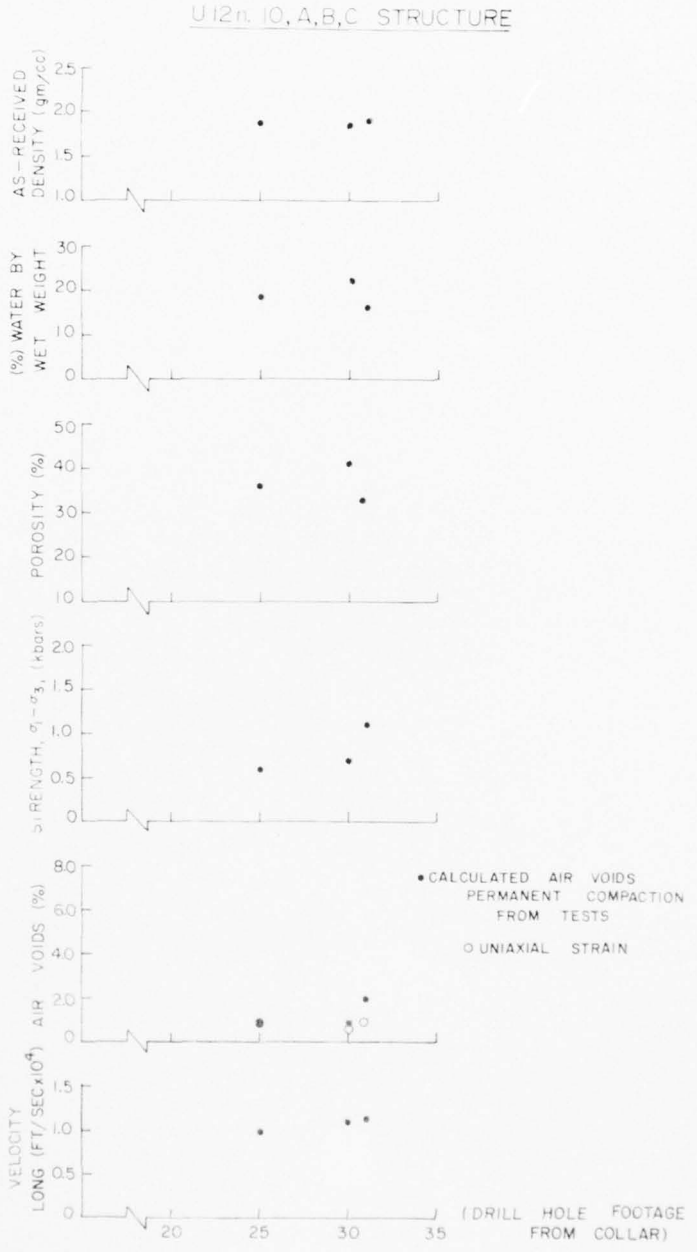

Figure 8. U12n.10 A, B, and C Structures Selected Properties as a Function of Drill Hole Footage.

TABLE 2

SOME AVERAGE PROPERTIES OF

THE STRUCTURES TUFF*

	AVERAGE	STANDARD DEVIATION
As Received Density (gm/cc)	1.95	0.05
Water Content by Wet Weight (%)	15.7	2.6
Porosity (%)	31	7
Air Voids (%)**	1.0	0.43
Ultrasonic Longitudinal Velocity (ft/sec)	10,300	1,000

* The averages includes all values (with the exception of the last 4 samples from U12n.10 UG#4 which were not considered as representative) on samples from U12n.10 UG#4, UG#6a, ISS#5 and ISS#7.

** The air void content is taken here as the permanent volume compaction from the uniaxial strain test.

AD-A048 165 DEFENSE NUCLEAR AGENCY WASHINGTON D C F/G 18/3
HUSSAR SWORD SERIES. MIGHTY EPIC EVENT, CONSOLIDATED MIGHTY EPI--ETC(U)
APR 77 H L PIPER

UNCLASSIFIED DNA-POR-6962 ERDA-WT-6962 NL

3 OF 3
ADA
048165

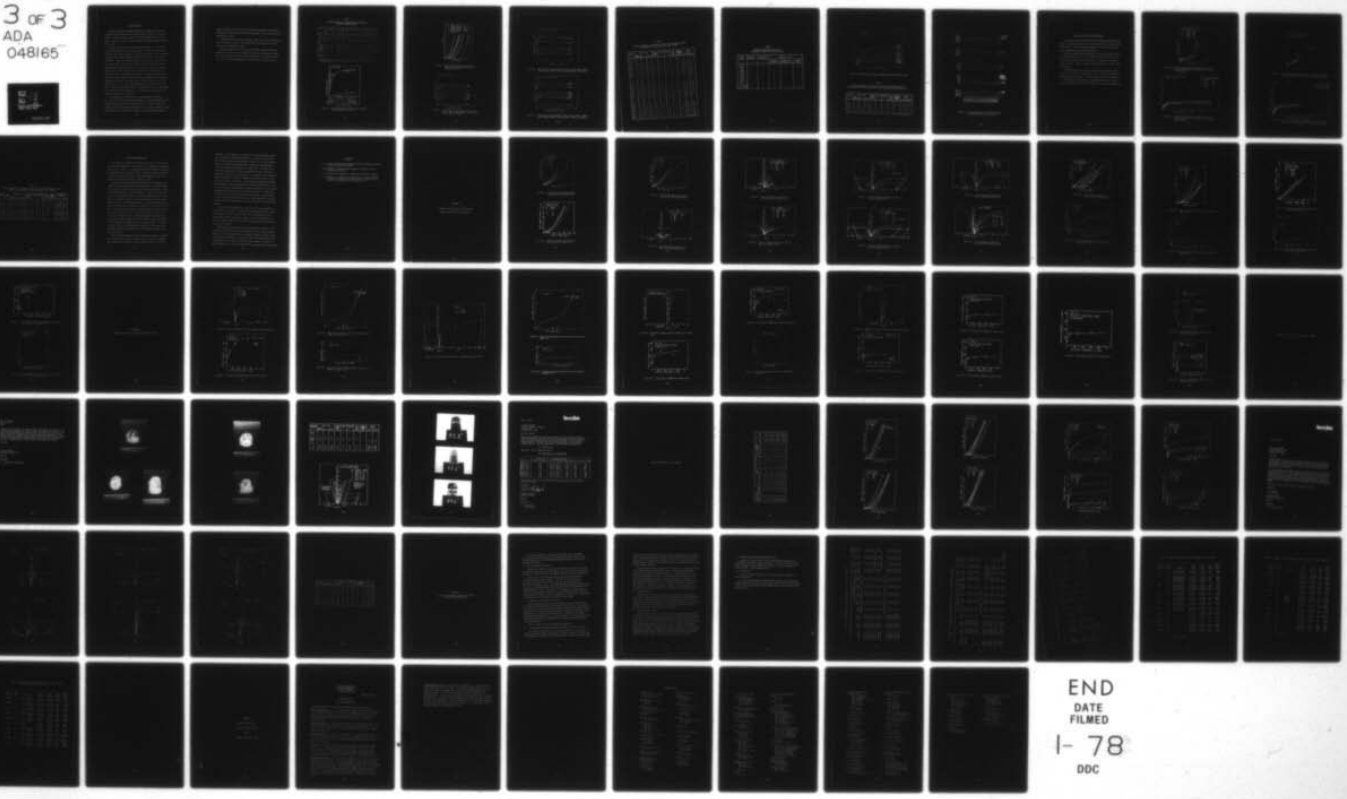

END
DATE
FILMED
1-78
DDC

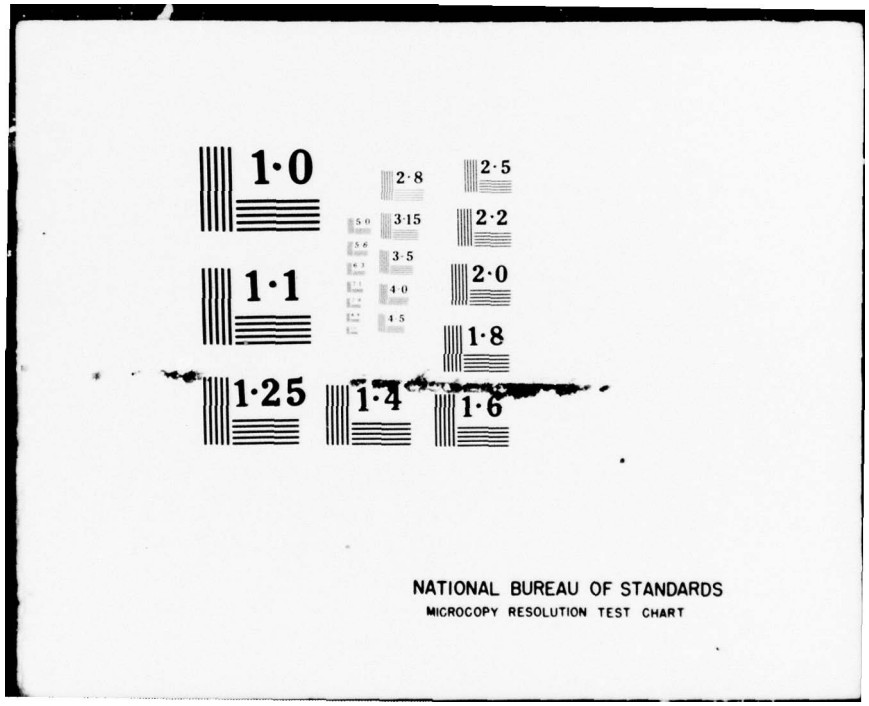
1·0
2·8
2·5
3·15
2·2
3·5
1·1
2·0
4·0
4·5
1·8
1·25
1·4
1·6
NATIONAL BUREAU OF STANDARDS
MICROCOPY RESOLUTION TEST CHART

GROUT PROPERTIES

Material properties have been determined on a number of grout types during the last several years of the Nevada Test Site program. Grout types were all variations of basic super lean, rock matching and high strength grouts. Table 3 and Figures 9 and 10 summarize selected properties of these basic types[4].

Following the preliminary estimate of the structures tuff properties, nine different mixtures of grout, used mainly in stemming and containment systems of past events, were sent to Terra Tek for testing. The grout designations were HPRM-1, HPRM-2, HPRM-3, HPRM-4, HPRM-5, HPSL-16, HPNS-1, HPNS-2 and HPRM-3C. Hydrostatic compression tests, triaxial compression tests, uniaxial strain tests, physical property measurements and ultrasonic velocity measurements were conducted on these grout types at 14, 28 and 56 day ages. These data are listed in tabular form in Table 4 and as the triaxial compression derived failure envelopes in Figure 11. These data indicate variations in the shear strength from tens of bars to hundreds of bars, ultrasonic longitudinal velocities from 7,000 to 11,000 feet per second, air void contents from 1.5% to 4.5%, and as-received densities from 1.86 gm/cc to 2.10 gm/cc. Based on these grout properties, changes were made in mix constituents to "fine tune" the grout properties, (i.e., bring all of the properties of a single mix close to that of the tuff).

The subsequent grout mixtures were designated ME8Ø1 through ME8-11. In most cases, each grout mixture was reproportioned in the developmental studies based on the properties of the previous mixture. The tests on these grout mixtures varied from unconfined compression tests to triaxial compression tests to verify the shear strength of the mixture. If other properties were also

needed, uniaxial strain tests, physical property measurements and ultrasonic longitudinal and shear wave velocities were conducted - Table 5 summarizes the measurements and tests.

The Mighty Epic grout failure envelopes, based on the triaxial compression tests, are shown in Figure 12 while the physical properties and ultrasonic velocities are tabulated in Table 6.

Selected properties of all grout mixtures (HPRM-1 through ME8-11) are summarized in Figure 13 with the average structures tuff shown for reference. This plot, along with the shear strength data (Figure 12), substantiate the evolution of the grout development for the Mighty Epic structures program.

TABLE 3

SELECTED PROPERTIES OF SUPER LEAN, ROCK MATCHING AND HIGH STRENGTH GROUTS

Type	Density gm/cc			H_2O by Wet Wgt. %	Saturation %	Porosity Total %	Air Voids %	Meas. Perm Comp. %	Velocity (Ft/Sec)	
	As Rec.	Dry	Grain						Long	Shear
SLG	Meas.	Calc.	Meas.	Meas.	Calc.	Calc.	Calc.	Meas.	Meas.	Meas.
14-45* Day Age	1.74 ±0.03	1.25 ±0.03	2.63 ±0.02	28 ±2.0	94	52	3	2-4	5800	2600
RMG										
14-45* Day Age	2.04 ±0.03	1.51 ±0.03	3.20 ±0.02	26 ±2.0	100	53	0	2-4	7400	3600
Full** Strength	2.02	1.62	3.20	20	82	49	7	7	8300	4500
HSG										
Full** Strength	1.95	1.68	2.70	14	56	38	11	10+	11500	6800

* Average of about 10 batches for physical properties and permanent compactions and one batch only for velocities.
** One batch only for all values. For the RMG, see RMG test data section for explanations of the change in physical properties with age.

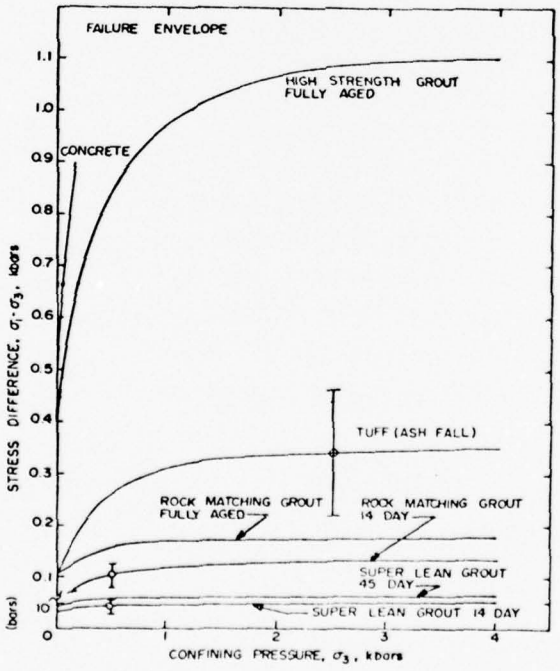

Figure 9. Failure Envelopes of Several Grout Mixtures and a Typical Ash Fall Tuff.

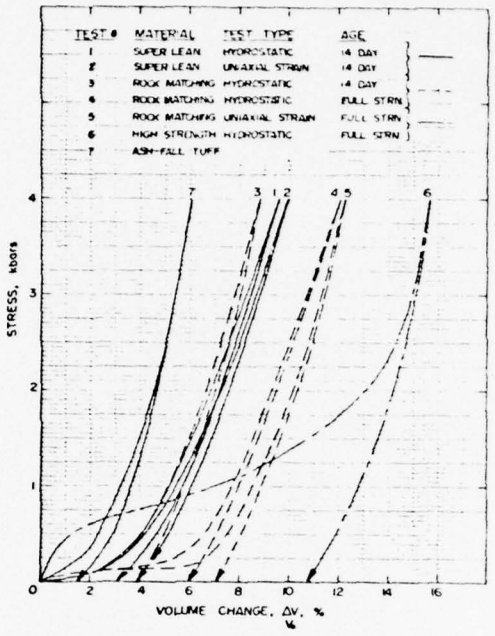

Figure 10. Hydrostatic Compression and Uniaxial Response of Several Grout Mixtures and a Typical Ash Fall Tuff.

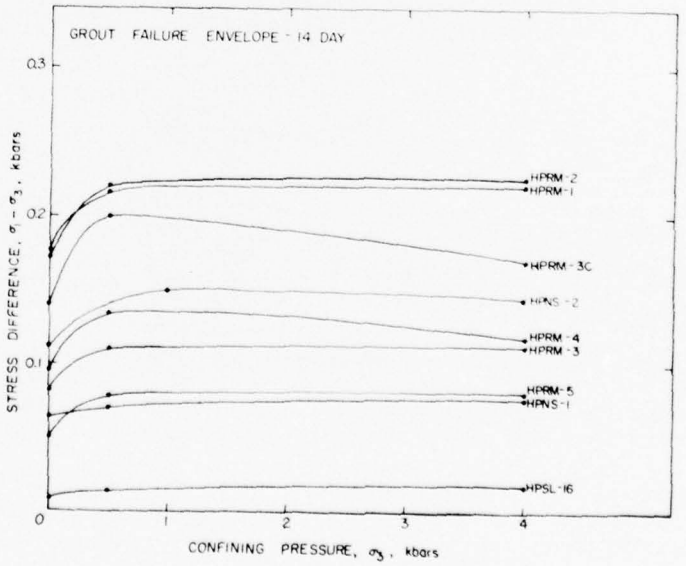

Figure 11a. 14 Day Age Failure Envelope on Grout Mixtures HPRM-1, HPRM-2, HPRM-3, HPRM-4, HPRM-5, HPSL-16, HPNS-1, HPRM-3C and HPNS-2.

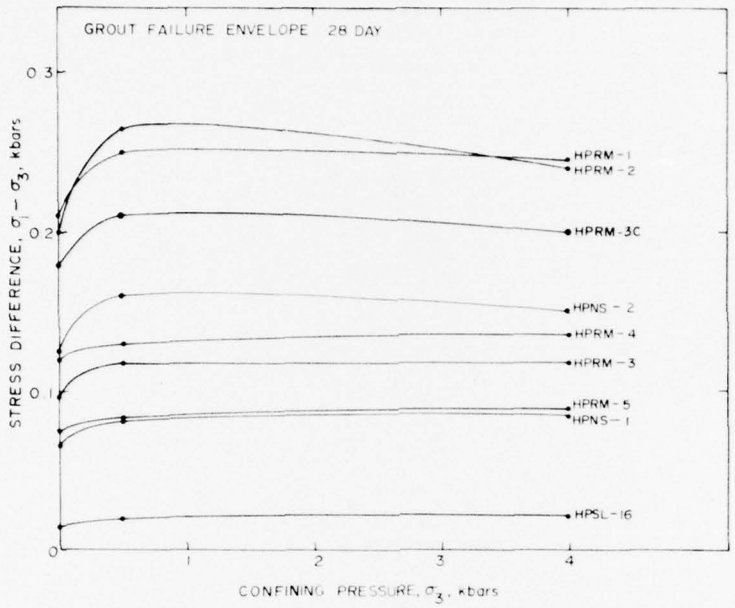

Figure 11b. 28 Day Age Failure Envelope on Grout Mixtures HPRM-1, HPRM-2, HPRM-3, HPRM-4, HPRM-5, HPSL-16, HPNS-1, HPRM-3C and HPNS-2.

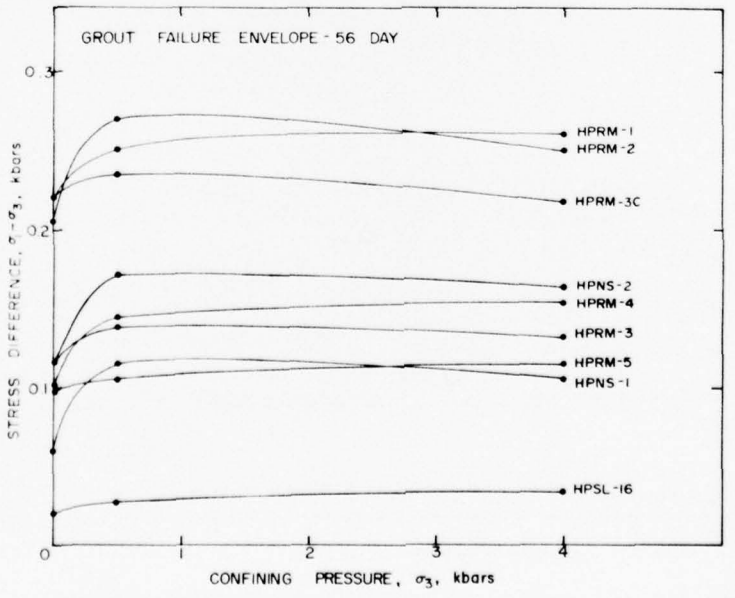

Figure 11c. 56 Day Age Failure Envelope on Grout Mixtures HPRM-1, HPRM-2, HPRM-3, HPRM-4, HPRM-5, HPSL-16, HPNS-1, HPRM-3C and HPNS-2.

TABLE 4

PHYSICAL PROPERTIES, ULTRASONIC VELOCITIES AND PERMANENT VOLUME COMPACTION ON NINE INITIAL GROUT TEST MIXTURES

GROUT MIXTURES	DENSITY (gm/cc)			WATER BY WET WEIGHT (%)	POROSITY (%)	SATURATION (%)	CALC. AIR VOIDS (%)	MEAS PERMANENT COMP. (%)	VELOCITY (ft/sec)	
	AS-RECEIVED	DRY	GRAIN						LONG	SHEAR
Grout 14 Day								Hyd. 1-D		
HPRM-1	2.06	1.65	2.97	20.1	44	93	3.0	2.1 2.3	9478	5274
HPRM-2	2.04	1.64	3.01	19.8	46	89	5.1	2.2 2.2	9166	5022
HPRM-3	2.07	1.58	3.11	23.6	49	99	0.5	1.5 1.6	8366	4472
HPRM-4	2.01	1.55	3.06	22.9	49	94	3.2	3.1 3.5	9084	4640
HPRM-5	1.92	1.46	3.02	23.9	52	88	5.9	3.5 4.0	7910	3753
HPSL-16	1.86	1.37	2.94	26.5	54	92	4.3	2.4 2.5	6579	2459
HPNS-1	2.04	1.51	3.35	25.9	55	96	2.0	1.8 1.8	7213	3427
HPRM-3C	2.10	1.71	3.03	18.9	44	91	3.9	2.4 2.6	9850	5333
HPNS-2	1.92	1.40	3.21	27.1	56	92	4.3	3.7 4.9	8240	4240
Grout 28 Day										
HPRM-1	2.02	1.56	2.97	22.9	48	97	1.3	2.2 2.8	10259	5696
HPRM-2	2.04	1.61	3.01	21.0	46	93	3.3	1.7 2.7	11591	6363
HPRM-3	2.08	1.61	3.11	22.7	48	98	1.0	1.5 1.9	8871	4695
HPRM-4	1.98	1.53	3.06	22.9	50	91	4.5	3.5 3.9	9058	4678
HPRM-5	1.94	1.45	3.02	27.4	52	95	2.6	2.9 3.1	7707	3796
HPSL-16	1.86	1.36	2.94	27.0	54	93	3.7	2.4 2.7	6303	2717
HPNS-1	2.05	1.51	3.35	26.7	55	99	0.2	2.0 2.5	7519	3619
HPRM-3C	2.12	1.70	3.03	19.6	44	95	2.3	2.0 2.5	9786	5275
HPNS-2	1.94	1.41	3.21	27.4	56	95	2.9	3.2 3.4	8360	4265
Grout 56 Day										
HPRM-1	2.05	1.63	2.97	20.5	45	93	3.2	2.5 3.0	10269	5545
HPRM-2	2.02	1.57	3.01	22.4	48	94	2.7	1.5 2.9	11591	6368
HPRM-3	2.10	1.65	3.11	21.2	47	95	2.5	1.6 2.5	9672	5230
HPRM-4	1.96	1.49	3.06	24.1	51	92	4.3	4.3 4.4	8215	3976
HPRM-5	1.97	1.48	3.02	24.8	51	96	2.0	2.5 2.7	8064	4117
HPSL-16	1.85	1.34	2.94	27.4	54	93	3.6	2.3 3.0	8291	3819
HPNS-1	2.09	1.58	3.35	24.2	53	96	2.2	2.1 2.6	8015	4006
HPRM-3C	2.15	1.73	3.03	19.5	43	98	1.0	1.9	10780	5480
HPNS-2	1.88	1.34	3.21	28.7	58	93	4.3	2.4 5.7	8780	4560

TABLE 5

SUMMARY OF MEASUREMENTS AND TESTS
CONDUCTED ON MIGHTY EPIC GROUT MIXTURES

GROUT MIXTURES	PHYSICAL PROPERTIES	ULTRASONIC VELOCITIES	MECHANICAL TESTS		
			TRIAXIAL COMPRESSION	HYDROSTATIC COMPRESSION	UNIAXIAL STRAIN
ME8Ø1	X	X	X	X	X
ME8Ø2	X	X	X	X	X
ME8Ø4	X		X		
ME8Ø5	X	X	X	X	
ME8Ø6	X		X		
ME8Ø7			X		
ME8Ø8			X		
ME8-11	X	X	X		
ME8-11(R) (Field Cast)	X	X	X	X	X

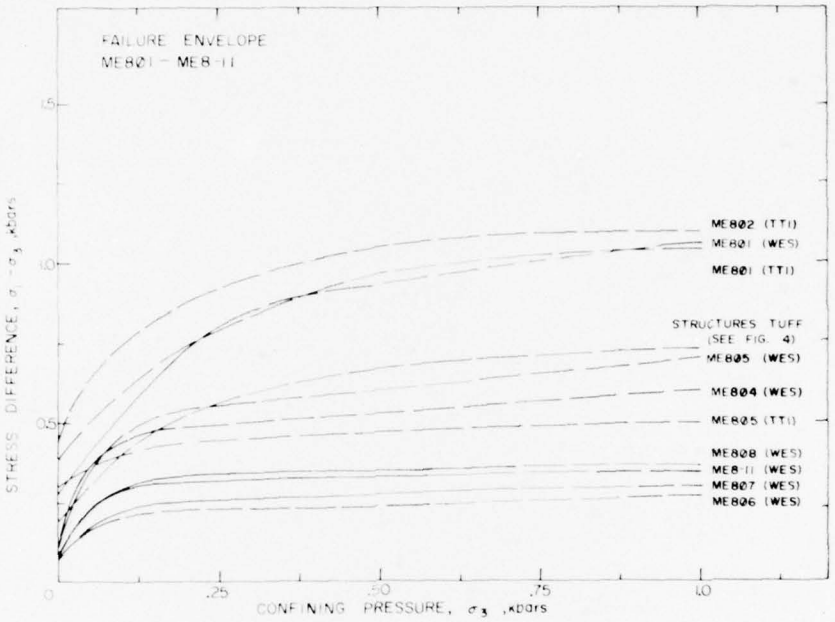

Figure 12. Combined Failure Data on ME8Ø1 through ME8-11 Grout Samples.

TABLE 6

PHYSICAL PROPERTIES, ULTRASONIC VELOCITIES AND PERMANENT VOLUME COMPACTION ON GROUT MIXTURES ME8Ø1, ME8Ø2, ME8Ø4, ME8Ø5, ME8Ø6 and ME8-11

GROUT MIXTURES	DENSITY (gm/cc)			WATER BY WET WEIGHT (%)	POROSITY (%)	SATURATION (%)	CALC. AIR VOIDS (%)	MEAS. PERMANENT COMP. (%)	VELOCITY (ft/sec)	
	AS-RECEIVED	DRY	GRAIN						LONG	SHEAR
								Hyd. 1-D		
ME8Ø1	1.95	1.61	2.57	17.4	38	90	3.7	3.9 4.5	12670	7402
ME8Ø2	1.89	1.57	2.54	17.0	38	84	6.1	4.0 5.1	12864	7188
ME8Ø4	1.91	1.56	2.52	18.5	38	92	2.9			
ME8Ø5	1.97	1.67	2.53	15.5	34	89	3.7		12700	7100
ME8Ø6	2.01	1.74	2.50	13.6	31	90	3.2			
ME8-11	2.05	1.77	2.53	13.7	30	93	2.0	3.4	9420	4272

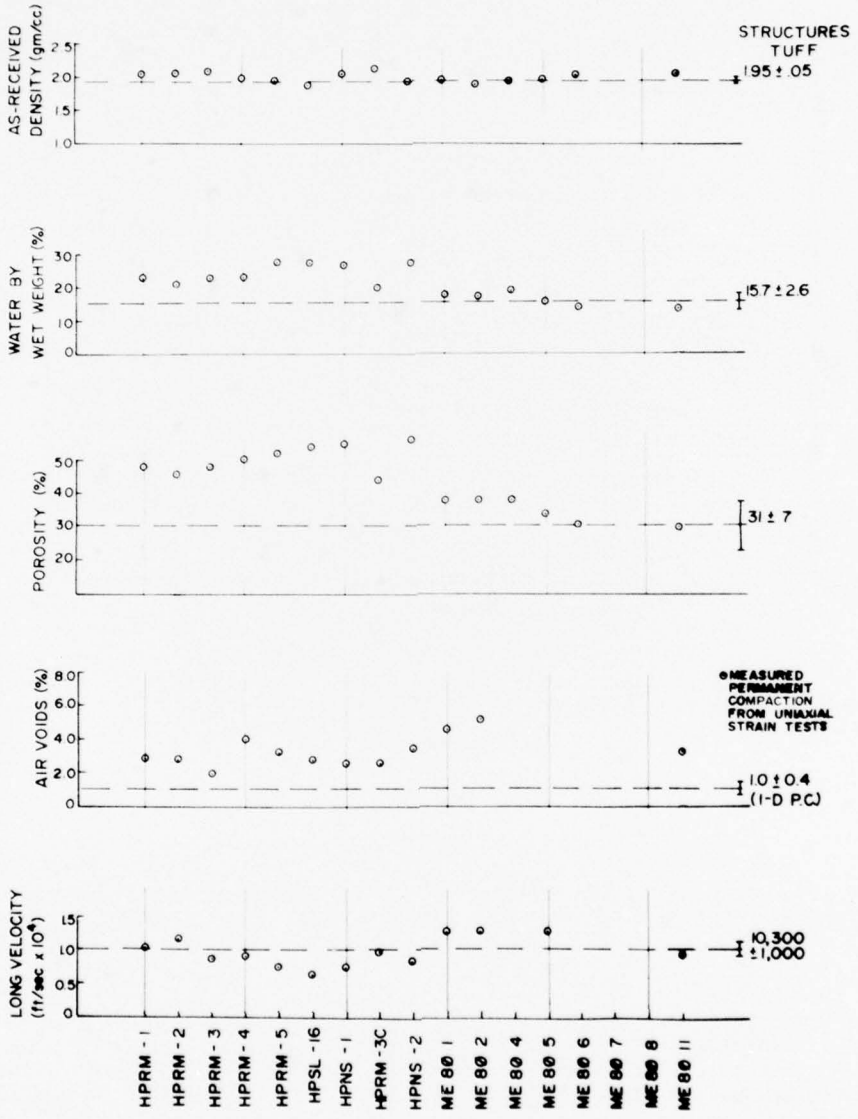

Figure 13. Selected Properties of all Grout Mixtures Tested During this Grout Development.

VERIFICATION OF FIELD GROUT MIXTURES

An added precaution, and one that has been standard procedure for past events, is periodic sampling of the grout mixes that are actually implaced in the tunnels. This was especially necessary for the structures grout where the properties were of upmost importance.

Selected samples obtained from batches of the field cast ME8-11 grout were tested by WES and TTI. The test results are shown in Figure 14 and 15 during the aging process and in Figure 16 for grout tests conducted close to shot day. Table 7 summarizes selected properties on these field cast mixtures.

The finalized mixture contained; Portland cement, expansive cement, flyash, Barite, Bentonite, pumice sand, fine silica sand, water reducing-retarder admixture and water. The water-cementitious ratio by weight was 1.4. The theoretical unit weight and theoretical cementitious content were 125.9 pounds per cubic feet and 5.0 bags per cubic yard, respectively.

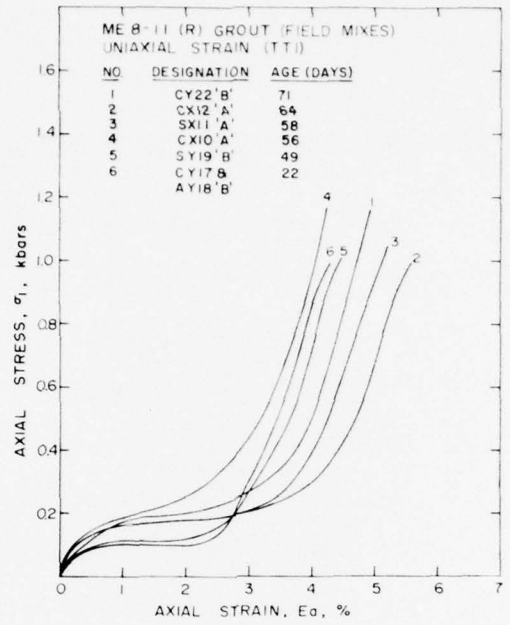

Figure 14a. Uniaxial Strain Results on Samples from Several Mixtures of ME8-11(R) Field Mixes (TTI) -- Stress-Strain Response.

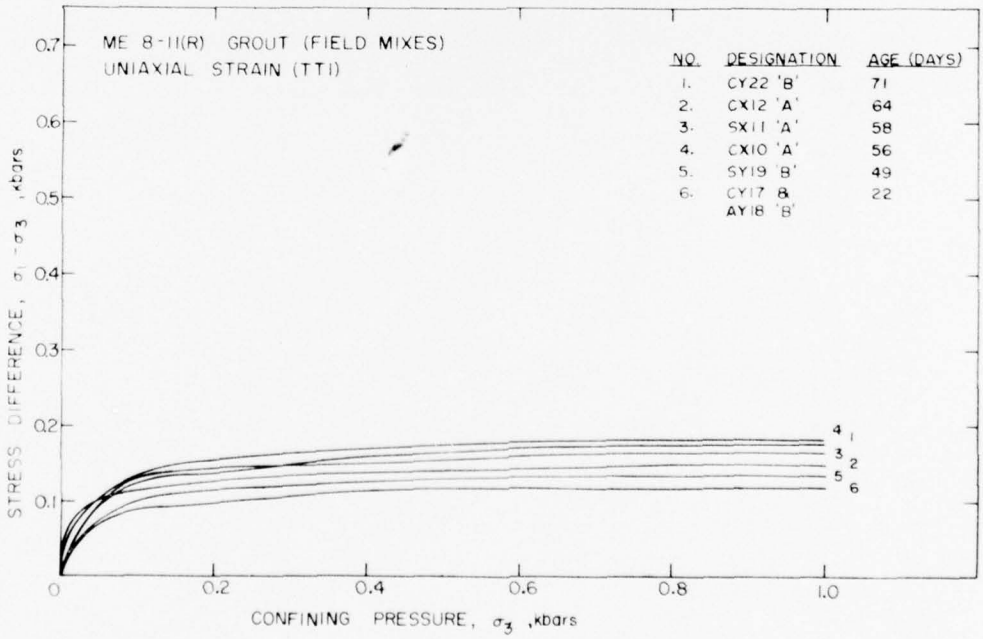

Figure 14b. Uniaxial Strain Results on Samples from Several Mixtures of ME8-11(R) Field Mixes (TTI) -- Stress-Stress Response.

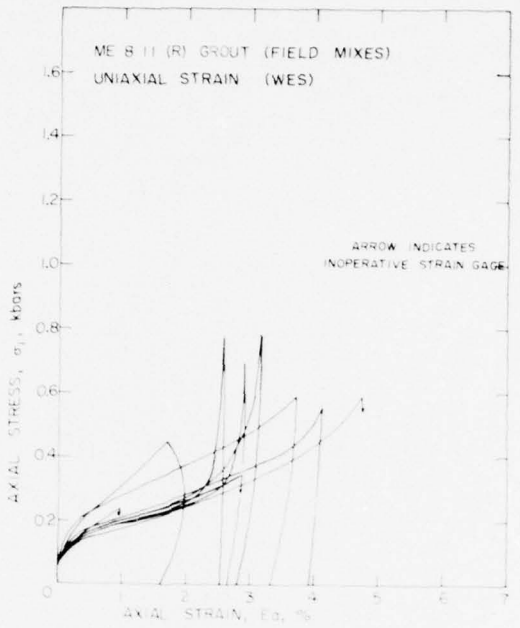

Figure 15a. Uniaxial Strain Results on Samples from Several Mixtures of ME8-11(R) Field Mixes (WES) -- Stress-Strain Response.

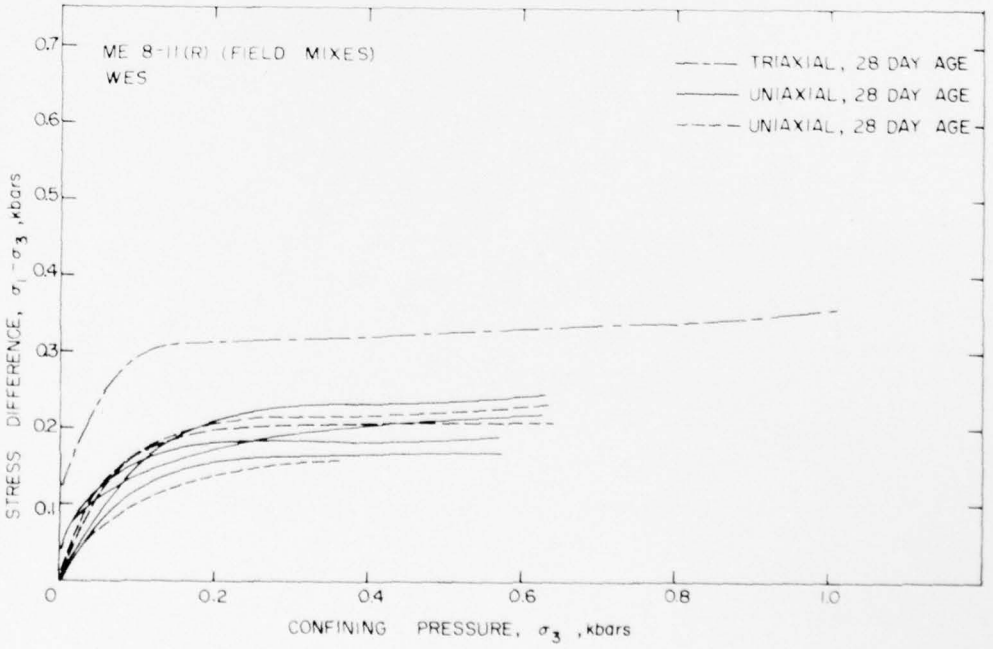

Figure 15b. Uniaxial Strain Results on Samples from Several Mixtures of ME8-11(R) Field Mixes (WES) -- Stress-Stress Response.

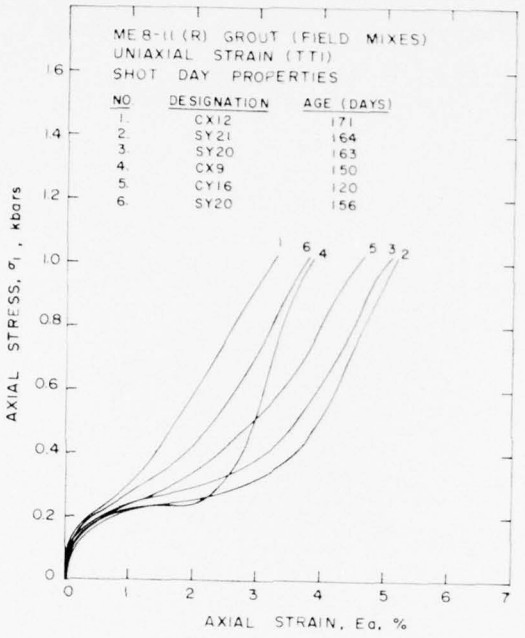

Figure 16a. Uniaxial Strain Results on Samples from Several Mixtures of ME8-11(R) Field Mixes (TTI) -- Stress-Strain Response. Tests were conducted close to Mighty Epic Shot Day.

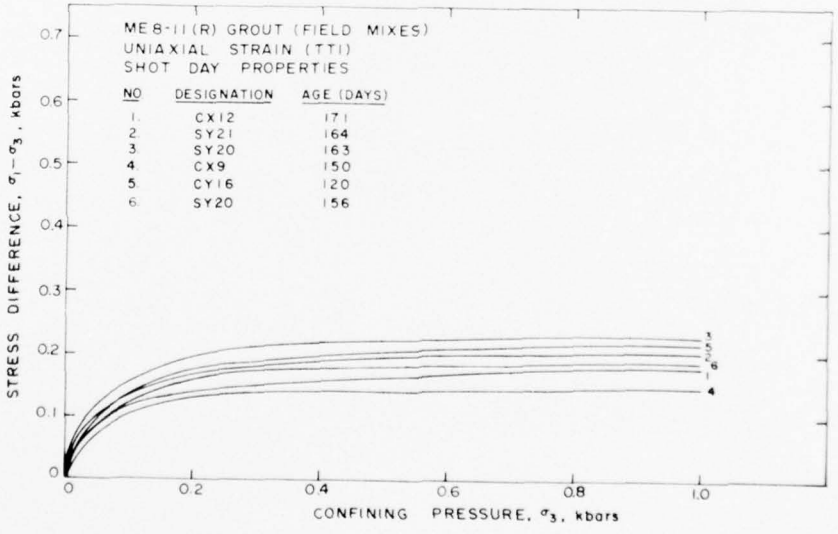

Figure 16b. Uniaxial Strain Results on Samples from Several Mixtures of ME8-11(R) Field Mixes (TTI) -- Stress-Stress Response. Tests were conducted close to Mighty Epic Shot Day.

TABLE 7

PHYSICAL PROPERTIES, ULTRASONIC VELOCITIES AND MEASURED PERMANENT VOLUME COMPACTION ON SEVERAL FIELD CAST BATCHES OF ME8-11 GROUT

DESIGNATION	AGE (DAYS)	DENSITY (gm/cc)			WATER BY WET WEIGHT (%)	POROSITY (%)	SATURATION (%)	CALC. AIR VOIDS (%)	MEAS. PERMANENT COMP. (%)	ULTRASONIC VELOCITY (ft/sec)	
		AS-RECEIVED	DRY	GRAIN						LONG	SHEAR
CY22 'B'	71	2.12	1.75	3.01	17.7	42	90	4.3	4.0	10,240	5300
CX12 'A'	64	2.14	1.77	3.05	17.6	42	90	4.3	4.9	10,490	5300
SX11 'A'	58	2.09	1.73	2.94	17.5	41	88	5.1	4.7	11,260	5600
CX10 'A'	56	2.12	1.75	3.03	17.5	42	87	5.4	5.4	10,500	5540
SY19 'B'	49	2.12	1.73	3.00	18.1	42	91	3.9	4.0	11,150	5360
CY17 & AY18 'B'	22	2.11	1.73	2.96	17.8	42	90	4.1	3.9	9,700	4970
CX12(FFSH)	171	2.10	1.73	2.96	17.6	42	89	4.6		11,125	5789
SY21	164	2.09	1.73	3.00	17.5	43	86	6.0		10,614	5425
SY20(FFSH)	163	2.13	1.77	3.07	16.8	42	85	6.6		10,904	5450
SY20	156	2.17	1.79	3.03	17.5	41	93	2.9		10,564	5721
CX9	150	2.19	1.83	3.07	16.5	40	90	4.2		9,570	5179
CY16	120	2.12	1.75	3.03	17.3	42	87	5.6		10,287	5520

DISCUSSION AND CONCLUSIONS

The mechanical and physical properties of the tuff in the structures area are well documented. The structures tuff, as compared to the typical ash fall tuff in Area 12, has about twice the shear strength with densities and sound speeds 10 to 20 percent higher, porosities and water contents 10 to 20 percent lower and air void contents approximately the same. The scatter in the material properties is typical of tuff.

Once the tuff properties had been established, the development of a matching grout required several major considerations. The shear strength of the grout was of utmost importance, not only unconfined, but as a function of confining pressure (failure envelope). Grout mixtures with high porosity and saturation are much less pressure dependent than tuff. This behavior is primarily a function of the pore pressure and the resulting effective stress. The most obvious means to increase the pressure dependence of the grout shear strength was to decrease the water content of the grout. Lowering the water content and reproportioning with various types of mixture constituents not only assisted in matching the shape of the tuff failure envelope but also in producing the overall increase in the shear strength needed. However, with this decrease in water and increase in shear strength, the pumpability of the grout was lowered. It should be obvious that with this dependence of properties on one another, the development required considerable effort and a number of changes in the grout constituents.

Aside from predicting what mixture changes were necessary to produce the desired results, the aging history of each test batch was important. Time, temperature and humidity all add an important factor to the grout

properties. Grout implaced in essentially a 100 percent humidity environment can develop a considerable temperature rise over a period of time. Also, the grout would be implaced weeks or months prior to test execution. Obviously, to have simulated these exact conditions on the development grouts would require a prohibitive test program time. Therefore, prior experience and knowledge of the aging characteristics were utilized to a considerable degree in this grout program. As an example, note the differences in the uniaxial strain test response of the ME8-11 grout as tested by WES and Terra Tek, Figure B15. The WES data was generated from samples which had been at elevated temperature and 100 percent humidity for 7 days. This aging history is approximately equivalent to 28 days of curing at room temperature while maintaining the water content constant. The Terra Tek tests were on 14 day age room temperature cured samples. The WES samples (7 day accelerated) produced about twice the shear strength and a much different stress-strain response than the Terra Tek samples (14 day room temperature).

In summary, the development of a grout to match select properties of the tuff was very successful. The ME8-11 grout mixture matches very closely the shape of the tuff failure surface, the as-received density, the sound speed, porosity and the water content. The air void content of the grout is slightly higher but will not be a problem because of the relatively thin layer of grout.

Concerning the absolute magnitude of the grout shear strength, it was the general consensus of the persons responsible for the structures experiments, that in consideration of the tuff material scatter, they would prefer to have the grout strength on the low side rather than the high side of the "representative" tuff strength. The ME8-11 grout mixture is therefore expected to peak out at a strength lower than the "representative" tuff strength.

REFERENCES

1. R. L. Stowe, Concrete and Rock Properties Branch, Waterways Experiment Station, Vicksburg, Mississippi.

2. Ralph Bendenelli, Grouting Branch, Waterways Experiment Station, Vicksburg, Mississippi.

3. J. W. LaComb, Civil Engineering, Nevada Test Site, Mercury, Nevada.

4. S. W. Butters, R. K. Dropek, S. J. Green and A. H. Jones, "Material Properties in Support of the Nevada Test Site Nuclear Test Program," Terra Tek Report TR 75-27, October 1975.

APPENDIX A

Mechanical Test Results on U12n.10 UG#4,

UG#6a, ISS#5 and ISS#7 Core Samples.

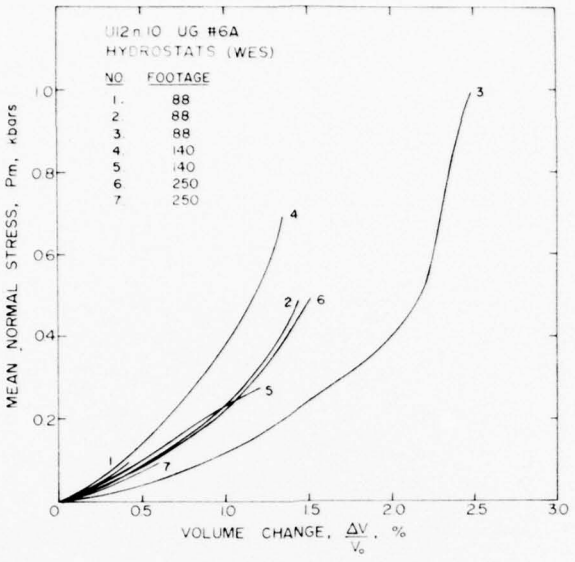

Figure A1. Hydrostatic Compression Results on U12n.10 UG#6a Core Samples (WES).

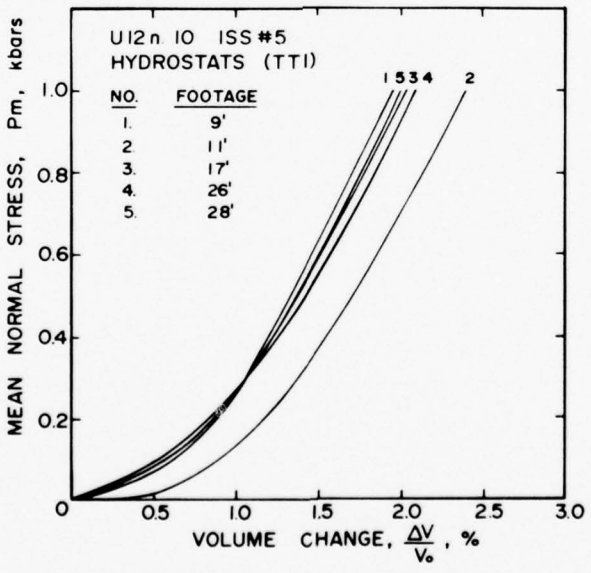

Figure A2. Hydrostatic Compression Results on U12n.10 ISS#5 Core Samples (TTI).

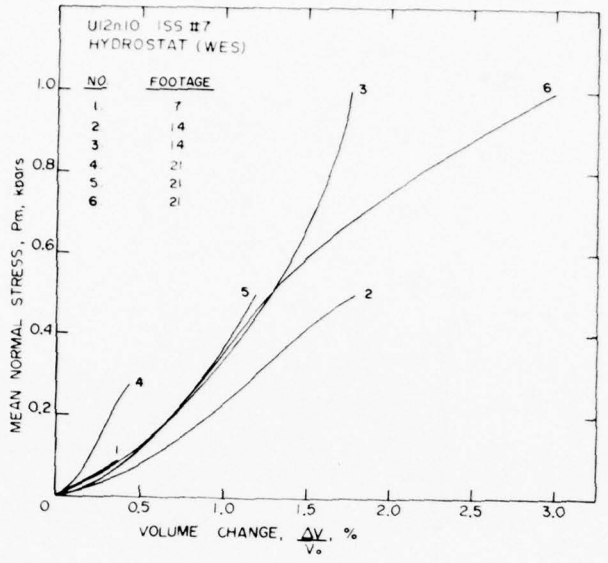

Figure A3. Hydrostatic Compression Results on U12n.10 ISS#7 Core Samples (WES).

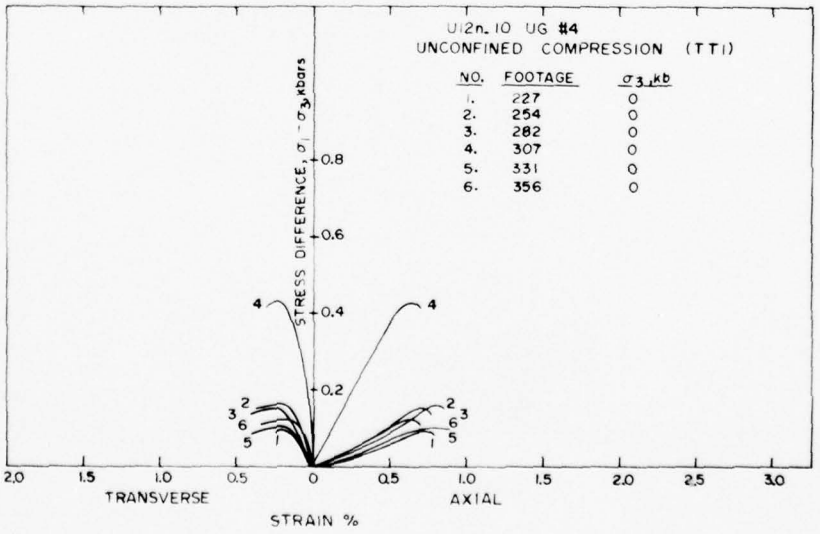

Figure A4. Unconfined Compression Results on U12n.10 UG#4 Core Samples (TTI).

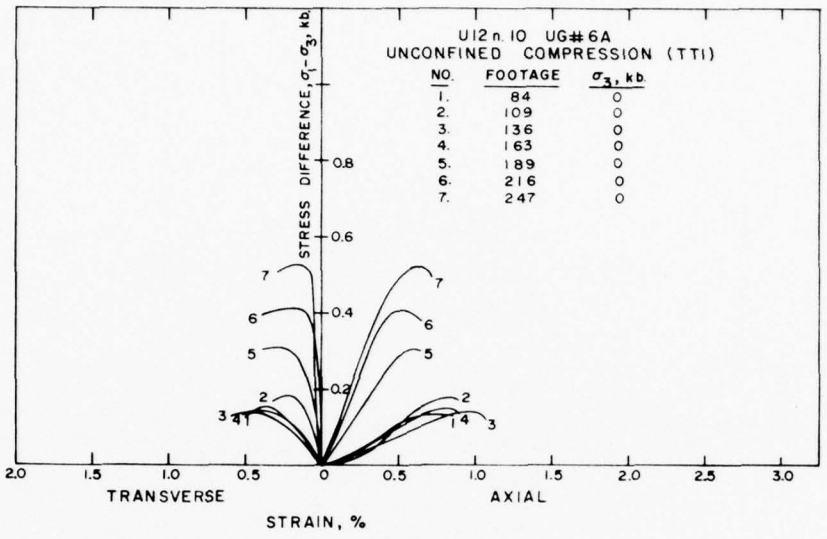

Figure A5. Unconfined Compression Results on U12n.10 UG#6a Core Samples (TTI).

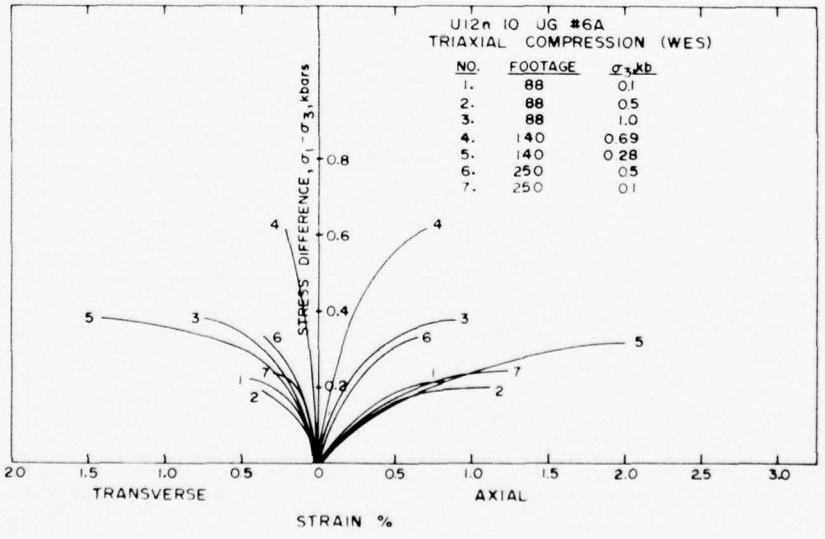

Figure A6. Triaxial Compression Results on U12n.10 UG#6a Core Samples (WES).

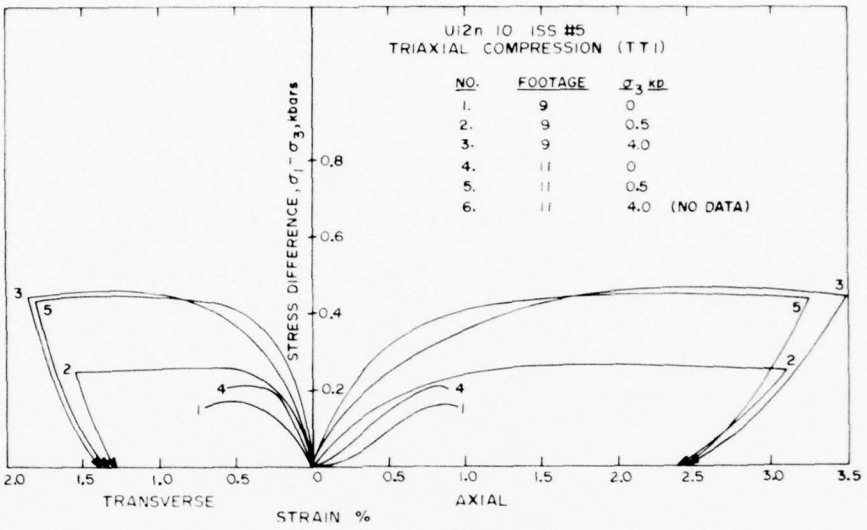

Figure A7. Triaxial Compression Results on U12n.10 ISS#5 Core Samples (TTI).

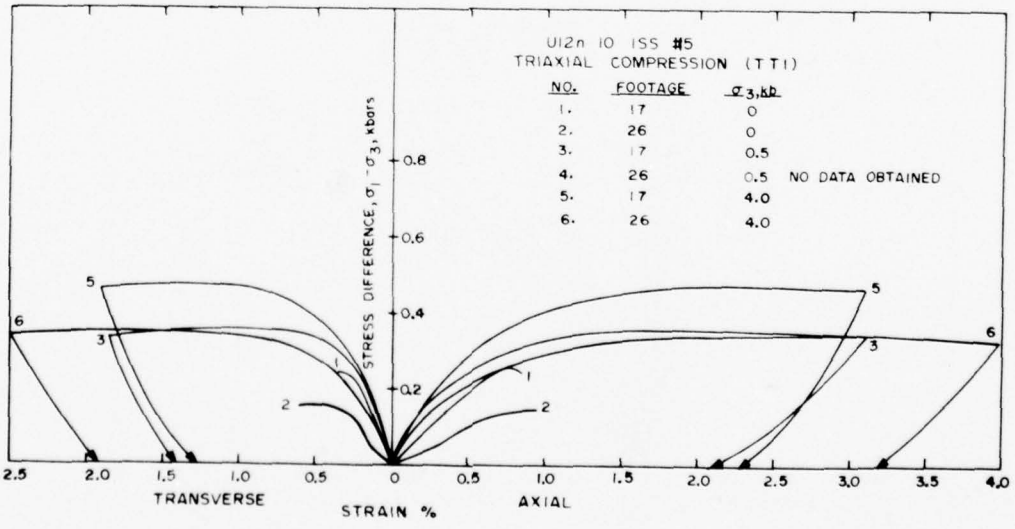

Figure A8. Triaxial Compression Results on U12n.10 ISS#5 Core Samples (TTI).

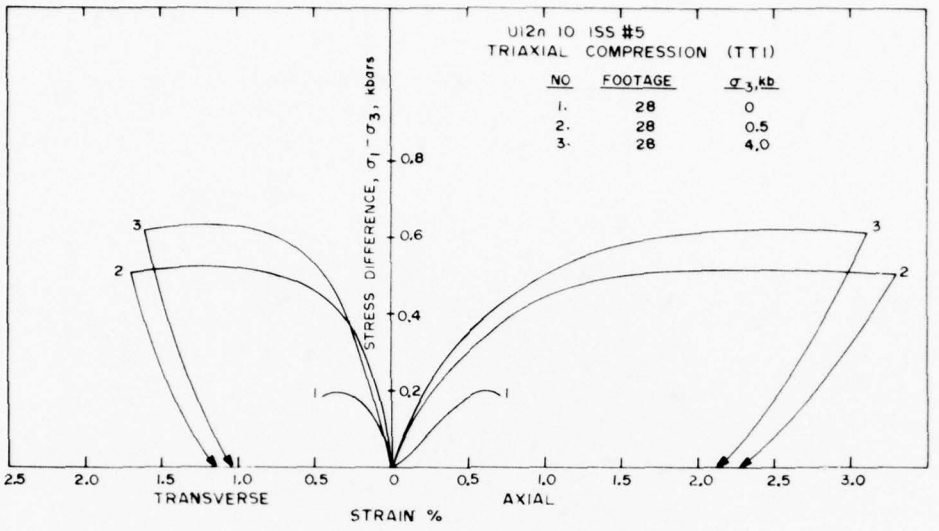

Figure A9. Triaxial Compression Results on U12n.10 ISS#5 Core Samples (TTI).

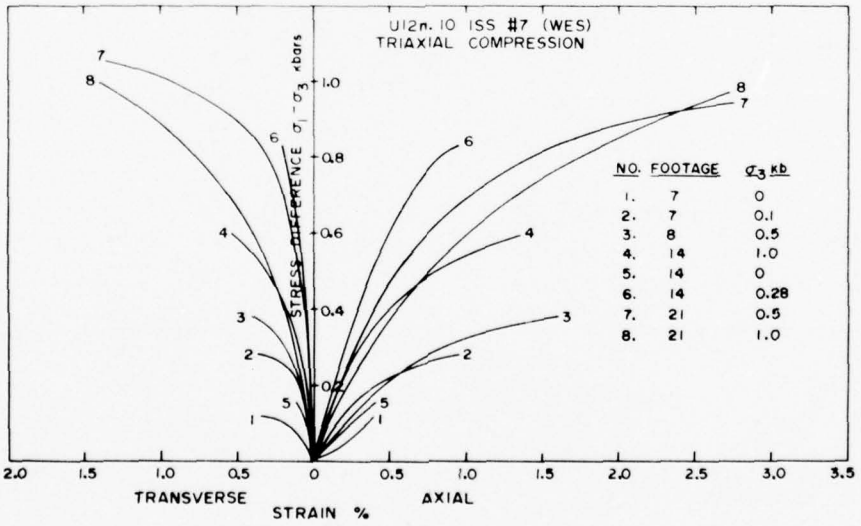

Figure A10. Triaxial Compression Results on U12n.10 ISS#7 Core Samples (WES).

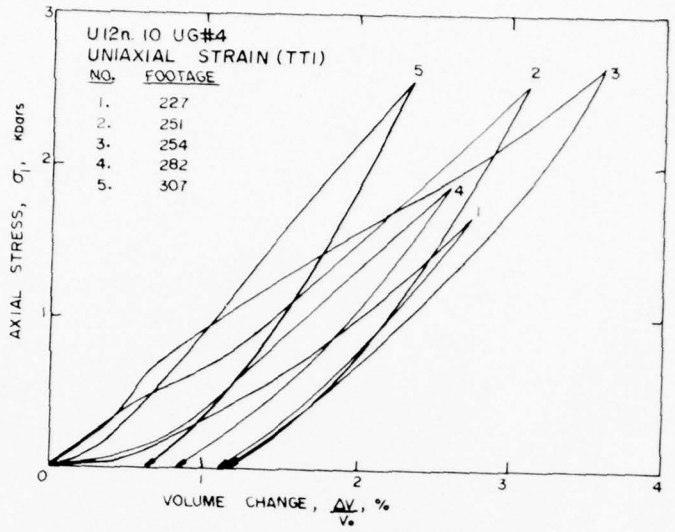

Figure A11a. Uniaxial Strain Results on U12n.10 UG#4 Core Samples (TTI).

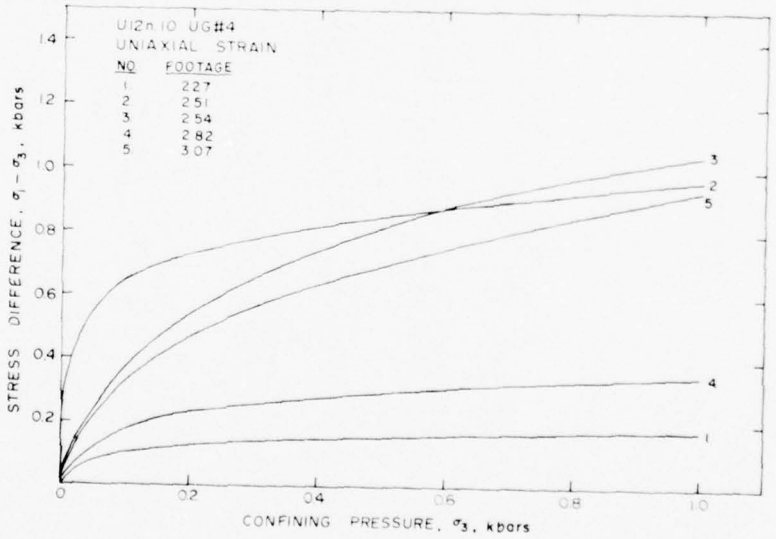

Figure A11b. Uniaxial Strain Results on U12n.10 UG#4 Core Samples (TTI).

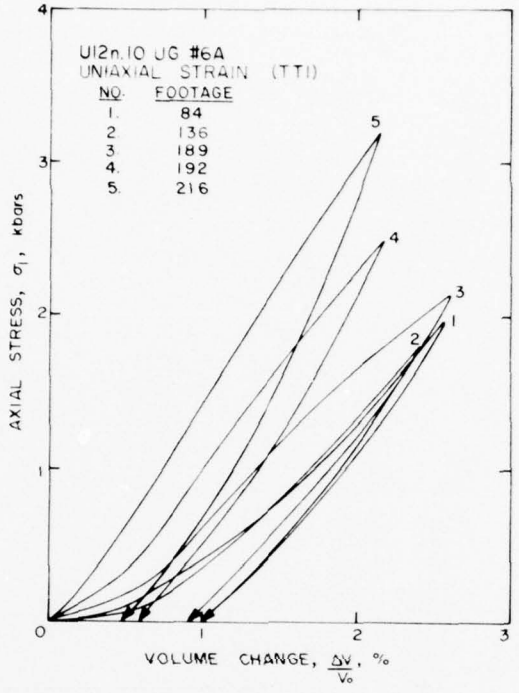

Figure A12a. Uniaxial Strain Results on U12n.10 UG#6a Core Samples (TTI).

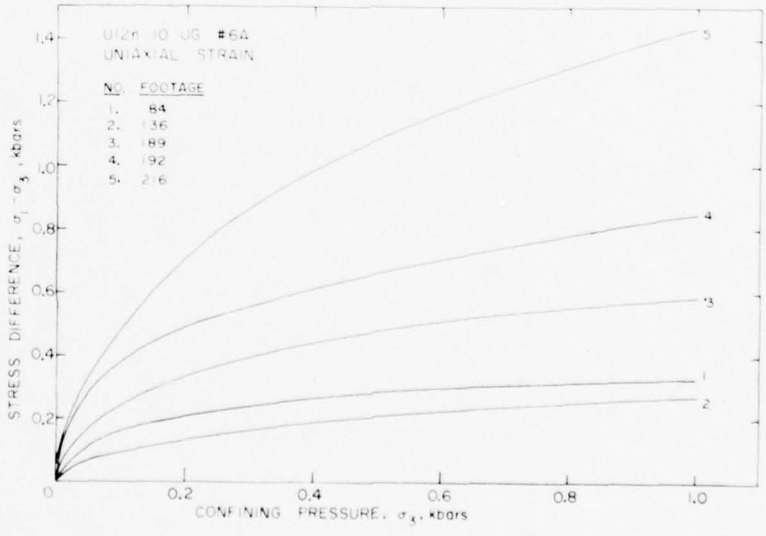

Figure A12b. Uniaxial Strain Results on U12n.10 UG#6a Core Samples (TTI).

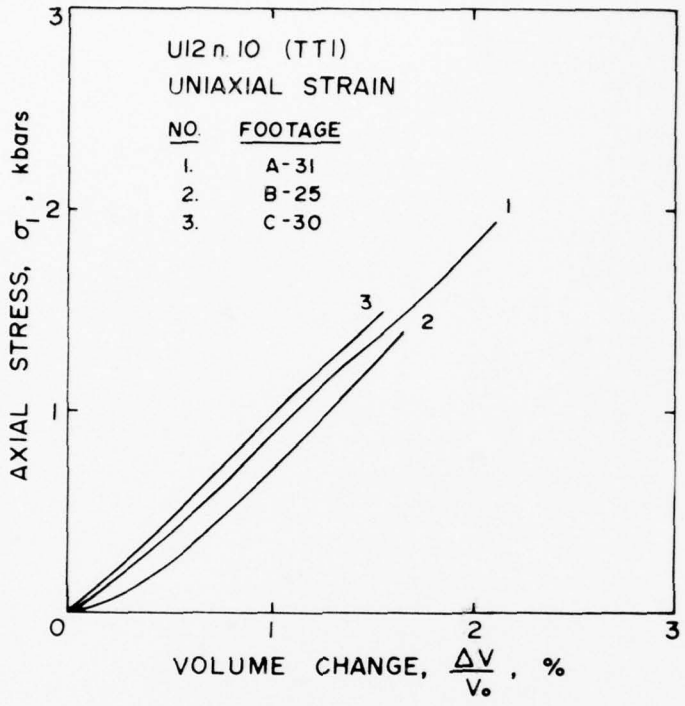

Figure A13a. Uniaxial Strain Results on U12n.10 A, B, and C Drift Samples (TTI).

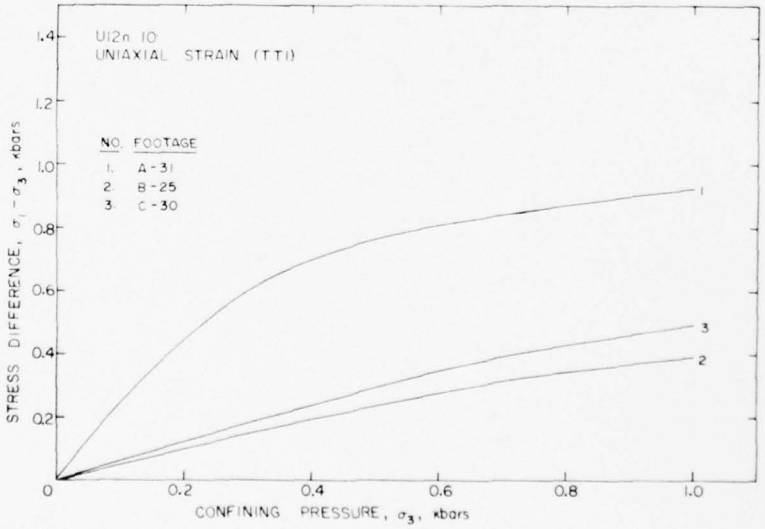

Figure A13b. Uniaxial Strain Results on U12n.10 A, B, and C Drift Samples (TTI).

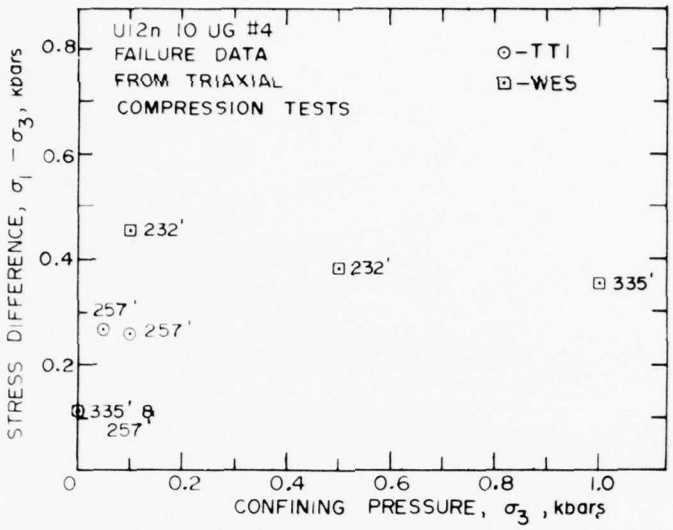

Figure A14. Failure Data from Triaxial Compression Tests on U12n.10 UG#4 Core Samples.

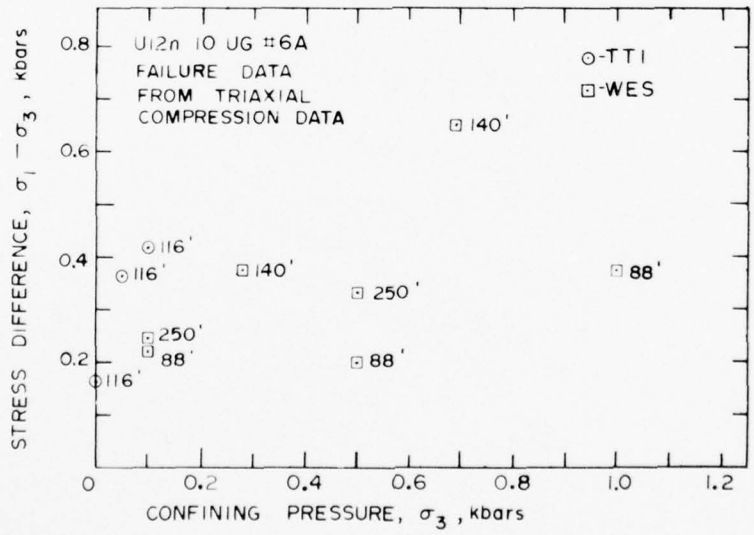

Figure A15. Failure Data from Triaxial Compression Tests on U12n.10 UG#6a Core Samples.

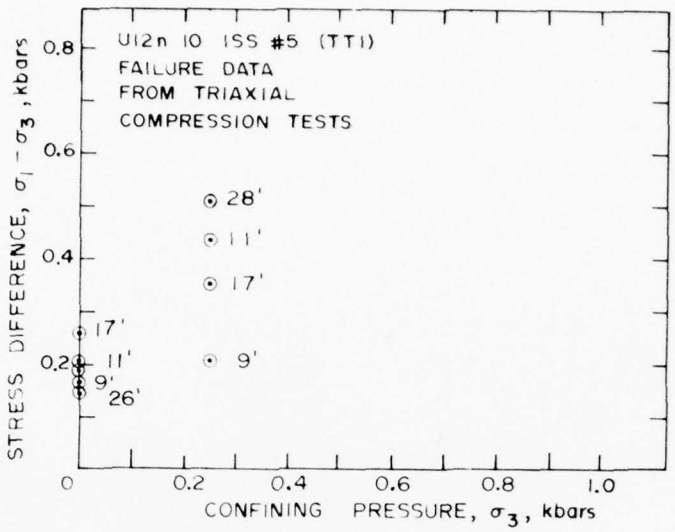

Figure A16. Failure Data from Triaxial Compression Tests on U12n.10 ISS#5 Core Samples (TTI).

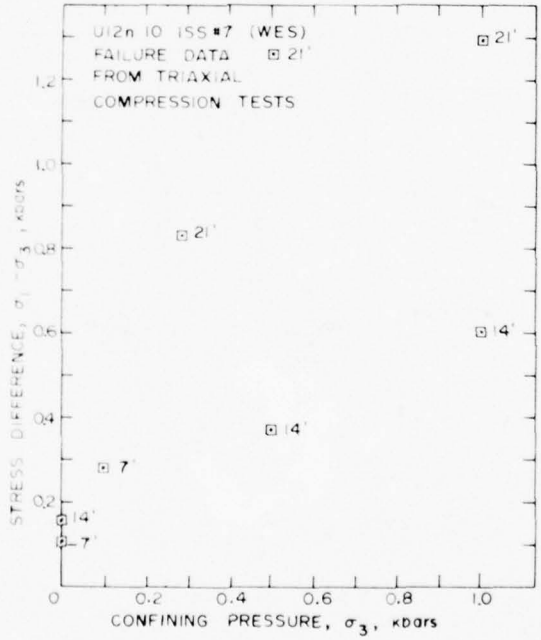

Figure A17. Failure Data from Triaxial Compression Tests on U12n.10 ISS#7 Core Samples (WES).

APPENDIX B

Mechanical Test Results on Mighty Epic Grout Mixtures

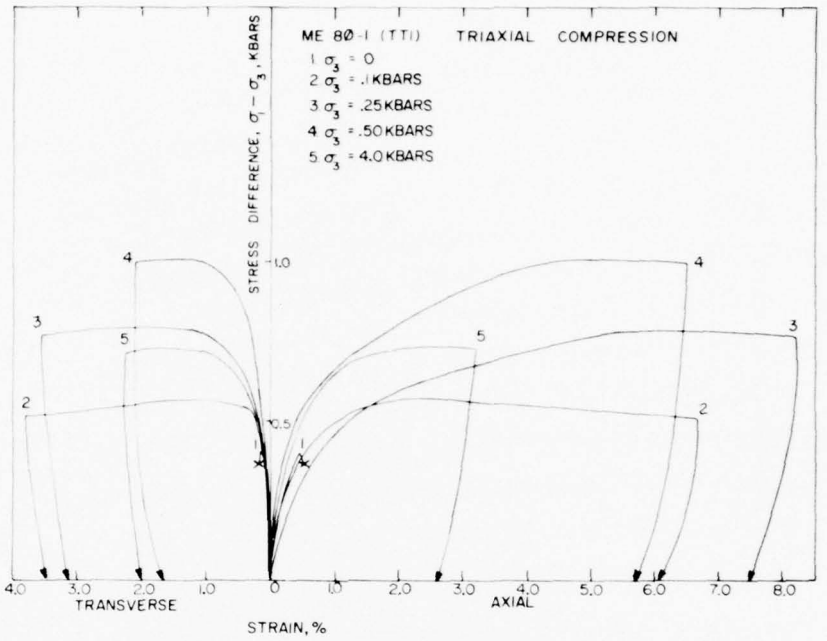

Figure B1. Triaxial Compression Tests on ME8Ø1 Grout Samples (TTI).

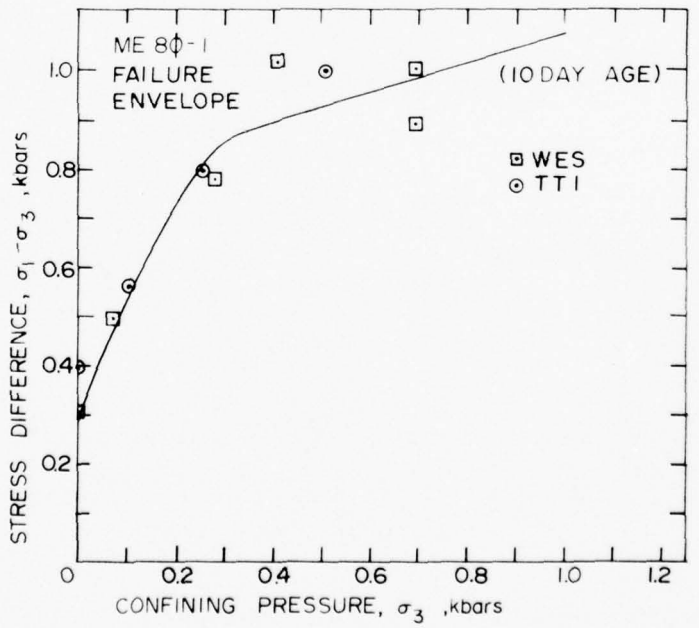

Figure B2. Failure Data on ME8Ø1 Grout Samples (WES and TTI).

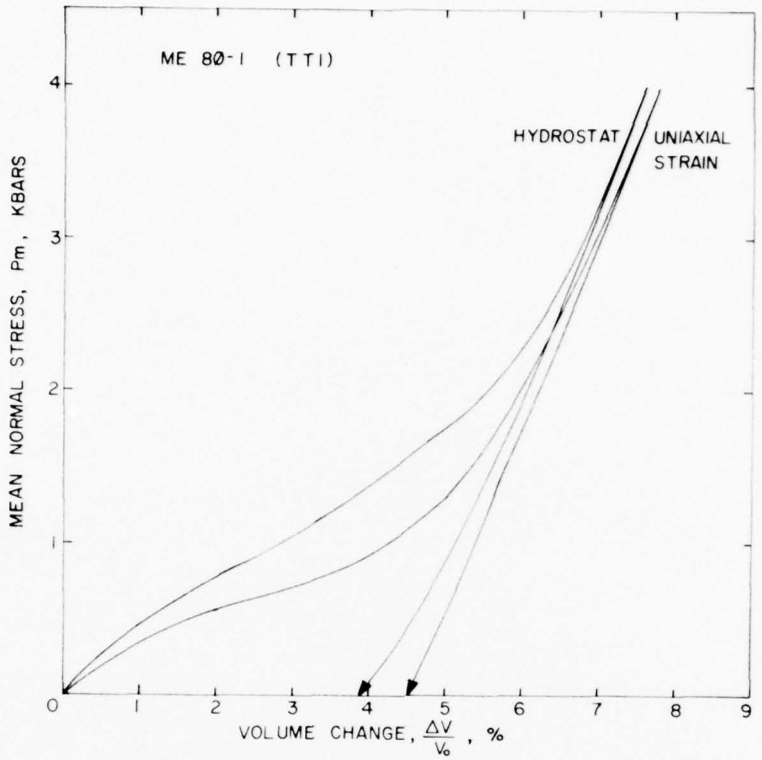

Figure B3a. Hydrostatic Compression and Uniaxial Strain Tests on ME8Ø1 Grout Samples (TTI).

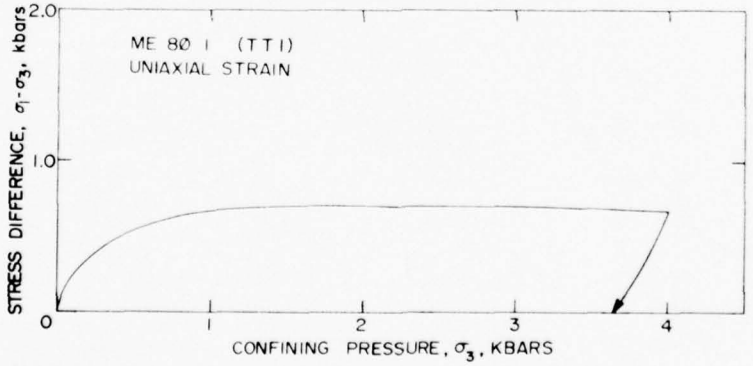

Figure B3b. Hydrostatic Compression and Uniaxial Strain Tests on ME8Ø1 Grout Samples (TTI).

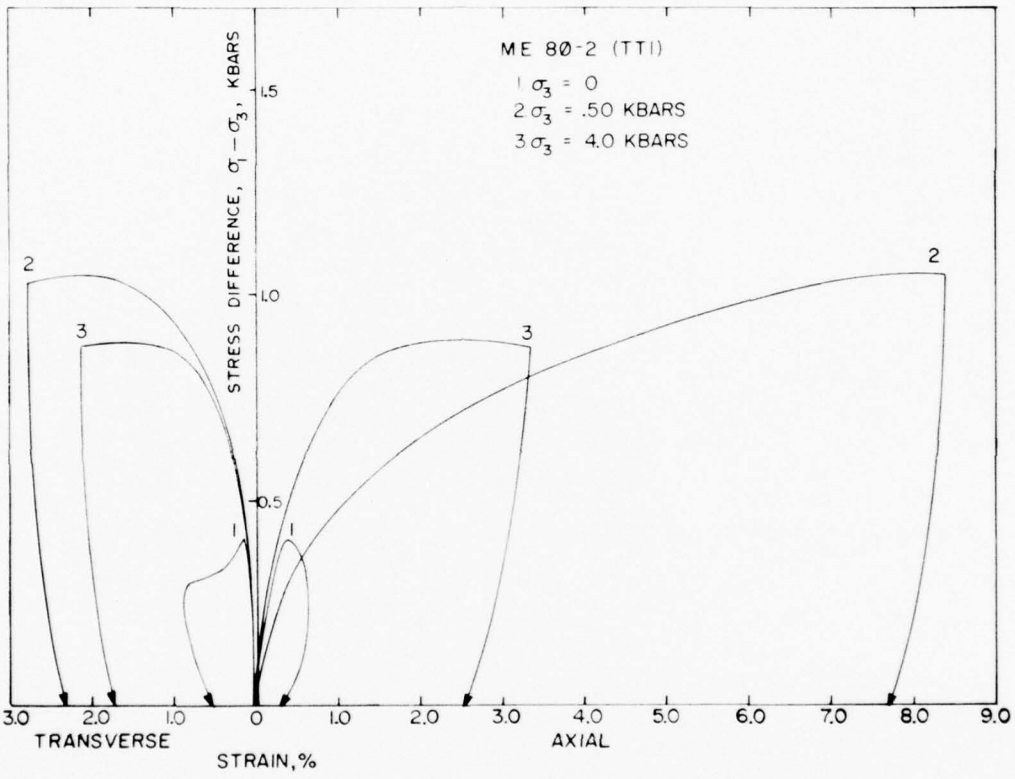

Figure B4. Triaxial Compression Results on ME802 Grout Samples (TTI).

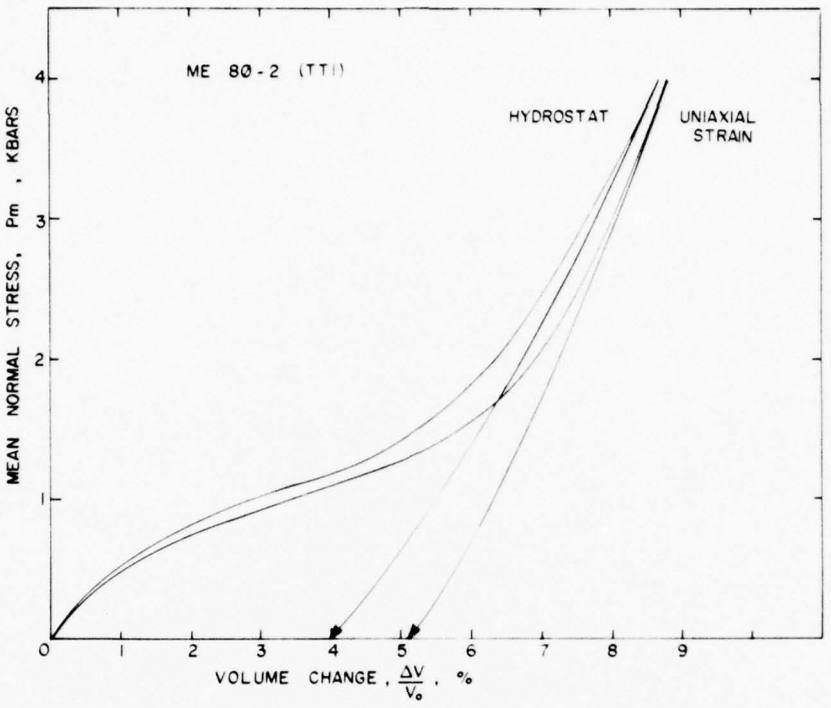

Figure B5a. Hydrostatic Compression and Uniaxial Strain Results on ME802 (TTI).

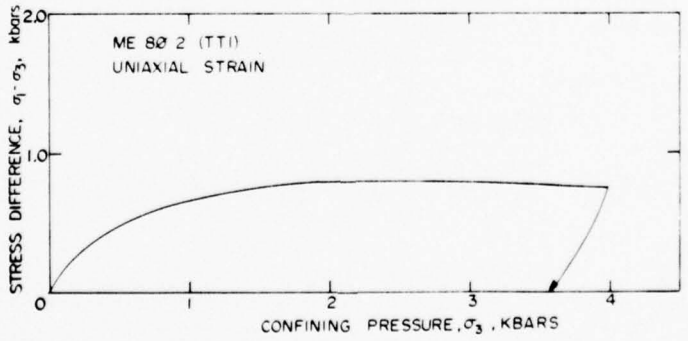

Figure B5b. Hydrostatic Compression and Uniaxial Strain Results on ME802 (TTI).

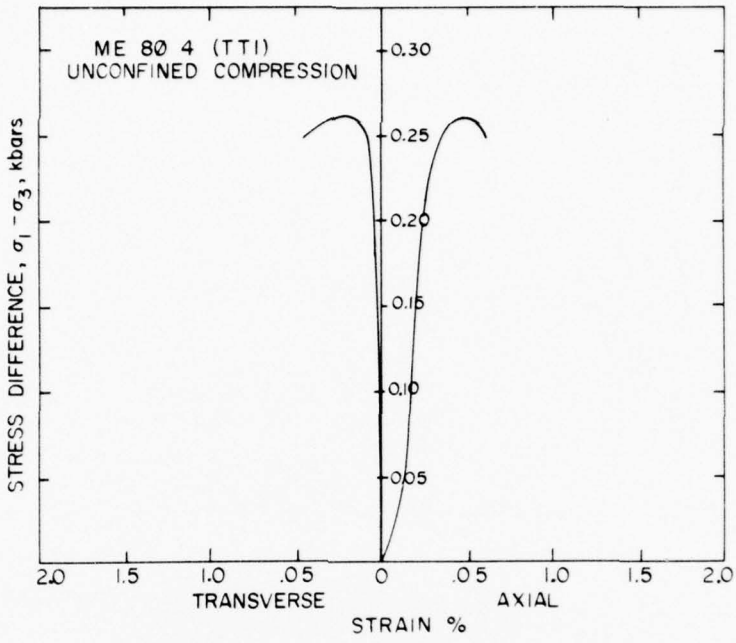

Figure B6. *Unconfined Compression Tests on ME8Ø4 Grout Samples* (TTI).

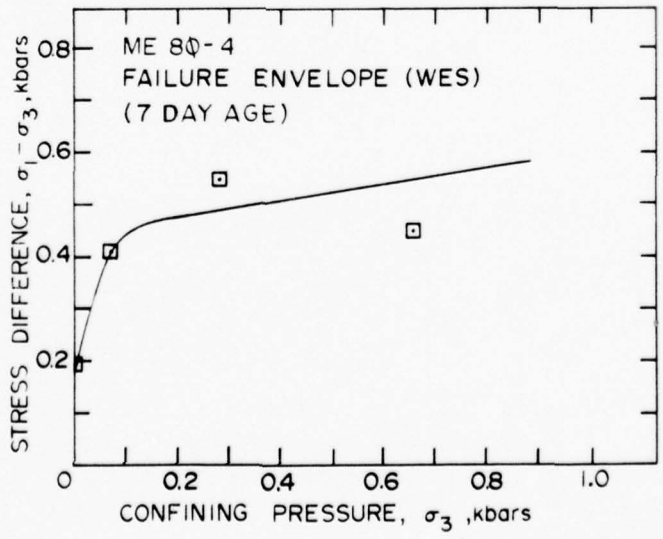

Figure B7. Failure Data on ME8Ø4 Grout Samples (WES).

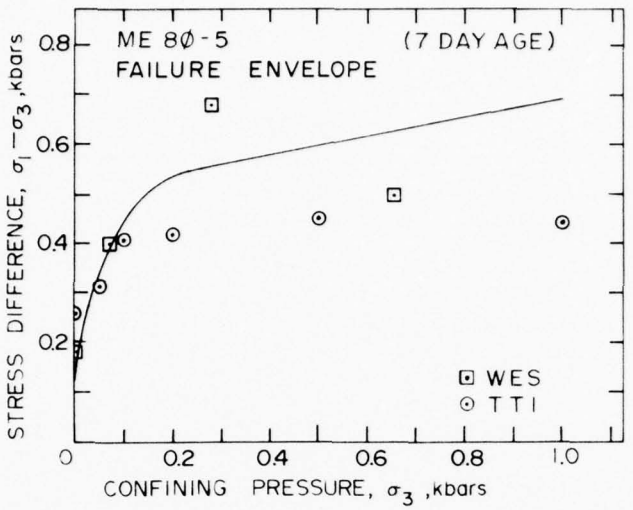

Figure B8. Failure Data on ME8Ø5 Grout Samples (WES and TTI).

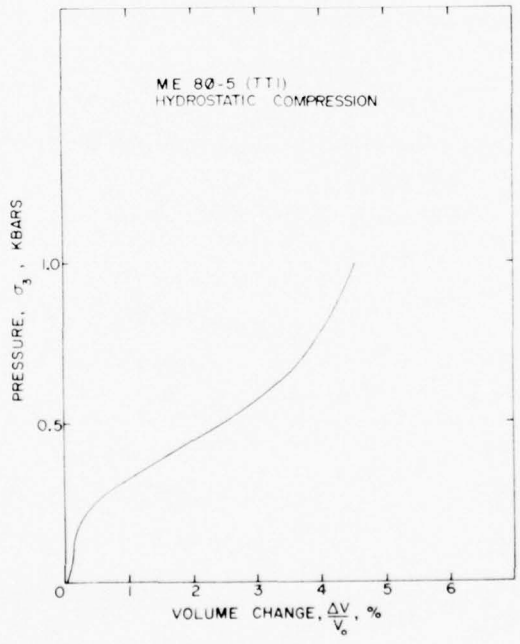

Figure B9. Hydrostatic Compression Results on ME8Ø5 Grout Samples (TTI).

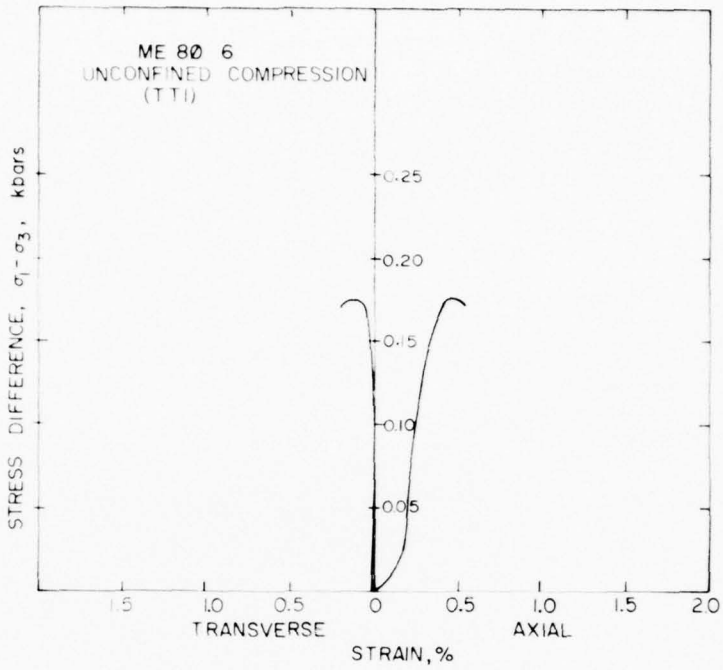

Figure B10. Unconfined Compression Results on ME80 6 Grout Samples (TTI).

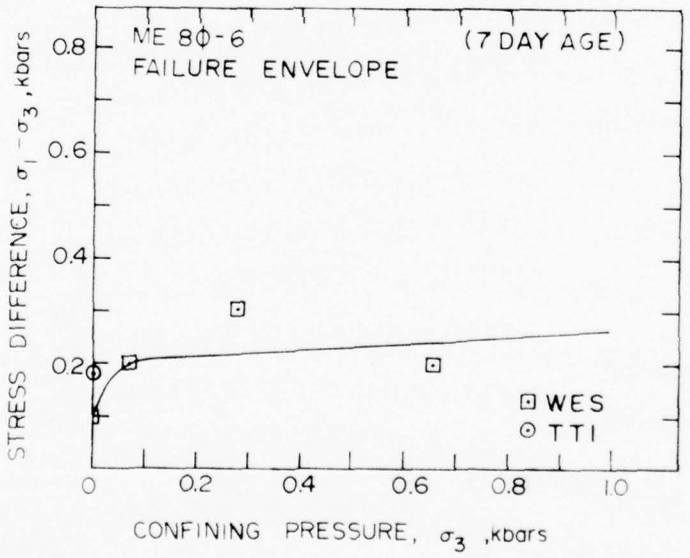

Figure B11. Failure Data on ME80 6 Grout Samples (WES and TTI).

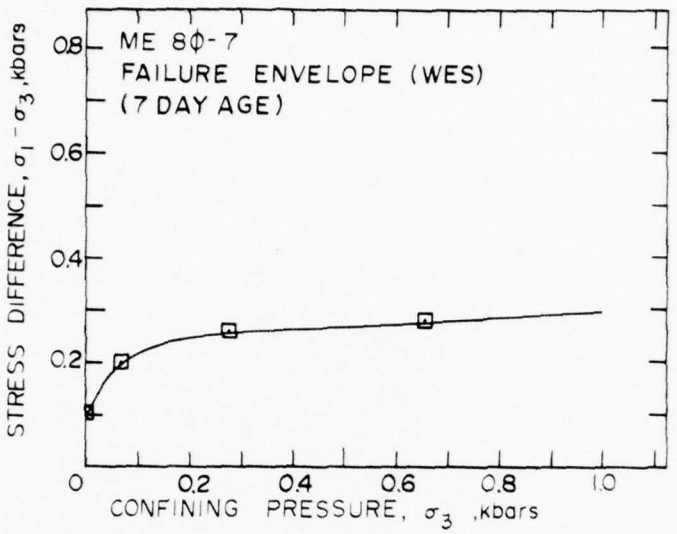

Figure B12. Failure Data on ME8Ø7 Grout Samples (WES).

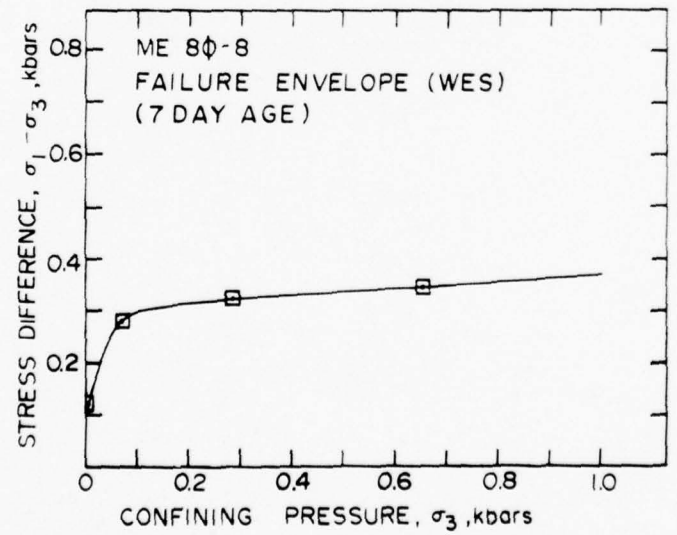

Figure B13. Failure Data on ME8Ø8 Grout Samples (WES).

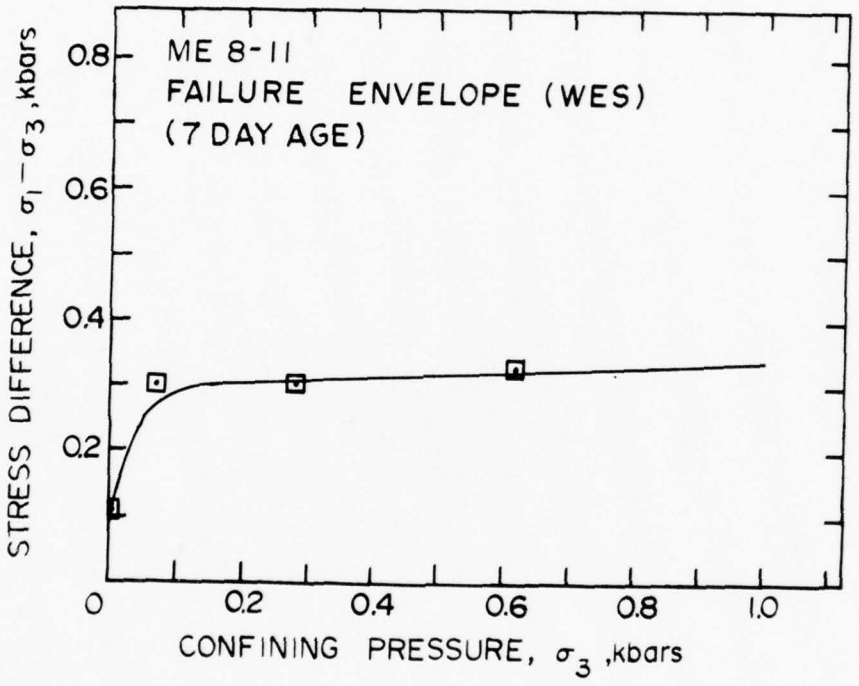

Figure B14. Failure Data on ME8-11 Grout Samples (WES).

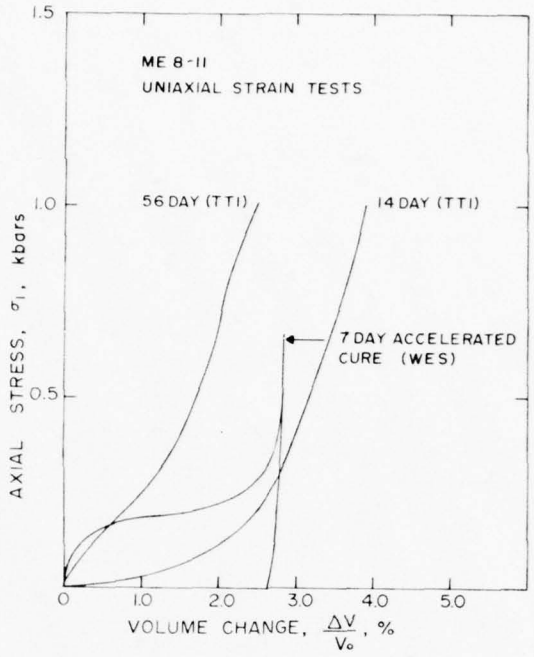

Figure B15a. Uniaxial Strain Results on ME8-11 Grout Samples (WES and TTI).

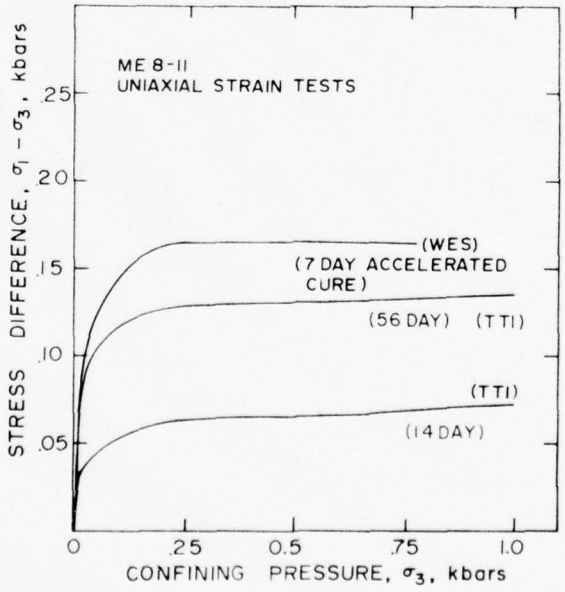

Figure B15b. Uniaxial Strain Results on ME8-11 Grout Samples (WES and TTI).

PROPERTIES OF U12n.10 MH#2 AND MH#3 CORE SAMPLES

TerraTek

June 2, 1976

Mr. J. W. LaComb
Defense Nuclear Agency
Nevada Test Site
Mercury, NV 89023

Dear Joe:

Properties have been measured on core samples from U12n.10 MH#2 (90') and U12n.10 MH#3 (48', 51', 54', 57') interface drill holes. Physical properties and ultrasonic velocities were obtained on all samples while limited mechanical data was produced.

Attached are photographs showing the tuff sample from MH#3 at 48 feet, a combination tuff and rubble at 51 and 54 feet and a more competent palezoic material at 57 feet. The MH#2 90 foot sample shown appears to be from the same region of the interface as the MH#3 51 and 54 foot samples.

The table following the photographs lists the physical properties and ultrasonic velocities of the samples. As noted by the data along a 2 inch length of the 90 foot sample, there is a considerable amount of variation in the interface region. The actual insitu physical properties would obviously require knowing the percentage of each type of material in the whole; although the material from 48' thru 57' does, in general, show higher densities, lower water contents and higher ultrasonic velocities than the Mighty Epic tunnel bed tuff.

Triaxial compression tests were conducted, with limited success, at confining pressures of 0.1 and 0.5 KB. The attached data indicates that the tuff sample (48') showed only slightly higher shear strength than the average tunnel bed tuff while the sample at 51 foot showed a shear strength within the lower bound of the tunnel bed tuff. Two tests were conducted on the 54 foot sample, both at a confining pressure of 0.5 kilobars, to determine the effect of the inhomogeneities in the material. One sample contained a number of rubble fragments on the order of 1 to 3 centimeters in diameter while the other sample contained fragments no greater than 1 centimeter in diameter. The former sample produced a maximum failure stress of 0.25 kilobars while the latter sample produced a maximum failure stress of 1.07 kilobars. This amount of variation is not at all unreasonable for the type of sample being tested. The 57 foot sample produced a maximum failure stress of 1.04 kilobars which would have, in all probability, been much higher had it not failed along the bedding plane shown in the earlier photograph. The 90 foot sample from MH#2 was noticeably weaker, but again, seemed to be a result of the size and orientation of the rubble fragments in the test sample.

Preliminary direct shear test results on MH#2 - 84', MH#3 - 47' and MH#3 - 52' indicate shear strengths of 0.117 KB, 0.133 KB and .069 KB, respectively. The normal stress was constant at 0.069 kilobars. The coefficient of sliding friction was difficult to obtain as the initial fracture was not entirely in the shearing plane and continued fracturing occurred as the displacement increased. The data suggests, however, a coefficient of sliding friction on the order of 0.6 to 0.7. Photographs of the direct shear test samples are attached.

Sincerely,

Scott W. Butters
Engineering Supervisor

SWB/jlg

Enclosures

cc: Mighty Epic Distribution

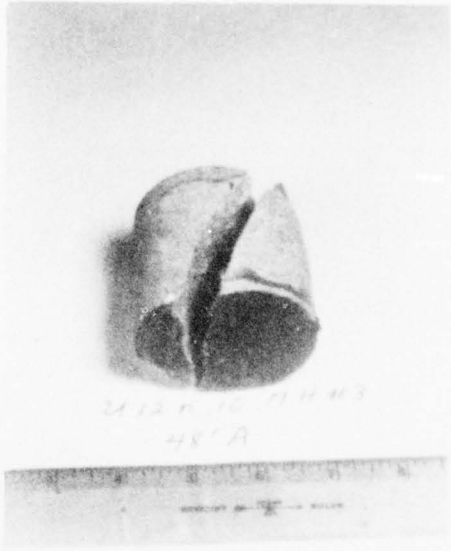


21 12 N. 10 M H #3
57' B


21 12 N. 10 M H #2
92.8' B

DRILL HOLE FOOTAGE	DENSITY (gm/cc) AS-RECEIVED	DRY	GRAIN	WATER BY WET WEIGHT (%)	POROSITY (%)	SATURATION (%)	CALC. AIR VOIDS (%)	MEAS. PERMANENT COMP. (%)	VELOCITY (ft/sec) LONG	SHEAR
U12n.10 MH#2										
90'										
Sample A	2.12	1.86	2.77	12.2	30	88	3.5	--	--	--
Sample B	2.23	1.97	2.81	11.9	33	78	7.2	--	--	--
Sample C	2.47	--	--	--	--	--	--	--	4710	2600
MH#3										
48'	2.15	1.91	2.56	11.0	25	93	1.9	--	12,420	6780
51'	2.65	2.48	3.05	6.7	19	95	0.9	--	12,840	6580
54'	2.44	2.26	2.86	7.3	21	86	3.0	--	9220	3840
57'	2.81	2.80	2.85	0.5	2	84	0.3	--	14,270	7540

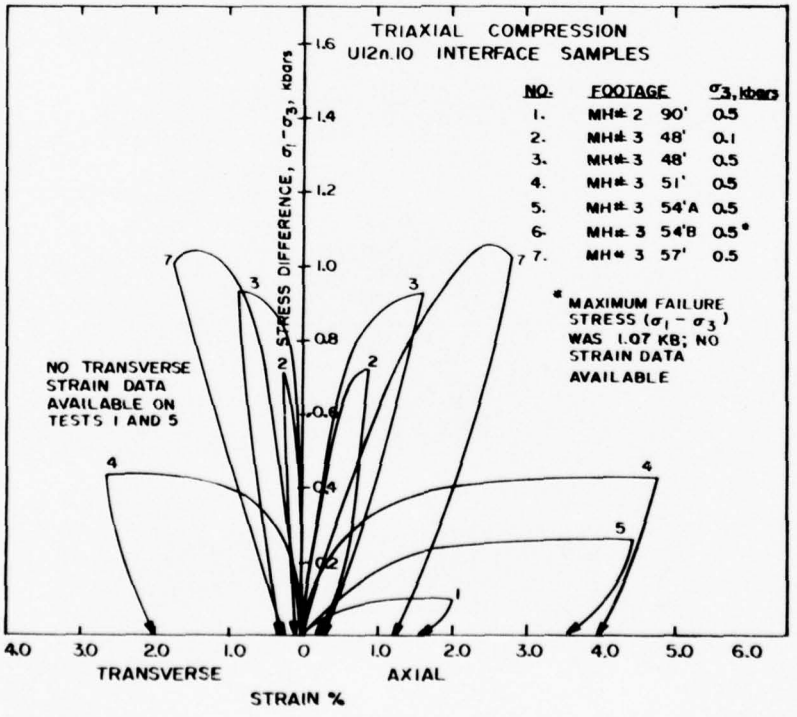

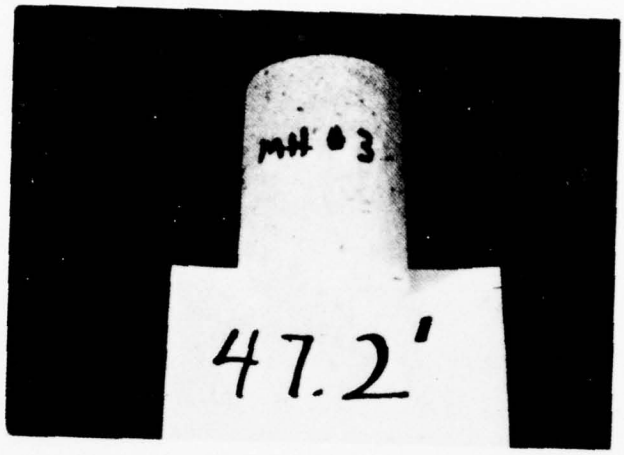
MH #3
47.2'


52.6'


#2
84.6'

TerraTek

May 17, 1976

Mr. Phil Coleman
Systems, Science & Software
P.O. Box 1620
La Jolla, CA 92037

Dear Mr. Coleman:

The following table lists the true susceptibilities as calculated from the apparent susceptibilities (Ka) for each of the footages from U12n.10 MH#2 and MH#3. The true susceptibilities were determined using Vc as the volume of powdered material, M as the mass of the material and Da as the calculated apparent density. The true susceptibility (Km) was then calculated as:

$$Km = (Dm/Da) \times Ka$$

where Dm is the true material density.

TRUE SUSCEPTIBILITY DETERMINATION

Sample I.D.	As-Received Density, Dm,gm/cc	Powdered Material Vc(cc)	Powdered Material M(gm)	Powdered Material Da,gm/cc	Ka,10^{-6}emu	Km,10^{-6}emu
MH#2 52.5'	1.61	93.0	97.9	1.05	285	437
MH#2 82.4'	2.11	90.5	111.5	1.23	576	988
MH#2 95.3'	2.65	90.0	143.6	1.60	412	682
MH#2 128.2'	2.64	92.0	144.0	1.57	605	1017
MH#3 42.2'	1.73	47.0	49.9	1.06	114	186
MH#3 56.4'	2.16	92.5	127.9	1.38	343	537
MH#3 65.55'	2.80	87.0	125.3	1.44	106	206
MH#3 80.0'	2.82	93.0	130.3	1.40	166	334

Enclosed are copies of the susceptibility procedures and the susceptilibity machine description.

Sincerely,

Richard K. Dropek

Richard K. Dropek
Research Engineer

RDK/jlg

Enclosures

cc: Joe LaComb
Scott Butters

MISCELLANEOUS MIGHTY EPIC PROPERTIES

DRILL HOLE		DENSITY (gm/cc)			WATER BY WET WEIGHT (%)	POROSITY (%)	SATURATION (%)	CALC. AIR VOIDS (%)	MEAS. PERMANENT COMP. (%)	VELOCITY (ft/sec)	
DIST. FROM COLLAR	DIST. FROM W.P.	AS-RECEIVED	DRY	GRAIN						LONG	SHEAR
U12n 10 UG#5											
23'		1.86	1.53	2.42	17.6	37	89	3.9	1.4	9,440	4,450
53'		1.92	1.59	2.40	17.4	34	98	0.4	1.0	10,240	5,010
71'		1.94	1.62	2.48	16.7	35	94	2.1	1.0	10,830	5,550
83'		1.91	1.63	2.40	15.0	32	89	3.6		10,030	4,980
126'		1.95	1.66	2.41	14.8	31	93	2.2	1.8	8,740	3,380
181'		2.04	1.80	2.42	11.4	26	91	2.3	2.6	12,550	6,270
224'		1.82	1.52	2.26	16.6	33	93	2.4	1.0	11,800	5,850
273'		1.95	1.65	2.41	15.1	32	93	2.2	2.0	8,380	4,050
327'		1.88	1.52	2.43	19.3	37	97	1.2	2.0	9,740	5,020
378'		1.93	1.61	2.40	16.5	33	97	1.1	1.1	10,540	5,780
422'		1.94	1.61	2.51	17.4	36	94	2.1	1.4	10,020	4,650
474'		1.95	1.63	2.46	16.6	34	96	1.4	0.7	9,350	4,610
522'		2.00	1.69	2.50	15.9	33	97	0.8	1.1	10,430	5,360
573'		1.98	1.66	2.59	15.9	35	91	3.1	1.3	11,000	5,490
626'		1.98	1.67	2.55	15.6	34	90	3.5	1.1	12,600	6,380
674'		2.137	1.87	2.59	12.8	28	97	0.8	0.9	10,780	5,050

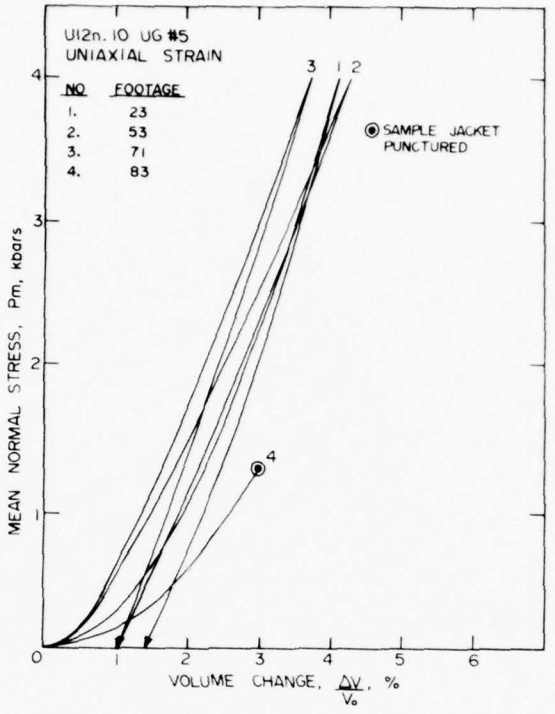
U12n.10 UG #5
UNIAXIAL STRAIN
NO. FOOTAGE
1. 23
2. 53
3. 71
4. 83
SAMPLE JACKET PUNCTURED
MEAN NORMAL STRESS, Pm, kbars
VOLUME CHANGE, ΔV/Vo, %

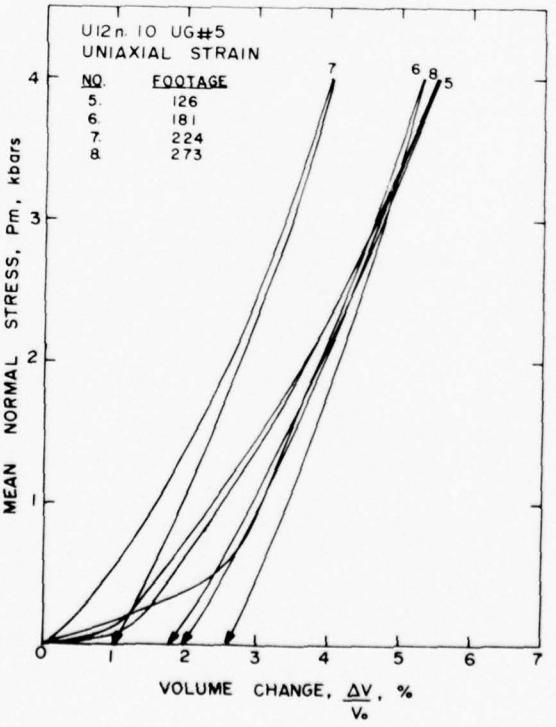
U12n.10 UG#5
UNIAXIAL STRAIN
NO. FOOTAGE
5. 126
6. 181
7. 224
8. 273
MEAN NORMAL STRESS, Pm, kbars
VOLUME CHANGE, ΔV/Vo, %

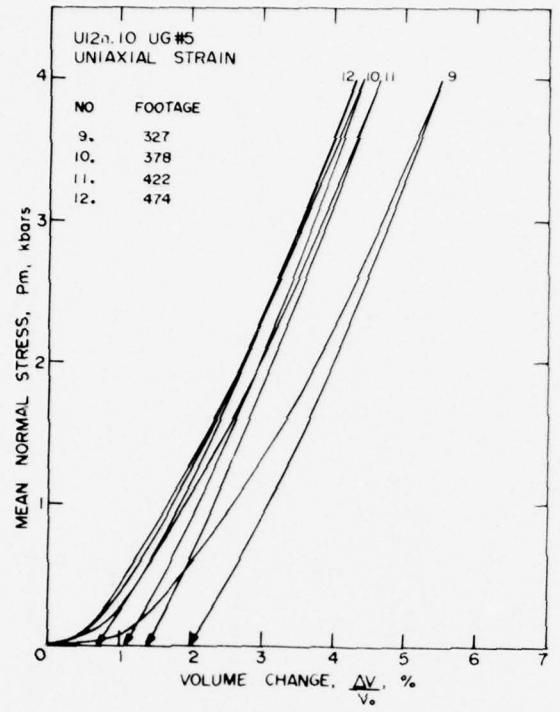
U12n.10 UG#5
UNIAXIAL STRAIN
NO FOOTAGE
9. 327
10. 378
11. 422
12. 474
12
10,11
9
MEAN NORMAL STRESS, Pm, kbars
VOLUME CHANGE, ΔV/Vo, %

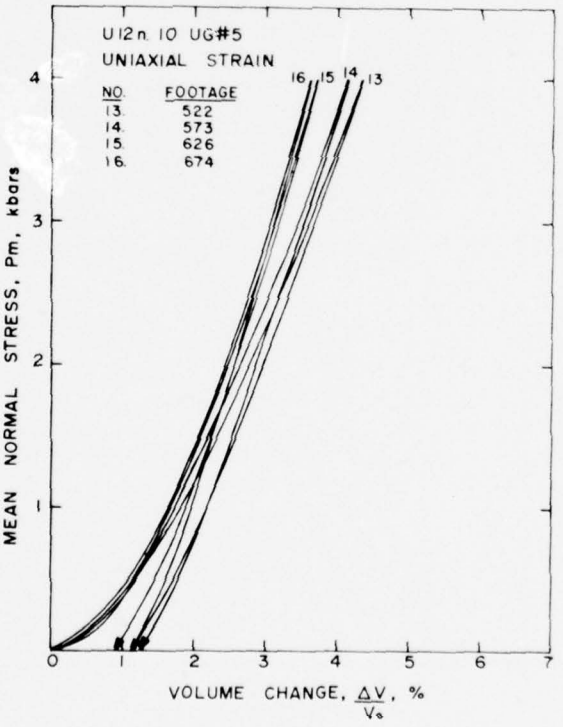
U12n.10 UG#5
UNIAXIAL STRAIN
NO FOOTAGE
13. 522
14. 573
15. 626
16. 674
16
15
14
13
MEAN NORMAL STRESS, Pm, kbars
VOLUME CHANGE, ΔV/Vo, %

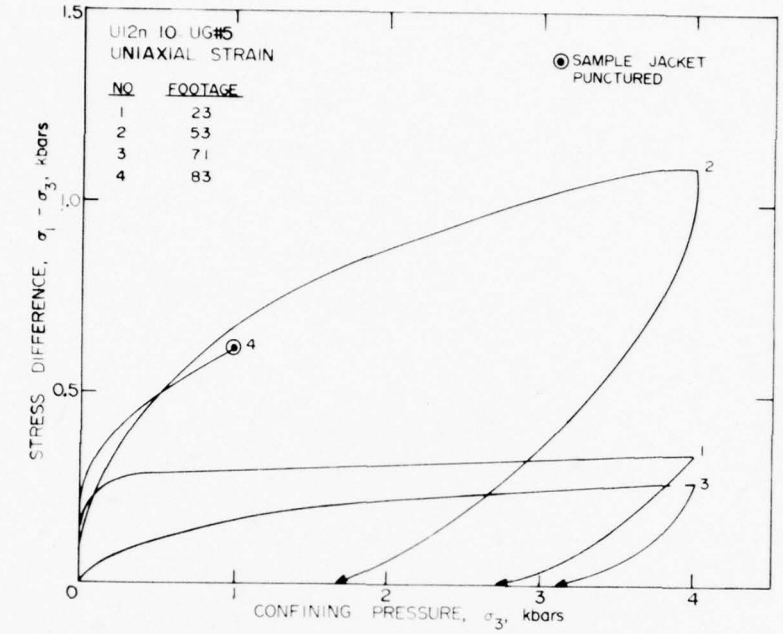
U12n.10 UG#5
UNIAXIAL STRAIN
NO FOOTAGE
1 23
2 53
3 71
4 83
SAMPLE JACKET PUNCTURED
STRESS DIFFERENCE, $\sigma_1 - \sigma_3$, kbars
CONFINING PRESSURE, σ_3, kbars
0
0.5
1.0
1.5
1
2
3
4

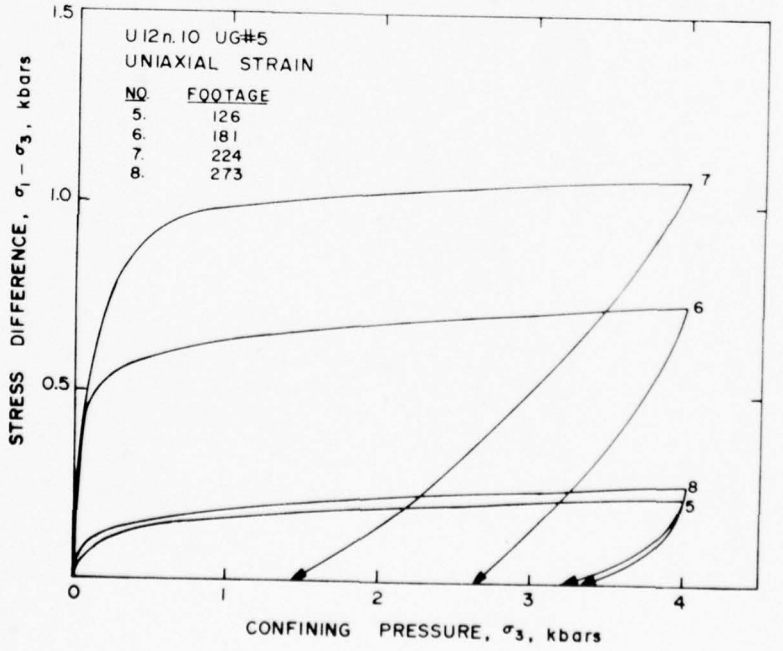
U12n.10 UG#5
UNIAXIAL STRAIN
NO FOOTAGE
5. 126
6. 181
7. 224
8. 273
STRESS DIFFERENCE, $\sigma_1 - \sigma_3$, kbars
CONFINING PRESSURE, σ_3, kbars
0
0.5
1.0
1.5
1
2
3
4

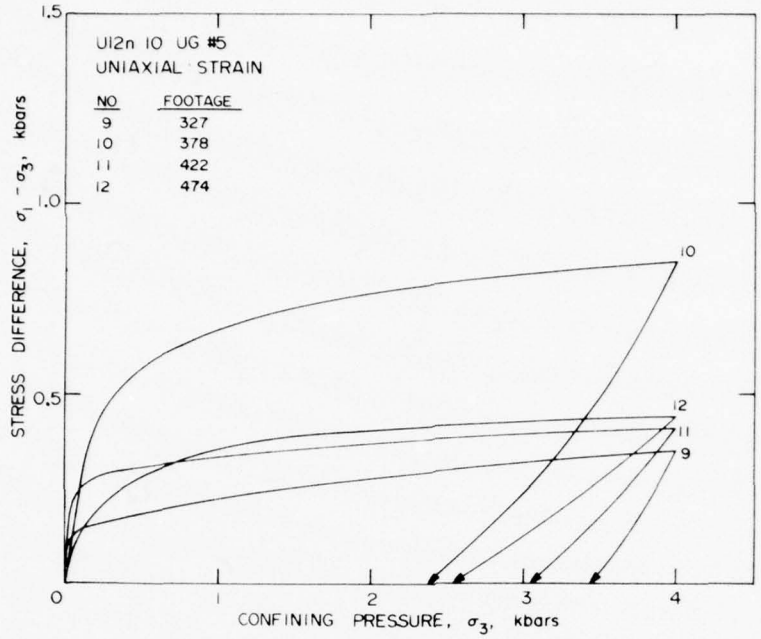
U12n 10 UG #5
UNIAXIAL STRAIN
NO FOOTAGE
9 327
10 378
11 422
12 474
STRESS DIFFERENCE, $\sigma_1 - \sigma_3$, kbars
CONFINING PRESSURE, σ_3, kbars
0
0.5
1.0
1.5
1
2
3
4
10
12
11
9

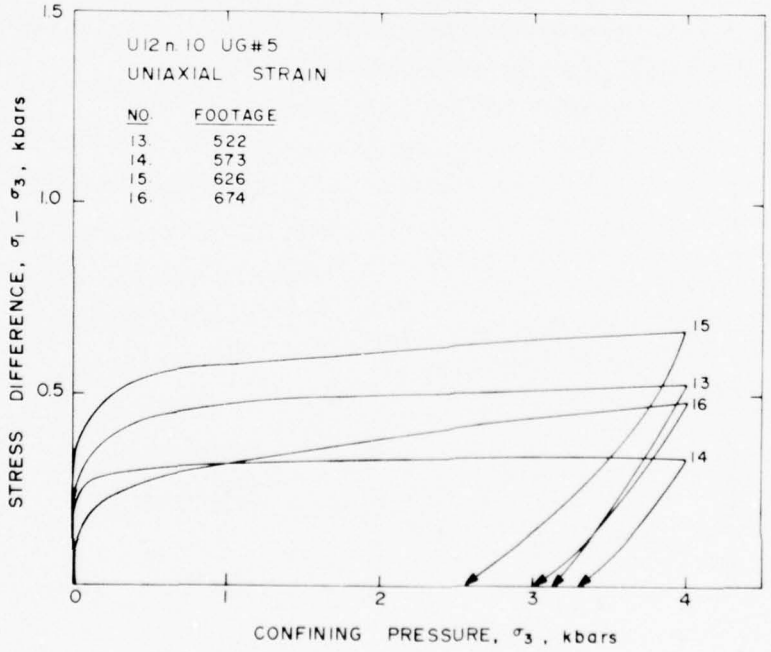
U12n 10 UG#5
UNIAXIAL STRAIN
NO. FOOTAGE
13. 522
14. 573
15. 626
16. 674
STRESS DIFFERENCE, $\sigma_1 - \sigma_3$, kbars
CONFINING PRESSURE, σ_3, kbars
0
0.5
1.0
1.5
1
2
3
4
15
13
16
14

TerraTek

March 30, 1976

Mr. J. W. LaComb
Defense Nuclear Agency
Nevada Test Site
Mercury, NV 89023

Dear Joe:

We have completed the triaxial compression tests on the U12n.10 ISS drill hole samples. The apparent Young's Moduli and Poisson's ratios have been scaled from the slopes of the stress-strain curves and are listed in the attached table. The individual stress-strain curves and the physical properties are also attached.

The data indicates a consistent increase in the Young's Moduli with increasing confining pressure. The Poisson's ratios listed for the unconfined compression tests ($\sigma_3 = 0$) were obtained by using the "linear portion" of the stress difference-axial strain curve. The "foot" that was not scaled on these curves would have produced much lower Poisson's ratios -- on the order of 0.05 to 0.10. The Poisson's ratios at the two confining pressure levels appear consistently between 0.20 and 0.25 regardless of the value of Young's Moduli.

Please call if you have any questions concerning the data.

Sincerely,

Scott W. Butters
Engineering Supervisor

SWB/jlg

Enclosures

cc: Bill Ellis, USGS

ELASTIC MODULI FROM

TRIAXIAL COMPRESSION TESTS

SAMPLE	CONFINING PRESSURE σ_3, BARS	YOUNG'S MODULUS E,KB	POISSON'S RATIO ν
U12n.10 ISS#1 23'	0	28	0.32
	34	48	0.24
	69	49	0.24
U12n.10 ISS#3 21'	0	27	0.40
	34	44	0.27
	69	37	0.23
U12n.10 ISS#5 5'	0	47	0.26
	34	54	0.22
	69	42	0.25
U12n.10 ISS#6 28'	0	130	0.25
	34	150	0.23
	69	160	0.23
U12n.10 ISS#7 17'	0	54	0.32
	34	75	0.22
	69	95	0.23
U12n.10 ISS#8 12'	0	64	0.15
	34	70	0.20
	69	80	0.23

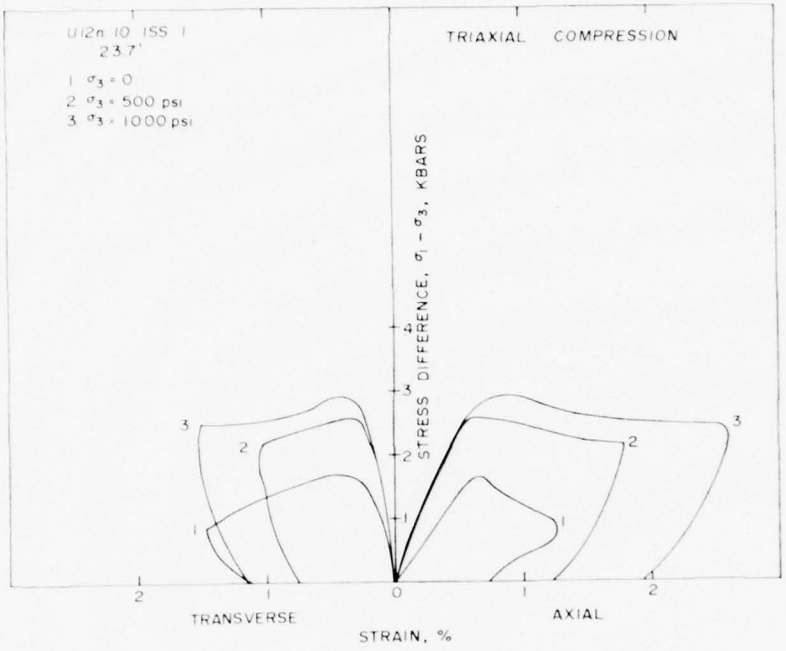
UI2n 10 ISS 1
23.7°
1. σ_3 = 0
2. σ_3 = 500 psi
3. σ_3 = 1000 psi
TRIAXIAL COMPRESSION
STRESS DIFFERENCE, $\sigma_1 - \sigma_3$, KBARS
TRANSVERSE
AXIAL
STRAIN, %

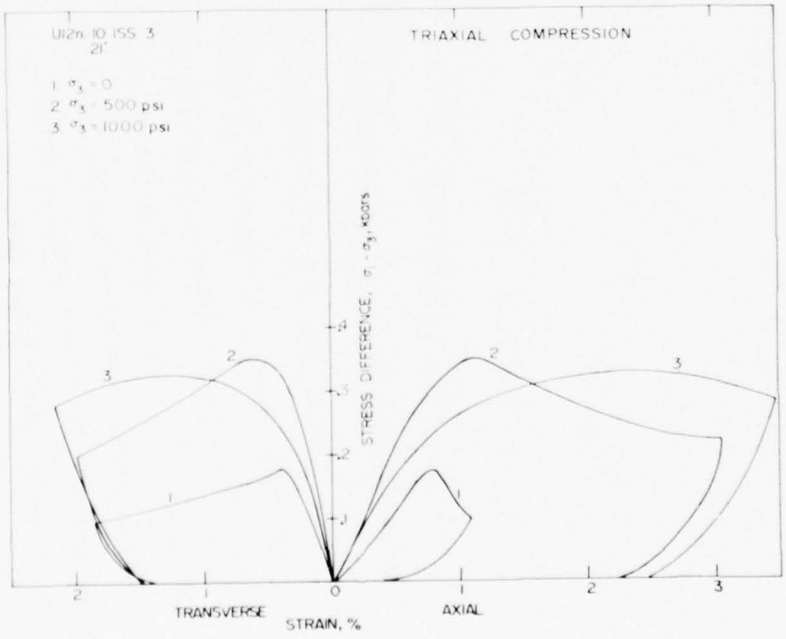
UI2n 10 ISS 3
21°
1. σ_3 = 0
2. σ_3 = 500 psi
3. σ_3 = 1000 psi
TRIAXIAL COMPRESSION
TRANSVERSE
AXIAL
STRAIN, %

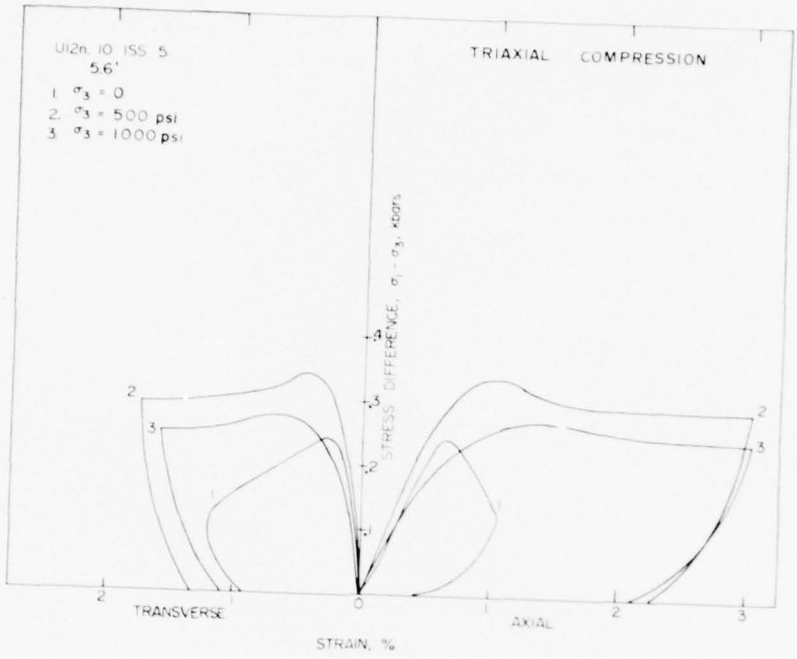
U12n.10.1SS.5
5.6'
1. σ_3 = 0
2. σ_3 = 500 psi
3. σ_3 = 1000 psi
TRIAXIAL COMPRESSION
STRESS DIFFERENCE, $\sigma_1 - \sigma_3$, KSI
TRANSVERSE
AXIAL
STRAIN, %

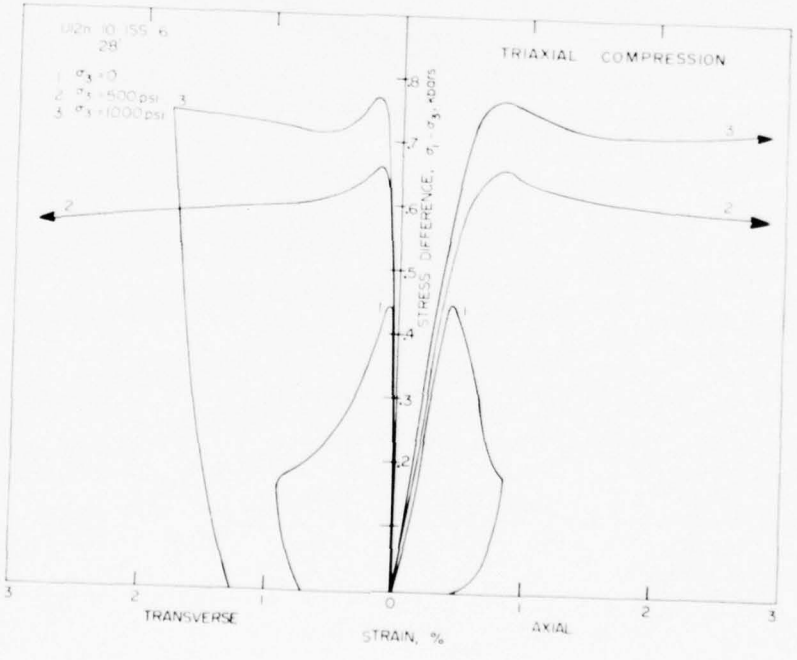
U12n.10.1SS.6
28
1. σ_3 = 0
2. σ_3 = 500 psi
3. σ_3 = 1000 psi
TRIAXIAL COMPRESSION
STRESS DIFFERENCE, $\sigma_1 - \sigma_3$, KSI
TRANSVERSE
AXIAL
STRAIN, %

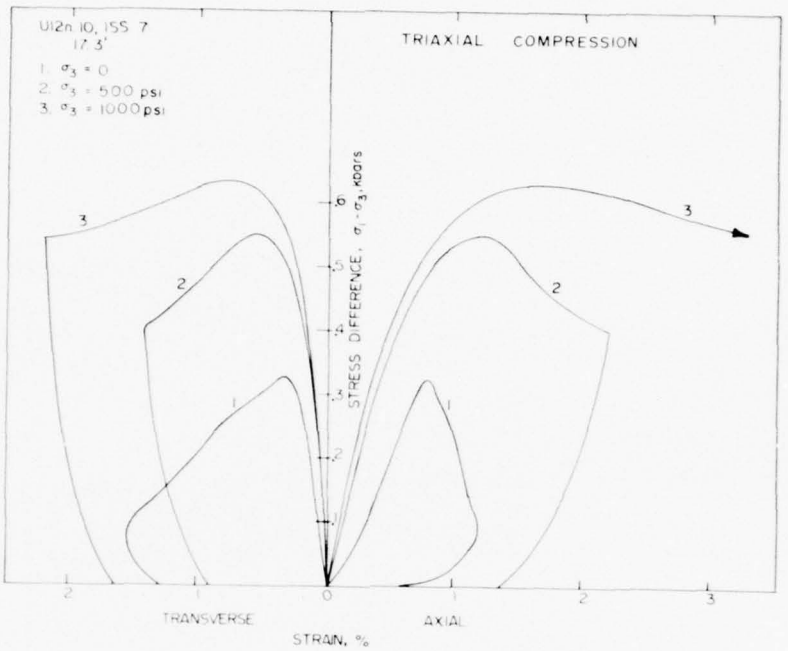
U12n.10, ISS 7
17.3'
1. σ_3 = 0
2. σ_3 = 500 psi
3. σ_3 = 1000 psi
TRIAXIAL COMPRESSION
STRESS DIFFERENCE, $\sigma_1 - \sigma_3$, kbars
TRANSVERSE
AXIAL
STRAIN, %

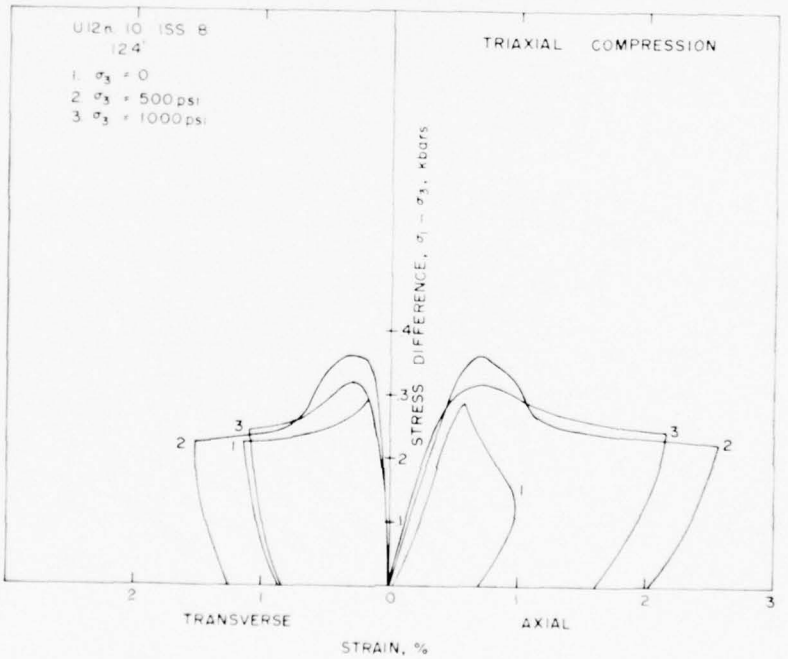
U12n.10 ISS 8
12.4'
1. σ_3 = 0
2. σ_3 = 500 psi
3. σ_3 = 1000 psi
TRIAXIAL COMPRESSION
STRESS DIFFERENCE, $\sigma_1 - \sigma_3$, kbars
TRANSVERSE
AXIAL
STRAIN, %

DRILL HOLE		DENSITY (gm/cc)			WATER BY WET WEIGHT (%)	POROSITY (%)	SATURATION (%)	CALC AIR VOIDS (%)	MEAS PERMANENT COMP (%)	VELOCITY (ft/sec)	
DIST FROM COLLAR	DIST FROM W.P.	AS-RECEIVED	DRY	GRAIN						LONG	SHEAR
U12n.10											
ISS#1 23.7'		1.89	1.53	2.41	18.8	37	97	1.0		10,460	5,290
ISS#3 21.0'		2.00	1.70	2.45	14.7	30	96	1.0		10,800	5,140
ISS#5 5.6'		1.95	1.65	2.37	15.2	30	98	0.3		10,540	5,180
ISS#6 28.4'		1.88	1.50	2.42	20.2	38	99	0.1		10,040	4,980
ISS#7 17.3'		2.01	1.72	2.51	14.7	32	94	2.1		9,590	4,330
ISS#8 12.4'		1.95	1.63	2.49	16.6	35	93	2.6		9,680	4,710

APPENDIX B

EXTRACT FROM WATERWAYS EXPERIMENTAL STATION MIGHTY EPIC CONCRETE STUDY

This report and Tables B.1 through B.3 were taken from a 1977 MIGHTY EPIC Cellular Standard and Steel Fiber Reinforced Concrete Study done by the Concrete Laboratory, U.S. Army Engineers Waterways Experiment Station (WES) Vicksburg, Mississippi.

B.1 CELLULAR CONCRETE TEST RESULTS

Standard 152-x 305-mm (6-x 12-inch) cylinder molds were used to cast the specimens which were protected from moisture loss after casting. The specimens were kept, in the molds, in the same ambient conditions as were the structures.

Usually, there are three values used to describe stress-deformation characteristics of cellular concrete. These are (1) yield stress, σ_y, (2) stress at 40 percent deformation, $\sigma_{0.40}$, and (3) average stress to 40 percent deformation, $\bar{\sigma}_{0.40}$. The percent deformation at which average stress, $\bar{\sigma}_{0.40}$, occurs is halfway between yield strain and 40 percent deformation on the stress-deformation curves. The values of yield strain, ε_y, yield stress, σ_y, and stress at 40 percent deformation, $\sigma_{0.40}$, were obtained directly from the stress-deformation graphs. Percent deformation was calculated by dividing depth of penetration of the load head by the total specimen height.

B.1.1 Preparation of Specimens for Testing

About two days before test date, the cardboard molds were stripped from the specimens and the middle 152 mm (6 inches) of the cylinders were prepared for testing. The resulting test specimens were measured to the nearest 0.254 mm (one-hundredth of an inch) (height and diameter), weighed to the nearest gram, and then placed in moisture tight plastic bags. Computations were made to determine the hardened density, γ_d, for each specimen. On test date 12 May 1976, the constrained compressive strength of each specimen was determined by the slow-loading method.

Table B.1 gives the results of these determinations.

B.1.2 Slow-Loading Constrained Compressive Strengths of Cellular Concrete

The 152 mm by 15 mm (6 by 6 inch) specimen was placed in a split-wall confining pipe and tested in compression. The steel pipe had a 152-mm (6-inch) inside diameter with 6.35-mm (1/4-inch) thick walls. There was only negligible

lateral strain in the pipe walls for the vertical loads applied to the specimen. After the specimen was placed in the pipe, both closure bolts on the pipe were torqued to a final closure of 6.78 joules (5 ft-lb). Compression loads were applied through a 102-mm (4-inch) diameter loading piston centered on the 152-mm (6-inch) diameter specimen.

Load was applied to the 152-by 152-mm (6- by 6-inch) cylindrical specimens using a 13600 kilogram (30,000 pound) capacity Universal testing machine operating at a constant rate of piston travel of 7.62 mm/min (0.30 in./min) (5 percent deformation per minute). Deformations were measured with a linear slide-wire potentiometer attached to the base platform and the moving load head of the testing machine. An X-Y recorder was linked electronically to the dial gage of the testing machine and so calibrated that loads (in pounds) were recorded as stresses (in pounds per square inch) on the recorder. The resulting stress-deformation data for each specimen are recorded in Table B.1.

B.2 STANDARD CONCRETE

Quality control of standard concrete was maintained by monitoring the batch weights, performing slump tests and where applicable, performing percent-of-air tests. When all these specification requirements were met, specimens were cast during placement operations. Standard 152-mm x 305-mm (6- x 12-inch) cylinder molds are used for specimen casting and were cured or otherwise protected in the same manner as were the structures.

B.3 FIBER REINFORCED CONCRETE

Quality control of fiber reinforced concrete was maintained by monitoring batch weights, performing slump test, and, where applicable, performing percent-of-air tests. The main item controlled was the proper inclusion of the steel fibers into the mix. The proper technique for this depended on the type batching and mixing equipment used on a particular project. However, experience has shown that a technique that will disperse the fibers into the mix along with the aggregates (as opposed to introducing the fibers separately or after the cement has been added) was the most desirable. When the project specifications have been met, standard cylinder molds were used to cast the test specimens.

B.4 STANDARD AND FIBER REINFORCED CONCRETES (FRC)

Compressive strength of each FRC and standard concrete specimen was determined by loading the standard cylinder to failure in a Universal testing machine [200,000 kilogram (440,000 lb) capacity]. Table B.2 and Table B.3 give the results of these determinations.

B.5 SPECIAL NOTES

a. Unless otherwise stated, test results given in this Appendix are those tested at WES.

b. None of the specimens representing CASES "donuts" cast at WES were tested because this material was later removed from the structure and replaced. Cellular concrete data represent that material placed on the structure at the Nevada Test Site.

Table B.1. Slow-loading constrained compression tests - cellular concrete.

Spec No.	Date Cast	Date Tested	Age Days	Physical Properties: Height in.	Diameter in.	Weight lb	Dry Unit Weight γ_d pcf	Yield Strain ε_y in./in.	Yield Stress σ_y psi	Stress @ 40% deform psi	Average Stress @ 40% deform psi
CASES STRUCTURE - INTERIM TESTING - RECAST AT NTS											
5 (Batch 1)	2-18-76	4-8-76	50	6.05	6.052	4.68	46.5	0.012	700	950	775
10 (Batch 1)	2-18-76	4-8-76	50	5.97	6.051	5.65	56.9	0.007	675	1200	975
1 (Batch 2)	2-18-76	4-8-76	50	5.93	6.056	4.525	45.8	0.017	675	975	800
2 (Batch 2)	2-18-76	4-8-76	50	5.95	6.050	5.155	52.1	0.010	525	950	725
1 (Batch 3)	2-18-76	4-8-76	50	6.01	6.057	5.34	53.3	No distinct yield points			
2 (Batch 3)	2-18-76	4-8-76	50	6.07	6.050	5.49	54.4	0.010	1150	1750	1450
2 (Outside)	2-18-76	4-8-76	50	6.01	6.050	5.25	52.5	0.020	850	1350	1175
6 (Outside)	2-18-76	4-8-76	50	6.01	6.028	4.36	43.9	No distinct yield points			
CASES STRUCTURE - SHOT DATE TESTING - RECAST AT NTS											
7 (Batch 1)	2-18-76	5-20-76	92	6.05	6.047	5.38	53.3	0.0099	975	1500	1350
4 (Batch 1)	2-18-76	5-20-76	92	5.94	6.051	4.88	49.3	0.010	625	1000	825
1 (Batch 2)	2-18-76	5-20-76	92	6.02	6.050	4.65	46.4	0.015	875	1225	1025
3 (Batch 2)	2-18-76	5-20-76	92	6.20	6.053	4.69	45.5	0.011	700	1225	1000
8 (Batch 2)	2-18-76	5-20-76	92	5.95	6.048	4.57	46.2	0.017	750	1100	1000
1 (Batch 3)	2-18-76	5-20-76	92	6.07	6.059	5.53	54.5	0.0198	1300	2100	1750

Table B.1. Slow-loading constrained compression tests - cellular concrete (continued).

Spec No.	Date Cast	Date Tested	Age Days	Physical Properties: Height in.	Diameter in.	Weight lbs	Dry Unit Weight γ_d pcf	Yield Strain ε_y in./in.	Yield Stress σ_y psi	Stress @ 40% deform psi	Average Stress @ 40% deform psi
2 (Batch 3)	2-18-76	5-20-76	92	6.06	6.053	5.44	53.8	0.015	1100	2025	1650
	2-18-76	5-20-76	92	5.98	6.050	5.10	51.2	0.015	850	1600	1350
	2-18-76	5-20-76	92	6.05	6.045	5.30	52.7	0.0099	900	1600	1250
2	2-18-76	5-20-76	92	5.93	6.053	5.135	52.0	0.020	775	1400	1125
6	2-18-76	5-20-76	92	5.93	6.050	5.34	54.1	0.012	1000	1600	1325
10	2-18-76	5-20-76	92	5.94	6.052	4.575	46.3	0.015	825	1200	1050
SRI STRUCTURES - 28 DAY TESTING											
SX-11-1	10-7-75	11-4-75	28	6.05	6.090	6.38	62.6	0.025	1300	2375	@ 33%
SX-11-2	10-7-75	11-4-75	28	6.10	6.070	6.93	67.8	No distinct points			
SX-11-3	10-7-75	11-4-75	28	6.00	6.050	6.91	69.2	No distinct points			
SY-21-1	10-10-75	11-7-75	28	6.02	6.020	4.67	47.1	0.010	400	1000	775
SY-21-2	10-10-75	11-7-75	28	5.90	6.050	4.87	49.6	0.010	500	1200	875
SY-21-3	10-10-75	11-7-75	28	5.92	6.050	5.15	52.3	0.015	775	1525	1050
SY-20-A	10-30-75	12-1-75	32	5.95	6.038	5.62	57.0	0.010	950	2050	1525
SY-20-C	10-30-75	12-1-75	32	5.95	6.045	5.51	55.8	0.005	700	2075	1425
SY-19-1	10-31-75	12-2-75	32	5.97	6.046	6.80	68.6	0.020	1775	2400	@ 10% deform
SY-19-2	10-31-75	12-2-75	32	5.92	6.045	6.49	66.0	0.020	1450	2400	@ 15% deform
SY-19-3	10-31-75	12-2-75	32	5.81	6.042	6.02	62.5	*	*	2400	@ 25% deform

Table B.1. Slow-loading constrained compression tests - cellular concrete (continued).

Spec No.	Date Cast	Date Tested	Age Days	Physical Properties: Height In.	Diameter In.	Weight lbs	Dry Unit Weight Yd pcf	Yield Strain ϵ_y In./In.	Yield Stress σ_y psi	Stress @ 40% deform psi	Average Stress @ 40% deform psi
SZ-2-1	11-7-75	12-5-75	28	5.94	6.050	4.82	48.8	0.010	550	1150	900
SZ-2-2	11-7-75	12-5-75	28	6.00	6.050	4.90	49.1	0.010	525	1140	840
SZ-2-3	11-7-75	12-5-75	28	5.96	6.050	4.79	48.3	0.009	575	1075	840
				SBI STRUCTURES - SHOT DATE TESTING							
SX-11-2-A	10-7-75	5-20-76	226	5.90	6.043	6.650	67.9	*	*	2400	@ 5% deform
SX-11-2-B	10-7-75	5-20-76	226	5.95	6.040	6.240	63.0	0.015	1250	3740	@ 30% deform
SY-21-B	10-10-75	5-20-76	223	5.96	6.000	4.620	47.9	0.010	550	1550	1225
SY-20-2	10-30-75	5-20-76	203	5.95	6.040	5.405	54.6	0.010	975	2375	@ 35% deform
SY-19-2-A	10-31-75	5-24-76	206	5.95	6.044	6.66	67.3	0.025	2400	4770	@ 30% deform
SY-19-2-B	10-31-75	5-24-76	206	5.91	6.046	6.65	67.9	0.015	2700	4770	@ 24% deform

SZ-2 28 day tests only

* No distinct yield points

Table B.2 Standard concrete compressive strengths shot date testing

Structure No.	Spec No.	Remarks	Date Cast	Date Tested	Age Days	Comp Strg psi
5A3	1	Dome Closures	11-11-75	5-26-76	197	8260
	2	Dome Closures	11-11-75	5-26-76	197	7820
5B1	1	Dome Closures	11-12-75	4-1-76	141*	8070
	2	Dome Closures	11-12-75	4-1-76	141*	8430
	3	Dome Closures	11-12-75	5-26-76	196	9550
	4	Dome Closures	11-12-75	5-26-76	196	9340
5B2	1	Dome Closures	11-14-75	4-1-76	139*	7390
	2	Dome Closures	11-14-75	4-1-76	139*	7210
	3	Dome Closures	11-14-75	5-26-76	194	9370
	4	Dome Closures	11-14-75	5-26-76	194	8540
5C1	1	Dome Closures	9-22-75	5-26-76	247	6600
	2	Dome Closures	9-22-75	5-26-76	247	5040
5C2	1	Dome Closures	9-24-75	5-26-76	245	10,630
	2	Dome Closures	9-24-75	5-26-76	245	10,810
5C3	1	Dome Closures	10-27-75	5-26-76	212	7890
	2	Dome Closures	10-27-75	5-26-76	212	7850
5C4	1	Dome Closures	10-29-75	5-26-76	210	8670
	2	Dome Closures	10-29-75	5-26-76	210	8370
C-X-5	1		12-8-75	5-26-76	170	11,690
	2		12-8-75	5-26-76	170	9,550
C-X-7	1		11-4-75	5-27-76	205	8980
C-X-8	1		11-20-75	5-27-76	189	8630
C-X-10	1		10-29-75	5-26-76	210	10,010
	2		10-29-75	5-26-76	210	9,800
C-X-13	1		10-13-75	5-26-76	226	8070
	2		10-13-75	5-26-76	226	8720

*Not Shot Day

Table B.2 Standard concrete compressive strengths shot date testing (Continued)

Structure No.	Spec No.	Remarks	Date Cast	Date Tested	Age Days	Comp Strg psi
C-Y-12	1		12-18-75	5-27-76	161	9870
C-Y-13	1		12-3-75	5-26-76	175	9,530
	2		12-3-75	5-26-76	175	10,170
C-Y-14	1		11-14-75	5-26-76	194	8300
	2		11-14-75	5-26-76	194	8140
C-Y-15	1		11-10-75	5-26-76	198	7230
	2		11-10-75	5-26-76	198	6830
C-Y-16	1		10-30-75	5-26-76	209	9370
	2		10-30-75	5-26-76	209	9900
C-Y-17	1	Stud	11-27-75	5-26-76	181	9,550
	2	Stud	11-27-75	5-26-76	181	9,370
	3	Sphere	11-27-75	5-26-76	181	11,000
	4	Sphere	11-27-75	5-26-76	181	11,320
C-Y-22	1		10-15-75	5-26-76	224	10,650
	2		10-15-75	5-26-76	224	10,330
C-Y-23	1		10-24-75	5-26-76	215	8580
	2		10-24-75	5-26-76	215	8450
C-Z-1	1		12-10-75	5-27-76	179	10,770
	2		12-10-75	5-27-76	179	10,650
C-Z-3	1		10-15-75	5-26-76	224	9920
	2		10-15-75	5-26-76	224	9480
LAB	1		12-17-75	4-1-76	106*	8540
	2		12-17-75	4-1-76	106*	9000
	3		12-17-75	4-1-76	106*	8950
	4		12-17-75	4-1-76	106*	9070

*Not Shot Day

Table B.2 Standard concrete compressive strengths shot date testing (Continued)

Structure No.	Spec No.	Remarks	Date Cast	Date Tested	Age Days	Comp Strg psi
5A1	1	Dome Closures	11-5-75	5-26-76	203	8720
	2	Dome Closures	11-5-75	5-26-76	203	8100
5A2	1	Dome Closures	11-7-75	5-26-76	201	8810
	2	Dome Closures	11-7-75	5-26-76	201	8120

Table B.3 Steel fiber reinforced concrete compressive strength shot date (12 May 1976) testing

Structure No.	Spec No.	Remarks	Date Cast	Date Tested	Age Days	Comp Strg psi
501-6A1	1	Sphere; Batch 1	12-9-75	5-27-76	170	8240
	2	" Batch 2	12-9-75	5-27-76	170	8630
501-6A2	1	Sphere; Batch 1	12-13-75	5-26-76	165	9780
	2	" Batch 3	12-13-75	5-26-76	165	9140
501-6A3	1	Sphere; Batch 1	12-17-75	5-26-76	161	8350
	2	" Batch 2	12-17-75	5-26-76	161	8310
501-6A4	1	Sphere; Batch 2	12-22-75	5-26-76	156	9020
	2	" Batch 3	12-22-75	5-26-76	156	8450
501-6A6	1	Sphere; Batch 1	1-5-76	5-26-76	142	8770
	2	" Batch 3	1-5-76	5-26-76	142	8930
501-6A7	1	Sphere;	1-8-76	5-26-76	139	9370
	2	"	1-8-76	5-26-76	139	9800
503-6B1	1	Sphere; Batch 1	1-12-76	5-26-76	135	8670
	2	" Batch 3	1-12-76	5-26-76	135	9940
503-6B2	1	Sphere; Batch 1	1-16-76	5-26-76	131	10,030
	2	" Batch 3	1-16-76	5-26-76	131	9,250
503-6B3	1	Sphere; Batch 1	1-20-76	5-26-76	127	10,520
	2	" Batch 3	1-20-76	5-26-76	127	10,290
505-6E1	1	Sphere; Batch 1	12-27-75	5-26-76	151	9710
	2	" Batch 3	12-27-75	5-26-76	151	9130

APPENDIX C

FENIX AND SCISSON, INC.

MIGHTY EPIC GROUTING REPORT

OF THE

INTERFACE DRIFT DRILL HOLES

FENIX AND SCISSION, INC.
ENGINEERS-CONTRACTORS
P.O. BOX 15408
LAS VEGAS, NEVADA 89114

March 15, 1976

GROUTING REPORT

U12n.10 INTERFACE DRIFT

In the interface drift of U12n.10 the following holes have been grouted.

Magnet Hole (MH) No. 1 - Four inch (HQ) hole at interface construction station (CS) ± 2 + 10, total depth 193 feet. This hole was grouted to the collar in one lift with HUSKY PUP neat slurry II CS 6.0 using 29.8 ft^3 of grout on 2-16-76. The grouting was done through the Systems Science and Software (S^3) experiment installation pipe.

Magnet Hole (MH) No. 2 - HQ hole at interface CS ± 03, total depth 150 feet. This hole was grouted to the collar in one lift with HUSKY PUP neat slurry II CS 6.0 using 19.85 ft^3 of grout on 3-8-76. The grouting was done through the S^3 experiment installation pipe.

Magnet Hole (MH) No. 3 - HQ hole at interface CS ± 4 + 04, total depth 115 feet. This hole was grouted to the collar in one lift with HUSKY PUP neat slurry II CS 6.0 using 15.3 ft^3 of grout on 3-1-76. The grouting was done through the S^3 experiment installation pipe.

UE12n No. 9 - HQ hole drilled from the mesa, intersects U12n.10 interface drift at CS ± 2 + 10. Grouted with 26.18 ft^3 of neat concrete slurry (NCS) II chem chomp (CC) (CS 6.0). Maximum static pressure of 235 psi. Top of grout plug is at ± 285 above back of drill chamber (calculation based on Halliburton tables of hydrostatic head for lbs/gal. of NCS II CC (CS 6.0)). Hole grouted on 3-2-76.

Instrumentation Hole No. 3 - 17-1/2" hole at interface CS ± 4 + 04, 183' of 17-1/2" hole and ± 9' of 9-7/8" hole. This hole was grouted through a string of 2-3/16" outside diameter (BQ) drill rod that was suspended in the hole prior to the emplacement of the Develco experiment. The grouting was done in two lifts. The first lift consisted of 222 ft^3 of quartzite matching grout (QMG)-R1 and was tagged at a depth of 62'. The second lift consisted of 70 ft^3 of MIGHTY EPIC 8-11 R1 with final grout elevation determined by the experimenter. Grouting done 3-1-76 and 3-2-76.

Instrumentation Hole No. 2 - 17-1/2" hole at interface CS ± 3 + 03, 360 feet of 17-1/2" hole and ± 9' of 9-7/8" hole. This hole was grouted through a string of BQ drill rod that was suspended in the hole prior to the emplacement of the Develco experiment. The first lift consisted of 510 ft^3 of QMG-R1 and was tagged wet at 90'. After the grout hole set, it was tagged dry at 112', grouting done on 3-8-76. One 3-15-76, 35 ft^3 of QMG-R1 was pumped into the hole bringing the level to 96' below grade. 160 ft^3 of MIGHTY EPIC 8-11 R1 was then pumped into the hole through the drill rod to bring the level to 12' 6" below grade. Solid grout was tagged at 14' below grade on 3-16-76.

DISTRIBUTION LIST

DEPARTMENT OF DEFENSE

Assistant to the Secretary of Defense
Atomic Energy
ATTN: Document Control

Director
Defense Advanced Rsch. Proj. Agency
ATTN: NMRO
ATTN: PMO
ATTN: STO

Director
Defense Communications Agency
ATTN: Code 930
ATTN: CCTC/C672, Franklin D. Moore

Defense Documentation Center
Cameron Station
12 cy ATTN: TC

Director
Defense Intelligence Agecny
ATTN: DB-4C2, Timothy Ross

Director
Defense Nuclear Agency
ATTN: STVL
ATTN: TISI, Archives
ATTN: DDST
2 cy ATTN: STRA
2 cy ATTN: STSP
3 cy ATTN: TITL, Tech. Library
3 cy ATTN: SPSS
26 cy ATTN: SPTD

Under Secretary of Def. for Rsch. & Engrg.
ATTN: S&SS (OS)

Commander, Field Command
Defense Nuclear Agency
ATTN: FCTMD
ATTN: FCPR
2 cy ATTN: FCTMOF
4 cy ATTN: FCTMC

Director
Joint Strat. Tgt. Planning Staff, JCS
ATTN: JLTW-2

Chief
Livermore Division, Field Command, DNA
Lawrence Livermore Laboratory
ATTN: FCPRL

Chief
Test Construction Division
Field Command, Test Directorate
Defense Nuclear Agency
6 cy ATTN: FCTC

DEPARTMENT OF THE ARMY

Program Manager
BMD Program Office
ATTN: DACE-BMT
ATTN: CRDABM-NE

DEPARTMENT OF THE ARMY (Continued)

Director
BMD Advanced Tech. Ctr.
Huntsville Office
ATTN: ATC-T, Melvin T. Capps
ATTN: CRDABH-S
ATTN: 1CRDABH-X

Commander
BMD System Command
ATTN: BDMSC-TEN, Noah J. Hurst
ATTN: R. DeKalb

Dep. Chief of Staff for Rsch. Dev. & Acq.
ATTN: DAMA-CSM-N

Chief of Engineers
ATTN: DAEN-MCE-D
ATTN: DAEN-RDM

Commander
Harry Diamond Laboratories
ATTN: DRXDO-RBH, James H. Gwaltney
ATTN: DRXDO-TI, Tech. Lib.
ATTN: A. J. Baba
ATTN: DRXDO-NP

Commander
Picatinny Arsenal
ATTN: SMUPA-ND-W

Director
U.S. Army Ballistic Research Labs.
ATTN: Tech. Lib., Edward Baicy

Commander
U.S. Army Engineer Center
ATTN: ATSEN-SY-L

Division Engineer
U.S. Army Engineer Div, Huntsville
ATTN: HNDED-SR

Director
U.S. Army Engr. Waterways Exper. Sta.
ATTN: J. D. Day
ATTN: J. K. Ingram
ATTN: William Flathau
ATTN: Guy Jackson

Commander
U.S. Army Missile Command
ATTN: DRS-RKP, W. B. Thomas

Commander
U.S. Army Nuclear Agency
ATTN: Tech. Lib.

DEPARTMENT OF THE NAVY

Chief of Naval Operations
ATTN: Op 981

DEPARTMENT OF THE NAVY (Continued)

Officer-in-Charge
Civil Engineering Laboratory
Naval Construction Battalion Center
ATTN: Stan Takahashi
ATTN: Technical Library
ATTN: L51, Warren Shaw
ATTN: J. Crawford
ATTN: R. J. Odello

Commander
Naval Facilities Engineering Command Hqs.
ATTN: Technical Library
ATTN: Code 04B

Naval Plant Representative
Naval Plant Representative Office
Strategic Systems Project Office
Lockheed Missile & Space Company
2 cy ATTN: SPL 325

Director
Naval Research Laboratory
ATTN: Code 2600, Tech. Lib.

Officer-in-Charge
Naval Surface Weapons Center
ATTN: WA50
ATTN: Kurt Inkenhaus

Director
Strategic Systems Project Office
ATTN: NSP-272
ATTN: NSP-27201
ATTN: NSP-273
ATTN: NSP-27331

DEPARTMENT OF THE AIR FORCE

AF Weapons Laboratory, AFSC
ATTN: RNB(NS)
ATTN: DED
ATTN: DES-G, Mr. Melzer
ATTN: RN(NT)
ATTN: DES-C, Robert Henny
ATTN: SUL
ATTN: RNE(EL)
ATTN: DES-S, M. A. Plamondon
2 cy ATTN: RND(DY)

Headquarters
Air Force Systems Command
ATTN: DLCAW
ATTN: Technical Library
ATTN: R. Cross

Commander
Foreign Technology Division, AFSC
ATTN: ETDP
ATTN: PDBG
ATTN: PDBF, Mr. Spring
ATTN: NICD Library

Hq. USAF/RD
ATTN: RDQSM

SAMSO/DE
ATTN: DEB

DEPARTMENT OF THE AIR FORCE (Continued)

SAMSO/MN
ATTN: MMH
ATTN: MNNH

SAMSO/RS
ATTN: RSSE

Space & Missile Systems Organization
ATTN: Director, ABRES

DEPARTMENT OF ENERGY

University of California
Lawrence Livermore Laboratory
ATTN: Tech. Info. Dept. L-3
ATTN: T. Boster, L-45
ATTN: Victor Karpenko, L-113
ATTN: Doc. Con. Off. for J. Morton
ATTN: J. Carothers, L-18
ATTN: David Oakley, L-21
ATTN: Jack Shearer
ATTN: Joseph E. Keller, Jr., L-125
ATTN: Ray Birkett, L-34
ATTN: Harry Reynolds, L-21
ATTN: O. T. Vik, L-24

Los Alamos Scientific Laboratory
ATTN: Doc. Con. for Robert Brownlee
ATTN: Doc. Con. for Pruitt Ginzberg, WX-7
ATTN: Doc. Con. for Fred App
ATTN: Doc. Con. for Reports Lib.
ATTN: Doc. Con. for Jack Fuller, WX-6
ATTN: Doc. Con. for Paul Whalen
ATTN: Doc. Con. for Robert Skaggs
ATTN: Doc. Con. for John McQueen
ATTN: Doc. Con. Off. for R. Dingus

Sandia Laboratories
Livermore Laboratory
ATTN: Doc. Con. for Tech. Library

Sandia Laboratories
ATTN: Doc. Con. for Luke J. Vortman
ATTN: Doc. Con. for 3141, Sandia Rpt. Coll.
ATTN: Doc. Con. for George Kinoshita, 1535
ATTN: Doc. Con. for Wendell D. Weart
ATTN: Doc. Con. for Jim Plimpton
ATTN: Doc. Con. for Lynn Tyler
ATTN: Doc. Con. for Ben Bader
ATTN: Doc. Con. for M. L. Merritt
ATTN: Doc. Con. for Carter Broyles

OTHER GOVERNMENT AGENCIES

Department of the Interior
U.S. Geological Survey
Special Projects Center
ATTN: William Twenhofel
ATTN: Arthur Fernald

Department of the Interior
U.S. Geological Survey
ATTN: J. H. Healy
ATTN: Cecil B. Raleigh

DEPARTMENT OF DEFENSE CONTRACTORS

Aerospace Corporation
2 cy ATTN: Tech. Info. Services
ATTN: V. Stephenson
ATTN: J. McClelland
ATTN: Richard Crolius, A2-Rm. 1027
ATTN: Larry Selzer
ATTN: Frank Hai
ATTN: W. Barry
ATTN: S. P. Bower
ATTN: Prem N. Mathur

Agbabian Associates
ATTN: Carl Bagge
ATTN: M. Agbabian

Analytic Services, Inc.
ATTN: George Hesselbacher

Applied Theory, Inc.
2 cy ATTN: John G. Trulio

Artec Associates, Inc.
ATTN: Steven Gill

Battelle Memorial Institute
ATTN: Technical Library

The BDM Corporation
ATTN: Tech. Lib.

The Boeing Company
ATTN: Robert Dyrdahl
ATTN: Aerospace Library

Brown Engineering Company, Inc.
Cummings Research Park
ATTN: Manu Patel

California Research & Technology, Inc.
ATTN: Sheldon Shuster
ATTN: Technical Library
ATTN: Ken Kreyenhagen

Civil/Nuclear Systems Corp.
ATTN: Robert Crawford

Electromechanical Sys. of New Mexico, Inc.
ATTN: R. A. Shunk

Engineering Decision Analysis Co., Inc.
ATTN: Robert Kennedy

General Electric Company
TEMPO-Center for Advanced Studies
ATTN: DASIAC

H-Tech. Laboratories, Inc.
ATTN: B. Hartenbaum

IIT Research Institute
ATTN: Technical Library

University of Illinois at Chicago
College of Engineering
ATTN: Ted Belytschko

Institute for Defense Analyses
ATTN: IDA Librarian, Ruth S. Smith

DEPARTMENT OF DEFENSE CONTRACTORS (Continued)

IRT Corporation
ATTN: Ralph H. Stahl
ATTN: C. Pepper

J. H. Wiggins, Co., Inc.
ATTN: Jon Collins

Kaman Sciences Corporation
ATTN: W. Foster Rich
ATTN: Frank H. Shelton
ATTN: Walter E. Ware
ATTN: H. Hollister
ATTN: Dave Foxwell
ATTN: Paul A. Ellis

Lockheed Missiles & Space Co., Inc.
ATTN: A. Risso, Dept. 58-10, Bldg. 102
ATTN: Jack Wilson, Dept. 58-10
ATTN: Edwin A. Smith, Dept. 85-85

Lockheed Missiles & Space Company, Inc.
ATTN: Tom Geers, D/52023, Bldg. 205
ATTN: S. R. Salisbury
ATTN: Lloyd F. Chase

McDonnell Douglas Corporation
ATTN: J. Kirby
ATTN: H. M. Berkowitz

Merritt CASES, Inc.
ATTN: J. L. Merritt
ATTN: Technical Library

Mission Research Corporation
ATTN: Conrad L. Longmire

Mission Research Corporation
ATTN: David E. Merewether

Mission Research Corporation-San Diego
ATTN: V. A. J. Van Lint

The Mitre Corporation
ATTN: Library

University of New Mexico
Dept. of Campus Security & Police
ATTN: G. E. Triandafalidis

Nathan M. Newmark
Consulting Engineering Services
ATTN: Nathan M. Newmark
ATTN: W. Hall

Pacifica Technology
ATTN: G. Kent
ATTN: R. Bjork

Physics International Company
ATTN: Doc. Con. for Fred M. Sauer
ATTN: Doc. Con. for Charles Godfrey
ATTN: Joe Kochley
ATTN: Doc. Con. for Dennis Orphal
ATTN: Doc. Con. for Coye Vincent
ATTN: Doc. Con. for Larry A. Behrmann

The Rand Corporation
ATTN: Armas Laupa
ATTN: Technical Library

DEPARTMENT OF DEFENSE CONTRACTORS (Continued)

R&D Associates
ATTN: Henry Cooper
ATTN: Harold L. Brode
ATTN: F. A. Field
ATTN: Cyrus P. Knowles
ATTN: William R. Graham, Jr.
ATTN: Robert Port
ATTN: Richard R. Schaefer
ATTN: J. G. Lewis
ATTN: Technical Library

Science Applications, Inc.
ATTN: Larry Scott
ATTN: R. Parkinson
ATTN: Olan Nance

Science Applications, Inc.
ATTN: R. I. Miller

Science Applications, Inc.
ATTN: J. Roger Hill
ATTN: James Cramer

Science Applications, Inc.
ATTN: Burt Chambers

SRI International
ATTN: T. Morita
ATTN: George R. Abrahamson
ATTN: H. E. Lindberg
ATTN: George Carpenter

DEPARTMENT OF DEFENSE CONTRACTORS (Continued)

Systems, Science & Software, Inc.
ATTN: Bud Pyatt
ATTN: Donald R. Grine
ATTN: Russell E. Duff
ATTN: Charles R. Dismukes
ATTN: Technical Library
ATTN: Phil Coleman

Terra Tek, Inc.
ATTN: Sidney Green
ATTN: Technical Library

TRW Defense & Space Sys. Group
ATTN: Norm Lipner
ATTN: Peter K. Dai, R1/2170
ATTN: Dick Cramond
ATTN: Tech. Info. Center/S-1930

TRW Defense & Space Sys. Group
San Bernardino Operations
ATTN: G. D. Hulcher

Weidlinger Assoc. Consulting Engineers
ATTN: Melvin L. Baron